ol. 118 No. 2, August, 1980
ompleting Vol. 118

ISSN 0003-2670

ANALYTICA CHIMICA ACTA

International journal devoted to all branches of analytical chemistry

EDITORS
A. M. G. MACDONALD (Birmingham, Great Britain)
HARRY L. PARDUE (West Lafayette, IN. U.S.A.)

Editorial Advisers

F. C. Adams, Antwerp
R. P. Buck, Chapel Hill, NC
G. den Boef, Amsterdam
G. Duyckaerts, Liège
D. Dyrssen, Göteborg
W. Haerdi, Geneva
G. M. Hieftje, Bloomington, IN
J. Hoste, Ghent
A. Hulanicki, Warsaw
E. Jackwerth, Bochum
G. Johansson, Lund
D. C. Johnson, Ames, IA
J. H. Knox, Edinburgh
P. D. LaFleur, Washington, DC
D. E. Leyden, Denver, CO
F. E. Lytle, West Lafayette, IN
H. Malissa, Vienna
A. Mizuike, Nagoya
E. Pungor, Budapest
W. C. Purdy, Montreal
J. P. Riley, Liverpool
J. Růžička, Copenhagen
D. E. Ryan, Halifax, N.S.
J. Savory, Charlottesville, VA
W. D. Shults, Oak Ridge, TN
W. Simon, Zürich
W. I. Stephen, Birmingham
G. Tölg, Schwäbisch Gmünd, B.R.D.
A. Townshend, Birmingham
B. Trémillon, Paris
A. Walsh, Melbourne
H. Weisz, Freiburg i. Br.
P. W. West, Baton Rouge, LA
T. S. West, Aberdeen
J. B. Willis, Melbourne
Yu. A. Zolotov, Moscow
P. Zuman, Potsdam, NY

ELSEVIER SCIENTIFIC PUBLISHING COMPANY

ANALYTICA CHIMICA ACTA

International journal devoted to all branches of analytical chemistry
Revue internationale consacrée à tous les domaines de la chimie analytique
Internationale Zeitschrift für alle Gebiete der analytischen Chemie

PUBLICATION SCHEDULE FOR 1980 (incorporating the section on Computer Techniques and Optimization).

	J	F	M	A	M	J	J	A	S	O	N	D
Analytica Chimica Acta	113/1 113/2	114	115	116/1	116/2	117	118/1	118/2	119	120/1	120/2	121
Section on Computer Techniques and Optimization			122/1			122/2			122/3			122/4

Scope. *Analytica Chimica Acta* publishes original papers, short communications, and reviews dealing with every aspect of modern chemical analysis, both fundamental and applied. The section on *Computer Techniques and Optimization* is devoted to new developments in chemical analysis by the application of computer techniques and by interdisciplinary approaches, including statistics, systems theory and operation research. The section deals with the following topics: Computerized acquisition, processing and evaluation of data. Computerized methods for the interpretation of analytical data including chemometrics, cluster analysis, and pattern recognition. Storage and retrieval systems. Optimization procedures and their application. Automated analysis for industrial processes and quality control. Organizational problems.

Submission of Papers. Manuscripts (three copies) should be submitted as designated below for rapid and efficient handling:

Papers from the Americas to: Professor Harry L. Pardue, Department of Chemistry, Purdue University, West Lafayette, IN 47090, U.S.A.

Papers from all other countries to: Dr. A. M. G. Macdonald, Department of Chemistry, The University, P.O. Box 363, Birmingham B15 2TT, England.

For the section on *Computer Techniques and Optimization:* Dr. J. T. Clerc, Universität Bern, Pharmazeutisches Institut, Sahlistrasse 10, CH-3012 Bern, Switzerland.

American authors are recommended to send manuscripts and proofs by INTERNATIONAL AIRMAIL.

Information for Authors. Papers in English, French and German are published. There are no page charges. Manuscripts should conform in layout and style to the papers published in this Volume. Authors should consult Vol. 111, p. 343 for detailed information. Reprints of this information are available from the Editors or from: Elsevier Editorial Services Ltd., Mayfield House, 256 Banbury Road, Oxford OX2 7DE (Great Britain).

Reprints. Fifty reprints will be supplied free of charge. Additional reprints (minimum 100) can be ordered. An order form containing price quotations will be sent to the authors together with the proofs of their article.

Advertisements. Advertisement rates are available from the publisher.

Subscriptions. Subscriptions should be sent to: Elsevier Scientific Publishing Company, P.O. Box 211, 1000 AE Amsterdam, The Netherlands. The section on *Computer Techniques and Optimization* can be subscribed to separately.

Publication. *Analytica Chimica Acta* (including the section on *Computer Techniques and Optimization*) appears in 10 volumes in 1980. The subscription for 1980 (Vols. 113–122) is Dfl. 1390.00 plus Dfl. 160.00 (postage) (total approx. U.S. $795.00). The subscription for the *Computer Techniques and Optimization* section only (Vol. 122) is Dfl. 139.00 plus Dfl. 16.00 (postage) (total approx. U.S. $79.50). Journals are sent automatically by airmail to the U.S.A. and Canada at no extra cost and to Japan, Australia and New Zealand for a small additional postal charge. All earlier volumes (Vols. 1–112) except Vols. 23 and 28 are available at Dfl. 150.00 (U.S. $77.00), plus Dfl. 10.00 (U.S. $5.00) postage and handling, per volume.

Claims for issues not received should be made within three months of publication of the issue, otherwise they cannot be honoured free of charge.

Customers in the U.S.A. and Canada who wish to obtain additional bibliographic information on this and other Elsevier journals should contact Elsevier/North Holland Inc., Journal Information Center, 52 Vanderbilt Avenue, New York, NY 10017. Tel: (212) 867-9040.

An Atlas of Spectral Interferences in ICP Spectroscopy

by **M. L. Parsons, Alan Forster,** and **Donn Anderson**
Arizona State University

This volume provides the information necessary to determine if a specific system will be subject to spectral interferences. An indispensable tool for inductively coupled plasma (ICP) analytical spectroscopists, this volume will be an aid in the choice of analysis line, the prevention of errors due to spectral overlap, and in the identification of sources of stray radiation. 654 pp., 1979, $59.50 ($71.40/£37.49 outside US)

Auger Electron Spectroscopy Reference Manual
A Book of Standard Spectra for Identification and Interpretation of Auger Electron Spectroscopy Data

by **G. E. McGuire**
Texas Instruments Inc., Dallas

This volume can be used as a laboratory guide for the most frequently encountered elements in the periodic table. The data include a general survey scan from 0–2000 eV taken with a 5 keV primary beam energy, 5 μA beam current and a 6 eV peak-to-peak modulation voltage. 280 pp., 1979, $39.50 ($47.40/£24.89 outside US)

Multiple Electron Resonance Spectroscopy

edited by **Martin M. Dorio**
General Electric
and **Jack H. Freed**
Cornell University

Multiple Electron Resonance Spectroscopy presents an account of the techniques and applications of multiple resonance that use electron paramagnetic resonance (EPR) for detection. The book details theoretical and experimental material on inorganic, organic, biochemical, and polymer systems, and critically points out areas of controversy and future research. 524 pp., illus., 1979, $49.50 ($59.40/£31.19 outside US)

Practical Mass Spectrometry
A Contemporary Introduction

edited by **Brian S. Middleditch**
University of Houston

Practical Mass Spectrometry is a unique text directed to the novice who wishes to acquire a working knowledge of the techniques and capacities of modern mass spectrometers. The text provides a detailed examination of three currently available mass spectrometers, an introduction to gas chromatography–mass spectrometry, available methods for comparing spectra, and applications of mass spectrometry in a broad range of disciplines. 404 pp., illus., 1979, $29.50 ($35.40/£18.59 outside US)

Introduction to Analytical Electron Microscopy

edited by **John J. Hren**
University of Florida
Joseph I. Goldstein
Lehigh University
and **David C. Joy**
Bell Laboratories, New Jersey

This volume is a tutorial guide for the practicing electron microscopist wishing to learn newly available methods of analysis. The approach is practical, with a heavy reliance on examples. 626 pp., 1979, $42.00/£22.05 outside US)

Ion-Selective Electrodes in Analytical Chemistry
Volume 1

edited by **Henry Freiser**
University of Arizona

"[This volume] is a comprehensive monograph treating both conceptual and practical aspects, and serves as an introduction to ion-selective electrodes while stimulating interest in the development of applications. . . . A recommended acquisition for scientists and engineers."

—*Electrochemical Progress*

A volume in the *Modern Analytical Chemistry* series. 454 pp., 1978, $42.50 ($51.00/£26.78 outside US)

THE LANGUAGE OF SCIENCE
Plenum
PUBLISHING CORPORATION

227 West 17th Street, New York, N.Y. 10011
In United Kingdom: Black Arrow House
2 Chandos Road, London NW10 6NR, England

Euroanalysis III

edited by **D. M. CARROLL,** *Institute for Industrial Research and Standards, Dublin, Ireland*

6 × 9″ (15·5 × 23 cm). xvi + 428 pages. 137 illus. 1979.

This book contains the plenary and keynote lectures presented at the Third European Conference on Analytical Chemistry, Euroanalysis III, held in Dublin in August 1978, organised by the Institute of Chemistry of Ireland on behalf of the Working Party on Analytical Chemistry of the European Federation of Chemical Societies.

It provides a comprehensive review of the present situation and future prospects in chemical, pharmaceutical and environmental analysis as well as the role of analytical chemistry in the earth sciences and the analysis of solid surfaces.

CONTENTS: 1. Irish contributions to European analytical chemistry. 2. Stable free radicals—electron spin resonance—analytical chemistry. 3. Are you still eating? Chemical food analysis—fact and fiction. 4. Clinical laboratory reference materials and methods—present status and future prospects. 5. Atomic spectrochemical analysis in soil science research. 6. *In-situ* microanalysis and surface analysis by electron probe techniques. 7. Computers in spectroscopy. 8. Reference materials: Their production, certification and use in compatible measurement networks. 9. Ion-selective electrodes—application in flowing systems. 10. Modern polarographic and voltammetric techniques. 11. Recent developments in high performance liquid chromatography. 12. Infrared spectroscopy of biocontact surfaces. 13. Analytical chemistry in the dairy industry. 14. Electron spectroscopy for chemical analysis. 15. Analytical chemistry in the earth sciences. 16. Conformational analysis: An account of experimental and theoretical methods applied to the analysis of mixtures and of constituent structures. 17. Hydrocarbon analysis. 18. Environmental analysis—air quality evaluation. 19. Pharmaceutical analysis. 20. Clinical biochemical analysis. Index.

APPLIED SCIENCE PUBLISHERS Ltd
Ripple Road, Barking, Essex, England

216 AS

ANALYTICA CHIMICA ACTA
VOL. 118 (1980)

ANALYTICA CHIMICA ACTA

International journal devoted to all branches of analytical chemistry

EDITORS
A. M. G. MACDONALD (Birmingham, Great Britain)
HARRY L. PARDUE (West Lafayette, IN, U.S.A.)

Editorial Advisers

F. C. Adams, Antwerp
R. P. Buck, Chapel Hill, NC
G. den Boef, Amsterdam
G. Duyckaerts, Liège
D. Dryssen, Göteborg
W. Haerdi, Geneva
G. M. Hieftje, Bloomington, IN
J. Hoste, Ghent
A. Hulanicki, Warsaw
E. Jackwerth, Bochum
G. Johansson, Lund
D. C. Johnson, Ames, IA
J. H. Knox, Edinburgh
P. D. LaFleur, Washington, DC
D. E. Leyden, Denver, CO
F. E. Lytle, West Lafayette, IN
H. Malissa, Vienna
A. Mizuike, Nagoya
E. Pungor, Budapest
W. C. Purdy, Montreal
J. P. Riley, Liverpool
J. Růžička, Copenhagen
D. E. Ryan, Halifax, N.S.
J. Savory, Charlottesville, VA
W. D. Shults, Oak Ridge, TN
W. Simon, Zürich
W. I. Stephen, Birmingham
G. Tölg, Schwäbisch Gmünd, B.R.D.
A. Townshend, Birmingham
B. Trémillon, Paris
A. Walsh, Melbourne
H. Weisz, Freiburg i. Br.
P. W. West, Baton Rouge, LA
T. S. West, Aberdeen
J. B. Willis, Melbourne
Yu. A. Zolotov, Moscow
P. Zuman, Potsdam, NY

ELSEVIER SCIENTIFIC PUBLISHING COMPANY

Anal. Chim. Acta, Vol. 118 (1980)

25 FEB 2523

© Elsevier Scientific Publishing Company, 1980.
All rights reserved. No part of this publication may be reproduced, stored in a retrieval system or transmitted in any form or by any means, electronic, mechanical, photocopying, recording or otherwise, without the prior written permission of the publisher, Elsevier Scientific Publishing Company, P.O. Box 330, 1000 AH Amsterdam, The Netherlands.

Submission of an article for publication implies the transfer of the copyright from the author to the publisher and is also understood to imply that the article is not being considered for publication elsewhere.

Submission to this journal of a paper entails the author's irrevocable and exclusive authorization of the publisher to collect any sums or considerations for copying or reproduction payable by third parties (as mentioned in article 17 paragraph 2 of the Dutch Copyright Act of 1912 and in the Royal Decree of June 20, 1974 (S. 351) pursuant to article 16 b of the Dutch Copyright Act of 1912) and/or to act in or out of court in connection therewith.

Printed in The Netherlands.

Analytica Chimica Acta, 118 (1980) 1—9
© Elsevier Scientific Publishing Company, Amsterdam — Printed in The Netherlands

A THREE-CHANNEL FLAME ATOMIC ABSORPTION/EMISSION SPECTROMETER FOR THE RAPID, ROUTINE DETERMINATION OF MAJOR CATIONS IN SOIL EXTRACTS AND PLANT ASH SOLUTIONS

A. M. URE*, G. J. EWEN and M. C. MITCHELL

The Macaulay Institute for Soil Research, Craigiebuckler, Aberdeen AB9 2QJ (Gt. Britain)

(Received 29th February 1980)

SUMMARY

A 3-channel instrument for the simultaneous routine determination of calcium, magnesium and sodium by atomic absorption/emission spectrometry is described. The instrument uses a novel burner for a nitrous oxide/air/acetylene flame with two nebulizers, one for nitrous oxide and one for air. This permits continuous nebulization of an ionization suppression solution by one nebulizer and nebulization of sample and buffer solutions by the second nebulizer fitted with a branched, capillary aspirator tube. With this technique, time-consuming additions of buffering materials to sample solutions are eliminated. Examples of its application to acetic acid extracts of soils and solutions of plant ash are given and the freedom from aluminium and phosphate interference in the determination of calcium is demonstrated.

In the agricultural chemical laboratory, the analysis of large numbers of soil extracts and solutions of ashed plant materials for major nutrient cations, such as calcium, potassium, magnesium and sodium, demands rapid methods of determination with the minimum of sample pretreatment. Part of the solution to this problem involves the use of simple, simultaneous, multi-element instrumentation and this has been achieved with flame emission spectrometers [1—3] and to a more limited extent with atomic absorption spectrometry [4].

The present paper describes a simple three-channel instrument for the simultaneous determination of calcium and magnesium by atomic absorption and sodium by atomic emission spectrometry. This uses a nitrous oxide/air/acetylene flame, on a twin-nebulizer burner, to which sample and ionization suppression solutions can be presented simultaneously by means of the two nebulizers. This is practicable, since ionization, and its suppression by an easily-ionized element such as potassium, occur as gas-phase reactions in the flame, and not in the solution or solid clotlet phases. In contrast, a lanthanum or strontium buffer is required in the sample and standard solutions for the suppression of aluminium or phosphate interference on calcium and magnesium. This is achieved by using a branched, nebulizer capillary tube, one branch to aspirate the sample or standard solution and the other the strontium or lanthanum buffer solution. These techniques obviate the need for time-

consuming additions of buffering materials to sample and standard solutions. Finally the need for dilutions is minimized by making use of burner rotation to reduce the absorbing path length for atomic absorption and by using electronic gain-control for atomic emission measurements.

EXPERIMENTAL

Burner/nebulizer

The burner/nebulizer assembly is illustrated in elevation in Fig. 1a and in plan in Fig. 1b, with the 5-cm slot, high-temperature burner-top (Varian Techtron, AB40) removed. The twin nebulizers, A and C (modified Corning-EEL Cat. No. 100-99008) are fitted into the stainless steel base, D, of the burner together with the acetylene jet, B. Coarse and fine vertical movements of the whole burner assembly are provided by the clamp, E, and the elevating screw, F. The burner-top, G, is free to rotate in the teflon insert, H, at the top of burner-tube, I. The base, D, acts as spray chamber from which surplus solution drains out at J.

Details of the construction of the spray-chamber burner-base are shown in Fig. 2. The two nebulizers, A and C, are mounted on either side of the acetylene jet, B, in polyethylene bushes, K, and aligned so that the jets of spray produced impinge at the same point on the rear of the chamber, L. This acts as a flow-spoiler and ensures mixing of the two streams. Nebulizer C, supplied

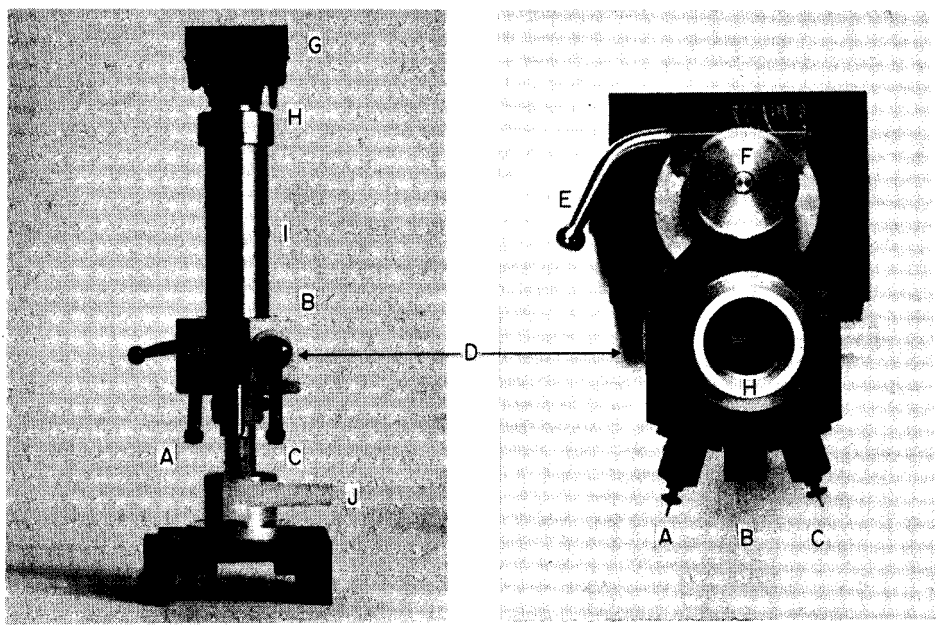

Fig. 1. Burner/nebulizer assembly shown in elevation (a) and plan (b): A and C, nebulizers; B, acetylene jet; D, stainless steel base; E and F, the clamp and elevating screw, respectively, for coarse and fine vertical movements; G, burner top in teflon inset, H; I, burner tube; J, drain.

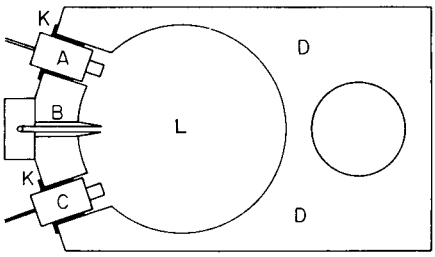

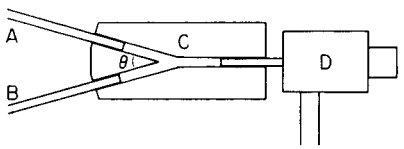

Fig. 2. Plan of spray chamber, L, in burner base, D, showing nebulizers A and C, mounted in polyethylene bushes, K, and the acetylene jet, B.

Fig. 3. Branched nebulizer adaptor: A and B, solution inlet capillaries; C, teflon body; D, nebulizer; $\theta = 20°$.

with nitrous oxide, is used to aspirate the potassium ionization suppression solution (500 mg l^{-1}). The other nebulizer, A, is supplied with compressed air and fitted with a teflon Y-piece whose two branches are connected to two capillary tubes, one supplying sample solution and the other strontium or lanthanum buffer solution to the nebulizer. The teflon Y-piece adaptor shown schematically in Fig. 3 consists of a teflon body, C, fitted on to the steel capillary of the nebulizer, D, with the two inlet capillaries, A and B, at an angle of 20° to each other. This Y-form has been found to be more reliable than T-form designs [5] in its self-starting and self-clearing abilities. The nebulizers themselves have been modified, to accommodate the gas flow rates used, by enlarging the guide hole in the nebulizer (to 0.89 mm) and fitting a larger (0.64 mm o.d.) stainless steel capillary.

Air and acetylene are supplied from conventional regulators, and the nitrous oxide from a regulator with an integral heat-exchanger (Victor SR300 supplied by Pye Unicam). All flow rates are controlled by needle valves and monitored by flow-meters.

In addition to the advantages already mentioned, the twin-nebulizer design allows intrinsically safe, operational gas conditions to be used for this nitrous oxide/air/acetylene flame.

Instrument description

The instrument, shown schematically in Fig. 4, consists of three hollow-cathode lamps and three monochromators (Rank Hilger D220) fitted round a high-temperature, 5-cm slot burner. Of the three channels, only the central one is described as they are essentially identical. In one channel, used for sodium determination by atomic emission spectrometry, the hollow-cathode lamp and its lens (shown dashed in Fig. 4) are not required. Each spectrometer consists of a d.c.-fed hollow-cathode lamp, A; a twin-lens optical system, B; a 180° sector chopper, D, fitted with an opto-electronic relay, C, to provide sector position information to a trigger circuit and LED driver circuit, K; a burner, E; monochromator, F; and a photomultiplier, G, whose output is displayed on a digital panel meter, H (3 digit). In operation, the

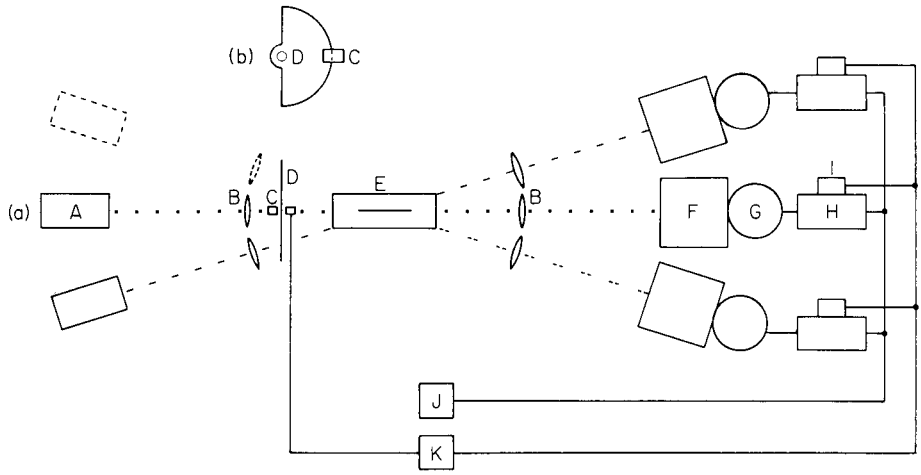

Fig. 4. Schematic diagram of instrument. The major part of the diagram (a) shows: A, Hollow-cathode lamp; B, lenses: C, opto-electronic relay; D, 180° sector rotating chopper; E, burner; F, monochromator (Rank Hilger D220); G, photomultiplier, RCA IP28; H, digital panel meter; I, LED display; J, start and reset controls; K, electronic trigger and LED driver circuitry. The top section (b) shows the side elevation of 180° sector rotating chopper D, and opto-electronic relay, C.

sector chopper rotates continuously, alternately opening and closing the light path from the hollow-cathode lamp to the flame for 3-s periods. The light intensities displayed at the digital panel meter therefore have two alternating values, each of which persists for 3 s, and which correspond respectively to the readings with the hollow-cathode lamp sector shutter open and closed. The position of the sector is indicated on an LED display, I, as a "1" or a "2" corresponding to open and closed, respectively. Start and reset controls are provided electronically at J. After each sample insertion, the digital display is blanked out for 20 s to allow the nebulizers and flame conditions to reach equilibrium before readings are made.

In the emission mode, the operation of the sector chopper is redundant and only one measurement level is displayed on the digital panel-meter.

Principle of atomic absorption measurement

If, for a blank solution, the two measurements corresponding to the above "1" (open) and "2" (closed) conditions are M_1 and M_2, then

$$M_1 = I_D + E_B + I_0 - A_B \text{ and } M_2 = I_D + E_B$$

where I_D is the photomultiplier dark-current signal, E_B is the flame background emission signal, I_0 the hollow-cathode lamp intensity, and A_B the flame background absorption signal. Then

$$M_1 - M_2 = I_0 - A_B = I_0' \quad (1)$$

where I_0' is the resultant hollow-cathode lamp intensity corresponding to 100% transmittance (100%T).

If, in the same way, for a sample or standard solution, two measurements are again made, M_3 and M_4, corresponding respectively to the "1" and "2" conditions, then

$M_3 = I_D + E_B + E_L + I_0 - A_B - A_L$ and $M_4 = I_D + E_B + E_L$

and, from eqn. (1) $M_3 - M_4 = (I_0 - A_B) - A_L = I'_0 - A_L = I_T$

where E_L is the spectral line emission signal from the flame, A_L is the spectral line atomic absorption signal, and I_T ($= I'_0 - A_L$) is the resultant transmission signal.

The percentage transmittance signal (%T) is equal to $(100\ I_T)/I'_0$ for the sample solution and the corresponding absorbance is equal to $2 - \log (100\ I_T/I'_0)$. Thus, the absorbances corresponding to the aspirated sample or standard solutions can be calculated from the four measurements M_1, M_2, M_3 and M_4.

Operation

A fuel-rich air/acetylene flame (air 2.2 l min^{-1}, acetylene 0.5 l min^{-1}) is first ignited. The acetylene flow is slowly increased to ca. 1 l min^{-1}, while the nitrous oxide supply is gradually increased from zero to 2.1 l min^{-1} with the air flow unaltered. The final reducing flame has a 4-mm orange-red "feather" above a blue 2-mm primary combustion zone. The flame conditions were chosen to minimize the interference effects of aluminium on calcium. For all analyses, an ionization suppressor solution (500 mg K l^{-1}) is aspirated by the "nitrous oxide" nebulizer. A potassium concentration of 500 mg l^{-1} was found to be sufficient to suppress the ionization of sodium (5 mg l^{-1}) in a standard solution containing in addition calcium (75 mg l^{-1}) and magnesium (3.6 mg l^{-1}). One branch of the "air" nebulizer is fed with a buffer solution while the other branch aspirates the sample and standard solutions. Typical nebulizer solution uptake rates are: air nebulizer, sample branch 8.5 ml min^{-1}; air nebulizer, buffer branch 8.5 ml min^{-1}; and nitrous oxide nebulizer 6 ml min^{-1}.

A blank solution is first aspirated to make measurements M_1 and M_2; measurements of M_3 and M_4 are then made by aspirating a series of standard solutions containing the appropriate amounts of calcium, magnesium and sodium (see operational concentration ranges). Prior to the analysis of a series of samples, an additional standard solution containing aluminium (100 mg l^{-1}) and calcium (30 mg l^{-1}) is aspirated, in order to verify that flame conditions are such that there is no significant depression of the calcium absorbance by aluminium.

Computation

Calcium and magnesium absorbances are calculated from the readings $M_1 - M_4$ by using a pre-programmed calculator (Texas Instruments SR52). Blank and check standard absorbances, measured before and after each seven samples, are averaged and normalized to a reading of 100 for the check standard (normally the upper standard of the operational range). The normalizing factor is applied to the sample readings.

The concentrations of the analyses in the sample solutions can be calculated from calibration graphs of normalized absorbance versus concentration for the range of standard solutions. In practice, incremental tables of normalized absorbance versus concentration, derived from the calibration curves, are used to evaluate the concentrations for each solution.

A similar normalizing procedure is adopted for sodium (atomic emission spectrometry) by using the digital meter readings of intensity directly.

RESULTS AND DISCUSSION

Interference effects

The effect of aluminium on the determination of calcium was investigated by measuring the absorbance for calcium obtained with standard solutions containing aluminium concentrations ranging from zero to 500 mg l^{-1} and calcium, magnesium and sodium in proportions suitable for soil extracts (see operational concentration ranges). These solutions were examined by aspirating them in one branch of the air nebulizer capillary, while distilled water or a 1250 mg l^{-1} or 2500 mg l^{-1} strontium solution was aspirated in the other branch. In all cases, the ionization suppressor (500 mg K l^{-1}) was aspirated by the nitrous oxide nebulizer. Typical effects for calcium are illustrated in Fig. 5 for a standard solution containing 15 mg Ca l^{-1}, 0.72 mg Mg l^{-1} and 1.0 mg Na l^{-1}. The results are also compared with those for a conventional 10-cm air/acetylene burner. It can be concluded that, in the absence of strontium, the nitrous oxide/air/acetylene flame reduces the degree of aluminium interference compared with an air/acetylene flame, but that the presence of 2500 mg Sr l^{-1} is necessary to limit the interference to less than 5%. Since the expected range of aluminium in acetic acid soil extracts for example will seldom exceed 50 mg l^{-1} [6], aluminium interference should present no problems. A concentration of 2500 mg Sr l^{-1} was therefore adopted for the buffer solution.

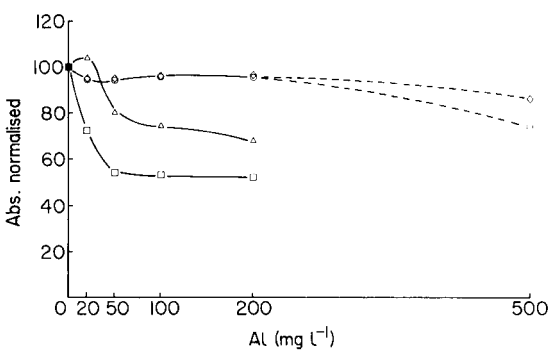

Fig. 5. The interference of aluminium on the absorbance of calcium (15 mg l^{-1}) and its suppression in: (□) a conventional 10-cm air/C_2H_2 burner; (△) N_2O/air/C_2H_2 burner described herein; (○) N_2O/air/C_2H_2 burner with 1250 mg Sr l^{-1} nebulized in second nebulizer; (◇) N_2O/air/C_2H_2 burner with 2500 mg Sr l^{-1} nebulized in second nebulizer.

Similar experiments with phosphorus interference on calcium showed that no significant interference occurred up to phosphorus concentrations of about 200 mg l^{-1} with small (<10%) but significant depression for levels of 500 mg l^{-1}. The combined effect of aluminium (100 mg l^{-1}) and phosphorus (50 mg l^{-1}) was also found to be negligible (<3%). No interference is likely to occur in most herbage materials where the phosphorus content in the analysed solution is expected to be in the range 10—200 mg l^{-1}.

Operational concentration ranges

The minimum and maximum concentrations measurable in practice with the different burner orientations are indicated in Table 1. Modes A and B (Table 1) are used principally for acetic acid and other extracts of soils, the expected calcium contents of the sample solution being the main criterion for choosing A or B.

Typical standard solutions for acetic acid extracts of soils (20 g of soil with acetic acid at 800 mg l^{-1}, as described by Scott et al. [7]), are prepared in 2.5% acetic acid by dilution of a basic standard solution containing calcium (300 mg l^{-1}), magnesium (14 mg l^{-1}) and sodium (20 mg l^{-1}). Mode C is used mainly for the analysis of solutions of ashed plant materials in 0.06 M hydrochloric acid (2 g of plant material with 100 ml of 0.06 M hydrochloric acid [7]).

Samples are analysed directly without dilution and without the addition of buffering solutions. Typical ranges of solution concentrations for acetic acid extracts of soils and solutions of plant ash are given in Table 2.

TABLE 1

Minimum and maximum concentrations determined (mg l^{-1})

Mode	Burner alignment	Minimum concentration			Maximum concentration		
		Ca	Mg	Na	Ca	Mg	Na
A	On central axis (Ca channel)	0.2	0.06	0.1	60	14	20
B	Offset 20° to central axis (Mg channel)	0.7	0.03	0.1	150	7	10
C	Perpendicular to central axis	1.0	0.2	0.4	200	48	80

TABLE 2

Typical solution concentration ranges for acetic acid extracts of soils and plant ash solutions (mg l^{-1})

Sample type	Ca	Mg	Na
Acetic acid extracts of soil (mode B)	6—150	0.30—7	0.4—10
Plant ash solutions (mode C)	4—200	1.0—48	1.6—80

Precision and accuracy

The precision of the method is indicated by the relative standard deviations obtained for calcium (±3.1%), magnesium (±3.6%) and sodium (±2.5%) in ten replicate analyses of an acetic acid soil extract containing mean concentrations of 63.2 mg l^{-1}, 4.56 mg l^{-1} and 2.38 mg l^{-1}, respectively.

An indication of the accuracy of the method is provided by the comparative analysis of acetic acid extracts of soils by the present method and by a conventional atomic absorption procedure with an Instrumentation Laboratory 751 instrument and an air or nitrous oxide/acetylene flame. The results in Table 3 show good agreement for all three elements.

Another confirmation of the accuracy was obtained by the determination of the calcium and magnesium contents of NBS Orchard Leaves (SRM 1571); the results are shown in Table 4. Determinations with the three-channel instrument were carried out directly on the ash solution, whereas for the a.a.s. (IL 751) procedure the solutions were diluted a further 200 times and potassium and strontium buffers were added as indicated in Table 3. The agreement between the two methods is good, and for calcium the contents agree closely with the certified value. Both methods, however, provide magnesium contents which are significantly lower, presumably as a result of inadequate ash dissolution.

TABLE 3

Calcium, magnesium and sodium contents (mg l^{-1}) of acetic acid soil extracts. (A) Direct analysis of original solution as described with the three-channel instrument; (B) conventional a.a.s. with an IL751 and an air/acetylene flame for sodium and magnesium or a nitrous oxide/acetylene flame for calcium[a]

Sample	Calcium		Magnesium		Sodium	
	A	B	A	B	A	B
1	57	56	1.7	1.6	2.5	2.8
2	55	53	1.6	1.6	2.7	2.6
3	79	74	2.9	3.0	2.8	2.6
4	52	52	2.0	2.0	2.5	2.5
5	104	90	15.8	14.0	1.6	1.8
6	19	16	1.7	1.6	1.5	1.5
7	19	17	2.1	1.9	1.5	1.5

[a]With diluted solutions containing 2500 mg Sr l^{-1} and 1000 mg K l^{-1}.

TABLE 4

Calcium and magnesium contents (% dry weight) of NBS Orchard Leaves SRM 1571

Element	Proposed method	Conventional a.a.s.	Certified value
Ca	2.04	1.91	2.09 ± 0.03
Mg	0.55	0.55	0.62 ± 0.02

REFERENCES

1 R. L. Mitchell, Spectrochim. Acta, 4 (1950) 62.
2 B. L. Vallee and M. Margoshes, Anal. Chem., 28 (1956) 175.
3 A. M. Ure, Brit. Commun. Electron., 5 (1958) 846.
4 R. A. G. Rawson, 4th Int. Conf. on Atomic Spectroscopy, Toronto, 1973.
5 I. Rubeška, M. Mikšovský and M. Huka, At. Absorpt. Newsl., 14 (1975) 28.
6 R. O. Scott and A. M. Ure, Analyst, 83 (1958) 561.
7 R. O. Scott, R. L. Mitchell, D. Purves and R. C. Voss, Spectrochemical Methods for the Analysis of Soil, Plant and other Agricultural Materials, Bulletin 2, Consultative Committee for Development of Spectrochemical Work, The Macaulay Institute for Soil Research, 1971.

Analytica Chimica Acta, 118 (1980) 11—28
© Elsevier Scientific Publishing Company — Printed in The Netherlands

AMMONIA-FILLED DISCHARGE TUBES FOR OPTICAL EMISSION SPECTROMETRIC DETERMINATION OF ^{15}N : ^{14}N ISOTOPE RATIOS

J. C. BURRIDGE* and I. J. HEWITT

Department of Spectrochemistry, The Macaulay Institute for Soil Research, Craigiebuckler, Aberdeen AB9 2QJ (Gt. Britain)

(Received 5th March 1980)

SUMMARY

A procedure is described for filling a discharge tube, permanently attached to a vacuum line, with ammonia in the pressure range 1.5—5 Torr, without any carrier gas. The ^{15}N : ^{14}N isotope ratio is determined from the N_2 spectrum emitted when the tube is excited by a 2450-MHz microwave source. Cooling one end of the discharge tube to —60°C enables the N_2 (1,0) bandheads at 316 nm to be used for ^{15}N contents down to about 0.04 atom-%. Unidentified interfering bands and emission from NH, OH, H_2 and H are discussed. Samples containing 1—30 mg of nitrogen can be analysed with an accuracy and precision suitable for most soil—plant studies employing ^{15}N as a tracer.

The molecular emission spectrum of nitrogen, in particular the (2,0) bandhead of the Second Positive N_2 system at 298 nm, is widely used for the determination of ^{15}N : ^{14}N isotope ratios. Three factors that have led to the increasing use of optical emission spectrometry (o.e.s.) for ^{15}N determination are the ease with which this N_2 system can be excited in discharge tubes, the isotopic wavelength shifts which are large enough for bandheads to be resolved by spectrometers having only a moderate dispersing power, and the ability to determine isotope ratios using only a few micrograms of nitrogen. Discharge tubes containing nitrogen gas are generally prepared by conversion of ammonium salts using the Dumas or Rittenberg reactions [1, 2].

These reactions are not convenient for o.e.s., however, when the samples used contain milligram amounts of nitrogen, as may arise in soil—plant studies. In a previous report [3] it was shown that such large amounts of nitrogen can readily be analysed by using discharge tubes containing ammonia and argon, omitting the conventional prior conversion to nitrogen gas. Further investigations have now established conditions under which discharge tubes filled with ammonia alone are stable and suitable for the determination of the nitrogen isotope ratio. Some of the properties of these discharge tubes, filled after separating sample ammonia from potentially contaminating atmospheric nitrogen by liquid-nitrogen cooling, are described.

Elimination of the argon flow and rare-gas purifier and the introduction of 'on-line' collection of ammonia, have simplified the apparatus and allow

a more efficient use of the sample nitrogen than in the earlier procedure [3]. Replicate measurements can be more readily made, improving analytical precision and reducing cross-contamination memory effects. It is also shown that ^{15}N contents well below the natural abundance of 0.37 atom-% can be determined by using the alternative (1,0) bandhead at 316 nm, providing OH emission is suppressed by cooling one end of the discharge tube to about —60°C.

EXPERIMENTAL

General vacuum equipment arrangement for discharge tube filling

The arrangement of equipment used to fill discharge tubes with ammonia for isotope analysis is shown schematically in Fig. 1. It consists of four units, the ammonia preparation tube A (Quickfit MF 24/3 borosilicate tube approximately 30 mm × 150 mm long), discharge tube B (silica, outer diameter 6 mm × 500 mm long, wall thickness 1 mm), thermopile vacuum gauge C, calibrated for the air pressure range 5—5000 mTorr (Hastings EVH-3 with gauge head DV-23), and rotary vacuum pump D (Edwards EDM6), interconnected with stainless steel tubing (type 316, outer diameter 0.25 in. (6.35 mm) to suit Cajon Ultra-Torr couplings) via four shut-off valves V_1—V_4 (Nupro bellows valves SS-4H). The bellows valves are oriented with their stem dead-space on the pumped side.

The temperature of tube A, when connected to the apparatus, can be varied by adjusting the height of a wide-mouth Dewar flask containing liquid nitrogen and positioned below A. The discharge tube B is permanently situated within the microwave cavity (Electro Medical Supplies, type 210 L), and the lower 200 mm of the 500 mm-long tube can be cooled to about —60°C by sheathing it with a copper tube, of about 8 mm internal diameter, which is fixed in good thermal contact to the flexible probe of a small refrigerator (Neslab Cryocool CC-60). Adequate insulation is provided by wrapping several alternate layers of cellular foam plastic and aluminium foil around the probe. Temperature control is not required; —60°C is approximately the minimum temperature attainable with this cooling unit. A liquid-nitrogen-

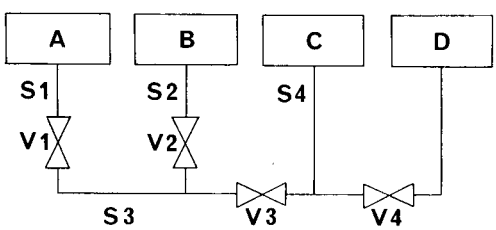

Fig. 1. Schematic arrangement of apparatus for filling the discharge tube with ammonia. (A) Ammonia preparation tube; (B) discharge tube; (C) vacuum gauge; (D) vacuum pump; (V1—V4) bellows valves; (S1—S4) sections connecting units A—D and valves V1—V4 with stainless steel tubing.

cooled trap is used in the vacuum line to condense oil vapour from the pump and to reduce possible cross-contamination between samples from back-streaming ammonia.

Tube-filling procedure

In the following description, reference is made to the items A—D, valves V_1—V_4 and interconnecting sections S1—S4 in Fig. 1. Approximate volumes of the interconnecting sections are: S1(A—V_1) 60 ml; S2(B—V_2) 8 ml; S3(V_1—V_2—V_3) 5 ml; and S4(C—V_3—V_4) 15 ml.

Preliminary leak check. With tube A detached, V_1 closed, V_2, V_3 and V_4 open, the apparatus is evacuated to below 10 m Torr, then checked for possible leaks or excessive outgassing by closing V_4 and noting the rate of pressure increase on gauge C. Increases of less than 1 m Torr h^{-1} are readily attained and considered satisfactory. After this check, valve V_4 is re-opened and pumping continued.

Ammonia release. A sample containing 1—2 mg of nitrogen as the ammonium ion in 0.1—0.2 ml of aqueous solution is placed in the bottom of the detached, dry tube A. The quantity of nitrogen and solution volume are not critical. The end of tube A is dipped into liquid nitrogen, and as soon as the sample is completely frozen (generally in less than 1 min) it is removed and 2 or 3 sodium hydroxide pellets are dropped into the tube where they rest on the sample but do not react with it yet. Tube A is immediately attached to the apparatus, valve V_2 closed and valve V_1 opened; when gauge C indicates a pressure of 5 Torr or less, valve V_1 is closed. This operation removes most of the air from the sample preparation tube A and takes place before the sample melts. Closing V_2 avoids flushing the discharge tube B with air.

With V_1 remaining closed, the sample is allowed to thaw slowly at room temperature, thus dissolving the sodium hydroxide and releasing ammonia which mixes with the residual air in tube A. The reaction is not vigorous and no precautions against frothing are required.

Final isolation of sample ammonia. When the reaction releasing ammonia is complete (in about 5 min), the Dewar flask is placed below tube A and raised until the end of tube A dips about 10 mm into the liquid nitrogen. After 5 min, sufficient ammonia for analysis has condensed, allowing valve V_1 to be opened and the final traces of residual air and any uncondensed ammonia to be pumped away. This completes the separation of sample ammonia, now in the solid phase, from potentially-contaminating atmospheric nitrogen. Valve V_1 is then closed, the Dewar flask removed, and the temperature of tube A allowed to rise to about 0°C. The Dewar flask is replaced and slowly raised until the cold end of tube A reaches a temperature of about −70°C. The approximate temperature of the end of tube A, kept about 20 mm above the liquid nitrogen, is monitored with an external thermocouple resting in contact with it (Comark Electronic Thermometer type 1602-BP, with flexible probe TC4).

A 2-mg sample of nitrogen provides an ammonia pressure of around 40 Torr in the 60-ml preparation tube A, most of which is at room temperature. At −70°C the vapour pressure of water over ice is about 2mTorr, while the saturated vapour pressure of ammonia is about 100 Torr. Thus cooling one end of tube A to −70°C enables the gaseous ammonia to be held in a sufficiently dry condition. This can conveniently be done by using a 1-l Dewar flask having a diameter of about 80 mm, with the liquid nitrogen level about 50—70 mm below its rim.

Discharge-tube filling. The arrangement adopted, shown in Fig. 1, allows the discharge tube B to be filled without the main stock of sample ammonia in tube A coming into direct contact with it, and also without the subsample in the discharge tube B coming into contact with the vacuum gauge C. This facilitates effective 'rinsing' of the apparatus with each sample and thus reduces cross-contamination 'memory' effects. The operational sequence of valve opening and closing is as follows.

(1) Sections S2, S3 and S4 are evacuated, then V_2 and V_3 are closed.

(2) V_1 is opened, then closed, thus filling section S3 with ammonia at the same pressure as the sample stock in tube A.

(3) V_2 is opened, then closed; V_4 is closed and then V_3 opened; the pressure registered on gauge C is noted.

(4) If this pressure is above 1 Torr, V_4 is opened and when sections S3 and S4 have been evacuated, V_3 is closed.

(5) V_2 is opened, then closed, effectively reducing the pressure in the discharge tube B by the volume factor (section S2)/(sections S2 + S3), which is about 2/3.

(6) V_4 is closed, then V_3 opened and the pressure again noted on gauge C.

Steps 4, 5 and 6 are repeated as necessary until the gauge C reading lies in the range 0.5—1 Torr. Readings on the vacuum gauge C are multiplied by the volume factor (sections S3 + S4)/(section S3), which is about 4 with the present apparatus, to determine the pressure in the discharge tube.

Excitation and recording of the N_2 spectrum

A microwave power supply (EMS Microtron Mk 3) operating at 2450 MHz with meter output of 50 W excites the discharge in a tuned 3/4-wave cavity, as used previously for the ammonia—argon discharge tubes [3]. The discharge tube is fixed about 15 cm in front of the entrance slit of a modified spectrometer (Optica CF4, dispersion 1.9 nm mm^{-1}), no condensing lens being required. The coupled entrance and exit slits are set to the smallest width that gives adequate signals when the output photomultiplier (EMI 6256 B) is operated at 1000 V or less (EHT power supply, Brandenberg 475 R). The actual slit widths could not be determined, mainly because of uncertainty in the zero setting of the adjusting mechanism; they were estimated to be about 40 μm. In addition to the maker's wavelength scanning drive (Optica 6-2007), an intermediate gear-train was constructed giving a further speed reduction of 25:1. This permits the wavelength to be scanned at approxi-

mately 0.5, 1 or 2 nm min^{-1}, the intermediate speed normally being used. The photomultiplier output load resistor of 10 MΩ is shunted with a 0.02-μF capacitor, giving an RC value of 0.2 s which enables rapid variations of output signal arising from narrow spectral lines to be traced without significant distortion.

Output signals are fed to a pen recorder (Servoscribe IS RE541.20) via an auto-ranging digital voltmeter (DVM, Datron 1041) fitted with an analogue output. This permits the recorder to be operated on its 2-V range, with the automatic range change of the voltmeter on rising signals coinciding with full deflection of the pen. Two particular advantages of this recording arrangement that reduces tracing 'noise' are that the use of large signals, up to 20 V, from the photomultiplier is made possible by the very high input impedance of the DVM, and that the pen recorder is used on a range that is relatively insensitive to the pick-up of stray signals from other electrical apparatus in the surrounding laboratory.

Isotope ratio measurement

Immediately after the discharge tube has been filled with ammonia (see above), the emission is initiated by an external high-voltage spark (Edwards H.F. Tester T.I.). Within the pressure range and power conditions stated above, a stable discharge readily forms. The spectrum tracing is started after a delay of 90 s, which allows conditions in the tube to stabilize (see 'Stabilization' below). When the appropriate wavelength range has been recorded, generally taking 3—4 min, the discharge tube is evacuated, and refilled with ammonia for a further tracing if required. Three tracings are generally made, but if a mean value for the ^{15}N : ^{14}N ratio with a greater precision is necessary, ten or more replicate fillings and tracings can be made by using the sample stock in tube A. Although tubes filled with ammonia as described are sufficiently stable to run continuously for several hours without attention and with only a slow increase in the intensity of N_2 emission, interfering bands from other molecules steadily increase and can cause errors in the isotope ratio determination. For this reason, replicate measurements are made by refilling the discharge tube from tube A, rather than by repeated tracings from the same filling.

The (2,0) bandhead at 298 nm or the (1,0) bandhead at 316 nm is used depending on the level of ^{15}N being determined. The ^{15}N : ^{14}N ratio is calculated in the normal way from background-corrected measurements of bandhead peak heights on the pen recordings [2]. Background measurements are made at wavelengths just greater than each of the bandheads, since the bands of the Second Positive N_2 system are degraded towards the ultraviolet. Calibration curves are not required.

Spectral emissions other than N_2

Apart from the Second Positive N_2 system, several other emissions from the ammonia-filled discharge tube were identified. They include spectra from NH, CN, OH, H_2, O_2, H and Si. All except CN can arise from dissociation products of ammonia, water and silica. The CN emission was greatly reduced by the use of the liquid-nitrogen trap in the vacuum line. Weak residual CN emission not removed by this trap most likely originates from the organic material of the O-ring seals in the connector used to join the silica discharge tube to bellows valve V_2 (Fig. 1). The NH_2 ammonia α-bands and Schuster's NH_3 bands have not yet been examined in detail. Preliminary investigation of the 475—600 nm region indicates that the many-lined H_2 spectrum is predominant, and that NH_3 and NH_2 bands, if present, are very weak.

NH. The strong triplet system at 336.0 nm is always well developed, the (0,0) and (1,1) heads at 336.0 nm and 337.0 nm respectively being indicated in Fig. 2. The NH (1,1) bandhead at 337.0 nm is not resolved from the strong N_2 (0,0) bandhead at 337.1 nm, nor is the triplet structure resolved in the sequence of apparently single NH bands at 339—342 nm.

OH. Unless the discharge tube is cooled, the 306.4 nm band system occurs strongly, not only the (0,0) bands with heads at 306.4 nm, but also the (1,0) bands with heads at 281—283 nm. The intensity of the OH bands increases quite rapidly in continuously-run, uncooled discharge tubes, and numerous experiments strongly suggest that they are not derived only from traces of water vapour introduced with the sample ammonia. Two likely alternative sources are SiOH groups on the surface of the silica tubing, and the combination of hydrogen, produced by dissociation of ammonia, with oxygen derived from the silica tubing. Cooling the bottom part of the discharge tube to —60°C as described above reduces OH emission to a negligible intensity. This cooling temperature is essential as even at —40°C the saturated vapour pressure of water over ice is nearly 0.1 Torr. The temperature must, however, be kept above —77°C to avoid condensing the sample ammonia in the discharge tube.

H_2. The well-known continuum spectrum of H_2 is strongly developed. The removal of water by cooling the tube has little effect on the intensity of this continuum, indicating that the majority of the hydrogen is derived from the dissociation of ammonia and not of water.

O_2. The spectrum of this molecule was illustrated and discussed by Leicknam et al. [4]. The part of its spectrum that could affect the nitrogen isotope ratio determination when measurements are made on the N_2 (2,0) bandhead is shown in Fig. 3, which was obtained from a discharge tube containing argon at low pressure with impurity traces of oxygen and nitrogen. It is not certain which oxygen system produces these bands, but it is possibly the Second Negative O_2^+. In the cooled ammonia-filled discharge tubes, as

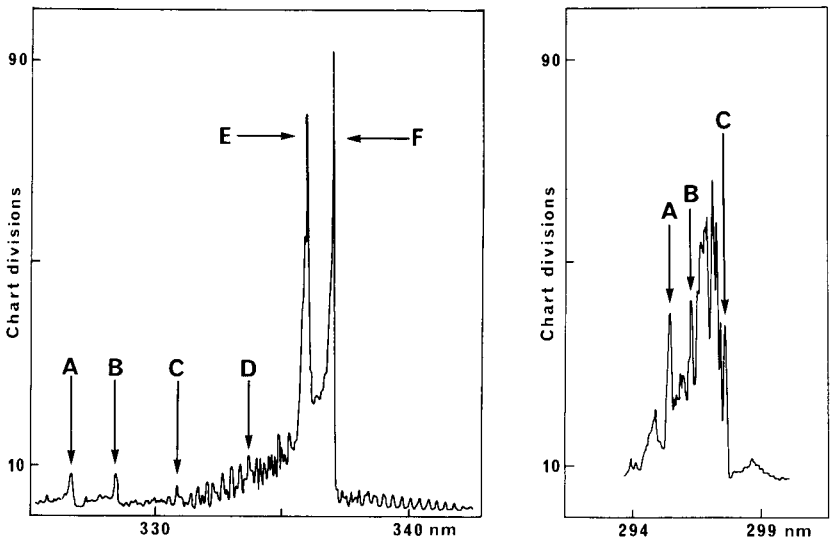

Fig. 2. Emission of NH and overlapping N_2 bands. (A) N_2(4,4) 326.8 nm, (B) N_2 (3,3) 328.5 nm, (C) N_2 (2,2) 330.9 nm, (D) N_2 (1,1) 333.9 nm, (E) NH (0,0) 336.0 nm, (F) NH (1,1) 337.0 nm and N_2 (0,0) 337.1 nm, not resolved.

Fig. 3. Oxygen bands at 295—298 nm underlying the N_2 bands. (A) N_2 (4,2) 295.3 nm, (B) N_2 (3,1) 296.2 nm, (C) unresolved combination of N_2 (2,0) head at 297.7 nm and part of the oxygen system.

used for analysis in this study, they are not observed. When OH bands are present, however, caused for example by inadequate cooling or overheating of the discharge tube by excessive microwave power, these O_2 bands generally appear.

H. The atomic hydrogen spectrum is strongly emitted and contributes to the red colour of the discharge.

Si. The sensitive atomic line at 288.2 nm is not detectable under normal operating conditions; however, if the walls of the discharge tube are raised to red-heat, by raising the microwave source power, this Si line is emitted. It can be readily observed provided that the OH bands with heads at 281—283 nm are efficiently suppressed.

Effect of ammonia pressure and tube cooling on emission

Changes in emission intensity resulting from variations in the initial pressure of ammonia in the discharge tube, as well as from the effect of cooling the lower part of the tube to about −60°C, are shown in Figs. 4 and 5. These summarize intensity measurements on the H_2 continuum at about 300 nm (Fig. 4a); N_2 (2,0) bandheads for the $^{14}N^{14}N$ head at 297.7 nm and $^{15}N^{14}N$ head at 298.3 nm, at about 5 atom-% ^{15}N ammonia (Fig. 4b); the NH (0,0) bandhead at 336.0 nm (Fig. 5a); the OH (0,0) bandheads at about 306.4 nm (Fig 5b); and the H_α 656.28 nm line (Fig. 5c). The signals, apart from the H_2 continuum, were all corrected for underlying background;

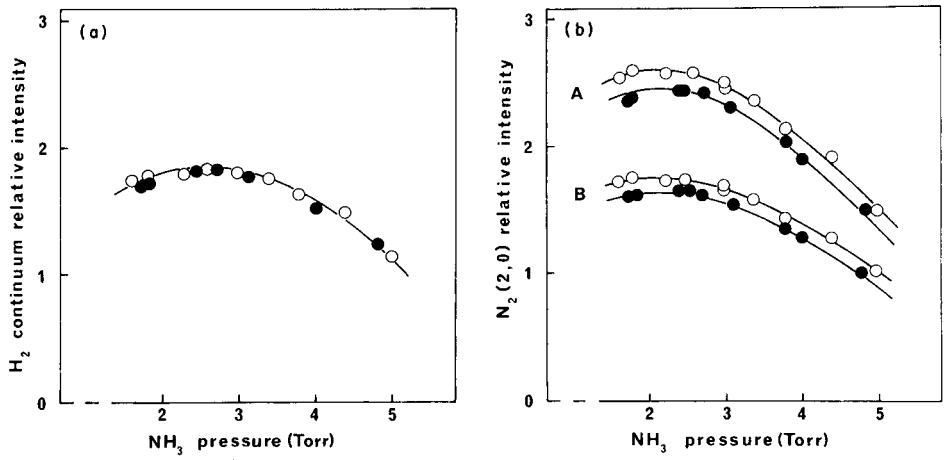

Fig. 4. Effect of initial ammonia pressure in the discharge tube and of cooling one end of the discharge tube to —60°C (a) on the intensity of the H_2 continuum at 300 nm, and (b) on the intensity of N_2 (2,0) heads; (A) $^{14}N^{14}N$, 297.7 nm; (B) $^{15}N^{14}N$, 298.3 nm, using ammonia containing about 5 atom-% ^{15}N. Curves (A) and (B) are based on different intensity scales. (•) Cooled; (○) uncooled.

they were measured about 2—3 min after initiating the discharge. The emission intensities, however, as is well known, are not proportional to the amounts of these molecular species present in the discharge tube.

It is apparent from the Figures that the intensity of the NH (Fig. 5a) and OH (Fig. 5b) emissions both fell rapidly with increasing ammonia pressure. The N_2 emission (Fig. 4b) passed through a maximum at about 2.5 Torr, falling rapidly above that pressure, and the H_α line intensity (Fig. 5c) followed a similar pattern. The H_2 continuum (Fig. 4a) varied least, having a broad maximum around 2—3 Torr and decreasing slowly at higher pressures. It is also clear that cooling the discharge tube greatly reduced the OH intensity, but had a negligible effect on the H_2 continuum or the NH bands, and produced a small reduction in N_2 emission and a moderate reduction in H_α emission.

The similar behaviour of the $^{14}N^{14}N$ and $^{15}N^{14}N$ bandhead intensities (Fig. 4b) demonstrates that the measured ^{15}N : ^{14}N ratio does not vary with pressure or cooling. The ^{15}N contents calculated from the data used for Fig. 4(b), expressed as the mean and standard error of the mean, were 5.34 ± 0.02 and 5.33 ± 0.02 atom-% ^{15}N for the cooled and uncooled exposures, respectively.

Rate of stabilization of the discharge

The way in which emissions from the discharge tube varied during the period immediately following initiation was examined by setting the spectrometer at the required wavelength, and operating the pen-recorder at the fast chart speed of 12 cm min^{-1}. Emissions from the N_2 and NH bands,

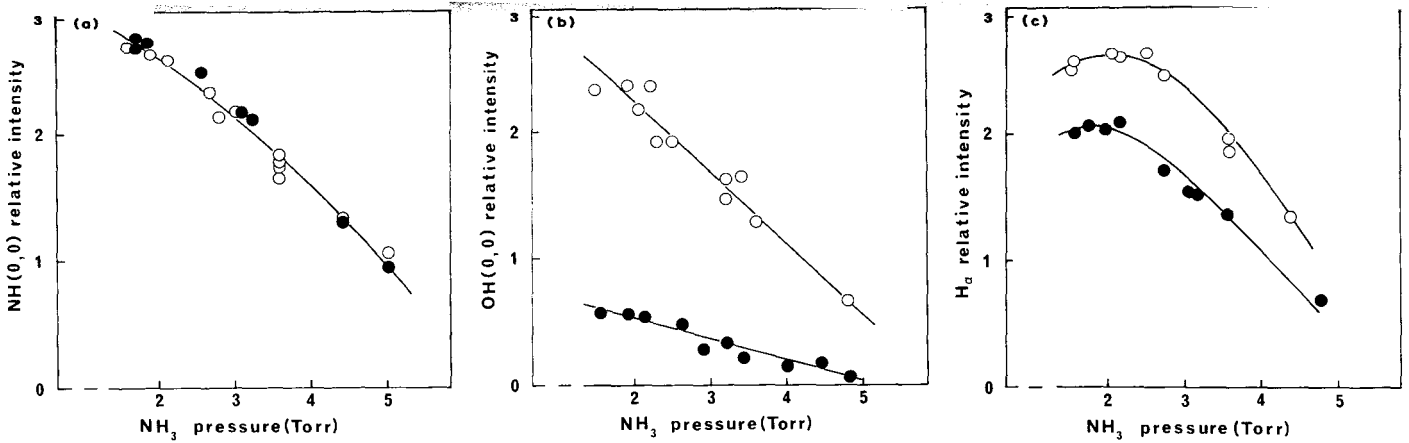

Fig. 5. Effect of initial ammonia pressure in the discharge tube and of cooling one end of the discharge tube to −60°C, on the intensity of (a) the NH (0,0) head at 336.0 nm; (b) the OH (0,0) head at 306.4 nm; and (c) the H_α line at 656.28 nm. (•) Cooled; (○) uncooled.

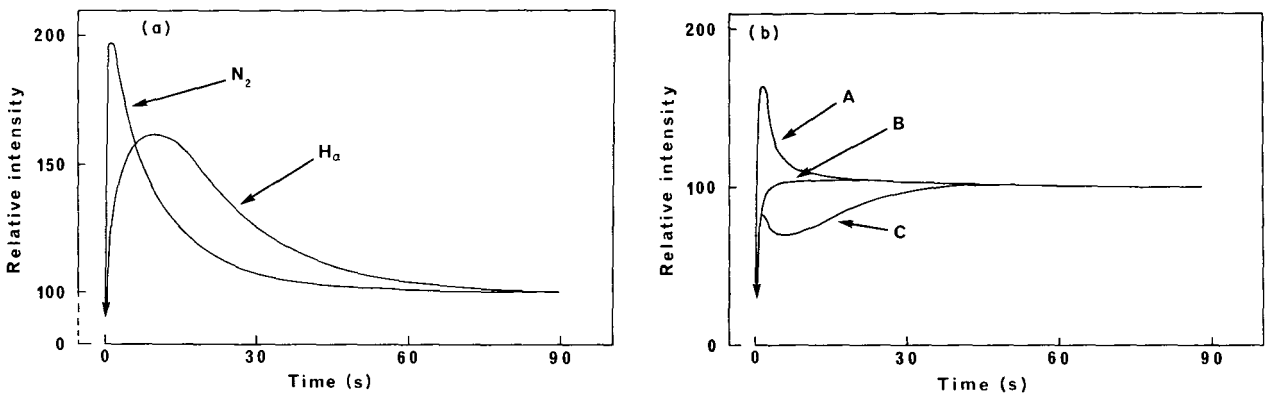

Fig. 6. Intensity changes after initiating the discharge: (a) for the N_2 (2,0) head at 297.7 nm and the H_α line at 656.28 nm, averaged over initial ammonia pressures of 1.5—5 Torr; and (b) for the H_2 continuum at 300 nm, showing the effect of initial ammonia pressures of (A) 1.5 Torr; (B) 1.8 Torr; (C) 3.8 Torr.

H_2 continuum and H_α line were measured over a range of initial ammonia pressures, both with and without cooling. A limited amount of the information obtained is shown, for N_2 bands and the H_α line (Fig. 6a) and for the H_2 continuum (Fig. 6b). The pattern of change for NH was very similar to that for N_2 and is not shown.

Cooling had no effect on the pattern for any of the emissions; pressure variation affected only the H_2 continuum. All the curves in Fig. 6 have been normalized to a steady state intensity value of 100 after 90 s.

A sharp peak for N_2 emission occurred within 2 s of starting the discharge (Fig. 6a), but since the overall response time of the measurement system was of the order of 1 s, the true peak intensity was probably higher and earlier. It is clear that after 1 min the N_2 emission intensity was within 1 % of the steady-state value. In contrast, the H_α atomic hydrogen line took longer to reach its maximum, around 5—10 s, and approached its steady state more slowly.

The H_2 continuum approached its steady state in a way that depended on the initial ammonia pressure (Fig. 6b). At the lowest pressure for which a stable discharge could be operated, around 1.5 Torr, the continuum reached a maximum within 2 s of starting the discharge and then fell, reaching a steady value after about 30 s. In contrast, at 3.8 Torr, which is approaching the highest pressure (5 Torr) for operating a stable discharge, the intensity of the continuum attained 75% of its final value within 1 s, fell slightly and then increased steadily towards its final value, reached after about 30 s. At intermediate pressures near 1.8 Torr, the final steady intensity was reached rapidly, usually within 5—10 s.

When isotope ratios are to be measured, the spectrometer is set to about 300 nm or 318 nm, depending on the bands to be used, before the discharge is initiated, so that observation of the H_2 continuum background intensity displayed on the digital voltmeter can confirm that a steady state exists before the spectrum is recorded. The stabilization period of 90 s used for isotope ratio measurement was based on the information summarised in Fig. 6.

Interfering bands

Typical tracings of the (2,0) bandheads at natural ^{15}N abundance (0.37 atom-%) and when enriched to 5 atom-% are shown in Fig. 7. When intensity measurements are to be made on these bands, the wavelength is scanned from 300—297 nm. The only interferences found to be of any consequence are from oxygen (Fig. 3), which has a band coincident with the $^{14}N^{14}N$ head at 297.7 nm, and a weak, as yet unidentified, band coincident with the $^{15}N^{14}N$ head at 298.3 nm. The even trace of the H_2 continuum from 300—298 nm (Fig. 7a) demonstrates the absence of potentially interfering NO and CO bands; in cooled tubes, OH bands are of negligible intensity (cf. ref. 4).

The oxygen bands are generally too weak to be observed or to affect the

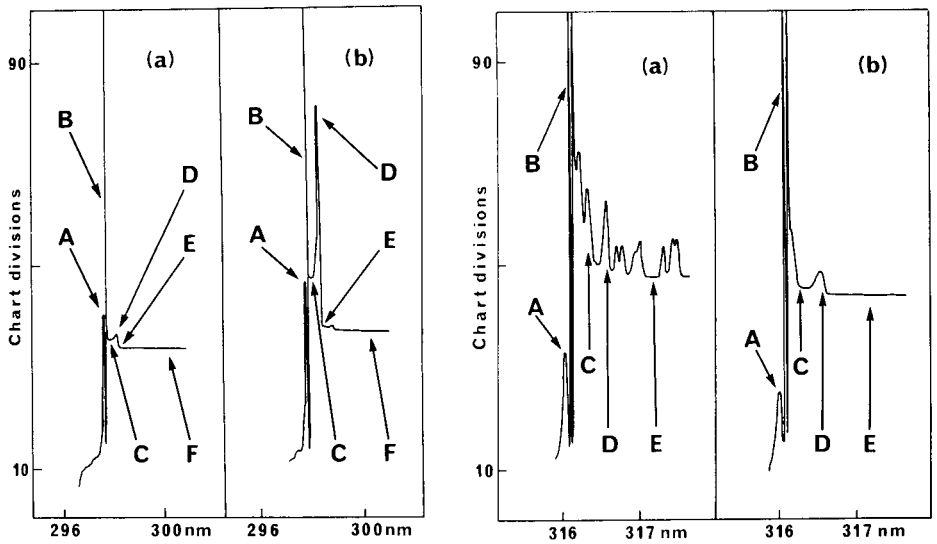

Fig. 7. Typical signal tracings of the N_2 (2,0) head using a cooled tube: (a) natural abundance (0.37 atom-%) of ^{15}N; (b) ^{15}N enriched to 5 atom-%. (A) $^{14}N^{14}N$, 297.7 nm; (B) digital voltmeter autochange X10; (C) background wavelength for $^{14}N^{14}N$; (D) $^{15}N^{14}N$, 298.3 nm; (E) background wavelength for $^{15}N^{14}N$; (F) H_2 continuum.

Fig. 8. Typical signal tracing of the N_2 (1,0) head using highly depleted NH_3 containing 0.01 atom-% ^{15}N: (a) discharge tube not cooled; (b) one end of discharge tube cooled to −60°C. Note the suppression of OH bands. (A) $^{14}N^{14}N$, 315.9 nm; (B) double autochange X 10 X 10; (C) position of $^{15}N^{14}N$, 316.3 nm; (D) position of $^{15}N^{15}N$, 316.6 nm; (E) H_2 continuum.

isotope ratio measurement. Their appearance would indicate an incomplete separation of air from ammonia during sample stock preparation, air leaking into the discharge tube, or the presence of water vapour resulting from inadequate cooling of the discharge tube. The weak unidentified bands at 298.3 nm have a variable strength equivalent to about 0.05—0.10 atom-% ^{15}N. Although their general appearance is very similar to that of the N_2 bands, numerous experiments with highly depleted ammonia containing 0.01 atom-% ^{15}N, and measurements on the (1,0) bandheads (see below) established that they were not residual traces of $^{15}N^{14}N$ in the apparatus. In addition, the use of a different spectrometer (Hilger and Watts E760), as well as the examination of strong, sharp atomic emission lines of Cu and Al, removed the possibility that these weak unidentified bands were a grating 'ghost' image of the much stronger $^{14}N^{14}N$ bands.

Tracings of the (1,0) bandhead using ammonia containing 0.01 atom-% ^{15}N are shown in Fig. 8, which demonstrates the removal of OH emission by cooling the discharge tube. Wavelengths are scanned from 318 to 314 nm when the (1,0) bands are used. One of the OH bands is coincident with the $^{15}N^{14}N$ head at 316.3 nm and without cooling, measurement of the isotope

ratio would be impossible. The efficient suppression of OH emission in the apparatus described here enables ^{15}N contents to be determined down to about 0.04 atom-%, i.e. to well below natural abundance. There is an unidentified bandhead at about 316.6 nm (Fig. 8b), almost coincident with the $^{15}N^{15}N$ head. This unidentified band is not removed by cooling and is also considered not to be a 'ghost' image since it occurred at an identical wavelength when the other spectrometer was used.

RESULTS

^{15}N measurement; range, precision and accuracy

The unidentified band underlying the $^{15}N^{14}N$ (2,0) bandhead at 298.3 nm sets a lower limit for the use of this band to ^{15}N contents of around 0.5 atom-%. Although the background signal from the H_2 continuum is about ten times stronger than the $^{15}N^{14}N$ signal at this ^{15}N content, an accurate correction for it is readily made. There are no interferences at the $^{15}N^{15}N$ bandhead at 298.9 nm, so that the upper limit to the use of the (2,0) bands is determined only by the need to correct the $^{15}N^{14}N$ bandhead for the underlying tail of the $^{15}N^{15}N$ bands. This has been found to be possible up to contents of 90—95 atom-% ^{15}N.

As can be seen from Fig. 8 (b), the lower limit for using the $^{15}N^{14}N$ (1,0) bandhead at 316.3 nm is determined by the height of the smallest peak that can be measured on the pen recordings. This is about 1—2 chart divisions, corresponding to ^{15}N contents of about 0.02—0.04 atom-%. This peak can be used up to around 80 atom-% ^{15}N. The use of the $^{15}N^{15}N$ (1,0) head is limited by the unknown interfering band at 316.6 nm to the range above 10 atom-% and up to about 90—95 atom-% ^{15}N.

The precision with which ^{15}N contents can be determined with the present apparatus is high, being largely dependent on the stability of the microwave power supply and errors in measuring peak positions on the recorder charts. For single determinations, with contents below 2 atom-%, the variance is about 0.01—0.02 atom-%. Above this content, a relative standard deviation of 1% is normally obtained.

The accuracy of this optical emission method, with the ammonia-filled discharge tube, has so far been assessed only by comparing the values obtained for ^{15}N content with those specified by the manufacturer of the salts used (Prochem Ltd.). Typical results are given in Table 1.

To achieve this accuracy, considerable care was taken to ensure that the speed of wavelength scanning and time-constants of the signal measurement equipment enabled spectra to be recorded without distortion. With this auto-ranging digital voltmeter system it was also necessary to ensure that the pen recorder zero and full-scale readings were in agreement with the voltmeter on all its ranges.

TABLE 1

Comparison of measured ^{15}N contents with values specified by the manufacturer of the salts used

Salt	^{15} N atom-%				Bandheads used
	Specified	Measured[a]			
		$\bar{x}$	s.e.m.	N	
NH_4Cl	30.15	30.84	0.07	7	(2,0)
NH_4Cl	5.14	5.24	0.01	9	(2,0)
NH_4Cl	(0.37)[b]	0.377	0.005	10	(1,0)
KNO_3[c]	(0.37)[b]	0.358	0.001	15	(1,0)
	(0.37)[b]	0.360	0.002	10	(1,0)
$(NH_4)_2SO_4$	0.01	<0.02[d]	—	10	(1,0)

[a]Mean ($\bar{x}$), standard error of mean (s.e.m.) and number of replicates (N) analyzed. [b]Assumed content of unenriched 'AnalaR' laboratory sample. [c]Duplicate samples, independently digested and reduced and then converted to $(NH_4)_2SO_4$ by steam distillation into dilute sulphuric acid. [d]All 10 values <0.02, i.e. less than 1 chart division.

Memory effect

The cross-contamination of one sample by residues of the previous sample remaining in the apparatus, i.e., the memory effect, must of course be kept as small as possible. Various experiments had established that in the present work the thermopile gauge-head was potentially the major source of such cross-contamination. The tube-filling procedure was specifically designed to minimise this. In section S1 (Fig. 1), the metal tube and adapter, to which the sample tube A is attached, are exposed for a relatively long period to the full ammonia pressure from each sample. They are also exposed to air while samples are being changed. It is important to note, however, that any memory effect occurring in this section would contaminate the whole of the stock in tube A, and thereby limit the value of 'rinsing' the rest of the apparatus with several subsamples from this stock. Section S3 is exposed to ammonia during the tube filling procedure, when it is briefly connected to sections S1 and S2 in turn, and then to S4 during measurement of the ammonia pressure. Residual ammonia in S3 is therefore not likely to affect the stock in S1, but will affect the subsample in the discharge tube. Although cross-contamination of S3 by S4 can occur while pressure is being measured, the discharge tube cannot be affected.

Since the discharge tube is not changed between samples, any memory effect arising from the tube itself is largely confined to S2, but could have a small effect on S3 and S4 during a sequence of pressure reductions (steps 4, 5 and 6 in the 'Tube-filling procedure', above). After the emission measurements have been completed for each filling of the discharge tube, sections S3 and S4 are evacuated before V_2 is opened. Dissociation products such as N_2, NH and H_2 formed in section S2 during the operation of the dis-

charge may contaminate S3 and S4 while being pumped away. It is less likely that any memory effect from S4 will affect S2 at this stage.

In view of the well-known ability of many materials to adsorb or absorb ammonia, an attempt was made to measure memory effects. The results of three such tests are given in Table 2. In each case, the equipment was thoroughly conditioned by the repeated analysis of the samples with high ^{15}N content before introduction of the two replicate samples with lower ^{15}N content. The memory effect is quantitatively defined as the difference between the measured and nominal ^{15}N contents, expressed as a percentage of the difference between the ^{15}N content of the material used to condition the apparatus and the nominal ^{15}N content of the sample being analyzed. It is apparent from Table 2 that there can be as much as 7% cross-contamination of the first-filled discharge tube, but that this is rapidly reduced to less than 1% in subsequent fillings from the same sample stock. The memory effect on the second and subsequent replicate samples is less than 1% (relative) and is small enough to be analytically acceptable. Test A is nearly the most severe possible, and in practice such an extreme contrast in successive sample contents will seldom occur. The three tests clearly indicate that very little contamination of the sample stock occurs. The values for the second sample in Test A are somewhat enhanced on account of the interfering band, but probably do reveal a slight contamination of the sample stock, of the order of 0.2%. Most of the memory effect is considered to arise within the discharge tube.

DISCUSSION

The earlier work [3] showed that N_2 formed by the dissociation of ammonia within a discharge tube also containing argon had the isotopic composition anticipated from the random recombination of nitrogen atoms. It also showed that the separation of ammonia from air, by condensation at low temperature, could form the basis of a simple analytical procedure. Further investigation subsequently established that discharge tubes containing ammonia without any carrier gas such as argon could also be used to determine the ^{15}N : ^{14}N ratio, and the findings reported above support the conclusion that a practical procedure for this isotope ratio measurement has been devised. Isotopic fractionation during condensation and vaporization of the ammonia samples is considered not to be a significant source of error, in view of the reported vapour pressures and melting points of $^{14}NH_3$ and $^{15}NH_3$ [5].

The pressure range within which a stable discharge can be maintained is quite narrow, from about 1.5—5 Torr with the apparatus used in this work. By increasing the incident microwave power to 150 W, for example, this range can be extended to both higher and lower pressures. This results, however, in localized overheating of the discharge tube, enhances several unwanted background emissions, and has no analytical advantages. Within

TABLE 2

Assessment of memory effect by the analysis of samples with ^{15}N content much lower than the preceding sample

Test[a]	Sample	Subsample[b]	^{15}N content (atom-%)		Memory effect[c] (%)
			Nominal	Measured	
A	1	1	0.01	7.00	7.0
		2		1.67	1.7
		3		0.97	1.0
		7		0.46	<1
	2	1	0.01	0.32	<1
		4		0.23	<1
B	1	1	5.14	6.79	6.6
		2		5.61	1.9
		3		5.39	1.0
		4		5.25	<1
		5		5.30	<1
	2	1	5.14	5.20	<1
		2		5.30	<1
		3		5.21	<1
		7		5.26	<1
C	1	1	0.37	0.65	5.9
		2		0.50	2.8
		3		0.45	1.7
		4		0.43	1.3
		5		0.40	<1
	2	1	0.37	0.37	<1
		2		0.39	<1
		3		0.37	<1
		4		0.38	<1
		5		0.38	<1

[a]Test A: 0.01 following 97 atom-% ^{15}N. Test B: 5.14 following 30.2 atom-% ^{15}N. Test C: 0.37 following 5.14 atom-% ^{15}N. The (2,0) bandheads were used for Tests A and B without correction for the interfering band, equivalent to 0.05—0.10 atom-% ^{15}N; the (1,0) bandheads were used for Test C.
[b]Subsamples were successive fillings of the discharge tube from the same sample stock.
[c]See text.

the stable range, it has been established that the measured isotope ratio does not vary with pressure. There is a practical advantage in using tubes filled at the higher end of the pressure range, especially when the N_2 (1,0) bands are to be used, because OH emission can be more effectively suppressed (Figs. 5b and 8).

The way in which the discharge approaches a steady state is obviously complicated (Fig. 6) and relatively slow. This may well reflect diffusion

processes in the discharge tube since the active discharge zone is only about 50 mm long, i.e. less than one tenth the length of the discharge tube when the metal tubing of S2 (Fig. 1), about 100 mm long, is taken into account. The use of a multi-channel spectrometer might enable the isotope ratio to be measured as soon as the discharge has been initiated, but in the method described here the scanning spectrometer requires the emission intensities to remain constant over the period needed to scan the related bandheads. The present apparatus fulfils this requirement provided that scanning is delayed for about 90 s.

The information presented in Figs. 4—6 does not allow any firm conclusions to be drawn about the way in which pressure or cooling affects the equilibria of the several reactions occurring in the discharge tube. It is of interest to note that the N_2 intensity is reduced by cooling while the NH intensity is not, and that the H_α and OH intensities fall while the H_2 continuum remains unchanged. It is reasonable to assume that the reduction in H_α and OH emissions reflect the active removal of water vapour by condensation as ice on the cold end of the discharge tube.

It has been shown that memory effects occur in the apparatus (Table 2), but that they are small enough to allow the repeated use of a single discharge tube. The procedure for analysing a succession of subsamples from a single ammonia stock not only allows a convenient 'rinsing' of the apparatus, but also readily allows a succession of replicate determinations to be made. The time taken from initially pipetting a sample solution into tube A (Fig. 1) to first filling the discharge tube is about 20 min. A cycle of filling the discharge tube and recording the spectrum takes about 5 min. Thus a typical analysis including 3 replicate determinations takes just over 30 min, and a more precise determination based on 10 replicates can be completed in a little over 1 h. This is much slower than the rate of analysis achieved, for example, by Goulden and Salter [6] with a technique based on a two-channel spectrometer and a continuous flow of helium carrier gas. A relatively slow spectrum-scanning method is almost mandatory if adequate corrections are to be made for background emissions in determinations of ^{15}N contents well below natural abundance.

It is of practical advantage to be able to determine isotope ratios by evaluation without calibration based on reference standards. This prevents systematic errors from contamination passing undetected, but necessitates accurate measurement of intensity ratios. At ^{15}N contents of 0.05 atom-% the ratio between $^{14}N^{14}N$ and $^{15}N^{14}N$ bandhead intensities is about 1000:1 which illustrates the photometric problem involved. Determining the true correction for background emission is probably the most important single factor limiting accuracy in the procedure described here, but the results given in Table 1 indicate that the simple method adopted is satisfactory. There are indications of a slight positive bias and this is still being investigated. The more elaborate procedures for background correction used by other workers [2, 4] are not easy to justify spectrometrically with the equipment used here.

The measurement precision attained with the current equipment is more than adequate for the soil—plant studies, including symbiotic nitrogen fixation, for which it was devised. There are two ways by which it is considered that the analytical precision could be improved, if the need should arise. First, the digital voltmeter is equipped with a BCD output so that signals could be readily stored and evaluated with a microcomputer using procedures such as signal-averaging; secondly, the stability of the microwave power supply could be improved. Two other parameters that may also affect emission stability are the dimensions, particularly the diameter, of the discharge tube and the frequency used to excite the discharge. Some workers have shown that discharge tubes containing nitrogen gas can be more stable at frequencies lower than the 2450 MHz applied here when using a 100-MHz source stabilized by a photo-electric feedback signal from the discharge emission intensity [7]. Local regulations sometimes restrict the use of frequencies within broadcast bands.

The procedure for filling the discharge tube appears to be complicated, but in practice is very simple to operate. It was adopted for two reasons, both associated with the vacuum gauge. First, in the earlier arrangement [3] the gauge head was included in the section containing the discharge; consequently it was exposed to all of the dissociation products for considerable periods. This proved to be the main source of a memory effect, which could only be removed slowly by 'rinsing' with ammonia or by operating a flow-through, argon-only discharge. Secondly, the type of thermopile gauge used has a markedly non-linear scale. It can easily display pressure differences of 1—2 mTorr at pressures below 20 mTorr, making it suitable both for checking for leaks in the vacuum system and for monitoring the removal of air during sample preparation. Above 2 Torr, however, the compressed scale permits only a rough estimate of pressure. Measurement of the optimum ammonia pressure in the discharge tube, around 4—5 Torr, necessitated a pressure reduction technique. The expansion of ammonia from section S3 to the combined sections S3 and S4 (Fig. 1), by a factor of 4, enabled such pressures to be measured on a more suitable part of the gauge scale.

Samples containing either greater or smaller amounts than the preferred 1—2 mg of nitrogen can be analyzed if necessary. The lower limit is set by the need for an initial ammonia pressure of at least about 5 Torr in the preparation tube A, and this can be attained with about 250 μg of nitrogen. This limit could be reduced by the use of a smaller preparation tube. The upper limit is determined only by the practical consideration that the ammonia pressure, during preparation, should not exceed atmospheric pressure, as this could force apart some of the O-ring seals. Some 30 mg of nitrogen can be safely analysed with the equipment in its present form.

In conclusion, two practical comments are made for the benefit of any other workers who might consider constructing similar apparatus. Firstly, bellows valves appear to be essential if atmospheric contamination is to be

avoided. Extensive tests were made with high-quality flow-control valves (Negretti MF Series), but problems associated with the rising-stem design could not be overcome. Secondly, satisfactory joins (Swagelok) between valves and tubing could not be made when stainless-steel ferrules were used, probably because the wall of the stainless-steel tubing tended to deform too easily. Ferrules made from PTFE (Teflon, Swagelok) were instantly successful, although they need occasional tightening as the plastic flows slightly under prolonged compression.

The authors thank the staff of the Institute's Technical Services Department: Mr. J. H. Normington for constructing the gear-box used to reduce the wavelength-scanning speed, and Mr. A. I. A. Wilson for making stainless-steel adapters to fit the sample preparation tubes.

REFERENCES

1 V. Middelboe, Prog. Water Technol., 8 (1977) 447.
2 R. Fiedler and G. Proksch, Anal. Chim. Acta, 78 (1975) 1.
3 J. C. Burridge and I. J. Hewitt, Commun. Soil Sci. Plant Anal., 9 (1978) 865.
4 J. P. Leicknam, V. Middelboe and G. Proksch, Anal. Chim. Acta, 40 (1968) 487.
5 H. G. Thode, J. Am. Chem. Soc., 62 (1940) 581.
6 J. D. S. Goulden and D. N. Salter, Analyst, 104 (1979) 756.
7 M. M. Ferraris and G. Proksch, Anal. Chim. Acta, 59 (1972) 177.

Analytica Chimica Acta, 118 (1980) 29—44
© Elsevier Scientific Publishing Company, Amsterdam — Printed in The Netherlands

A CRITICAL COMPARISON OF STUDIES OF COMPLEX FORMATION BETWEEN COPPER(II) AND FULVIC SUBSTANCES OF NATURAL WATERS

J. BUFFLE

Department of Inorganic and Analytical Chemistry, University of Geneva (Switzerland)

(Received 28th January 1980)

SUMMARY

The results obtained by various authors in discussing complex formation between copper(II) and fulvic substances in natural waters are compared; particular attention is given to results obtained in the natural pH range (6—9). The influence of the experimental conditions used for the complexation measurements is discussed, as well as the hypotheses used in interpretation of the data. The ligand concentration, and the possible formation of mixed complexes and precipitation of copper hydroxide, are considered. When these factors are taken into account, a better agreement may be found between the results of the various workers. Further, the relative importance of the various possible reactions may be defined from such a comparison. As a result, various recommendations are given about the features of the experimental conditions that must be considered to obtain meaningful data on complex formation.

A detailed study of complex formation between copper(II) and fulvic substances, by means of ion-selective electrodes (i.s.e.) has recently been reported [1]. Because of the very complex behaviour of fulvic substances [2] and the fact that these substances are a mixture of unknown compounds [3], the results of such studies should be considered as fully valid only after the influence of the maximum number of physicochemical factors on the complexation model has been tested, and only after it has been shown that the results obtained by the maximum number of methods as well as those published by different workers give similar results. The effects of various factors have already been reported [1]. The aim of the present paper is to compare these results with those given in the literature. It will be shown that, when discrepancies are observed, a detailed comparison may produce valuable supplementary information about the reactivity of copper(II) and fulvic substances in natural waters.

In the subsequent discussion, the data obtained in our earlier study [1] will often be used as reference for the sake of convenience. However, it must be borne in mind that no distinction has been made, a priori, between these results and those of other workers. The comparison will be made mainly with the results of three other teams of workers [4—8] because these are among the few studies that have been devoted to complexation of copper(II)

by the organic matter in natural waters, and also because the experimental conditions used in these works were very different.

FACTORS AFFECTING THE NUMERICAL VALUES OF THE MEASURED PARAMETERS IN COMPLEX FORMATION

Comparison of values of the complexation parameters quoted by various authors is not simple. This is partly because the values of the constants are not always expressed in standard forms but particularly because the constants reported are only conditional constants which depend strongly on the experimental conditions used. These conditions differ from one paper to another and are not always clearly specified. The factors that should be considered when such comparisons are made are as follows.

The nature of the sample. Information about the sample used for complexation measurements should include the source and the sample pretreatment (if any) such as fractionation. In this case the method used for fractionation as well as the characteristic parameters of the fraction used for the complexation study (e.g., % organic matter compared with the original sample, chemical composition, mean molecular weight, etc.) must be known.

Experimental conditions used for complexation measurements. This may be further divided into two types of factors. First, there are conditions which are common to all the methods, such as the pH, concentration of organic matter (g l^{-1}), the ratio of metal to ligand concentrations, duration of the measurements (i.e., time elapsed between the mixing of copper(II) and fulvic solution, and the end of complexation measurements), and the ionic strength. Secondly, there are special conditions that have to be used for the method chosen for complexation measurement. For instance, it may be necessary to consider the reactivity of the metal of interest towards ligands other than fulvic acids, e.g., Tris and OH^- [4]; CO_3^{2-} and OH^- [8]; OH^- [1, 6]. The importance of this factor in the interpretation of the data will be particularly discussed in later sections. Another factor is the possible interaction of the ligands under study with cations other than Cu^{2+} which are present in the medium (e.g., H^+, Ca^{2+}, etc.). Finally, there may be reactions between the ligands or the complexes with the measuring system, e.g., adsorption on the gel [4], ion exchanger [8], manganese dioxide [6], or at the electrode surface [1].

Mode of transformation of the complexation measurements into complexing parameters. In all the methods used for complexation measurements, e.g. i.s.e. [1], retention by gel [4], adsorption on resin [8] or manganese dioxide [6], the degree of complexation of the metal, α_m, is the parameter which is determined experimentally either directly or indirectly. In all cases, certain assumptions must be made in order to calculate the stability constants from α_m and some value of molecular weight of the ligand. This is done in order to try to obtain parameters which are independent of the experimental conditions. In reality, they are only conditional constants valid for a more or less limited range of experimental conditions.

Some of the assumptions made are as follows: (1) formation of CuL and CuL_2 via the reactions $Cu + LH \rightleftharpoons CuL + H^+$ and $Cu + 2LH \rightleftharpoons CuL_2 + 2H^+$, where L is one of the complexing sites of the molecule [9, 10]; (2) formation of 1:1 complexes with the complexing sites of the molecule, taking into account that there may be several sites having different complexing ability [4]; (3) formation of global 1:1 complex [6, 8]; (4) formation of successive CuL_n complexes (without making assumptions on the value of n) by reactions of the type $Cu + LH_x \rightleftharpoons CuL + xH^+$, where the value of x is not assumed and L is one of the complexing sites of the molecule [1].

The role of the assumptions made initially in the development of the final results is illustrated by the fact that the experimental points in Fig. 4 of ref. 4 yield a curve similar to curve 2 of Fig. 4 of ref. 11. A value of 2300 was obtained for M_{eq} by using this curve which is in accordance with the values given in Table 1 [1]. Also $\log \beta_1'$ was found to be equal to 7.3 at pH 8. Owing to the lack of data, $\log \beta_2'$ could not be calculated by the method described earlier [1]. However, considering the similarities in the curve obtained above and that shown in Fig. 4 of ref. 11, it is clear that these data can be interpreted equally well by either way (i.e. 2nd or 4th model mentioned above), but that two different sets of values will be obtained for the complexation parameters.

The molecular weight of the ligand is required for converting the stability constant unit from $l\ g^{-1}$ to $l\ mol^{-1}$ and can be determined by various methods. The molecular weight M_w of the whole molecule can be measured independently of the number of complexing sites on this molecule, e.g. by gel permeation [4]. The equivalent weight, M_{eq}, is defined as the mean weight of the organic compound per complexing site. It may be determined either by a method different from that used for the measurement of α_m [8] or by the same method [1, 6]. Only in particular studies is it possible to compare M_{eq} and M_w [4, 8, 11].

PRACTICAL CONSIDERATIONS FOR COMPARISON

From the foregoing list of factors it seems very difficult to make a rigorous comparison of results described by various authors. However, an attempt has been made to do this on the basis of the following considerations.

Influence of the nature of the samples and of conditions of measurement

Source of sample. It has been shown [1] that for the same type of water samples, the results obtained for complexation parameters are relatively independent of the origin of the samples provided that the same method and hypotheses are used for obtaining the results. This is illustrated, for example, by the fact that waters from Zaïre, France and Switzerland (plain and mountain waters) resembled each other [1]. Similar results have been observed for fulvic substances in soils by, for example, Stevenson [9, 10].

Sample pretreatment. Analogous results were obtained [1] with surface waters and peat water (Nos. 21, 41a, 50a) for the unfractionated samples

(i.e., filtered only through 0.2-μm filters) and the fractionated samples (UM05, PM10, 0.035 and 0.2-μm membranes). Anyway, in the case of surface waters, most of the fulvic-type compounds are in the fraction passing through a PM10 membrane but retained by a UM05 membrane [12] while a significant amount of the "non-humic" organic matter present in the waters, particularly during Spring, is eliminated through UM05.

Effects of metal–ligand ratios, ionic strength and duration of measurement. In most of the published work, the molar ratio of copper to ligand used varies roughly between 0.01 and 1 and the duration of metal–ligand "contact" is a few hours. The ionic strength used is either 0.01 [4, 6, 9] or 0.1 [1, 8, 9, 11] but this factor does not seem to affect strongly the values of the constants [9].

Thus, the factors considered in this section may be neglected in comparisons of the order of magnitude of the constants, especially considering that the statistical errors in the measured constants ($\Delta \log \beta \approx 0.2$ [1]) are relatively large and are of the same order of magnitude as the effects of these factors. This is confirmed by the results reported at the end of the section 'Results of Baccini and Suter [8]'.

Mixed ligand complexes

The influence of mixed ligand complexes in each of the published methods can be estimated by breaking up α_m into three complexing components:

$$\alpha_m = 1 + \delta_L + \delta_{L,A} + \delta_A \qquad (1)$$

where δ_X is defined as $\delta_X = \sum_i [MeX_i]/[Me^{2+}]$, and the subscripts L, A and L,A refer to complexation of the metal with the fulvic ligands under investigation, all the other ligands of the medium, and the mixed ligand complexes, respectively.

The nature of A and the stability constants of the corresponding complexes with the metal are generally known, and therefore δ_A in eqn. (1) can be evaluated. By subtracting this term from α_m, the overall degree of complexation of Me by L can be obtained:

$$\delta_L^T = \delta_L + \delta_{L,A} \qquad (2)$$

Published data for the stability constants of mixed ligand complexes are sparse. However, owing to the complexity of the medium under study, such reactions might play an important role in water chemistry; consequently it is important to get a better insight into the possibility of the formation of such complexes. Literature data [13, 14] on mixed ligand complexes of copper(II) were therefore used to obtain the plot in Fig. 1. It can be seen that, as a first approximation, the logarithm of the overall stability constants ($\beta_{1,1}^{L,A}$) for the mixed ligand complexes of copper(II) with L and A (CuLA), may be obtained simply by adding the individual logarithms of the constants of the 1:1 complexes of the two ligands (β_1^L and β_1^A). This rule will not hold if both ligands are strong chelating agents or if the number of binding sites

exceeds 4, as is the case for mixed ligand complexes with nitrilotriacetic acid and amino acids, and for mixed complexes with EDTA and ethylenediamine, 1,2-diaminopropane or hydrazine. The residual dispersion of points in Fig. 1 is partly due to the fact that values of the three stability constants for the same system are not always available at the same ionic strength and temperature, so that values reported for different conditions have sometimes been plotted in Fig. 1. Figure 1 also shows that mixed complexes of copper(II) with fulvic acids and other organic ligands [15] seem to follow the above rule.

When only 1:1 copper–fulvate complexes and 1:1:1 mixed complexes are formed, one has

$$\delta_L^T = \beta_1^L \frac{[LH_x]}{[H^+]^x} + \beta_{1,1}^{L,A} \frac{[LH_x]}{[H^+]^x}[A] \simeq \beta_1^L \frac{[LH_x]}{[H^+]^x} + \beta_1^L \beta_1^A \frac{[LH_x]}{[H^+]^x}[A]$$

where $[LH_x]$ is the total concentration of the uncomplexed fulvic acid, [A] is the free concentration of A and all the equilibrium constants given are independent of pH. For example, β_1^L is related to the conditional stability constant β_1', valid at a given pH, by $\log \beta_1^L = \log \beta_1' - x.\mathrm{pH}$. Values of x were determined [1] for different water samples by two methods. From the results obtained earlier, the values of x will be taken here as equal to the slope S_α of

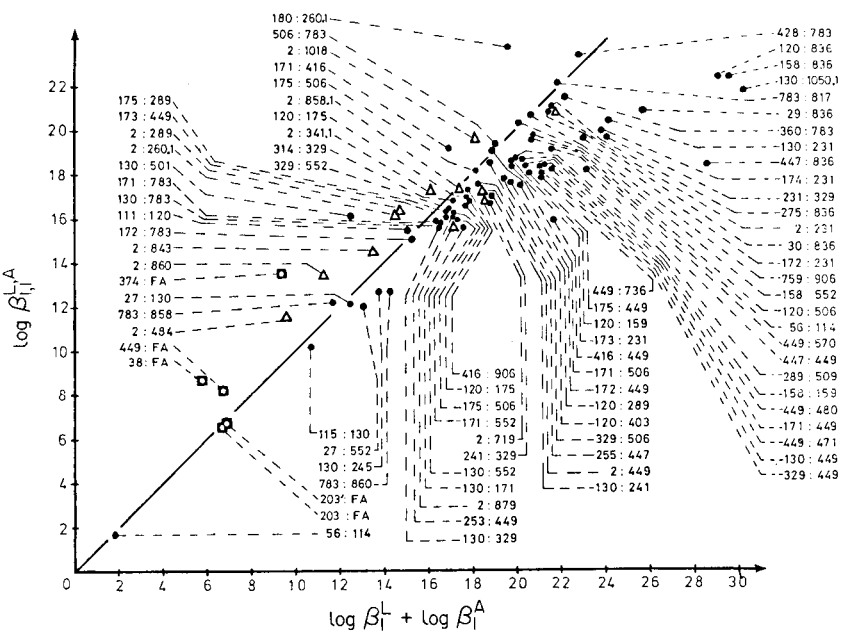

Fig. 1. Relationship between log $\beta_{1,1}^{L,A}$ and log β_1^L + log β_1^A for A—Cu—L complexes. The numbers refer to the nature of the ligands, according to the classification of Sillen and Martell [13]. FA = fulvic acids ligands; (□) mixed ligand complexes with FA; (△) mixed ligand complexes with OH^-; (•) all other mixed ligand complexes. The slope and the intercept of the straight line are equal to 1 and 0, respectively.

the plots $\log(\alpha - 1) = f(\mathrm{pH})$ (see Table 2 of ref. 1). If δ_L^T is then interpreted only in terms of Cu—L complexes with a global apparent constant K, then

$$K = \beta_1^L(1 + \beta_{1,1}^{L,A}[A]/\beta_1^L) \approx \beta_1^L(1 + \beta_1^A[A]) \quad (3)$$

This equation shows that if $\beta_1^A[A] \gg 1$ then important errors may be incurred in the measurement of the complexing ability of L, especially when the value of [A] used in the experimental measurements is considerably different from that present in the natural system of interest.

Influence of total concentration of organic matter

The overall degree of complexation, δ_L^T, is strongly dependent on the total concentration of organic matter $\{L\}_t$ (see Fig. 2 of ref. 1). Thus for comparison purposes, it is necessary to make a distinction between two kinds of experimental conditions: (1) those dealing with $\{L\}_t \leqslant 10$ mg l^{-1} [6, 8] where most probably 1:1 and mixed complexes are formed; and (2) those which deal with $\{L\}_t > 30$ mg l^{-1} [1, 4, 5, 9, 10] where, in addition to the complexes already mentioned, CuL_n may also be formed. In the latter case, the comparison will be made only for the values of $\log \beta_1$ obtained after correction to take into account the possible formation of mixed complexes and CuL_n ($n > 1$) complexes. From the earlier results [1], one may write, at constant pH:

$\delta_L = \beta_1'[L](1 + K_2'^L[L])$. Combination of this equation with the above results gives

$$\delta_L^T = \beta_1'[L] + \beta_1'K_2'^L[L]^2 + \beta_1'\beta_1^A[L][A] \quad (4)$$

If δ_L^T is interpreted only in terms of Cu—L complexes, then the global apparent constant at a given pH K' is given by

$$\log K' = \log(\delta_L^T/[L]) = \log \beta_1' + \log(1 + K_2'^L[L] + \beta_1^A[A]) \quad (5)$$

For correcting K' into β_1', the value of $K_2'^L$ was assumed to be independent of pH in the pH range 4—8. Moreover, it must be noted than higher complex aggregates than the dimer may be formed for $\{L\}_t > 100$ mg l^{-1} [1], so that overestimated corrected values of β_1' will probably be obtained from eqn. (5) in cases where the complexation parameters were measured for $\{L\}_t > 100$ mg l^{-1}.

Minimum value of δ_L^T

In view of the statistical errors in the measurement of α_m and of the error inherent in the computation of δ_A because of the variability in the constants given in the literature, the condition $\delta_L^T \geqslant 0.3 + \delta_A$ or $\alpha_m \geqslant 1.3 + 2\delta_A$ must be fulfilled in order that δ_L^T may be used with some degree of reliability.

In order to prevent the precipitation of CuO(s) the following condition must also be satisfied:

$$[Cu]_t [OH]^2/\alpha_m < K_{so}^{CuO} \quad (6)$$

or

$$\delta_L^T > ([Cu]_t[OH]^2/K_{so}^{CuO}) - (1 + \delta_A) \quad (7)$$

AN ATTEMPT TO COMPARE EARLIER RESULTS

Results of Buffle et al. [1]

Ligand A was mainly hydroxide, and δ_L was computed by subtracting δ_{OH} from the α_m term. Considering condition (7), meaningful complexation data can be obtained only at pH <8 (see Fig. 6 of ref. 1) which is the limit of precipitation of copper(II) oxide.

The main possible source of systematic error in the method used here arises from the assumption that the electrode response is Nernstian in the domain in which α_m is measured. The Nernstian behaviour of the electrode was checked with known ligands in this domain [11] but it might be that this would not be valid with fulvic substances. Another difficulty which may be encountered is the formation of mixed complexes with hydroxide as mentioned above. By using the best value for the constants ($\log \beta_{OH} = 5.52$ and $\log K_e = 13.18$; $\mu = 0.1$, $T = 25°C$ [16, 17]), one obtains $\beta_1^{OH}[OH] \geqslant 0.1$ at pH $\geqslant$ 7.26. Thus eqn. (3) shows that mixed complexes can no longer be neglected above this pH. This might then explain why the slope of the curve $\log \delta_L^T = f(pH)$ is close to 1 in the pH range 7—8 [1]. Indeed this value lies in between that found for the Cu—L complex alone (ca. 0.5) and the value that would be expected for the Cu—L—OH complex alone:

$$Cu + LH_x + H_2O \rightleftharpoons CuLOH + (1 + x)H^+$$

$(1 + x \approx 1.5)$. Combination of $\log \beta_1^L = \log \beta_1' - x.pH$ with eqn. (4) for δ_L^T gives

$$\delta_L^T[H]^x/[L]_t = \beta_1^L(1 + K_2'^L[L]_t) + \beta_{1,1}^{L,OH} K_e/[H^+] \quad (8)$$

Equation (8) is applicable when the total concentration of the uncomplexed ligand, $[LH_x]$, is almost equal to the total concentration $[L]_t$, i.e. $[LH_x] \approx [L]_t \gg [Cu]_t$, which was always the case in the T_H titrations [1]. Furthermore, in eqn. (8), the nature of the CuL_2 complexes is assumed to be $Cu(LLH_x)$ [1]. A typical example of the curves obtained by applying eqn. (8) to the T_H titrations obtained earlier [1] is given in Fig. 2. It can be seen that a reasonable straight line may be found for pH > 6.5. The values of $\log \beta_{1,1}^{L,OH}$ obtained in this way for all the surface waters are given in Table 1. Now, from the considerations for mixed ligand complexes outlined above, one must have

$$\log \beta_{1,1}^{L,OH} \simeq \log \beta_1^L + \log \beta_1^{OH} \quad (9)$$

Log β_1^L was computed for all the surface waters by substituting into the equation $\log \beta_1^L = \log \beta_1' - x.pH$, the values of $\overline{\log \beta_1'}$ (see Table 3 of ref. 1), and those of $x = S_\alpha$ (see Table 2 of ref. 1) obtained in the pH range 3.5—6.0. The values of $\log (\beta_{1,1}^{L,OH}/\beta_1^L)$ obtained in this way are given in Table 1. It can be seen that the mean value (5.6 ± 0.3) is very close to the value of $\log \beta_1^{OH}$ (5.52). This seems to confirm that mixed L—Cu—OH complexes are really

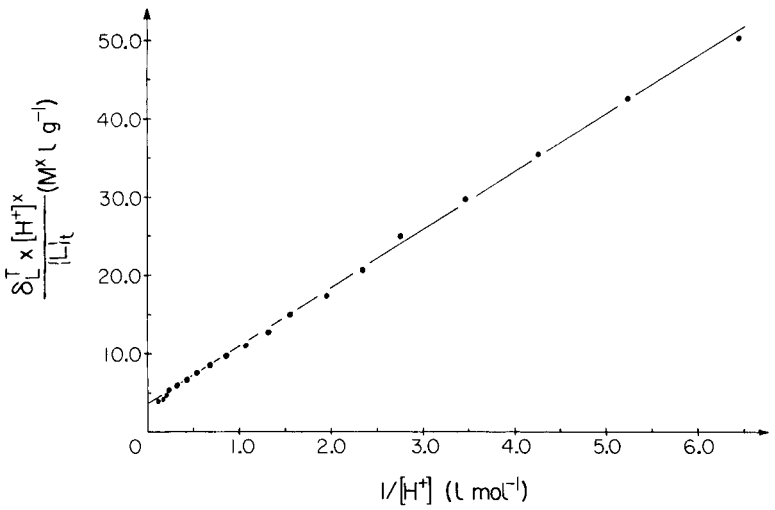

Fig. 2. Relationship between $\delta_L^T[H^+]^x/\{L\}_t$ and $1/[H^+]$ for water sample no. 24. This curve was computed from the T_H titration reported earlier (Figs. 4 and 5 of ref. 1).

formed, although it must be remembered that the curves $\log \delta_L^T = f(\mathrm{pH})$ may be also explained [1] by the formation of L—Cu–L complexes according to the reaction $Cu + 2LH_x \rightleftharpoons L\text{–}Cu\text{—}L + 2xH^+$. Figure 3 shows a typical change of $\log \beta_1'$ with pH, obtained by applying eqn. (5) to the T_H titrations [1].

Results of Mantoura and co-workers [4, 5]

In these papers the formation of CuL_n ($n > 1$) was not considered in spite of the high value of $\{L\}_t$ (ca. 270 mg l^{-1}) used for the measurements. Because of this high concentration, eqn. (5) is not rigorously applicable as CuL_n ($n \geqslant 2$) complexes might be formed. However, the ratio $[Cu]_t/[L]_t$ was varied greatly and it can reasonably be assumed that 1:1 complexes are the most important Cu–L complexes when this ratio is close to 1.0 or larger

TABLE 1

Values of $\log \beta_{1,1}^{L,OH}$ and $\log (\beta_{1,1}^{L,OH}/\beta_1^L)$, obtained from T_H titrations and eqn. (6), for surface water samples
(For the nature of the samples, see ref. [1].)

Sample no.	Nature of the sample	$\log \beta_{1,1}^{L,OH}$	$\log(\beta_{1,1}^{L,OH}/\beta_1^L)$
21	S_i	6.9	5.7
22	S_i	7.6	5.5
11	S_r	7.9	5.5
10	S_m	6.9	5.3
50a (2)	S_m	8.1	5.9
24	S_m—T	7.6	5.8

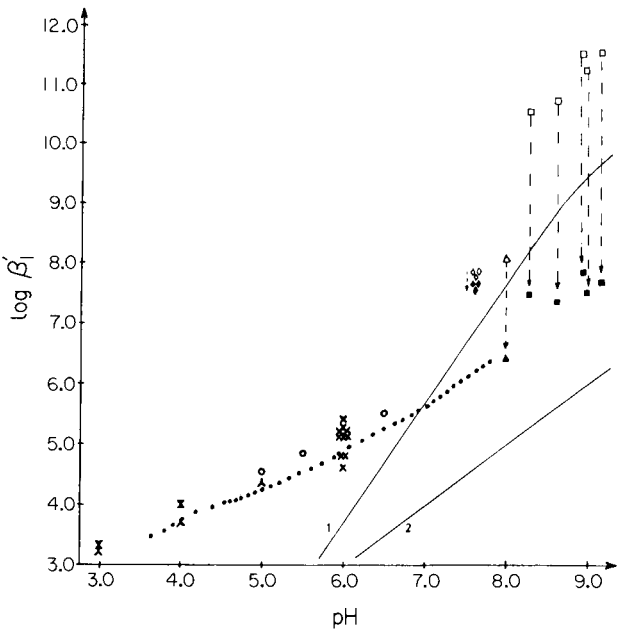

Fig. 3. Relationship between log β_1' and pH. (•) Values obtained by correcting the results of T_H titration of water sample no. 24 for CuL_n ($n > 1$) and OH—Cu—L complexes; (×) values of log β_1' at pH 6 obtained earlier [1] by T_{Cu} and T_L titrations for a series of fulvic substances in fresh waters; (○) values of log β_1' obtained earlier [1] at various pH for water sample no. 50a; (◇, △, □) values reported in refs. 6, 4 and 8, respectively (the values reported by Baccini and Suter [8] have been lowered by a factor 0.39 for the reasons discussed above); (♦, ▲, ■) values reported in refs. 6, 4 and 8, respectively, after correction for CuL_n ($n > 1$) and mixed ligand complexes. Curves 1 and 2 show the change of log β_1' with pH for complexes of Cu(II) with catechol and salicylic acid, respectively.

than this value. Under these conditions, the constant reported for lake water was log $K = 8.05$ at pH 8.0.

Under the conditions used, mixed ligand complexes with fulvic substances and Tris might also be formed. Therefore, β_1' may be computed from eqn. (3) applied at pH 8.0

$$K'/\beta_1' = 1 + \beta_1^{Tris}[Tris]_t/\alpha_H^T + \beta_1^{OH}[OH] \quad (10)$$

where $\alpha_H^T = 1 + \beta_H^{Tris}[H^+] = 2.15$ ($\mu = 0.01$, $T = 20°C$).

According to the above discussion of the results of Buffle et al. [1], the use of the constant β_1^{OH} for estimation of the mixed complexes with hydroxide ions seems to be a good approximation. From the prior discussion of mixed ligand complexes, the complexation term corresponding to the mixed complexes with Tris may be slightly overestimated because of the chelating or bulky nature of the fulvic and Tris ligands. However, values of the stability constants of Tris—copper(II) complexes are available only at higher ionic strength and temperature ($\mu = 0.1$, $T = 25°C$ [16]; $\mu = 0.5$, $T = 25°C$ [18])

than those used by Riley et al. (μ = 0.01, T = 20°C). Hence the available constants are presumably underestimated, so that the two above effects compensate each other at least partly. By using the best values of $\log \beta_1^{OH}$ (5.92 at μ = 0.01) and $\log \beta_1^{Tris}$ (3.98 at μ = 0.1), one has $\beta_1^{OH}[OH] = 1.05$ and $\beta_1^{Tris}[Tris]_t/\alpha_H^T = 44.4$, so that $\log(K'/\beta_1') = 1.67$. Accordingly, this factor might explain to a large extent the difference between the values of the stability constants reported by Riley et al. and those observed by Buffle et al. [1] (Fig. 3).

Although it is difficult, from the available data, to assess the relative importance of the two factors discussed above, it is clear that they both have to be considered in interpreting the data. A third factor which should be considered is the possible formation of CuO(s). Indeed by substituting the values of $\alpha_m = 1 + \delta_L^T + \delta_{OH} + \delta_{Tris} = 10^{5.06}$ and $K_{so}^{CuO} = 10^{-20.0}$ (μ = 0.01, T = 25°C) in eqn. (6), the concentration at which precipitation occurs can be evaluated: it was found to be 7.3×10^{-4} M. This is lower than the maximum concentration ($[Cu]_t = 1.5 \times 10^{-3}$) used by Mantoura and Riley [4]. It must be noted, however, that this effect would affect only the last points of the titration curve and would not modify fundamentally the results obtained.

Results of Schnitzer and Hansen [19] and Cheam and Gamble [20]

Figure 3 also shows values of $\log \beta_1'$ obtained in acidic medium for a soil fulvic fraction. The values plotted in Fig. 3 were chosen because, from the results, it was possible to ascertain with a relatively good degree of confidence that the measured stability constant corresponded to 1:1 Cu—fulvic acid complexes. Moreover, in the conditions used in these papers no corrections for mixed ligand complexes are required. It can be seen that these values agree well with the results of Buffle et al. [1], which is a further indication that the complexing properties of fulvic substances in fresh water and soil are similar [1].

Results of Baccini and Suter [8]

In this case, the precipitates which might be formed are CuO(s), $CuCO_3$(s), $Cu_2(OH)_2CO_3$(s) or $Cu_3(OH)_2(CO_3)_2$(s). By using the best values for the logarithm of the solubility products of these compounds at μ = 0.1 and T = 25°C (−19.64, −8.65, −32.07, −43.26, respectively [16, 17]) as well as the best values for the carbonato complexes ($\log \beta_1^C = 5.76$ and $\log \beta_2^C = 8.92$ for $CuCO_3$ and $Cu(CO_3)_2$, respectively [16, 17]), and the hydroxo complexes of copper(II) [1: section 'results for pH > 6'] and the best values for the acid—base constants of the carbonate system ($\log \beta_1^H = 10.0$, $\log \beta_2^H = 16.25$), calculation showed that none of these precipitates can be formed under the experimental conditions used.

There is, however, a problem with regard to selection of the value of the logarithmic stability constant for the Cu—NTA complex which is required for computing the fulvic—copper(II) complexes. A value of 12.2 was used

[8] for the conditional stability constant of this complex at pH 8.8, while the compilation of Smith and Martell [16] indicates that 12.03 would be more appropriate. Furthermore, no correction was made for Na—NTA complexes [16]. If this is also done, then, globally, the value of the apparent stability constant of the Cu--NTA complex is decreased by a factor of 0.39; this in turn lowers the value of the stability constant, K', found for the Cu(II)—fulvic acid complex by the same value. Although this effect is not sufficient to explain the difference between the larger values obtained by Baccini and Suter [8] compared to those obtained by Mantoura and Riley [4] and Buffle et al. [1], it exemplifies the order of magnitude of the systematic errors which may appear in measurements of complex formation based on competition between ligands.

One important factor in considering these results is the possible formation of mixed complexes with carbonate. When the CuLOH and CuL_2 complexes are also taken into account, the global stability constant becomes

$$K' = \beta_1' + K_2'^{L}\beta_1'[L]_t + (\beta_{1,1}^{L,OH})[OH] + (\beta_{1,1}^{L,CO_3})\,[CO_3]_t/\alpha_H^C$$

or, in view of eqn. (3),

$$\beta_1' = K'/(1 + K_2'^{L}[L]_t + \beta_1^{OH}[OH] + \beta_1^{C}[CO_3]_t/\alpha_H^C) \qquad (11)$$

where $\alpha_H^C = 1 + \beta_1^H[H] + \beta_2^H[H]^2$. By using the mean value of $K_2'^{L}$ obtained earlier [1], it can be shown that the first three terms in parentheses are negligible compared with the fourth. By using the values of log K' and of $[CO_3]_t$ given by Baccini and Suter [8], the corresponding values of log β_1' may be computed. Figure 3 shows that these values are much closer to the mean curve, log $\beta_1' = f$(pH), obtained for pH < 7, than the values of log K'.

It does therefore seem possible that L—Cu—CO_3 complexes could form under the conditions reported by Baccini and Suter [8] and this would explain at least partly the difference observed in the values of the constants reported [1, 8]. The mean value of d(log K')/d(pH) ≈ 1.5 observed by Baccini and Suter [8] seems also to be in accordance with the formation of mixed ligand complexes. Indeed, if the main complex formed under these conditions is L—Cu—CO_3, then

$$Cu^{2+} + LH_x + HCO_3^- \rightleftharpoons L\text{—}Cu\text{—}CO_3 + (1 + x)H^+ \qquad (12)$$

As x was observed [1] to be 0.53, the above value for the change in log K' is consistent with the existence of reaction (12).

Finally in order to check the influence of the method used on the values obtained for the complexation parameters, two water samples (Lake Bret (I) and Lake Alpnach (II), Switzerland) were studied by the procedures described by Buffle et al. [1] (method A) and by Baccini and Suter [8] (method B). For both samples, the values of the complexing parameters were found to be very similar to those reported by Buffle et al. [1] when measured by method A, but very similar to those reported by Baccini and Suter [8] when measured by method B. Furthermore, for sample II, the complexation parameters

measured according to method A were not strongly dependent on the pretreatment (either method A or B) used for concentrating the organic matter. These results show clearly that the differences reported for the values of the parameters are due to the method used for measuring them and to the way of interpreting the data, and not to the nature and pretreatment of the sample.

Results of Van den Berg and Kramer [6]

One important problem in interpreting these data is related to the hydrolysis of copper(II). α_m values were corrected for the $CuOH^+$ complex. The other hydroxo complexes were neglected but this omission is not important because δ_{OH} is small (see Fig. 6 of ref. 1). However, the possible formation of CuO(s) was also neglected. From $K_{so}^{CuO} = 10^{-20.0}$ with the experimental conditions used ($[MnO_2] = 10^{-4}$ M; 10^{-6} M $\leqslant [Cu]_t \leqslant 2 \times 10^{-5}$ M) and substituting in eqn. (1) of ref. 6, the values of log β and Γ_{max} given in Fig. 1 of ref. 6, the pH at which precipitation would occur in the absence of complexation can be computed. This was found to be pH $\geqslant$ 7.8. As these precipitates may be colloidal in nature, they can pass through a 0.45-μm membrane and in such a case it would be difficult to distinguish between precipitation and true complexation reaction. Hence the values given in Table 2 of ref. 6 for lake waters above pH 7.8 will not be used for comparison. Moreover, in these cases, in view of the very low values obtained for the complexing capacities there is uncertainty regarding the nature of the complexing agent.

Because of these effects, only those samples given in Table 2 of ref. 6 having sufficiently low pH (pH $\leqslant$7.6) and sufficiently large complexing capacities ($\{L\}_t > 2$ mg l^{-1}) will be considered for comparison purposes. The formation of mixed complexes with hydroxide may be computed in these cases, from eqn. (3). In view of the condition $\beta_{1,1}^{L,OH}/\beta_1^L \approx \beta_1^{OH}$ (see above), the result is log $(K'/\beta_1') = 0.15$.

Figure 3 shows that the values of log β_1' obtained in this case are higher than all other stability constants corrected for CuL_n ($n > 1$) complexes or mixed ligand complexes. It must be mentioned, however, that a problem which is not discussed by Van der Berg and Kramer [6] is the probable interaction between organic matter and manganese dioxide. Such interactions could involve adsorption of the fulvic compounds or their copper(II) complexes on manganese dioxide. In addition, a modification of the structure of the manganese dioxide particles in the presence of some organic samples was mentioned by these authors [7]; this could lead to passage of some MnO_2 particles, with their possible adsorbed copper(II), through the 0.45-μm filters. These results were obtained at very low concentrations of complexing agent; under such conditions some reactions may take place which do not occur at the higher concentrations used by other workers [1, 4, 5, 8]. These results are interesting in this respect, but the exact role of the above-mentioned secondary reactions needs to be checked before a more detailed interpretation is possible.

CONCLUSION

This comparative study of complexing parameters has brought out three important features. Firstly, the complexation depends on the concentration of fulvic compounds in a non-linear manner, so that the complexation data for concentrated solutions cannot be extrapolated to obtain information for dilute solutions by simply using an arbitrarily defined stability constant for a 1:1 complex.

Secondly, for interpretation of complexation data under natural water conditions ($7 < pH < 8$, $\{L\}_t < 10$ mg l^{-1}), the possible formation of precipitates of the hydrolysed metal must be taken into account. This precipitate may or may not be bound to the ligand under study. The contribution of this factor would be negligible if the experiments were carried out under real "natural" conditions as far as total metal concentration is concerned, i.e. $[Cu]_t < 10^{-7}$ M. At the present time, however, such low concentrations can be used in complexation studies only with voltammetric techniques, and these techniques are affected by adsorption processes [2, 21]. This study therefore emphasizes the desirability of developing methods of speciation and new techniques which would enable lower concentrations of ligand and metal to be examined without the need to introduce chemical reagents liable to produce ill-controlled secondary reactions.

Thirdly, for the interpretation of the complexation in natural systems, a detailed knowledge of the possible formation of "classical" mixed ligand complexes of copper(II) with L, OH^-, CO_3^{2-} and any other important ligand in natural waters is of prime importance, as was shown in several cases in this paper. Although the data available about the formation of mixed complexes of elements other than copper(II) are very sparse, Fig. 4 shows that an order of magnitude for the stability constants of mixed complexes of nickel(II) may be assessed in a similar way to those for copper(II); and this might be also valid for Cd^{2+}, Zn^{2+} and Co^{2+} (Fig. 4). Such relationships may be useful as a basis for more detailed studies of mixed complexes of heavy metals in natural waters. It must also be mentioned that, although only 1:1:1 (Me—L_1—L_2) mixed ligand complexes are discussed here because of lack of other data, other mixed complexes might be formed and should be taken into account, e.g., $CuL(OH)_2$ at relatively high pH values.

In view of the normal concentration of organic matter in natural waters, it is likely that only one ligand L is bound to copper in these conditions, so that β_1' is the important parameter that should be known, e.g., for speciation computations. Figure 3 shows that, depending on whether or not the measured constant is corrected for the possible formation of CuL_n ($n > 1$) complexes, or of mixed complexes, two different trends are observed at $pH > 6.5$ for the change of this constant with pH. For uncorrected values, there is an abrupt increase in the slope $d(\log K')/d(pH)$ at $pH > 7.0$, whereas the increase, if any, is much smaller with corrected values. This behaviour seems to be more likely for ligands having mainly carboxylic and phenolic complexing groups.

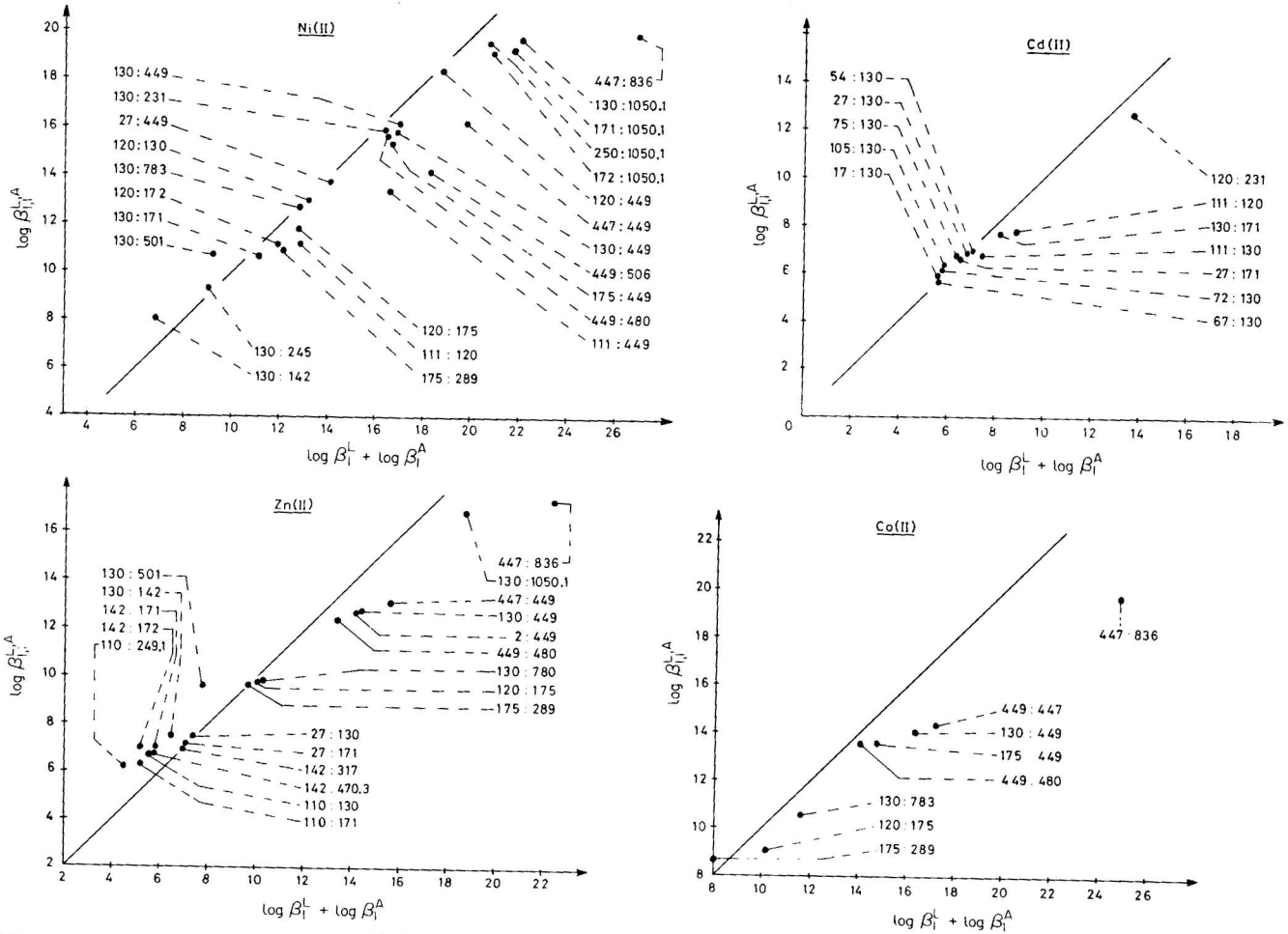

Fig. 4. Relationships between log $\beta_{1,1}^{L,A}$ and log β_1^L + log β_1^A for A—Me—L complexes, Me being Ni(II), Zn(II), Cd(II) and Co(II)). The numbers refer to the nature of the ligands according to the classification of Sillen and Martell [13]. The slopes and the intercepts of the straight lines are equal to 1 and 0, respectively.

However, as fulvic acids are a mixture of compounds, the nature of the complexing molecule might be different in acidic and alkaline medium. Curve 2 of Fig. 3 shows that the complexing ability of the salicylic acid group alone is never sufficient to explain the complexing properties of fulvic acids; in contrast, curve 1 for catechol shows that *o*-dihydroxy groups might play an important role at pH >7. However, the analysis of fulvic substances from fresh waters [3] shows that a very large proportion of the complexing groups of fulvic acids comprises carboxylic and phenolic groups, and that most of the oxygen atoms are included in —COOH groups (ca. 60%) rather than in phenolic groups (ca. 15%). In view of these figures, it is not very likely that the whole complexing capacity could be due only to *o*-dihydroxy groups at pH >7, at least when the conditions of the method used for the determination of $\log \beta_1'$ are such that the ligand is not in large excess compared to the metal. In the cases where a large excess is present, then it is necessary to consider the possible complexation of copper(II) by a minor component of the fulvic acid mixtures having stronger complexation properties than the "mean" components. For example, this could be an explanation for the high values of $\log K'$ found by Baccini and Suter [8].

At the present time, it is not possible to specify the exact role of the various factors discussed above. However, this work emphasizes that more data are needed on the complexing properties of fulvic acids at pH >7.0 and that a rigorous interpretation of these data must take into account the possible association of fulvic acids and the formation of CuL_n complexes and mixed ligand complexes.

This work was supported by the Swiss National Foundation (project 2.050-078). The author is very grateful to C. M. G. Van den Berg and P. Baccini for communication of their results before their publication, and to P. Baccini for having measured the complexation parameters of sample I (Lake Bret) by method B and for valuable discussions.

REFERENCES

1 J. Buffle, P. Deladoey, F. L. Greter and W. Haerdi, Anal. Chim. Acta, 116 (1980) 255.
2 J. Buffle and F. L. Greter, J. Electroanal. Chem., 101 (1979) 231.
3 M. Schnitzer and S. U. Kahn, Humic Substances in the Environment, M. Dekker, New York, 1972.
4 R. F. C. Mantoura and J. P. Riley, Anal. Chim. Acta, 78 (1975) 193.
5 R. F. C. Mantoura, A. Dickson and J. P. Riley, Estuarine Coastal Mar. Sci., 6 (1978) 387.
6 C. M. G. Van den Berg and J. R. Kramer, Anal. Chim. Acta, 106 (1979) 113.
7 C. M. G. Van den Berg and J. R. Kramer, in E. A. Jenne (Ed.), Chemical Modeling in Aqueous Systems, ACS Symposium Series 93 (1979).
8 P. Baccini and U. Suter, Schweiz. Z. Hydrol., 41(2) (1979) in press.
9 F. J. Stevenson, Soil Sci., 123 (1977) 10.
10 F. J. Stevenson, Soil Sci. Soc. Am. J., 40 (1976) 665.
11 J. Buffle, F. L. Greter and W. Haerdi, Anal. Chem., 49 (1977) 216.
12 J. Buffle, P. Deladoey and W. Haerdi, Anal. Chim. Acta, 101 (1978) 339.

13 L. G. Sillén and A. E. Martell, Stability Constants of Metal-Ion Complexes, Spec. Publ. No. 17, The Chemical Society, 1964, and Spec. Publ. No. 25, The Chemical Society, 1971.
14 H. Siegel (Ed.), Metal Ions in Biological Systems, Vol. 2, M. Dekker, New York, 1973.
15 P. G. Manning and S. Ramamoorthy, J. Inorg. Nucl. Chem., 35 (1973) 1577.
16 R. M. Smith and A. E. Martell, Critical Stability Constants, Vols. 2 and 4, Plenum Press, New York, 1976.
17 C. F. Baes and R. E. Messmer, The Hydrolysis of Cations, J. Wiley, New York, 1976.
18 D. P. Hanlon, D. S. Watt and E. W. Westhead, Anal. Biochem., 16 (1966) 225.
19 M. Schnitzer and E. H. Hansen, Soil Sci., 109 (1970) 333.
20 V. Cheam and D. S. Gamble, Can. J. Soil Sci., 54 (1974) 413.
21 F. L. Greter, J. Buffle and W. Haerdi, J. Electroanal. Chem., 101 (1979) 211.

Analytica Chimica Acta, 118 (1980) 45—52
© Elsevier Scientific Publishing Company, Amsterdam — Printed in The Netherlands

MINIATURIZATION IN ANALYTICAL CHEMISTRY—A COMBINATION OF FLOW INJECTION ANALYSIS AND ION-SENSITIVE FIELD EFFECT TRANSISTORS FOR DETERMINATION OF pH, AND POTASSIUM AND CALCIUM IONS

A. U. RAMSING*, J. JANATA**, J. RŮŽIČKA and M. LEVY**

Chemistry Department A, The Technical University of Denmark, Building 207, DK-2800 Lyngby (Denmark)

(Received 20th March 1980)

SUMMARY

The combination of flow injection analysis and ion-sensitive field effect transistors is described for determinations of pH, potassium and calcium ions. The reference electrode is placed in the bypass of the sample injector, thereby avoiding the detrimental effect of serum proteins on the liquid junction potential for the reference electrode. The reagent consumption is halved compared to the use of the conventional electrodes without adversely affecting the sampling rate and the standard deviation of the measurement. An attractive feature of this combination is the possibility of multi-ion analysis.

The applicability of ion-sensitive electrodes (ISE) as detectors in flow injection analysis (f.i.a.) has been demonstrated [1—4]. Although the feasibility of that combination has been proven, it has become apparent that f.i.a. would benefit from miniaturization of the electrochemical sensor. Recently developed ion-sensitive field effective transistors (ISFET's) [5] offer such a possibility, namely improved signal-to-noise ratio, speed of response and reduced detector dispersion.

The purpose of the work which is reported in this paper has been to explore the benefits which would be obtained by combining f.i.a. and ISFET's sensitive to pH, and potassium and calcium ions.

EXPERIMENTAL

Instrumentation and electrodes

The preparation of ISFET's, sensitive to hydrogen, potassium and calcium ions has been described [6]. The transistor chip was mounted on the outer wall of 3-mm o.d. glass tube. The 5 connecting wires were pulled through the tubing and terminated on a prefabricated edge connector. Apart from this change, the materials and procedures used for encapsulation were the same

**Permanent address: Department of Bioengineering, University of Utah, Salt Lake City, Utah 84112, U.S.A.

as described previously [6]. The calcium-selective membrane was prepared as described by Růžička et al. [7].

The f.i.a. system used has been described [1, 3] except for the mounting of the electrodes, which was different from the previous descriptions. The ISFET (glued to the glass tubing) was mounted in a holder. The plastic tube outlet was fixed over the gates of the ISFET at an angle of 45° (Fig. 1, inset a) as close to the gates as possible without touching the gate or the membrane, so that the fluid from the outlet covered the gates completely without

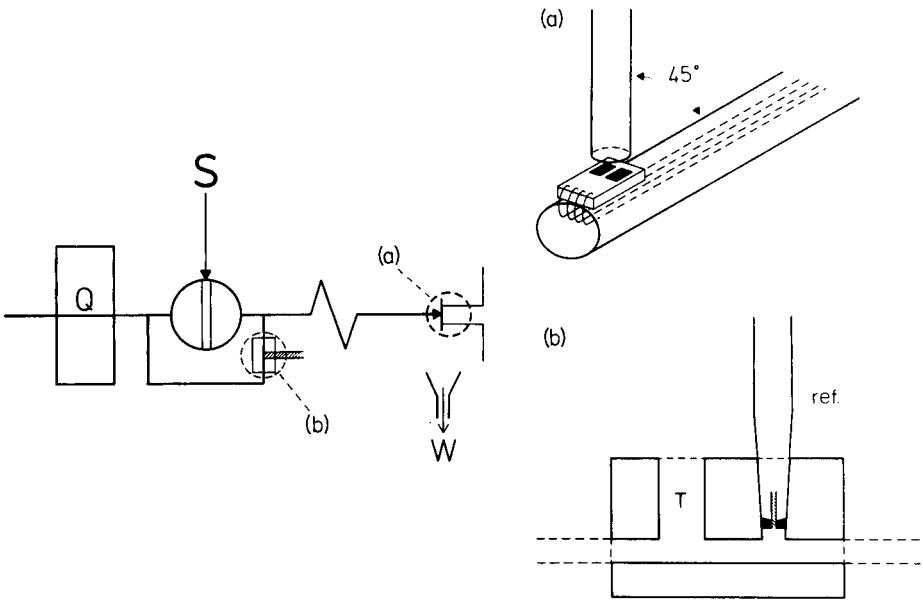

Fig. 1. Manifold for the determination of pH, and K^+ and Ca^{2+} ions. The sample (volume 30 μl) was injected (S) into a carrier stream having a composition of 25 mM Tris buffer in 0.14 M NaCl, adjusted to pH 7.4. All tubes were 0.5-mm i.d. The length between the point of injection (S) and the ISFET was 7 cm. The pumping rate was 0.70 ml min^{-1} (Q), and the residence time was 3.5 s. The plastic tube was mounted at an angle of 45° to the glass tubing to which the ISFET was glued (see inset a). After the fluid had passed the gates, it dripped down a funnel and was pumped to waste (W). The reference electrode was placed in the by-pass (see inset b).

Inset (a) shows the ISFET glued to the outer wall of a 3-mm o.d. glass tube with the connecting wires (only 4 of which are shown) pulled through the tubing to an edge connector. The gates (the black squares) were used directly (as bare gates) for pH measurements and were covered with an ion-selective membrane for the K^+ and the Ca^{2+} measurements. In the case of the dual sensor, one of the gates was a bare gate (pH) and the other gate was covered with an ion-selective membrane (K^+ and Ca^{2+}).

Inset (b) shows the perspex block used to fix the Ag/AgCl reference electrode in the bypass. The carrier solution flowed horizontally, while the reference electrode was placed vertically. Upstream from the bore for the reference electrode, the other bore (T) acted as a trap for air bubbles (if any), as bubbles might otherwise block the connection between the reference electrode and the ISFET.

danger of the membrane being lifted from the chip by contact with the plastic tube. After passing the gates, the fluid dripped from the ISFET down a funnel (Fig. 1) and was pumped to waste.

The reference electrode was placed in the bypass of the injection unit (Fig. 1, inset b) instead of the usual mounting in an electrode vessel together with the ion-selective electrode [1]. This was done in order to avoid changes in the reference electrode junction potential, when samples of a matrix different from the carrier solution were accumulated in the electrode vessel described earlier (e.g., serum samples, samples with proteins, etc.) [1]. Here the reference electrode was exposed to the pure carrier solution all the time, thereby preventing clogging of the asbestos-fibre junction.

The reference electrode used in this arrangement was an Ag/AgCl electrode. This Ag/AgCl (saturated KCl) reference electrode was made by sealing a strand of asbestos fiber in a disposable Pasteur pipette. The tip of the electrode was 1.3 mm wide. When potassium ions were determined, the inner solution of the reference electrode was replaced by 4 M sodium chloride.

The peristaltic pump was a Gilson Minipuls 2 (4 channels), and the recorder was a 4-channel Multirecorder (Type MC 642 4B, Watanabe Instruments Corp.), only two channels of which were used in this work.

The pH measurements (in adjusting the pH in the solutions) were done with a Beckman Expandometric IV pH meter in connection with an Altex pH electrode (Beckman Instruments) and a saturated calomel electrode (Electrode K401, Radiometer, Copenhagen, Denmark).

Chemicals

Deionized water was used throughout and all chemicals were of analytical-reagent grade. The pH was kept constant in the pH standards by addition of morpholinopropanesulfonic acid (MOPS; no. 475898, Ultrol, Calbiochem). Egg albumin was added to some of the standards to investigate the influence of proteins and viscosity on the signal. The egg albumin (ovalbumin; grade II, no. A5253, Sigma Chemical Company) was first dialyzed four times against physiological saline to exchange the potassium ions for sodium ions. The egg albumin (5%) was added to the standards and the viscosity of the samples was thus adjusted to 1.4 centipoise. The composition of the carrier solution was 25 mM Tris buffer in 0.14 M NaCl, adjusted to pH 7.4.

RESULTS

Combination of f.i.a. and ISFET

To investigate the combination of ISFET and f.i.a., the manifold shown in Fig. 1 was used to monitor hydrogen, potassium and calcium ions. The tube was mounted over the gates in an angle of 45° between the plastic tubing and the glass tubing, where the ISFET was mounted (Fig. 1, inset a). Parallel mounting and perpendicular mounting were also tried. With the parallel mounting, the signal was smaller (thicker diffusion layer) and in certain

cases, double peaks were observed, probably because the epoxy encapsulation, forming a small "well" at the gates, acted as a barrier, preventing a smooth wash of the sensitive surface. The perpendicular mounting resulted in a slower sampling rate, because the wash-out from the "well" at the gates was insufficient. The 45° mounting gave a large signal (diffusion layer minimized), and the rinsing of the gates was fast, thereby giving a sampling rate of 120—150 samples per hour with a pumping rate of 0.70 ml min^{-1}.

The magnitude of the signal was also dependent on the flow rate (Fig. 2). On increasing the flow rate, the diffusion layer decreased, thereby increasing the mass transport to the electrode surface. At high flow rates, however, the sample was flushed out before the maximum sample concentration reached the electrode surface, and the signal decreased slightly.

As the response time of the electrode depends, among other things, on the surface area [8], one may expect that the response time for the ISFET (because of its very small area) would be faster than that of the conventional ISE. This is indeed the case, especially for the pH sensor (Fig. 3), where the peak width for the pH signal is very narrow. The pH sensor is a bare gate sensor, utilizing the solid-state Si_3N_4 gate insulator as a pH membrane [6], whereas the potassium ion sensor has a membrane cast over the gate and so has a larger surface and greater resistance (and a type of memory effect), which indeed results in a longer response time for this sensor than for the pH gate sensor.

The influence of proteins on the sensor response was investigated by adding 5% egg albumin (dialyzed against physiological saline) to the standards.

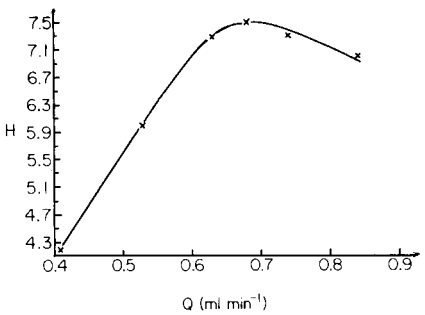

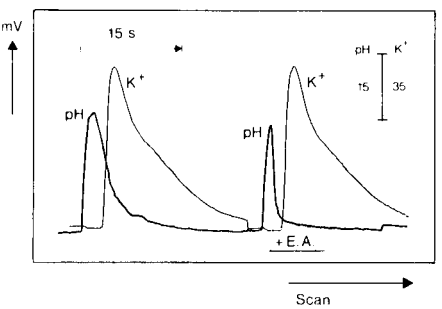

Fig. 2. The dependence of the signal on the flow rate for a K^+ sensor. The manifold shown in Fig. 1 was used, and Q was varied from 0.40 ml min^{-1} to 1.0 ml min^{-1}. The peak height (in inches, 1 in. corresponds to about 4 mV) is plotted.

Fig. 3. The shapes of the signals obtained for the dual ISFET sensor with a bare gate (pH) and a membrane gate (K^+). On the left, the curves for aqueous standards are shown; on the right, the recording shows the influence of 5% egg albumin added to the standards. The injected samples contained 1 mM K^+ in 0.14 M NaCl and were adjusted to pH 6.5. The differences in the positions of the rising edges of the recorded curves for pH and K^+ are due to the distance between the pens on the two-channel recorder. The manifold shown in Fig. 1 was used with a carrier consisting of 25 mM Tris buffer in 0.14 M NaCl adjusted to pH 7.4.

A comparison of the signals recorded for the pH and potassium sensors is shown in Fig. 3; the aqueous sample contained 1 mM KCl in 0.14 M NaCl at pH 6.5 (left-hand curves) whereas the protein solution also contained 5% egg albumin (right-hand curves). Interestingly, the response curve of the potassium sensor remains unaffected by albumin, whereas the response of the pH sensor is changed in a peculiar way. The surprising point is that the shape of the leading edges of the response curves of the pH sensor in the absence or presence of albumin are identical up to 90% of the peak height. Also the peak recorded in the presence of albumin has only half the width of the peak recorded in the absence of albumin (measured at 0.61 peak height). It is even more remarkable that the wash-out is faster in the presence of albumin (i.e. the tailing is less severe) than when an aqueous solution is injected. This is due to less tailing of a more viscous sample zone.

In the absence of a reference method, it is difficult to decide which of the processes (i.e. sample material transport to the electrode, sample zone dispersion, washing of the electrode surface or speed of the electrode response) causes these differences in the response of the pH sensor. It is likely, however, that the difference is mainly due to a combination of electrode geometry and the speed of electrode response. The rapidly responding gate of the pH sensor is situated in a well created by epoxy encapsulation, into which the more viscous solution penetrates only partially during the short sampling period. In contrast, the potassium sensor responds slowly, as the gate is covered by a relatively thick PVC membrane which fills the gate and in fact protruded a little over its edges, thus allowing a smoother flow over its sensing surface. Thus the combination of a better liquid contact and a slower sensor response provides a beneficial compensating effect. It should be noted, however, that in practice, the differences in response in the presence and absence of proteins would not play any role, because the f.i.a.—ISFET system — like any other automated instrument used in clinical measurements — will be calibrated with standards of known pK and pH values having a typical protein content and viscosity quite close to those of the unknown samples to be assayed.

A calibration recording obtained for 5×10^{-4}—10^{-2} M calcium chloride solutions at a sampling rate of 115 samples per hour is shown in Fig. 4. The carrier solution was 25 mM Tris buffer in 0.14 M NaCl at pH 7.4. The slope of the calibration plot was 25 mV/pCa, the relative standard deviation was less than 1%, and the calibration graph was linear over the range specified with a regression coefficient of 0.9998.

Figure 5 is the recording of the simultaneous determination of pH and K^+ using the ISFET as dual sensor. One of the gates on the ISFET was covered with a K^+-selective membrane, whereas the other gate was bare (sensitive to pH). The samples contained 1, 2, 4, 6, 8 and 10 mM potassium ion at pH 6.0, 6.5, 7.0, 7.5, 8.0 and 6.0, respectively, in 0.1 M MOPS—0.14 M NaCl. The slopes of the calibration plots for the pH sensor and the K^+ sensor were 35 mV/pH and 54 mV/pK, respectively. The relative standard deviation

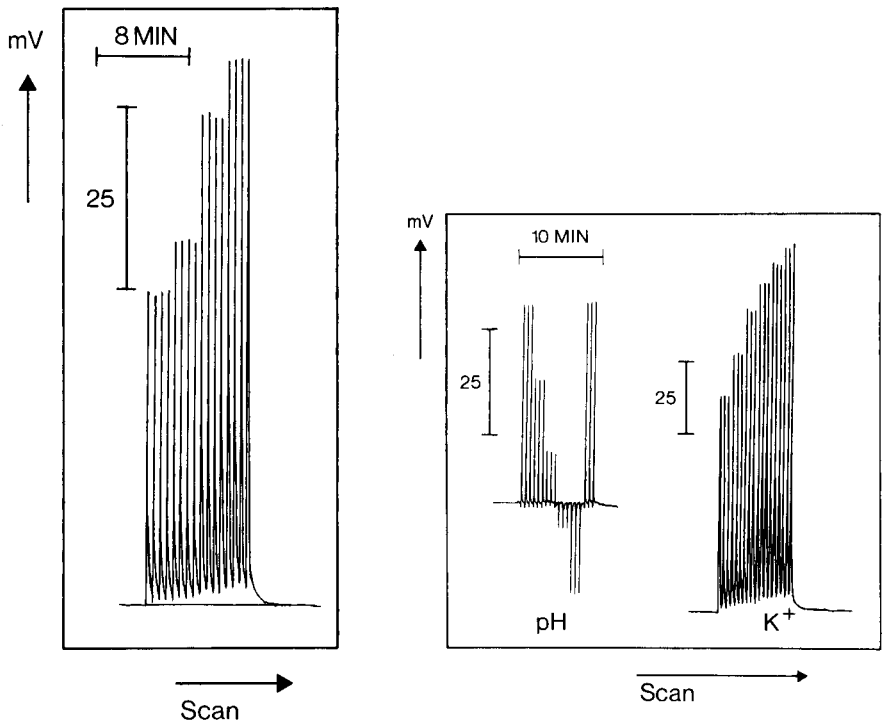

Fig. 4. Response curves for the calcium sensor. From left to right a series of calcium standards (5×10^{-4} M, 10^{-3} M, 5×10^{-3} M and 10^{-2} M $CaCl_2$). in 0.14 M NaCl was injected in quadruplicate. The carrier was 25 mM Tris buffer in 0.14 M NaCl adjusted to pH 7.4. Sample volume, 30 µl; pumping rate, 0.70 ml min^{-1}; sampling rate, 115 samples per hour.

Fig. 5. Calibration recording for the pH/K^+ dual sensor. From left to right the samples, injected in triplicate, were pH/K^+: 6.0/1 mM; 6.5/2 mM; 7.0/4 mM; 7.5/6 mM; 8.0/8.0 mM and 6.0/10.0 mM, all in 0.1 M morpholinopropanesulfonic acid and 0.14 M NaCl. The carrier was 25 mM Tris buffer in 0.14 M NaCl adjusted to pH 7.4. Flow rate, 0.70 ml min^{-1}; sample volume, 30 µl; sampling rate, 125 samples per hour.

was less than 1% for both standard curves. Both the calibration plots were linear with a regression coefficient of 0.9994 for pH and 0.9996 for K^+. The carrier solution was 25 mM Tris buffer in 0.14 M NaCl, and pH was adjusted to 7.4.

Because the reference electrode is placed in the bypass, the baseline signal changes by approximately 1 mV each time the injection valve is turned. This is due to the change in the flow rate of the carrier solution which passes the reference electrode. Thereby, both the liquid junction potential, and the baseline are changed; this effect can be observed as small negative peaks on the recording of pH (Fig. 5). These negative peaks do not disturb the measurement, as the same change occurs every time the valve is turned; the shift of the baseline is easily reproducible, and the peak height can be measured reliably.

DISCUSSION AND CONCLUSIONS

It is evident from this study that ISFET's and f.i.a. are compatible. The small size of the sample (30 μl) is matched by the small sensing area of the ISFET (0.008 mm^2). The dispersion [9] of the sample zone is greater with a conventional ISE than with an ISFET, as the sample is diluted over a larger surface of the electrode. The use of the ISFET's in combination with f.i.a. makes it possible to minimize dispersion in the detector because the surface area of the gates is smaller than the cross-section of the area of the fluid coming from the tube. Accordingly, an ISFET is a better tool than a normal ISE for investigating dispersion. It should be emphasized, however, that the dispersion measured by these electrochemical sensors (both ISE and ISFET) cannot be compared directly with the dispersion values obtained with colorimetric detectors [10], which are not affected by diffusion to the sensing surface.

The electrochemical sensors sense through a surface, and the signal therefore depends on the flow rate at the sensor surface, because the thickness of the diffusion layer depends on the flow rate. Therefore ISFET's would seem to be ideal tools for investigating dispersion in electro-analytical applications, because the contribution of the detector to the total dispersion can be neglected compared to that from other electrochemical sensors.

The experiments with the dual sensor (Fig. 5) indicate the most attractive feature of the f.i.a.-ISFET combination: multi-ion analysis. It is customary to place hundreds of transistors on a chip of the size used in the present study. Simultaneous multi-ion analysis is then only a matter of depositing various ion-selective membranes on the transistor gates. Although a two-ion combination has been tried [1], it is difficult to imagine a multi-ion potentiometric detector based on conventional ISE's, because of the relative bulkiness of the system for each individual sensor and because the detector dispersion is increased considerably with each additional ISE. This is avoided with the ISFET's, because all the sensors are placed on the same chip.

The multi-ion possibility immediately suggests the most attractive application, i.e. the analysis of biological fluids such as serum. In order to avoid the detrimental effect of serum proteins on the liquid junction on the reference electrode [1], this electrode was placed in the bypass loop of the sampling valve (Fig. 1). This arrangement represents an almost ideal situation in that the liquid junction is exposed to a solution of constant composition thus avoiding the effects of changing matrix from sample to calibration solutions. This arrangement was found to function even with a conventional ISE, but was less satisfactory because of the accumulation of effluent on the sensing electrode surface. With the ISFET, the need for the "washing" solution [1] which was essential when the reference electrode was placed in the effluent reservoir has been eliminated. Preliminary analyses of human serum for potassium ion gave encouraging results.

Summing up, the use of ISFET's with f.i.a. has the advantages that the response time for the electrochemical sensor is very short, and that the experimental arrangement is much smaller than is required by conventional ISE's. Because of the simpler set-up, it is easier to control the flow over the sensor surface, i.e. to obtain optimum rinsing of the electrode surface. This has reduced the necessary amount of carrier to half the amount used for conventional ISE without affecting the sampling rate. The sampling rate is 120—150 samples per hour with a relative standard deviation less than 1%. A really attractive feature of this combination is the possibility of multi-ion analysis with a single transistor in the f.i.a. system.

This work was partly supported from NIGMS grant, number 22952 and by a travel grant from Pernovo, Sweden.

REFERENCES

1 E. H. Hansen, J. Růžička and A. K. Ghose, Anal. Chim. Acta, 100 (1978) 151.
2 H. Bergamin F°, B. F. Reis and E. A. Zagatto, Anal. Chim. Acta, 97 (1978) 427.
3 E. H. Hansen, A. K. Ghose and J. Růžička, Analyst, 102 (1977) 705.
4 E. H. Hansen, F. J. Krug, A. K. Ghose and J. Růžička, Analyst, 102 (1977) 714.
5 J. Janata and R. J. Huber, Ion Select. Elect. Rev., 1 (1979) 31.
6 P. T. McBride, J. Janata, P. A. Comte, S. D. Moss and C. C. Johnson, Anal. Chim. Acta, 101 (1978) 239.
7 J. Růžička, E. H. Hansen and J. C. Tjell, Anal. Chim. Acta, 47 (1969) 475.
8 E. Lindner, K. Tóth and E. Pungor, Anal. Chem., 48 (1976) 1071.
9 J. Růžička and E. H. Hansen, Anal. Chim. Acta, 99 (1978) 37.
10 A. Ramsing, M. Sc. thesis, Technical University of Denmark, 1978.

Analytica Chimica Acta, 118 (1980) 53—64
© Elsevier Scientific Publishing Company, Amsterdam — Printed in The Netherlands

REDUCTIVE POTENTIOMETRIC STRIPPING ANALYSIS

JOAN KAI CHRISTENSEN and LARS KRYGER*

Department of Chemistry, Aarhus University, DK-8000 Aarhus C (Denmark)

(Received 21st January 1980)

SUMMARY

The feasibility of determining trace elements by anodic preconcentration and subsequent reductive potentiometric stripping analysis is demonstrated. The determination of manganese is chosen as an example. The interferences of various anodic films formed on the platinum working electrode are discussed. Certain interferences may be minimized by a careful choice of electrolysis potential and pH. The technique is suitable for the determination of manganese in the $\mu g\ l^{-1}$ range. The accuracy of the technique, tested on standard biological materials, is satisfactory.

Potentiometric stripping analysis (p.s.a.) [1, 2] is a new electrochemical approach to the determination of trace elements in solution. Like voltammetric stripping analysis, p.s.a. is characterized by high sensitivity, and the resolution compares well with that of differential pulse anodic stripping voltammetry [3]. P.s.a. requires only very simple equipment [2], although the introduction of a digital computer for data acquisition, signal averaging and background correction improves the performance of the technique [3, 4]. So far p.s.a. has been applied to the determination of metals which can be preconcentrated either as dilute amalgams in a mercury film electrode (Zn, Cd, Pb, Cu, Bi, Tl) or be directly cathodically deposited on glassy carbon electrodes or gold-film electrodes (Hg, As) [5, 6]. In these p.s.a. applications the preconcentrated analytes are stripped from the working electrode by some oxidizing agent in the test solution.

There are, however, cases where trace elements cannot be cathodically deposited, either because of low solubility in mercury or because of very cathodic half-wave potentials for reduction. Such elements may sometimes be preconcentrated anodically and determined by cathodic stripping voltammetry [7]. Moreover, in favourable cases, interference problems may be solved by going from anodic to cathodic stripping analysis. This paper deals with the analogous extension of p.s.a.: the analyte is preconcentrated by anodic oxidation, and the subsequent redissolution is achieved by a suitable reducing agent in the test solution. The paper is focused on the determination of manganese with hydroquinone as reducing agent, but the principles outlined are thought to be applicable to the determination of other elements.

THEORY

Manganese(II) can be anodically preconcentrated on various solid electrodes as (hydrated) manganese dioxide [8] through the overall process:

$Mn^{2+} + 2H_2O \rightleftharpoons MnO_2(s) + 4H^+ + 2e^-$ (E^0 = 1230 mV vs. SHE)

The oxidation can go further to soluble permanganate

$Mn^{2+} + 4H_2O \rightleftharpoons MnO_4^- + 8H^+ + 5e^-$ (E^0 = 1491 mV vs. SHE)

Similarly, lead(II) may be anodically deposited [9] and may interfere with the determination of manganese, since

$Pb^{2+} + 2H_2O \rightleftharpoons PbO_2(s) + 4H^+ + 2e^-$ (E^0 = 1455 mV vs. SHE)

Through most of this study hydroquinone was employed as the reducing agent. Hydroquinone can be anodically oxidized to form quinone

$C_6H_4(OH)_2 \rightleftharpoons C_6H_4O_2 + 2H^+ + 2e^-$ (E^0 = 700 mV vs. SHE)

Although hydroquinone is a weak acid, this is of no importance for the pH range used here (4.5—7.6).

The working electrodes were made from platinum and glassy carbon. During anodic preconcentration of trace elements, these electrodes are likely to react with the supporting electrolyte and films of platinum/carbon oxides/halides can be formed. The formation and stripping of such films depends on the electrolysis potential, the sample pH and on the history of the electrode.

EXPERIMENTAL

Instruments

For pre-electrolysis in conventional p.s.a., a laboratory-built potentiostat was employed, and the potential vs. time curves were recorded with a Radiometer PHM64 research pH meter and a Philips PM8132 $X_tY_1Y_2$ recorder. Most experiments, however, were done with the computerized instrument reported previously [3]. In these experiments the potential distributions rather than the potential vs. time curves were recorded during the stripping step [4].

Differential pulse voltammograms were recorded on a Metrohm-Herisau E506 Polarecord.

Electrochemical cell, electrodes and glassware

The electrochemical cell was a Metrohm EA876-20 cell, the temperature of which could be controlled by a Heto 08C-623 thermostat. The platinum electrodes used as the indicator and counter electrodes were made from platinum wires (1 mm thick, 5 mm long) sealed in glass tubes. The glassy carbon indicator electrode was made from Ringsdorff Glassartiger Kohle glued into glass tubing. Prior to use, this electrode was polished with diamond

paste (down to 0.25 μm). A Radiometer K401 saturated calomel electrode was used as the reference electrode. The cell could be stirred by means of a PTFE-coated magnetic bar. All glassware was thoroughly cleaned with nitric acid (1 + 1) before use.

Prior to analysis and to the addition of reducing agent, the sample solution was deaerated with argon passed through active charcoal. During analysis argon, which because of its high density is better suited than nitrogen, was passed over the sample.

Chemicals and biological standards

The nitric acid and sodium acetate employed were of Suprapur (Merck) grade; all other chemicals were of analytical grade. Manganese(II) and lead(II) stock solutions contained 0.01 M manganese(II) sulphate and 0.01 M lead(II) nitrate, respectively. Triply distilled water was used throughout the study. NBS standards 1571, 1577 (orchard leaves, bovine liver) were obtained from National Bureau of Standards, Washington, D.C. The standard kale was obtained from Dr. H. J. M. Bowen, University of Reading, U.K. [10].

Multichannel recording of potentiograms

In stripping potentiometry, the analytical signal for the stripping of a component is proportional to the time required to redissolve that component. As each component can be characterized by a potential interval where the component is redissolved, the natural mode of acquisition of a stripping potentiogram in a computerized approach is to record the time spent at any potential interval rather than to record the potential readings at equal time intervals [3, 4]. This mode of data acquisition is implemented by using a fast clock-pulse generator in conjunction with an A/D converter: a word in the computer memory is assigned to any potential interval. Whenever a clock pulse occurs, the potential of the electrochemical cell is recorded and the corresponding word in the computer memory is incremented, in the same manner as if a multichannel analyzer for monitoring the distribution of radiation energy was used. The result of this procedure can be seen from Fig. 1(B). A conventional stripping curve like Fig. 1(A) is readily obtained from 1(B) by integration of the number of clock pulses.

RESULTS AND DISCUSSION

The feasibility of obtaining a reductive potentiometric stripping signal of manganese deposited as manganese dioxide is demonstrated in Fig. 1. A stirred solution of 5×10^{-4} M hydroquinone in 0.1 M sodium acetate (50 ml; pH adjusted to 6.5 and thermostated at 50°C) was electrolysed for 5 min with a platinum indicator electrode at +600 mV vs. SCE. The potential versus time behaviour of the electrode was then recorded by using the simple (voltmeter) approach (curve a); in a subsequent experiment the potential distribution was obtained by the multichannel potentiometric approach (curve c). Then 4×10^{-6} M manganese(II) was added and the procedures

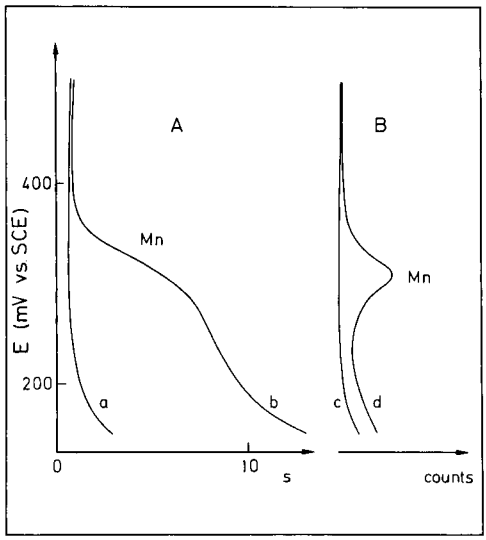

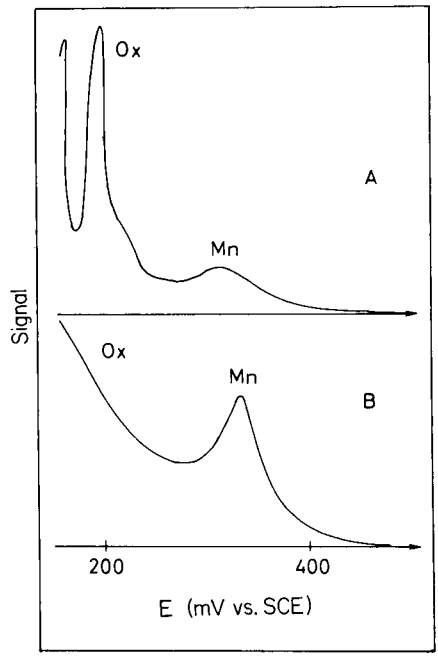

Fig. 1. Reductive potentiometric stripping potentiograms at a platinum electrode of 4×10^{-6} M manganese(II), 5×10^{-4} M hydroquinone in 0.1 M acetate buffer (pH 6.5, 50°C). Plating at +600 mV vs. SCE for 5 min. (A) Potential versus time recording of (a) blank, (b) sample; (B) multichannel potentiogram of (c) blank, (d) sample.

Fig. 2. Reductive potentiometric stripping analysis of 6×10^{-6} M manganese(II), 5×10^{-4} M hydroquinone in 0.1 M acetate buffer (pH 6.5, 50°C). Plating at +600 mV vs. SCE for 1 min. Indicator electrode: (A) glassy carbon; (B) platinum.

were repeated (curves b and d). Clearly a plateau (or peak) is developed, indicating the redissolution of manganese dioxide.

The analytical performance of reductive p.s.a., i.e. the selectivity, accuracy, precision and detection limit, depends on a number of experimental conditions, some of which are of lesser importance in oxidative p.s.a. When anodic preconcentration beyond the redissolution potential of mercury is employed, deposits can be formed only on solid electrodes. Such deposits are frequently of low electric conductivity and often exhibit heterogeneous morphology. Moreover, the electrode materials available for anodic work are likely to react with the solvent and hence cause interference problems. These effects and their impact on the analytical procedure are discussed in the following paragraphs.

Electrode material

Platinum and the various types of carbon are all potential candidates as working electrodes for anodic preconcentration of trace elements. Among the types of carbon available, glassy carbon is probably the most suitable

because it is rather resistant to oxidation and needs no prepolarization procedure to give reproducible results [11, 12]. Both glassy carbon and platinum indicator electrodes were tested: Fig. 2 shows the stripping potentiograms obtained after a polished glassy carbon electrode (A) and a platinum electrode (B) had been plated at 600 mV vs. SCE for 60 s in 6×10^{-6} M manganese(II)—5×10^{-4} M hydroquinone—0.1 M sodium acetate (pH adjusted to 6.5, 50°C).

Both the glassy carbon electrode and the platinum electrode produce a stripping signal for manganese. Although the potentiograms shown in Fig. 2 indicate that platinum is more sensitive for the determination of manganese, experiments with other electrodes indicate that this need not always be the case and that the sensitivity of the glassy carbon depends partly on the perfection of the polishing procedure and on the individual piece of glassy carbon used. Figure 2 also shows that other oxidation products (Ox) are formed on the electrodes during the anodic polarization. While the platinum electrode exhibits a rather constant and fairly simple broad band arising from the reduction of oxidation products even in chloride-containing medium, the behaviour of the glassy carbon electrode appears to depend on a number of factors such as the temperature and the degree of polishing employed. For glassy carbon the Ox-signal occasionally spreads out into a virtual fan of narrow peaks which are not reproducible. The interference from these products in the manganese determination is discussed later. Through the remaining part of the study, a platinum indicator electrode was used.

Influence of pH and plating potential

According to the reaction for deposition of manganese dioxide, the stripping potential can be expected to depend on the solution pH with, theoretically, $\Delta E/\Delta \mathrm{pH} = -128$ mV at 50°C. To test this, stripping experiments were run in various acetate and borax buffers with a constant plating potential of +600 mV vs. SCE (Fig. 3). An experimental value of $\Delta E/\Delta \mathrm{pH}$ of −105 mV was obtained. Figure 3 also indicates that the sensitivity decreases with pH. This effect is possibly due to less efficient preconcentration at low pH, where the stripping potential approaches the plating potential. Nevertheless, with a plating potential of +1200 mV vs. SCE it is possible to obtain a stripping signal for manganese dioxide even in 0.1 M hydrochloric acid.

To study the effect of the plating potential, a 5×10^{-6} M manganese(II)—5×10^{-4} M hydroquinone solution in 0.1 M acetate buffer (pH 6.57, 50°C) was electrolysed for 3 min at different potentials. The resulting potentiograms are shown in Fig. 4. The stripping peak potential depends slightly on the electrolysis potential, probably because the morphology of the deposit depends on the plating conditions. Furthermore, the interference of the stripping band corresponding to the redissolution of the Ox products clearly increases with increasing electrolysis potential. Obviously, the manganese signal initially increases with increasing difference between the plating and

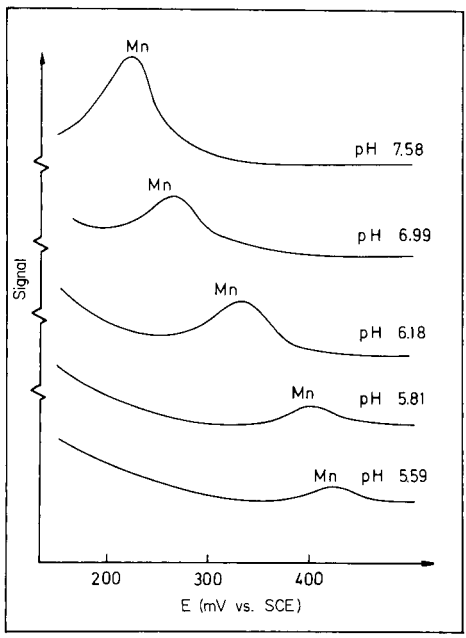

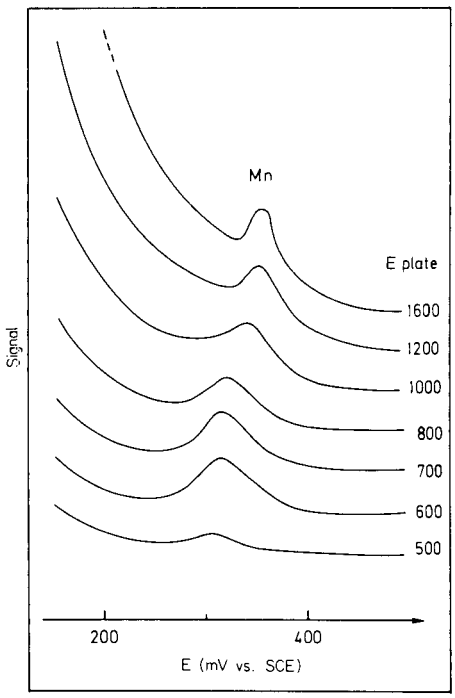

Fig. 3. Variation of potential and magnitude of the manganese signal with pH, for 5×10^{-6} M manganese(II), 5×10^{-4} M hydroquinone in 0.1 M acetate and borax buffers. Plating for 90 s at +600 mV vs. SCE, 50°C.

Fig. 4. Variation with the electrolysis potential of the magnitude of the stripping signals of manganese dioxide and other oxidation products: 5×10^{-6} M manganese(II), 5×10^{-4} M hydroquinone in 0.1 M acetate buffer, pH 6.57, 50°C. Plating time 3 min.

stripping potentials, but when this difference exceeds about 300 mV there is a slight decrease in the manganese signal. At these potentials, the electrode process involving oxidation to permanganate prevails and the permanganate formed stays in solution.

The stripping potential of manganese dioxide is plotted versus pH in Fig. 5. The results for the stripping of lead dioxide are also indicated; for lead dioxide the experimental value for $\Delta E/\Delta$pH was −105 mV at 50°C. To estimate the interference of the Ox band in the determination of manganese and lead by reductive potentiometric stripping analysis, the formation and redissolution of anodic films formed by reaction of platinum with acetate and borax buffers spiked with 10^{-3} M chloride were studied by differential pulse cyclic voltammetry at the platinum electrode. The line marked Ox in Fig. 5 roughly shows the variation with pH of the potential of the first peak observed at positive potentials on the anodic sweep of the voltammogram. The corresponding stripping maxima were generally found 100—200 mV

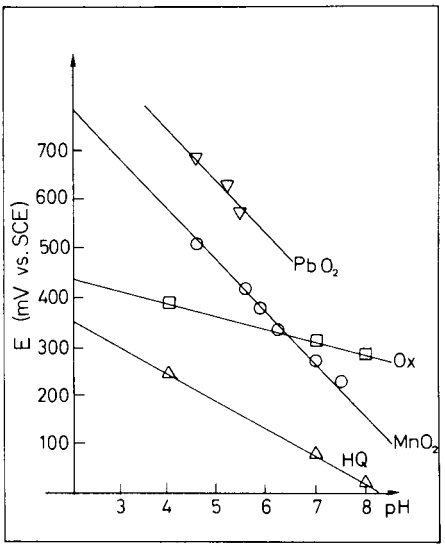

Fig. 5. pH dependence of the potentiometric stripping potentials of lead dioxide (▽) and manganese dioxide (○). Estimate of the pH dependence of the peak potential for the first oxidation peak (Ox) observed on platinum at positive potentials (□) by cyclic voltammetry. pH dependence of the most cathodic oxidation peak of hydroquinone (HQ) observed with cyclic voltammetry (△).

cathodic of this peak. Although the cathodic stripping signals of oxide/halide films from platinum electrodes are often the result of several overlapped peaks, the positions of which are variably dependent on pH, the general picture shown in Fig. 5 indicates that the interference of such films is best avoided at pH values lower than about 5.

Choice of reducing agent and pH

Two conditions must be fulfilled by the reagent to be used as the reducing agent in reductive p.s.a. First, its oxidation potential must be about 200 mV or more cathodic of the reduction potential of the preconcentrated analyte. Secondly, the redox process involved must be reasonably fast. Several reducing agents were investigated: hydroquinone, pyrogallol, sodium sulphite and tin(II) chloride. All four reagents were capable of reducing the manganese dioxide film, but sodium sulphite and tin(II) chloride were less suitable because the reduction of manganese dioxide, and especially of the Ox components, at the platinum electrode was very slow even at 50°C. With both hydroquinone and pyrogallol, however, reduction of all deposits was rapid.

The oxidation of hydroquinone, which was mostly used as the reducing agent, was studied in various buffers by anodic differential pulse voltammetry. In Fig. 5, the potential of the most cathodic peak is plotted as a function of pH (HQ). The value of $\Delta E/\Delta$pH found was -56 mV at 20°C (theoretical

value −59 mV). Since the distance between the reduction potential of manganese dioxide and the oxidation potential of hydroquinone increases with decreasing pH, the stripping procedure is best carried out at rather low pH values, where also the interference from platinum oxide/halide films is small. Moreover, in acidic solution the chance of disturbances from coprecipitation of other elements is generally low, but the decreasing sensitivity of the technique in very acidic solution, which is due to increasing solubility of the deposit, suggests that the manganese determination is best done at a pH of about 4.5. When the reducing agent is added to the sample solution, care must be taken to ensure that the solution is properly deaerated, otherwise a large amount of reducing agent may be consumed. In oxidative p.s.a., deaeration is usually not necessary [13]. In the experiments reported here, the hydroquinone stock solution was kept oxygen-free by the addition of 2.5 g of sodium sulphite per 50 ml of solution. As previously pointed out, the sulphite reaction with manganese dioxide is very slow, hence this addition does not affect the rate of manganese dioxide redissolution. The amount of hydroquinone to be added to the sample depends on the amount of reducible species present. Obviously, it is vital that all manganese be converted to manganese(II) before stripping analysis. For solutions of manganese(II) with no reducible species, a 50—100-fold excess of hydroquinone is suitable.

Effect of temperature and solution stirring

Redissolution of the manganese dioxide film is brought about by hydroquinone being transported towards the indicating electrode. At room temperature this process is very slow, and the stripping signals are not easily reproducible. At temperatures of 40—60°C, the quality and reproducibility of the stripping signal are significantly improved. This suggests that the redissolution process is not entirely transport-controlled: in order to maintain a well-defined electrode potential during the stripping of manganese dioxide, the corresponding redox pair must be present in appreciable amounts at the electrode—solution interface. If the redissolution process is fast compared with the rate at which the redissolved species escapes from the electrode by diffusion or convection (as is the case in potentiometric stripping from dilute amalgams of cadmium and lead) a high concentration gradient with respect to the analyte is created in the vicinity of the indicator electrode. Thus, although the bulk concentration of the analyte may be at or below the $\mu g\ l^{-1}$ level, the predominant electroactive species at the electrode—solution interface are the reduced and oxidized forms of the analyte and hence the characteristic potential is maintained for some time. In contrast, if the redissolution is slow compared with diffusion (or convection) the high concentration gradient is not formed and other redox pairs may govern the electrode potential. At a temperature of 40—60°C the reaction of manganese dioxide with hydroquinone appears to be sufficiently fast for potentiometric stripping analysis.

Moderate stirring of the solution during the stripping improves the repro-

ducibility. A small magnetic stirrer bar (1 cm long) rotating at about 200 rpm 2 cm below the indicator electrode was used. More vigorous stirring counteracts the advantages obtained from increased sample temperature, in accordance with the mechanism outlined above.

Since oxide deposits formed on anodically polarized platinum electrodes generally retard electron-transfer processes [12], kinetic control is likely to occur in reductive potentiometric stripping of other species.

Multiple-scanning potentiometric stripping analysis

In favourable cases, potentiometric stripping signals may be considerably enhanced by a computerized multiple scanning technique [4] where analytes, once preconcentrated, are forced through several plating/redissolution cycles. After the pre-electrolysis, the stripping potentiograms obtained are saved in the computer memory; immediately after the stripping of a component potentiostatic control is resumed and the potential is reset to plating conditions for a fraction of a second. Then a new potentiometric stripping curve is recorded and added to the previous one and so on. In cases where a high concentration gradient of analyte is formed around the indicator electrode, this procedure causes replating of a large fraction of the newly stripped material, so that a significant stripping signal can be achieved in several cycles. The multiple scanning procedure, however, completely fails to enhance the stripping signal in the reductive potentiometric stripping determination of manganese. This too indicates that the stripping process is not entirely governed by transport.

Electrode regeneration

To obtain reproducible results in the reductive p.s.a. for manganese and lead, any oxide layer formed on the platinum electrode must be removed completely before each experiment. Various procedures were tried: cleaning in concentrated nitric acid and hydrochloric acid at room temperature even for 10 min was insufficient to regenerate the electrode after a stripping experiment lasting for 1 min. The recommended procedure involves polarization of the electrode at a cathodic potential about 200 mV anodic of the hydrogen evolution potential in the test solution including hydroquinone at 50°C. The cleaning procedure follows immediately after the stripping procedure and is continued until the cathodic current decays to a stable value (usually after about 1 min). When not in use, the electrode is stored in a solution of hydroquinone.

Interferences

As previously pointed out, oxide and halide films on the platinum electrode may cause serious interferences with the determination of manganese. The formation of these films is minimized by employing as low a plating potential as possible to oxidize the manganese(II), i.e. about 250 mV anodic of the stripping potential. The separation of the manganese signal from the Ox signal at low pH is illustrated in Fig. 6.

Among the metallic elements which can be anodically plated (e.g. Tl, Fe, Co, Pb [14]), lead is most likely to interfere because its stripping potential at any pH is only about 200 mV anodic of the manganese dioxide stripping potential (cf. Fig. 5). Hrabánková et al. [8, 9] report that this interference is quite serious in cathodic voltammetric stripping analysis. This is not the case in reductive p.s.a., as is shown in Fig. 6. The reason is that stripping potentiograms are generally better resolved than linear sweep voltammograms, simply because the stripping of one component is essentially complete before stripping of the next component begins [3]. In voltammetric procedures, when the redissolution of a component is slow, that component may not be completely stripped before the controlled potential forces the next component to redissolve.

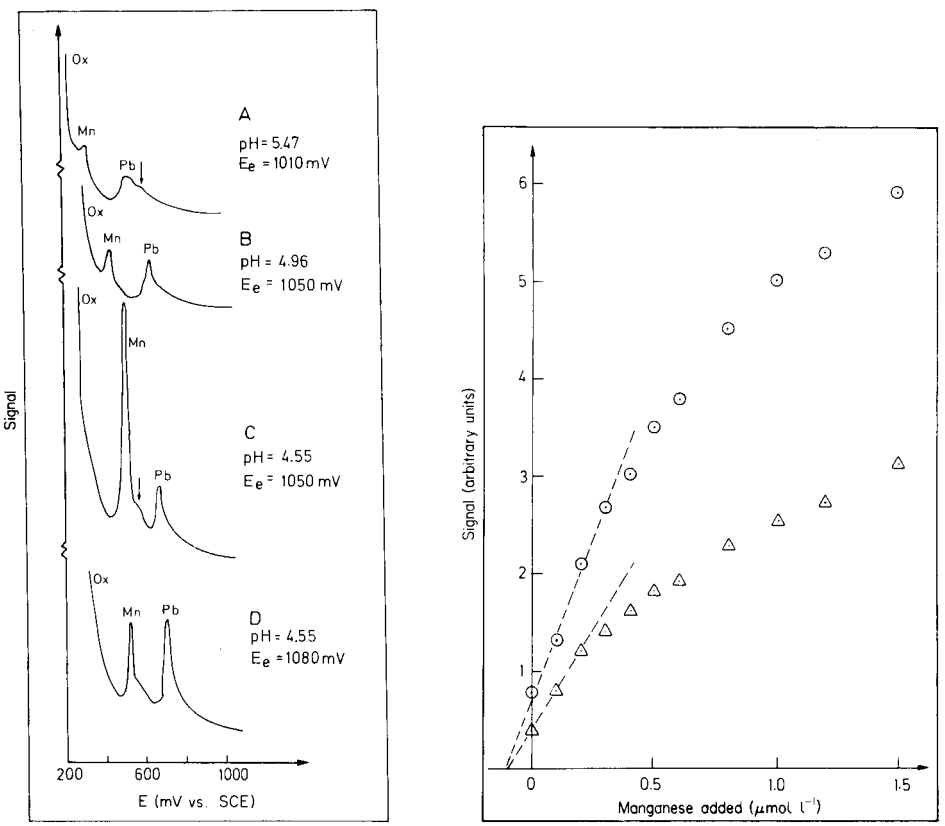

Fig. 6. Simultaneous determination of manganese and lead by reductive p.s.a., showing minimization of interference from other oxidation products (Ox) by lowering the pH, and the effect of plating potential on the relative magnitude of the manganese and lead signals. 5×10^{-6} M manganese(II), 15×10^{-5} M lead(II), 5×10^{-4} M hydroquinone in 0.1 M acetate buffers, 50°C. Plating for 3 min.

Fig. 7. Standard addition plots: 10^{-7} M manganese(II), 10^{-4} M hydroquinone in 0.1 M acetate buffer, pH 6.7, 50°C. Plating at +650 mV vs. SCE for 3 min (△) and 6 min (○). Standard additions up to 1.5×10^{-6} M manganese(II).

As shown in Fig. 6 (C and D), the lead peak increases simultaneously with a decrease in the manganese peak as the electrolysis potential E_e is increased from 1050 to 1080 mV vs. SCE. This is not, however, an interference effect because the same changes in peak heights are found if only one of the components is present. Thus, the decrement in the manganese peak is due to the formation of permanganate rather than manganese dioxide.

Signal evaluation, standard addition procedure

The analytical signals were taken as the peak heights in the potentiograms corrected for the background signal obtained with zero electrolysis time.

As indicated by arrows in Fig. 6, both manganese dioxide and lead dioxide may exhibit more than one stripping maximum. Such shoulders which occur when the deposits have reached a certain thickness and which indicate that the deposits are no longer homogeneous, were also observed by Hrabánková et al. [8, 9]. These secondary signals are not useful for quantitative analysis.

Experiments where the thickness of the manganese dioxide deposit is gradually increased either by addition of manganese(II) or by prolonged electrolysis show that the indicator electrode gradually becomes passive because of the low conductivity of the deposit. Signal versus electrolysis time plots and signal versus concentration plots therefore exhibit saturation effects above a certain film thickness. With the cell and electrodes reported here, saturation occurs after plating for about 3 min in a 2×10^{-7} M manganese(II) solution.

In order to use standard addition techniques on a given sample, it is necessary to ensure that the spiked solution will not cause such saturation problems. Therefore, before any standard is added to the sample solution, the signal versus plating time relationship should be recorded. Any non-linearity suggests that shorter plating time should be employed or the sample be diluted.

Figure 7 shows the standard addition plots for a 10^{-7} M manganese(II) solution. The plating times were 3 and 6 min. Obviously, only the parts of the curves for low concentrations approach straight lines, i.e. the electrode is passivated. However, when the same experiments were run in the region 10^{-8}—10^{-7} M straight lines were obtained.

Detection limit, precision and accuracy

The detection limit depends on the plating time. Thus 10^{-7} M manganese(II) produces a significant signal (ca. 3 times the standard deviation of the background) after 3 min of plating. The detection limit for lead is of the same magnitude.

The precision of the stripping procedure was tested by running eight consecutive experiments, each with 3-min plating times, on 8×10^{-7} M manganese(II), 10^{-4} M hydroquinone in 0.1 M acetate buffer (pH 4.53, 50°C). A relative standard deviation of 0.06 was found.

The accuracy was investigated by determining the total amount of manganese in certified biological materials. Prior to analysis, 0.2 g of the dried material was digested with 3 ml of concentrated nitric acid in a PTFE-

TABLE 1

Total manganese in standard biological materials

Material	Manganese ($\mu g\ g^{-1}$)	
	Found	Certified
Kale	15.0, 15.1	Range: 12.6—18 Best mean value: 14.73
Orchard Leaves (SRM 1571)	81, 91	91 ± 4
Bovine Liver (SRM 1577)	9.9, 10.4	10.3 ± 1.0

lined pressure bomb at 110°C overnight. The digests were buffered with sodium acetate and volumes made up to 50 ml (pH 4.50). Prior to the standard addition, a stripping signal vs. plating time curve was obtained. For the orchard leaves sample, a 10-fold dilution was necessary in order to avoid saturation effects with a plating time of 8 min. The stripping signal for manganese in a given sample was taken as the average from two consecutive stripping experiments on the sample.

The results are given in Table 1. The certified values for manganese, found by atomic absorption spectrometry and neutron activation analysis, are given for reference. Deviations from the certified values, in particular for the orchard leaves, can probably be attributed to two factors. First, because of the volume of the pressure bomb available, the sample weight had to be restricted to 0.2 g, i.e. slightly lower than the recommended minimum sample (0.25 g). Secondly, with the digestion procedure employed, a small residue of siliceous material may remain. Such a residue has previously been reported to contain manganese [15]. However, no visible residue remained in any of the digests examined here.

The support of the Danish Natural Science Research Council, grant no. 511-8032, for the computerized instrument is gratefully acknowledged.

REFERENCES

1 D. Jagner and A. Graneli, Anal. Chim. Acta, 83 (1976) 19.
2 D. Jagner, Anal. Chem., 50 (1978) 1924.
3 H. J. Skov and L. Kryger, Anal. Chim. Acta, 122 (1980) 179.
4 J. Mortensen, E. Ouziel, H. J. Skov and L. Kryger, Anal. Chim. Acta, 112 (1979) 297.
5 D. Jagner, Anal. Chim. Acta, 105 (1979) 33.
6 D. Jagner, unpublished results.
7 T. M. Florence, J. Electroanal. Chem., 97 (1979) 219.
8 E. Hrabánková, J. Doležal and U. Mašin, J. Electroanal. Chem., 22 (1969) 195.
9 E. Hrabánková, J. Doležal and P. Beran, J. Electroanal. Chem., 22 (1969) 203.
10 H. J. M. Bowen, J. Radioanal. Chem., 19 (1974) 215.
11 L. Dunsch and R. Naumann, Z. Chem., 14 (1974) 31.
12 L. Meites, Polarographic Techniques, 2nd edn., Wiley, New York, 1965, Ch. 8.
13 D. Jagner, Anal. Chem., 51 (1979) 342.
14 F. Vydra, K. Stulík and E. Juláková, Electrochemical Stripping Analysis, Ellis Horwood, Chichester, 1976, Ch. 5.
15 G. Duyckaerts and G. Gillain, in E. Wänninen (Ed.), Analytical Chemistry, Essays in Memory of Anders Ringbom, Pergamon, Oxford, 1977, p. 417.

Analytica Chimica Acta, 118 (1980) 65—71
© Elsevier Scientific Publishing Company, Amsterdam — Printed in The Netherlands

DETERMINATION OF GLUTAMATE PYRUVATE TRANSAMINASE AND PYRUVATE WITH AN AMPEROMETRIC PYRUVATE OXIDASE SENSOR

FUMIO MIZUTANI and KEISHIRO TSUDA

Research Institute for Polymers and Textiles, 1-1-4, Yatabe-Higashi, Tsukuba, Ibaraki-ken 305 (Japan)

ISAO KARUBE* and SHUICHI SUZUKI

Research Laboratory of Resources Utilization, Tokyo Institute of Technology, Nagatsuta-cho, Midori-ku, Yokohama 227 (Japan)

KUNIO MATSUMOTO

Toyo Jozo Co., Mifuku, Ohito-cho, Shizuoka-ken 410-23 (Japan)

(Received 29th October 1979)

SUMMARY

Pyruvate oxidase (E.C. 1.2.3.3.) is immobilized by adsorption on a porous acetyl-cellulose membrane, and combined with an oxygen electrode to provide a sensor for pyruvate (0.1—0.8 mM). The response time is 2 min. Glutamate pyruvate transaminase ($0.5—180 \times 10^{-3}$ I.U. ml^{-1}) is determined by its effect on pyruvate production by the alanine—α-ketoglutarate reaction. The sensor is stable for more than 10 days and 100 assays.

Determination of glutamate pyruvate transaminase (GPT) in serum is diagnostically important in clinical analysis. For example, the GPT level of viral hepatitis patients is very high [1]. The reaction catalyzed by GPT is

L-alanine + α-ketoglutarate → pyruvate + L-glutamate

Methods involving a combination of GPT and lactate dehydrogenase have been proposed for the assay of GPT [2—6], but generally require a long incubation time, additional reagents and expensive enzymes. In order to achieve a rapid and simple assay of GPT, an electrochemical method may have definite advantages.

Pyruvate oxidase catalyzes the reaction

$$\text{Pyruvate} + H_3PO_4 + O_2 \rightarrow CH_3OPO_3H_2 + \text{acetate} + CO_2 + H_2O_2$$

The amperometric determination of pyruvate can be carried out with the pyruvate oxidase sensor. Therefore, the use of the pyruvate oxidase sensor for the determination of the GPT activity via the production of pyruvate appears to be a suitable approach. In this paper, pyruvate oxidase is immobilized on a porous acetyl-cellulose membrane. The enzyme sensor,

composed of immobilized pyruvate oxidase and an oxygen electrode, is described and applied to the determination of GPT.

EXPERIMENTAL

Materials

The enzymes used were pyruvate oxidase (E.C. 1.2.3.3., from *Pediococcus* sp., 13 I.U. ml^{-1}; Toyo Jozo Co.) and glutamate pyruvate transaminase (E.C. 2.6.1.2., from pig heart, 80 I.U. ml^{-1}; Böehringer Mannheim GmbH). Human serum was obtained from Japan Red Cross Central Blood Center (Shibuya, Tokyo). Other reagents were analytical or laboratory-grade materials. Deionized water was used for all procedures.

Enzyme assay

Pyruvate oxidase was determined by the method of Hagar et al. [3], and GPT by the method of Wroblewski and Ladue [1].

Assembly of the enzyme sensor

Pyruvate oxidase was immobilized by adsorption as follows: 200 μl of solution (0.1 M phosphate buffer, pH 7.0, containing 20 I.U. of pyruvate oxidase) was dropped onto a porous acetyl-cellulose membrane (Millipore, Type HA, 0.45-μm pore, 140 μm thick, 25-mm diameter) with slight suction. This membrane was directly attached to the teflon membrane of an oxygen electrode (Ishikawa Manufacturing Co. Ltd.) and covered with a dialysis membrane (Visking Co., 20 μm thick, 25-mm diameter). The prepared sensor was stored in 0.1 M phosphate buffer (pH 7.0) at 5°C.

Figure 1 is a schematic diagram of the sensor. The sensor was immersed in a sample solution (25—80 ml) which was saturated with oxygen by bubbling air continuously (100 ml min^{-1}) and stirred magnetically while measurements were taken. The current from the sensor was converted to voltage by a 2 kohm resistance and displayed on a recorder (Riken Denshi SP-J5V).

Procedures

The standard solution used for characterization of the sensor was 0.04 M Tris—HCl buffer, 0.5 mM in potassium dihydrogenphosphate and 0.06 mM in thiamine pyrophosphate chloride. The temperature of the sample solution was kept at 30.0 ± 0.2°C during measurements.

For the determination of pyruvate, the sample solution was added to a solution of 0.04 M Tris—HCl buffer, pH 7.05 or 7.35, which was 0.5 mM in potassium dihydrogenphosphate and 0.06 mM in thiamine pyrophosphate chloride. The steady-state current obtained was measured 3 min after addition of pyruvate. The differences between the initial current and the constant currents obtained were plotted against pyruvate concentration to provide a calibration graph.

For the determination of GPT, the sample solution or serum was added to

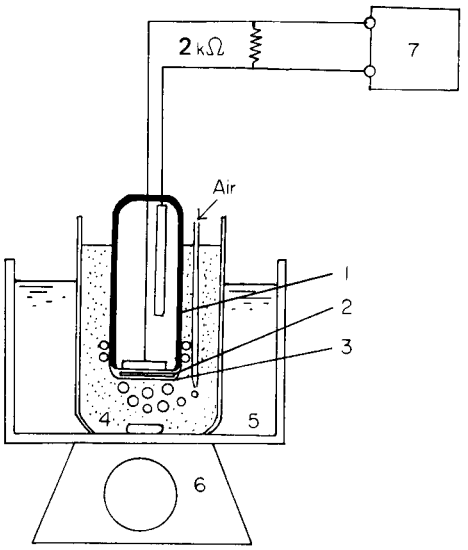

Fig. 1. Schematic diagram of the pyruvate oxidase electrode: (1) oxygen electrode; (2) enzyme membrane; (3) cellulose dialysis membrane; (4) cell; (5) thermostat; (6) magnetic stirrer; (7) recorder.

a 0.04 M Tris—HCl buffer solution, pH 7.35 which was 0.5 mM in potassium dihydrogenphosphate, 0.06 mM in thiamine pyrophosphate chloride, 250 mM in L-alanine, 50 mM in α-ketoglutarate and 0.5 mM in pyridoxal-5-phosphate. The initial constant rate of current decrease (within 5 min) was measured and the responses from standard solutions were plotted against GPT concentration to provide a calibration graph.

RESULTS

Response of the sensor

The assay is based on monitoring the decrease in dissolved oxygen resulting from the enzymatic reaction with pyruvate shown above. Figure 2 shows typical responses obtained when the sensor was inserted into a solution containing different amounts of pyruvate; about 2 min were required to obtain a steady current. The current decrease, i.e. the difference between the initial current and the steady-state current, increased with pyruvate concentration. When the sensor was inserted in a solution without pyruvate, the current returned to its initial level.

Effect of pH and various reagents

The effect of the buffer pH on the current decrease is shown in Fig. 3. The optimum pH of the immobilized pyruvate oxidase was 7.0 and an especially sharp decrease of the activity was observed above pH 7.2. This profile is almost the same as that of native pyruvate oxidase.

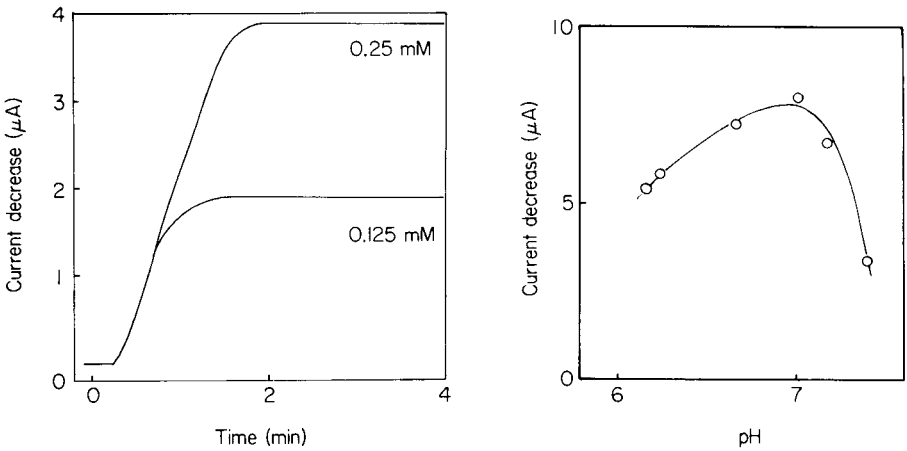

Fig. 2. Response curves of the pyruvate oxidase sensor under the recommended conditions to the pyruvate concentrations shown.

Fig. 3. Effect of pH on current decrease with Tris—HCl buffer solutions which were 0.5 mM in sodium pyruvate, 0.5 mM in KH_2PO_4 and 0.06 mM in thiamine pyrophosphate chloride.

Because phosphate ions, thiamine pyrophosphate, calcium ions and flavin adenine dinucleotide (FAD) are reported to be necessary for the enzymatic reaction and play important roles in increasing the accuracy and the reaction rate in the enzymatic determination of pyruvate [7], their effects on the sensor output were examined. The results obtained are shown in Fig. 4. The current decrease obtained was small (4 μA mM^{-1} pyruvate) in pyruvate solutions without phosphate ions. The current decrease increased linearly

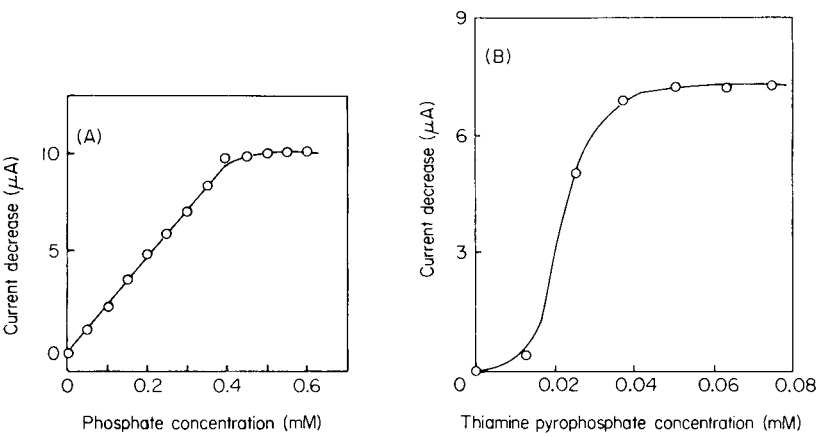

Fig. 4. Effects of (A) phosphate concentration and (B) thiamine pyrophosphate concentration on current decrease in Tris—HCl buffer solution (pH 7.05), 2 mM in sodium pyruvate; 0.06 mM in thiamine pyrophosphate chloride for (A) and 0.5 mM in KH_2PO_4 for (B).

with increasing phosphate ion concentration and became constant above 0.4 mM. Subsequent work was done at a phosphate ion concentration of 0.5 mM.

Thiamine pyrophosphate is also required as a cofactor of pyruvate oxidase. As shown in Fig. 4B, the current decrease increased with increasing concentration of thiamine pyrophosphate and became constant above 0.05 mM. Therefore, a thiamine concentration of 0.06 mM was used subsequently.

Inactivation of the bound pyruvate oxidase occurs when 0.01 M EDTA is present in the solution, presumably by binding calcium ions which are required for the enzymatic activity. However, no effect of calcium ions on the activity of pyruvate oxidase was observed in this study. Furthermore, addition of FAD to the reaction mixture did not affect the current decrease. Therefore, it is likely that the enzyme employed in the electrode contained enough FAD and calcium ions for the catalytic reaction, and none were added in subsequent studies.

Calibration

The calibration graphs obtained under the recommended conditions (Fig. 5) show a linear relationship between the current decrease and the concentration of pyruvate up to 0.8 mM, at pH 7.05 and pH 7.35. The minimum concentration which could be determined was 0.06 mM. The current decrease was reproducible to within ±4% for a sample containing 0.5 mM of pyruvate.

Determination of GPT with the pyruvate oxidase sensor

The GPT was determined by its catalysis of the production of pyruvate as shown above. A sample solution containing a large amount of L-alanine and α-ketoglutarate (ca. 10 K_m [8]) was employed. As described above, the optimum pH of the pyruvate oxidase sensor was 7.0, whereas the optimum pH range for GPT is 7.3—7.8 [8]. Therefore, the pH of the sample solution was adjusted to 7.35, at which pH the sensor is less than half as sensitive to pyruvate (Fig. 5). Figure 6 shows a typical response curve obtained when GPT (30×10^{-3} I.U. ml^{-1}) was present in the solution. The current decreased more with increasing reaction time, initially linearly for ca. 10 min. There is a linear dependence of this initial rate of current decrease on the GPT concentration over the range $0.5—180 \times 10^{-3}$ I.U. ml^{-1}. The lower limit of determination ($S/N = 5$) for GPT was 0.5×10^{-3} I.U. ml^{-1}. The reproducibility was ±6% for a GPT sample containing 11.7×10^{-3} I.U. ml^{-1}. Therefore, the proposed sensor can be used for the determination of GPT.

The GPT level of human sera was determined by the conventional spectrophotometric method [1] and by the proposed electrochemical method. The results showed satisfactory agreement (correlation coefficient 0.99) for 4 assays of GPT level over the range $8.4—16.4 \times 10^{-3}$ I.U. ml^{-1}.

The long-term stability of the sensor was studied: the current output on changes of pyruvate concentration was constant (within 30%) for more than 10 days and 100 assays.

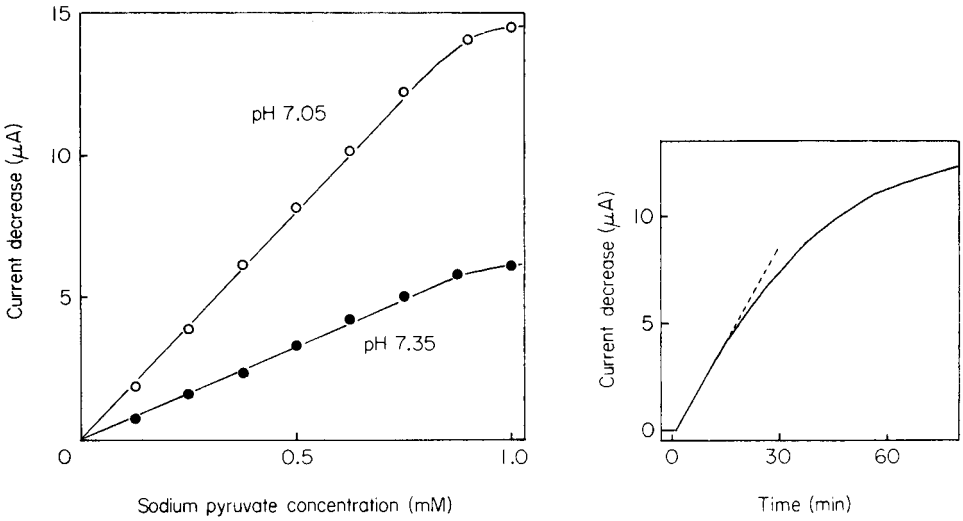

Fig. 5. Calibration graphs for pyruvate obtained under the recommended conditions.

Fig. 6. Response of the electrode to GPT (3×10^{-2} I.U. ml^{-1}) in a buffer solution 250 mM in L-alanine, 50 mM in α-ketoglutarate and 0.5 mM in pyridoxal-5-phosphate at 7.35. Other conditions as recommended for pyruvate determination.

DISCUSSION

Recently, many reports have been published on enzyme sensors, mainly for the determination of organic compounds in biological fluids. However, few reports have been published on the application of an enzyme sensor for the determination of an enzyme in biological fluids [9]. Immobilization of pyruvate oxidase on various membranes including collagen was attempted; high activity was obtained when the enzyme was simply adsorbed on the porous acetylcellulose membrane. As a slight leakage of enzyme was observed from this membrane, the membrane was covered with a cellulose dialysis membrane.

The enzyme sensor was applied to the determinations of pyruvate and of GPT activity. As would be expected, there is a linear relation between the initial rate of current decrease (i.e. initial rate of pyruvate formation) and GPT concentration. However, the rate of current decrease gradually slowed down. This might be caused by limiting diffusion of L-alanine and α-ketoglutarate to the enzyme membrane. The response to pyruvate became constant after 2 min (Fig. 2). This lag time was also observed after addition of GPT but had no influence on the determination of GPT.

REFERENCES

1 F. Wroblewski and J. S. Ladue, Proc. Soc. Exp. Biol. Med., 91 (1956) 569.
2 B. Rietz and G. G. Guilbault, Anal. Chim. Acta, 77 (1975) 191.

3 L. P. Hagar, D. M. Geller and F. Lipmann, Fed. Proc. Fed. Am. Soc. Exp. Biol., 13 (1954) 11.
4 K. Henley and H. Pollard, J. Lab. Clin. Med., 46 (1955) 785.
5 B. Rietz and G. G. Guilbault, Clin. Chem., 21 (1975) 1544.
6 J. Nixon and L. Cloutier, Clin. Biochem., 2 (1968) 115.
7 F. Lipmann, J. Biol. Chem., 155 (1944) 55.
8 M. Saier and W. Jenkins, J. Biol. Chem., 242 (1967) 101.
9 H. Booker and J. Haslam, Anal. Chem., 46 (1974) 1054.

Analytica Chimica Acta, 118 (1980) 73—79
© Elsevier Scientific Publishing Company, Amsterdam — Printed in The Netherlands

APPLICATION OF PULSE TECHNIQUES IN A POLAROGRAPHIC FLOW-THROUGH DETECTOR WITH POTENTIAL-CONTROLLED DROP SYNCHRONIZATION

H. B. HANEKAMP, W. H. VOOGT and P. BOS

Department of Analytical Chemistry, Free University Amsterdam, De Boelelaan 1083, 1081 HV Amsterdam (The Netherlands)

(Received 12th February 1980)

SUMMARY

The use of pulse techniques and current sampling available at the dropping mercury electrode (DME) is described for polarographic flow-through detectors. The necessary synchronization between the drop lifetime and the desired measuring technique is achieved by means of a potential pulse supplied to a horizontal DME with a partially-conical glass capillary.

Most commercially-available electrochemical detectors employ glassy carbon as the material for the working electrode. With this solid-state electrode excellent results can be obtained, especially when it is operated in the oxidation mode. For the reduction mode, glassy carbon is not the material of choice. As is well known from polarography, mercury has excellent characteristics for reductive measurements, namely a wide cathodic range, and the possibility of regular renewal of the electrode surface, hence avoiding electrode contamination. Therefore, several flow-through cells involving mercury electrodes have been developed [1] for application as detectors in liquid chromatography. The technical problems of constructing a dropping mercury electrode (DME) detector were overcome by introducing a conically ground horizontal mercury capillary, resulting in fast drop-times (ca. 25 ms). With direct-current amperometry (d.c.a.) good results were obtained [1, 2]. This fast system, however, does not allow the application of sampling techniques such as sampled d.c. (s.d.c.) or pulse techniques such as normal and differential pulse polarography or amperometry (n.p.p./n.p.a. and d.p.p./d.p.a.), because all these techniques require synchronization of the measurement with the drop lifetime.

This synchronization can be accomplished either by triggering the electronics with the drop-fall or by external control of the drop-time. The first case necessitates a detector to indicate the fall of the mercury drop. The trigger signal can be derived from the natural voltage change [3] or the change in a.c. impedance at drop-fall [4—10]. Another possibility is interruption of a light beam to provide the drop-fall signal [11—15]. In the second case,

the drop can be mechanically hammered off, as is usual in polarography, or the mercury drop formation can be regulated by means of a solenoid-actuated valve [16]. Unfortunately, mechanical types of regulation can cause undesired disturbance of the fluid flow pattern, especially at low flow-rates [16].

The aim of the present work was to make current sampling techniques and pulse amperometric detection applicable to flow-through cells, and so these synchronization techniques were considered. However, another means of drop synchronization, which can be applied even to relatively fast dropping systems, was found more satisfactory. It is based on the fact that the surface tension determines the natural drop time. Since the surface tension is potential-dependent, a potential change can induce a change in surface tension and cause, under certain conditions, the drop to fall. This effect is simple to realise in practice compared to drop-fall detectors, and avoids mechanical disturbance of the flow pattern.

EXPERIMENTAL

The dropping mercury electrode detector

In an earlier paper [17], it was reported that fast drop-rates are advantageous for establishing an improved signal-to-noise ratio. These short drop-times would give problems concerning the synchronization of mercury drops, pulse application and current sampling. Therefore it was necessary to apply longer drop-times than in the earlier detector designs. Again, a horizontal mercury capillary was used, of which the end was partially ground to a conical shape, which has excellent positioning and sealing characteristics (Fig. 1). The drop-times with a 8-cm long glass capillary are from 0.3 to 0.9 s, depending on the mercury height and flow rate. The longer drop-times made it impossible to point the eluent stream directly onto the drop, because of tear-off effects. Therefore, a straight flow channel was chosen, which results in less dependence of the drop-time on the flow rate[1]. The glass connecting tube of the reference electrode was ground conically and, as in earlier designs, attention was paid to correct positioning of all three electrodes [1, 17].

To control the drop-time electronically, a short negative potential pulse was applied in the last stage of the drop lifetime (Fig. 2). When the drop-time was controlled by such a pulse, it became possible to synchronize the electronics and the mercury drop.

Apparatus

The system consisted of a Perkin-Elmer 601 pump and a 25-μl or 1-ml loop injection valve (Valco Instruments Co., Houston, Texas). In some of the measurements a column (RVS, 10 cm $\times$ 4.6 mm i.d) was used, packed with LiChrosorb RP-8, 10 μm (Merck). The potential-pulse sequence was generated by a Tacussel UAP 4 pulse unit/PRT 30-01 potentiostat and

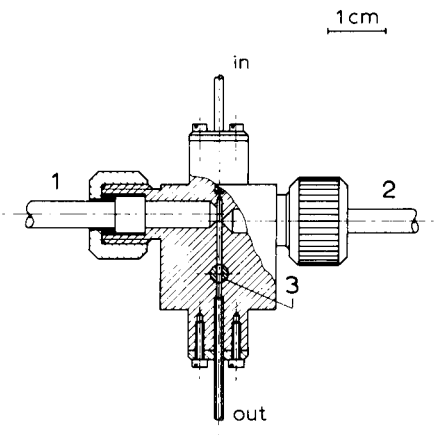

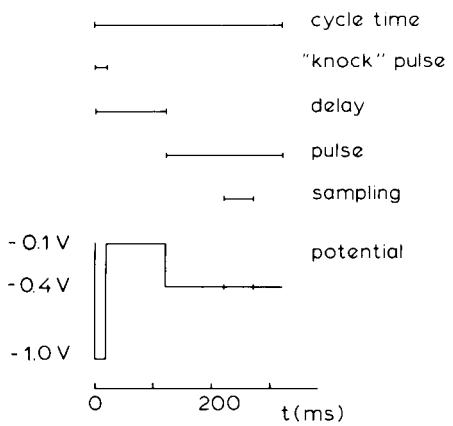

Fig. 1. The d.m.e. detector. (1) mercury capillary working electrode; (2) reference electrode; (3) auxiliary electrode.

Fig. 2. The pulse sequence.

the start of this pulse program triggered via a home-made interface a Princeton Applied Research PAR 175 programmer for the additional "knock" pulse. This pulse was superimposed on the pulse program of the Tacussel. The electrical currents were measured with the Tacussel PRT 30-01/UAP 4 and recorded with a Hewlett-Packard 7046 A dual-pen X-Y recorder. The potential-pulse program and the electrical currents were checked on a Tektronix 5103 N oscilloscope. The mercury capillary (Metrohm 1091/1) as delivered was machined to the desired shape in our workshop. The DME detector compartment was made of Plexiglas, and the counter electrode of platinum. The applied potential was measured vs. an Ag | AgCl | 1 M LiCl, methanol—water (50/50, v/v) reference electrode.

Chemicals

In every measurement water—methanol (50/50, v/v) was used as eluent, and contained 0.1 M potassium nitrate and 10^{-3} M nitric acid. The stock solution of this eluent was continuously de-aerated by purging with nitrogen (A 28). Methanol, lithium chloride, potassium nitrate, nitric acid and nitrobenzene (all Baker Analyzed chemicals) were used without further purification.

RESULTS AND DISCUSSION

Synchronization

With a "knock" pulse of 20 ms and a potential step from 0 to −1 V good results were obtained. This pulse duration is slightly above the minimum required to knock the mercury drop off the capillary, when this potential

change is applied. With a smaller potential step at this pulse duration no knocking off the drop occurs. Application of larger potential steps at smaller pulse durations is possible, but this can cause problems in the electronics with the decay of the current.

Synchronization by means of a knock pulse is possible if the cycle time is chosen to be just a little shorter than the natural mercury drop-time, which is dependent on the mercury height. Further, the range in which external regulation is possible depends, like the drop-time, on the flow rate (Fig. 3). With the chosen mercury height of 50 cm, at flow rates above 3.5 ml min^{-1}, it is no longer possible to synchronize the mercury drop and the measurements. At these high flow rates the drop-time is fully determined by the eluent stream.

Performance of the detector cell

As in an earlier paper [1], the important parameters for the detector cell performance, the time constant (τ) and the response volume, were determined by injecting 1-ml plugs of 10^{-4} M nitrobenzene (Fig. 4). The time constant of this detector cell is quite favourable, especially for flow rates above 1.25 ml min^{-1} ($\tau < 0.5$ s). The response volume decreases sharply between 1 and 2 ml min^{-1}, which behaviour is comparable to that of an earlier cell design with similar geometry [1].

Sampled d.c., normal pulse and differential pulse polarography

For these measurements, nitrobenzene (10^{-4} M) was added to the eluent, which was pumped through the detector. With sampled d.c. polarography (mercury column 30 cm, cycle time 0.90 s, sampling window from 80 to 90% of the cycle time, scan rate 5 mV s^{-1}), a well-developed wave was obtained (see Fig. 5). With normal pulse polarography (cycle time 0.90 s, delay 0.70 s, pulse 0.20 s, sampling window from 85 to 90% of the pulse)

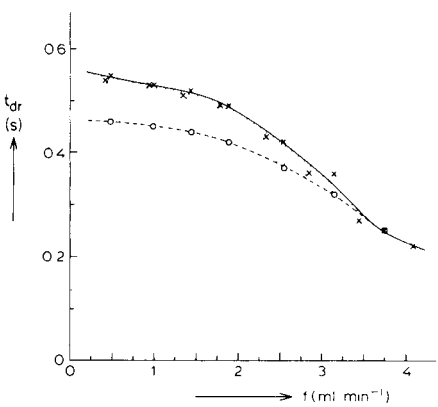

Fig. 3. Cycle time (t_{dr}) vs. flow rate (f). Cycle time: (×) maximum; (○) minimum, $E = 0$ V; for further conditions, see text.

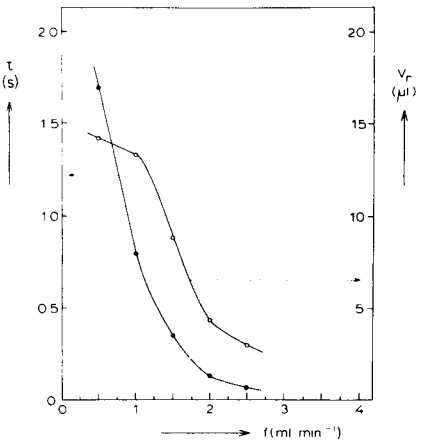

Fig. 4. The time constant (τ) and the response volume (V_r) vs. the flow rate. For conditions, see text.

the polarographic wave exhibited a maximum (Fig. 5). In differential pulse polarography (Fig. 6), the d.c. effect was very marked. This can be explained by the fact that the cycle time (the "drop-time") is short, which results in a relatively big difference in surface area between the two current-sampling times [18]. Differential pulse polarography has no greater sensitivity than s.d.c.p. or n.p.p. This probably happens because electrode reactions under hydrodynamic conditions seem to be less reversible than in corresponding batch experiments.

Sampled direct current, normal pulse and differential pulse amperometry

For these measurements, 25-μl de-aerated samples of 10^{-4} M nitrobenzene were directly injected into the detector at a flow rate of 1.0 ml min^{-1}. The potential for d.c. amperometry (d.c.a.) was fixed at —0.380 V and for n.p.a. and d.p.a. at E_1 = —0.150 V and E_2 = —0.380 V. In all cases, the conditions were: mercury column 74 cm, cycle-time 0.30 s, delay 0.10 s, pulse 0.20 s, sampling window 80—90% of pulse.

The principal result of the use of s.d.c.a. was a reduction of the noise. With n.p.a. the peak height was independent of the flow rate. This is in agreement with previously reported results [19, 20]. Normal pulse amperometry was used to study the influence of the current-sampling window and the delay (Fig. 2). The pulse was kept constant at 200 ms. Cycle-times between 0.30 and 0.90 s had no influence on the total current (oscilloscope) or the sampled current (recorder). The current-sampling window was varied in two ways; a constant window (20 ms) was taken between 5 and 95% of the pulse duration, or the window was increased in steps of 40 ms from 85—95% to 5—95% of the pulse duration. No influence on the sampled current peak height was found, which demonstrates that the capacitive current decayed within 5% of the pulse duration (10 ms).

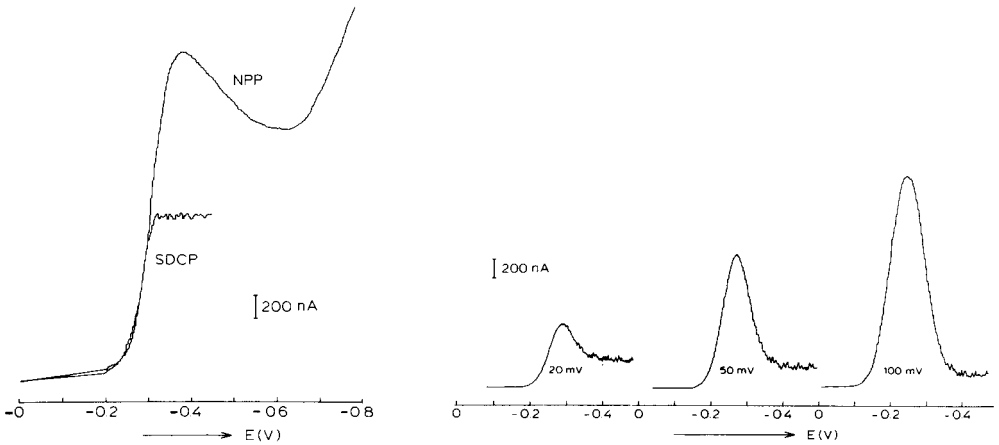

Fig. 5. Sampled d.c. and normal pulse polarograms. For conditions, see text.

Fig. 6. Differential pulse polarograms. For conditions, see text.

No further advantage in sensitivity was gained by using differential pulse amperometry. A possible advantage might have been selectivity [19, 21, 22], but this was not found in the case of nitro compounds with interfering oxygen, because of the irreversibility of the reduction of oxygen.

Linearity of response, sensitivity and detection limit as the n.p.a. detector for h.p.l.c.

For these measurements a chromatographic system was set up, again with nitrobenzene as the model component. With a flow rate of 1.0 ml min^{-1}, the capacity factor of nitrobenzene was 5.3 and the plate number of the column was 2000.

A linear dynamic range of 3—4 orders of magnitude was found (for conditions, see the n.p.a. experiment). The calibration curve was computed by linear regression; a sensitivity of 1.16 $\mu A\ \mu g^{-1}$ was found with a correlation coefficient of 0.9992. With a noise (peak-to-peak variation of the baseline) of 1.2 nA, the detection limit (3 × noise) was 3 ng per injection (25 μl). Especially from the measurement of the detection limit, it became clear that the noise was determined by eluent background effects and not by the detection system itself. The noise of the detection system was of the order of 0.1 nA. Thus the detection limit would be greatly improved if it were possible to minimize the eluent background effects. A means of eliminating the influence of eluent background effects has been described recently [23].

CONCLUSION

With this design the difficulties of applying pulse techniques in polarographic flow-through cells have been overcome. A knock pulse can successfully control the mercury drop-time. This makes synchronization of drop-time and electronics possible, without any mechanical disturbance of the flow pattern.

We thank W. P. van Bennekom for stimulating discussions and Prof. R. W. Frei for reviewing the manuscript.

REFERENCES

1 H. B. Hanekamp, P. Bos, U.A.Th. Brinkman and R. W. Frei, Fresenius Z. Anal. Chem., 297 (1979) 404.
2 H. B. Hanekamp, P. Bos and R. W. Frei, J. Chromatogr., 186 (1979) 489.
3 G. Willems and R. Neeb, Electroanal. Chem., 21 (1969) 69.
4 G. C. Barker and I. L. Jenkins, Analyst, 77 (1952) 685.
5 C. Auerbach, H. L. Finston, G. Kissel and J. Glickstein, Anal. Chem., 33 (1961) 1480.
6 R. C. Propst and M. H. Goosey, Anal. Chem., 36 (1964) 2382.
7 J. W. Hayes, D. E. Leyden and C. N. Reilley, Anal. Chem., 37 (1965) 1444.
8 B. Nygard, E. Johansson and J. Olofsson, J. Electroanal. Chem., 12 (1966) 564.
9 G. Papeshi, M. Costa and S. Bordi, Electrochim. Acta, 15 (1970) 2015.
10 Ch. Yarnitzky, Electroanal. Chem., 51 (1974) 207.
11 P. Corbusier and L. Gierst, Anal. Chim. Acta, 15 (1956) 254.
12 J. Riha, Advances in Polarography, Vol. I., 1960, p. 210.
13 H. P. Raayen and H. C. Jones, Anal. Chem., 34 (1962) 1594.
14 E. Verdier, R. Grand and P. Vanel, J. Chim. Phys., 66 (1969) 376.
15 B. K. Hahn and G. C. Enke, Anal. Chem., 46 (1974) 802.
16 E. G. and G. Princeton Applied Research, Model 310 (303) electrode, U.S. Patent 4, 142, 944; and manual.
17 H. B. Hanekamp, W. H. Voogt, P. Bos and R. W. Frei, Anal. Lett., 12 (A 2) (1979) 175.
18 J. H. Christie and R. A. Osteryoung, Electroanal. Chem., 49 (1974) 301.
19 D. G. Swartzfager, Anal. Chem., 37 (1976) 2189.
20 J. W. Dieker, W. E. van der Linden and H. Poppe, Talanta, 26 (1979) 511.
21 P. T. Kissinger, Anal. Chem., 49 (1977) 477 A.
22 W. A. McCrehan and R. A. Durst, Anal. Chem., 50 (1978) 2106.
23 H. B. Hanekamp, W. H. Voogt, P. Bos and R. W. Frei, Anal. Chim. Acta, 118 (1980) 81.

Analytica Chimica Acta, 118 (1980) 81—86
© Elsevier Scientific Publishing Company, Amsterdam — Printed in The Netherlands

AN ELECTROCHEMICAL SCRUBBER FOR THE ELIMINATION OF ELUENT BACKGROUND EFFECTS IN POLAROGRAPHIC FLOW-THROUGH DETECTION

H. B. HANEKAMP, W. H. VOOGT, P. BOS and R. W. FREI*

Department of Analytical Chemistry, Free University Amsterdam, De Boelelaan 1083, 1081 HV Amsterdam (The Netherlands)

(Received 12th February 1980)

SUMMARY

An electrochemical scrubber containing porous silver electrodes permits an efficient eluent clean-up for oxygen, metal traces and reducible organic impurities. The optimal working voltage can be determined for each system by obtaining a voltammogram. When the scrubber is used in conjunction with a dropping or hanging mercury electrode, a 100-fold reduction of the background current and a 10-fold reduction of the noise is achieved compared to a conventional nitrogen purge of the eluent. The influence of electrode surface area on noise and background current has been studied with various detector operation modes.

One of the problems in electrochemical flow-through detection is the large background current and the resulting baseline noise [1, 2]. This background current is caused by electrochemically active impurities in the eluent stream. In the reduction mode, one of the most important impurities is dissolved oxygen [3]. Other impurities that can cause interferences are metal ions and organic species if, for example, water—methanol mixtures are used. The dissolved oxygen can be removed by bubbling pure nitrogen through the eluent [1—4]. But even with this precaution the background current is typically 1 μA with our detector designs (−550 mV at the electrode with a flow rate of 1 ml min^{-1}, 50% (v/v) methanol—water, 0.1 M KNO_3, 10^{-3} M HNO_3). This background current is reasonably stable, hence it can to a certain extent be compensated electronically; but even a fluctuation of 0.1% in this current results in a variation in the baseline of 1 nA. Consequently, the variation in this background current is the major source of noise. Since peak currents of the order of nA have to be measured, the detection limits are unfavourably affected.

To eliminate these impurities a cell with porous silver flow-through electrodes was placed in the eluent stream. The impurities were electrochemically removed by applying a negative potential at these electrodes. This resulted in a very stable and much smaller background current, and so a very low noise level.

EXPERIMENTAL

The electrochemical eluent scrubber

This scrubber (Fig. 1) was designed to be used as a flow-through cell in the high-pressure part of a chromatographic system. The cell is able to withstand pressures up to 250 bar. The optimal position for this scrubber is immediately before the injection valve.

Porous electrodes were chosen to ensure a large electrode surface, hence it is possible to remove large quantities of impurities [4]. To increase the efficiency, the eluent stream is forced to pass through two electrodes (Fig. 1). Silver was chosen as electrode material because of its known, favourable behaviour in the reduction of dissolved oxygen [5, 6].

The cell is operated as a simple two-electrode system, which is sufficient for this kind of application. A stable high current potentiostat has to be used. Because of the large electrode area the electrical currents can be fairly high.

Apparatus

The eluent was pumped through by a Perkin-Elmer 601 pump. The eluent scrubber was constructed in our workshop. The potential on the silver electrodes was applied by a Wenking 68 FR 05 potentiostat (Gerhard Bank Elektronik, Göttingen) and controlled with a voltmeter. The chromatographic system consisted of an injection valve (Valco Instruments Co., Houston, Tex.) and a column (RVS, 10 cm, 4.6 cm i.d.) packed with LiChrosorb RP 8, 10 μm (Merck). The resulting background current and noise were measured with a Princeton Applied Research PAR 310 polarographic detector and with a PAR 174 polarograph. These currents were checked on a Tektronix 5103 N oscilloscope and recorded with a Kipp BD 30 X—Y recorder (Kipp —Zonen, Delft).

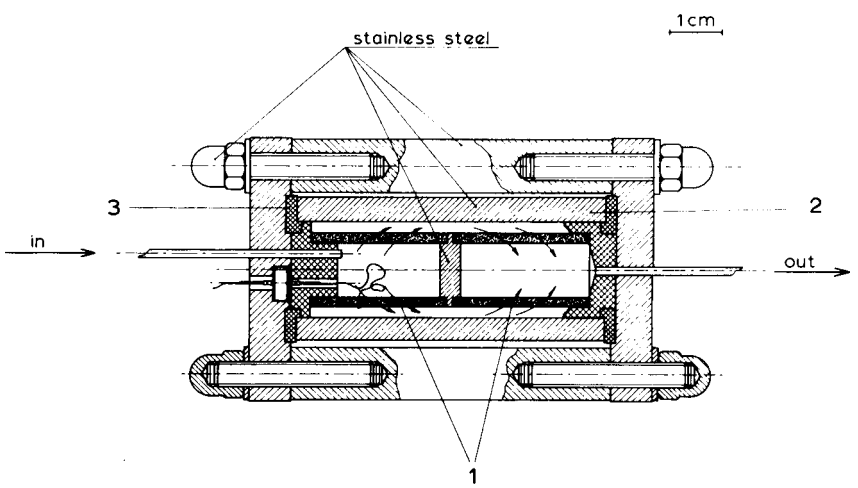

Fig. 1. The electrochemical eluent scrubber. (1) Porous silver electrodes; (2) steel housing, counterelectrode; (3) Delrin seals.

Chemicals

The eluent was deaerated by purging with nitrogen (A28) and/or ultrasonic treatment before it was poured into the pump cylinder. Methanol, nitric acid, potassium nitrate and sodium acetate (all Baker Analyzed chemicals) were used without further purification.

RESULTS AND DISCUSSION

The scrubbing potential

With an eluent flow rate of 1 ml min^{-1}, voltammograms were recorded with the scrubber. As can be seen from Fig. 2, simple addition of methanol greatly influences the background current, probably because of reducible organic impurities. This demonstrates that it is necessary to run a voltammogram of the eluent in order to find a suitable scrubber potential.

With a fast DME detector [1, 7] polarograms of the eluent were recorded at a fixed scrubbing potential. In Fig. 3 the values of the (background) current at −0.5 and −1.5 V are plotted vs. the scrubbing potential. As can be seen, the best results were obtained with a scrubbing potential of −1.4 to −1.5 V.

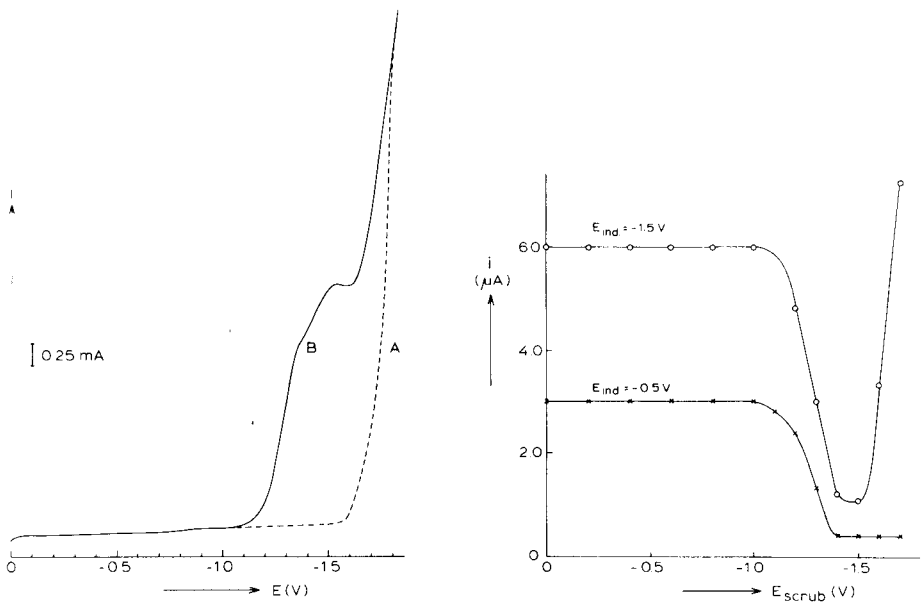

Fig. 2. Voltammograms of eluent recorded at the eluent scrubber; sweep-rate, 2 mV s^{-1}. (A) 0.25 M sodium acetate (or 0.1 M KNO_3) and 10^{-3} M HNO_3; (B) 3% methanol, 0.25 M sodium acetate (or 0.1 M KNO_3) and 10^{-3} M HNO_3; or 50% methanol, 0.1 M KNO_3 and 10^{-3} M HNO_3.

Fig. 3. Plot of background current in the polarographic detector vs. the scrubbing potential for two detector potentials (E_{ind}).

Similar results were obtained with other polarographic detectors. Once this scrubbing potential has been chosen, the background current is no longer dependent on the duration and the velocity of purging of the eluent with nitrogen. Nitrogen purging can be completely omitted but it is advisable to pre-clean the eluent with a nitrogen stream to diminish the electrical current in the electrochemical eluent scrubber.

The background current and noise

With a PAR 310 polarographic detector the effect of the use of a dropping mercury electrode (DME) or a hanging mercury drop electrode (HMDE) on the background current and noise were studied with different measuring techniques. A stock solution of eluent (0.25 M sodium acetate, 10^{-3} M nitric acid, 3% methanol) was purged by bubbling through nitrogen for at least 1 h. The eluent was ultrasonically degassed for a short time and poured into the pump cylinder. It was pumped through the scrubber and the chromatographic system at 1 ml min^{-1}. The background current and noise were measured without damping at −500 mV for the sampled d.c. and normal pulse (n.p.) techniques. With the differential pulse (d.p.) technique at a 25, 50 or 100-mV amplitude, the potential was varied between −475 and −500 mV, −450 and −500 mV, and −400 and −500 mV, respectively. The cathodic current was taken as positive. The noise was measured as the peak-to-peak variation in the baseline within a period of 2 min. The results are summarized in Tables 1 and 2.

As can be seen from the tables, the background current is far less than the current of 1 μA obtained without a scrubber, by just using nitrogen purging.

TABLE 1

The background current and noise at a DME detector (with column), after scrubbing

Drop-size[a]		Small (S)		Medium (M)				Large (L)			
Mode	Drop-time (s)	Baseline (nA)	Noise (nA)	Baseline (nA)	Ratio M:S	Noise (nA)	Ratio M:S	Baseline (nA)	Ratio L:S	Noise (nA)	Ratio L:S
Sampled d.c.	0.5	27.00	2.00	42.50	1.57	3.75	1.88	52.00	1.93	4.50	2.25
	1.0	20.75	1.50	37.00	1.78	1.75	1.77	47.75	2.30	2.50	1.67
N.p.	0.5	25.75	2.50	43.25	1.68	4.50	1.80	57.25	2.22	6.50	2.60
	1.0	21.25	1.50	35.50	1.67	4.00	2.67	48.50	2.28	5.50	3.67
D.p. 25	0.5	0.13	0.28	0.44		0.50	1.79	−0.69		0.64	2.29
	1.0	0.10	0.13	0.09		0.29	2.23	−0.71		0.30	2.31
D.p. 50	0.5	−0.31	0.25	0.85		0.36	1.44	−0.34		0.63	2.52
	1.0	−0.19	0.10	0.03		0.15	1.50	−0.61		0.17	1.70
D.p. 100	0.5	−0.34	0.28	1.48		0.56	2.00	−0.60		0.75	2.68
	1.0	−0.50	0.11	0.45		0.10	0.91	+0.15		0.24	2.18
Mean					1.68		1.74		2.18		2.39

[a]See text.

TABLE 2

The background current and noise at a HMDE detector (with column), after scrubbing

Drop-size		Small (S)		Medium (M)				Large (L)			
Mode	Drop-time (s)	Baseline (nA)	Noise (nA)	Baseline (nA)	Ratio M:S	Noise (nA)	Ratio M:S	Baseline (nA)	Ratio L:S	Noise (nA)	Ratio L:S
d.c.		10.12	0.60	19.00	1.88	0.98	1.63	20.00	1.98	1.35	2.25
Sampled d.c.	0.5	10.45	1.35	18.25	1.75	1.50	1.85	19.50	1.87	2.50	1.85
	1.0	10.10	1.10	17.75	1.76	1.25	1.14	18.75	1.86	2.50	2.27
N.p.	0.5	10.15	0.95	18.25	1.80	1.75	1.84	19.50	1.92	2.50	2.63
	1.0	10.10	0.80	17.88	1.77	1.38	1.73	18.75	1.86	1.88	2.35
D.p. 25	0.5	−0.43	0.23	−0.53		0.45	1.96	0.65		0.51	2.22
	1.0	−0.48	0.08	−0.54		0.10	1.25	0.68		0.15	1.88
D.p. 50	0.5	−1.05	0.30	−1.08		0.45	1.50	1.06		0.53	1.77
	1.0	−0.98	0.06	−1.13		0.10	1.67	1.18		0.14	2.33
D.p. 100	0.5	−1.98	0.23	−1.75		0.50	2.17				
	1.0	−2.10	0.06	−1.90		0.11	1.83				
Mean					1.81		1.69		1.90		2.17

The noise is also diminished by a factor of 10, compared to previous measurements under similar conditions (DME, d.c.) [1, 7]. The ratio for the surface area of the mercury drops designated small, medium and large is 1:1.59:2.52 (volume ratio 1:2:4). This ratio is similar to the ratio found for the noise for each size of drop, with all techniques. With the differential pulse technique the baseline is determined by the difference in background currents at the two potentials. For the other techniques the surface area ratio can be found at the DME (Table 1). At the HMDE (Table 2), the background current for the large mercury drop is slightly increased relative to that for the medium size drop.

Comparing the performance of the PAR detector in the DME and the HMDE modes, there is not much difference when the differential pulse technique is applied. However, with the sampled d.c. and normal pulse techniques the baseline and noise are larger for the DME. This is caused by the renewal of the electrode surface after every drop-life. At the HMDE there is the expected difference in baseline and noise with a longer cycle time. This results from the "time constant" introduced by the lower current-sampling frequency. Such a difference is larger at the DME, because of the decay of the faradaic current with longer drop-times. It should be kept in mind that with the PAR 310 electrode the drop-time and mercury drop surface area are governed electronically.

In a further set of experiments, the background current and noise were measured without a column in the system to investigate the influence of the column. The results for a HMDE (small drop-size) are presented in Table 3. With the d.c., sampled d.c. and n.p. techniques, the baseline and noise are

TABLE 3

The background current and noise at a HMDE detector (with column), after scrubbing

Mode	Drop-time (s)	Baseline (nA)	Noise (nA)	Mode	Drop-time (s)	Baseline (nA)	Noise (nA)
D.c.		4.10	0.02	D.p. 25	0.5	−6.45	0.08
					1.0	−5.45	0.03
Sampled d.c.	0.5	4.10	0.35				
	1.0	3.80	0.22	D.p. 50	0.5	−11.05	0.22
					1.0	−11.35	0.05
N.p.	0.5	3.43	0.53				
	1.0	3.33	0.40	D.p. 100	0.5	−25.38	0.29
					1.0	−26.38	0.05

decreased compared to the measurements with a column. In case of the d.p. technique the baseline is affected, but the noise is hardly changed, except with an amplitude of 25 mV. All these effects can be attributed to metal ions and can be decreased by using glass columns or glass-lined metal columns.

Conclusions

The background current and noise in electrochemical detection can be decreased if electrochemically active impurities are removed. This can be successfully accomplished by means of an on-line electrochemical eluent scrubber. The required potential to remove these impurities can be derived from a voltammogram recorded at this eluent scrubber. The time of continuous usage of such a scrubber can extend over several months without any change in performance. The background current in a polarographic flow-through detector is proportional to the electrode surface area, applying sampled d.c. or n.p. The noise is proportional to the electrode surface area, irrespective of the applied measuring technique.

It is conceivable that this scrubber principle can be used for other detection modes, for example, luminescence or other emission techniques.

We thank our workshop for their technical advice and skill which made this work possible.

REFERENCES

1 H. B. Hanekamp, W. H. Voogt, P. Bos and R. W. Frei, Anal. Lett., 12 (A2) (1979) 175.
2 H. B. Hanekamp, W. H. Voogt and P. Bos, Anal. Chim. Acta, 118 (1980) 73.
3 W. J. Blaedel and J. W. Todd, Anal. Chem., 30 (1958) 1821.
4 H. Khalifa, B. G. Ateya and E. A. S. Arafat, J. Electroanal. Chem., 81 (1977) 301.
5 E. A. Ostrovidov, Zh. Anal. Khim., 26 (1971) 1928.
6 R. E. Meyer, F. A. Posey and P. M. Lantz, Desalination, 11 (1972) 329.
7 H. B. Hanekamp, P. Bos, U. A. Th. Brinkman and R. W. Frei, Fresenius Z. Anal. Chem., 297 (1979) 404.

Analytica Chimica Acta, 118 (1980) 87—91
© Elsevier Scientific Publishing Company, Amsterdam — Printed in The Netherlands

DETERMINATION OF SELENIUM(IV) BY DIFFERENTIAL PULSE POLAROGRAPHY OF 4-CHLORO-*o*-PHENYLENEDIAMINE PIAZSELENOL

A. G. HOWARD*, M. R. GRAY and A. J. WATERS

Chemistry Department, The University, Southampton, Hampshire (Gt. Britain)

A. R. OROMIEHIE

Chemistry Department, Razi University, Kermanshah (Iran)

(Received 13th February 1980)

SUMMARY

Selenium(IV) can be determined by differential pulse polarography of the 4-chloro-*o*-phenylenediamine piazselenol. At pH 2.5 in formate buffer, the piazselenol gives two reduction peaks with peak potentials of —0.11 V and —0.63 V vs. SCE. At —0.11 V, the detection limit is 0.4 ng ml^{-1} (based on 3 times the standard deviation of the blank). Interferences from chromium(VI), copper(II), molybdenum(VI), nickel(II), tin(II), tellurium(IV) and vanadium(V) can be overcome by treatment of the sample with a chelating resin. The method is applicable to the determination of selenium(IV) in strongly saline solutions.

Selenium is a widely distributed essential element which may exhibit toxic effects at very low concentrations, and mimics sulphur in its speciation in biological and abiotic systems. Since the toxicological properties of different selenium compounds differ markedly [1], analytical procedures must be available to determine not only total selenium but also the various selenium species encountered in the environment. This paper deals with the determination of "inorganic" selenium(IV) compounds by differential pulse polarography and the application of the procedure to the analysis of polluted waters.

D.c. polarography of selenium(IV) gives two reduction waves as selenium(IV) is successively reduced to elemental selenium and then to selenium(—II) at the dropping mercury electrode [2, 3]. D.c. polarography of selenium(IV) is, however, insensitive and suffers from severe interference problems, especially from those metals which form insoluble selenides. Improved sensitivity can be achieved by differential pulse polarography of selenium(IV) and detection limits of 8 $\mu g\ l^{-1}$ have been obtained [4]. In order to increase sensitivity and selectivity, stripping techniques have been applied to the determination of selenium and detection limits of approximately 0.1 $\mu g\ l^{-1}$ have been reported [4—6].

Colorimetric and fluorimetric methods of analysis for selenium are dominated by the use of aromatic diamines and their reaction with selenium(IV)

to give piazselenols [7—9]. This piazselenol reaction has been exploited for the polarographic determination of selenium(IV) with 3,3′-diaminobenzidine [10]. In 0.1 M ammonium perchlorate at pH 2.5, two piazselenol waves were obtained ($E_{1/2}$ = −0.17 and −0.63 V vs. SCE) which could be used for quantitative analysis. Gas chromatography of piazselenols has proved useful in the determination of selenium in steel [11].

After initial studies of the polarographic behaviour of several piazselenols, 4-chloro-*o*-phenylenediamine was selected for further investigation. The results of those investigations are reported below.

EXPERIMENTAL

Reagents, glassware and instrumentation

Unless otherwise stated, all reagents were of analytical-reagent grade. Selenium standards were prepared from a 1000 μg Se ml^{-1} stock selenous acid solution. 4-Chloro-*o*-phenylenediamine (4-Cl-PDA; reagent quality) was used as supplied. A stock solution containing 0.5% (w/v) 4-Cl-PDA was prepared in aqueous ethanol (1 + 1). Formate buffer solutions were prepared by adjusting 0.6 M formic acid to the desired pH value with ammonia solution.

All glassware was soaked in 1 M hydrochloric acid and rinsed with distilled water before use.

The differential pulse polarograph was a Princeton Applied Research Model 174A Polarographic Analyser fitted with a Model 172 drop timer. The instrument was operated under the following conditions: pulse amplitude, 25 or 50 mV; drop time, 0.5 or 1 s; scan rate, 10 mV s^{-1}.

Procedure

The piazselenol solutions were prepared by the addition of microlitre quantities of the selenium(IV) stock solution to 2.5 ml of the complexing agent solution and the mixture was then made up to 50 ml with pH 2.5 buffer solution. The solutions were allowed to stand at room temperature for 1 h and were degassed with nitrogen prior to obtaining differential pulse polarograms of the piazselenol solutions.

RESULTS

Formation of 4-chloro-o-phenylenediamine piazselenol

The pH at which the piazselenol is formed determines the kinetics of formation, yield of the piazselenol and the product stability. To avoid decomposition of the piazselenol, it is not possible to adjust the solution pH prior to the polarographic determination although the peak potential is pH-dependent. The selection of solution acidity is, therefore, crucial to the optimization of the procedure. Preliminary spectrophotometric investigations of the piazselenol in formate buffer solutions indicated that the piazselenol formation was favourable at pH 2.5 but that the reaction yield dropped to

zero at pH 7. Over the pH range 1.5—3 the piazselenol solutions exhibited maximum absorbance (λ_{max} = 340 nm, ϵ = 31,250 l mol^{-1} cm^{-1}) and a pH 2.5 formate buffer solution was therefore selected for further investigations.

Polarographic studies of the rate of formation of the piazselenol indicated that the half-time for reaction was approximately 8 min at pH 2.5 (20°C) giving rise to an optimum reaction time of 1 h. No evidence of piazselenol decomposition was observed 3 h after mixing the reagents.

Polarographic behaviour of 4-chloro-o-phenylenediamine piazselenol

When the piazselenol solutions were prepared as described under Experimental, the resulting polarograms gave two selenium-dependent reduction peaks at −0.11 and −0.62 V vs. SCE. Two other reduction peaks, at −0.41 and −0.97 V vs. SCE were independent of selenium concentration (Fig. 1) and are believed to be due to impurities in the 4-chloro-*o*-phenylenediamine. Attempts to utilize the diamine dihydrochloride instead of the free diamine resulted in erratic results and failed to remove the peaks at −0.41 and −0.97 V vs. SCE peaks. Of the two selenium-dependent peaks, the more sensitive one at −0.11 V vs. SCE was selected for further investigation. The effect of the pH of the background electrolyte was investigated by obtaining differential pulse polarograms of the piazselenol solutions over the pH range 1.2—4.5. Over this range the peak potential of the first piazselenol reduction was dependent on pH and varied by 0.19 V (Fig. 2). The piazselenol yields discussed in the preceding section were confirmed by the polarographic results and a pH of 2.5 was therefore selected for further investigation.

Calibration, reproducibility and detection limits. Over the studied range of 1—200 ng Se ml^{-1}, the peak current was linear with respect to concentration. Based on three times the standard deviation of the blank, the detection limit

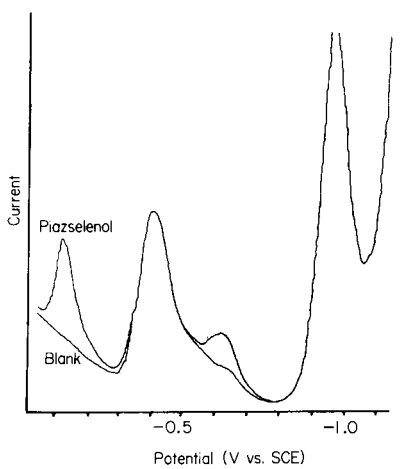

Fig. 1. Polarogram of 4-Cl-PDA piazselenol in formate buffer (pH 2.5).

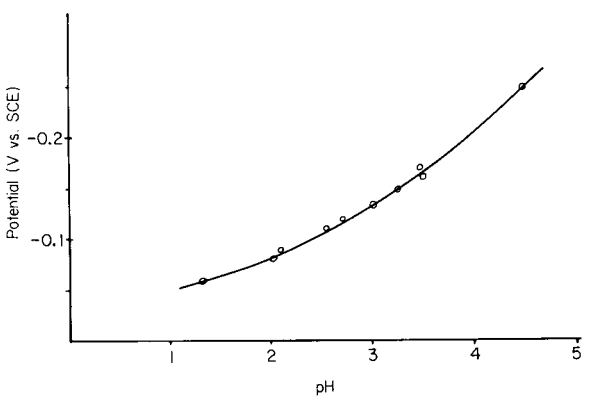

Fig. 2. Effect of pH on the potential of the initial piazselenol reduction peak.

was 0.4 ng Se ml^{-1}. Replicate analyses of 80 and 1 ng Se ml^{-1} solutions gave relative standard deviations of 1.9 and 6.8%, respectively.

Interference effects

Interferences were studied by the addition of an excess of foreign ions to standard solutions prior to formation of the piazselenol. The results of these experiments are given in Table 1; in addition there was no interference from bromide, fluoride, iodide, sulphate or phosphate at the 800 ng ml^{-1} level. Major interference effects were observed for chromium(VI), copper(II), molybdenum(VI), nickel(II), tin(II), tellurium(IV) and vanadium(V). In most cases, the interference problems arise from reduction peaks close to, or superimposed upon, the analyte reduction peak. In the case of those interferents exhibiting oxidizing properties, a reduction of the piazselenol peak height would be expected because of oxidation of selenium(IV) to selenium(VI).

An effective preliminary treatment for both fresh and sea-water samples is elution of the water sample through a Chelex-100 resin column. Chelex-100 (100—200 mesh) was packed into 5 cm × 1 cm i.d. glass columns and washed with distilled water, hydrochloric acid (1 M) and then formate buffer (pH 2.5). Filtered water samples (50 ml) were buffered to pH 2.5 with formate buffer in the volume ratio 10:1 and were passed through the Chelex-100 column at a flow rate of 2 ml min^{-1}. The column was washed with 20 ml of formate buffer and the combined eluents were made up to 100 ml with 0.5% (w/v) 4-Cl-PDA solution (5 ml) and formate buffer. Polarograms of the resulting solution were obtained one hour after the addition of the 4-Cl-PDA.

Initial studies demonstrated that the level of selenium(IV) present in local sea water (Southsea, Hampshire) was low and samples were therefore spiked with selenium(IV) to give concentrations between 15 and 60 μg Se l^{-1}. Following sample pretreatment with Chelex-100 as outlined above, an overall recovery of 99.5 ± 1.7% (range 96.7—102%) was obtained.

TABLE 1

Interferences and tolerance limits for diverse ions

No interference		No interference		Interference		
Ion	Concn. in cell (ng ml^{-1})	Ion	Concn. in cell (ng ml^{-1})	Ion	Concn. in cell (ng ml^{-1})	Interfering E_p[a] (V vs. SCE)
Ag(I)	1860	Cr(III)	2174	Cr(VI)	2000	−0.23
As(III)	100	Fe(II)	2144	Cu(II)	2000	−0.05
As(V)	100	Fe(III)	2016	Mo(VI)	800	−0.03
Ba(II)	3370	Mg(II)	2030	Ni(II)	2000	−0.22
Ca(II)	2030	Mn(II)	2020	Sn(II)	2638	−0.12
Cd(II)	2000	Pb(II)	2000	Te(IV)	2000	−0.15
Co(II)	2040	Zn(II)	2000	V(V)	2000	

[a]Only when the interferent gives a peak in the region of the piazselenol peak is the reduction potential quoted.

TABLE 2

Analysis of estuarine water samples

Sample	Grid reference	Selenium content ($\mu g\ l^{-1}$)	Comment
1	451156	12.2	Industrial discharge?
2	446155	<4.0	
3	440160	<4.0	
4	436145	19.2	Downstream from sewage works
5	435137	14.9	Downstream from sewage works

The procedure was applied to the determination of selenium(IV) in filtered samples of water obtained from the River Itchen (Hampshire). The results are given in Table 2.

DISCUSSION

Differential pulse polarography of the 4-chloro-*o*-phenylenediamine piazselenol provides a sensitive technique for the determination of selenium. At pH 2.5 the derivatization of the selenium is complete within 45 min of mixing the reactants, and the mixture, with certain limitations, can be analysed directly without further sample treatment. The sensitivity of the technique compares favourably with those of most other procedures.

The interferences from chromium(VI), copper(II), nickel(II), tin(II), tellurium(IV) and vanadium(V) will normally require the sample pretreatment prior to the polarographic step in applied work. In all cases except those of tin(II) and vanadium(V), the interfering reduction peaks can be observed and partially identified in a preliminary polarogram of the sample solution. For such elements, any observed interference effects are primarily due to incomplete resolution of the piazselenol and interfering peaks; although the peaks can be distinguished visually, such assessment is insufficient for quantification of the selenium. The procedure is suitable for the determination of selenium(IV) in samples containing high concentrations of sodium chloride, such as marine and estuarine waters, and should be applicable to a wide range of sample types.

REFERENCES

1 F. B. Cousins and I. M. Cairney, Aust. J. Agric. Res., 12 (1961) 927.
2 L. Schwaer and K. Suchy, Collect. Czech. Chem. Commun., 7 (1935) 135.
3 J. J. Lingane and L. W. Niedrach, J. Am. Chem. Soc., 70 (1948) 4115.
4 A. M. Shafiqual Alam, O. Vittori and M. Porthault, Anal. Chim. Acta, 87 (1976) 437.
5 F. Vajda, Acta Chem. Acad. Sci. Hung., 63 (1970) 257.
6 R. W. Andrews and D. C. Johnson, Anal. Chem., 47 (1975) 294.
7 J. Hoste, Anal. Chim. Acta, 2 (1948) 402.
8 J. H. Watkinson, Anal. Chem., 38 (1966) 92.
9 M. Tanaka and T. Kawashina, Talanta, 12 (1965) 211.
10 C. Le Peintre, C. R. Acad. Sci., 252 (1961) 1968.
11 M. Akiba, Y. Shimoishi and K. Toei, Analyst, 100 (1975) 648.

Analytica Chimica Acta, 118 (1980) 93—100
© Elsevier Scientific Publishing Company, Amsterdam — Printed in The Netherlands

THE USE OF EQUILIBRIUM REACTIONS IN POTENTIOMETRIC ANALYSIS
Determination of Weak acids, Bases and Electron-Pair Donors Forming Complexes of Low Stability

K. BURGER*, G. PETHÖ and B. NOSZÁL

Department of Inorganic and Analytical Chemistry, L. Eötvös University, P.O. Box 123, H-1443 Budapest (Hungary)

(Received 15th May 1979)

SUMMARY

Equilibrium reactions which do not proceed quantitatively at titration equivalence points, e.g. reactions involving weak bases or weak acids, or metal complexes or precipitates with low equilibrium constants, can be utilized analytically by plotting the concentration of the reagent consumed (e.g. the bound proton or bound metal concentration, etc., measured potentiometrically) as a function of the volume of titrant. Saturation (or maximum) curves are thus obtained and the limiting value is equivalent to the concentration of the base (or ligand) to be determined. The concentration of bound proton (or bound metal) is calculated from the difference between the total reagent concentration added and the concentration of the free protons (or uncomplexed metal ions) measured potentiometrically. The theoretical principles of this approach based on equilibrium calculations and some examples of its practical application are presented.

Many attempts have been made to apply equilibria which do not proceed quantitatively at the apparent end-point of potentiometric titrations. Most of these [1—5] are based on linearization of titration curves which do not show realistic inflection points. Rossotti [6] mentioned the use of Bjerrum's formation function [7] based on the average coordination number ($\bar{n}$) for the potentiometric determination of weak acids in aqueous solutions but results appear not to have been published. The present paper describes a rather general procedure for the use of weak electrolyte equilibria in potentiometric analysis which is also based on Bjerrum's $\bar{n}$ function.

THEORY

Molecules containing donor atoms or basic functional groups coordinate metal ions or protons to form metal complexes or weak acids, respectively. When an excess of a suitable metal ion (or proton) is added, each donor atom of the ligand coordinates a metal ion (or proton) and further increases in the titrant concentration have no further effect. Thus titration of a suitable electron-pair donor with a standard solution of the appropriate metal ion, or

titration of a base with a standard acid solution, followed by plotting the concentration of the metal ion bound to the donor molecule (or that of the protons bound to the base), i.e., the numerator in Bjerrum's $\bar{n}$ function, against the volume of the standard solution will yield a saturation curve. In practice, because of the effect of dilution during titration, maximum curves are formed. The concentration of the bound metal ion (or proton) at the maximum of this curve is equivalent to the concentration of the donor molecule (base) to be determined. The equivalent weight is given by the number of the donor groups in the molecule.

The bound metal (or proton) concentration can be calculated from the difference between the total known metal (or proton) concentration and the free (uncomplexed) metal ion (or proton) concentration measured potentiometrically, and so any ion or molecule A which reacts with reagent X, in one step or successively, in the equilibrium reaction

$$rA + pX \rightleftharpoons A_rX_p \tag{1}$$

can be determined by using a standard solution of X if a suitable potentiometric indicator electrode is available to determine the free (uncomplexed) concentration of X [X].

The analysis is done analogously to normal potentiometric titrations except that the ionic strength of all solutions must be kept constant by adding an inert salt (e.g., sodium perchlorate) and the volume of the solution at the beginning of the titration (v_0) must be known. Constant ionic strength is necessary to ensure that the activity coefficients remain constant; the electrode can thus be calibrated to measure the concentration of free X. The total concentration of X, C_i, is calculated after addition of v_i ml of the standard solution of concentration C_X at each point of the titration from the equation $C_i = C_X v_i/(v_0 + v_i)$, as well as the concentrations of free X from the Nernst Law:

$$[X] = 10^{(E_i - E_0)z/0.059} \tag{2}$$

The E_0 value is determined from e.m.f. measurements in solutions of identical ionic strength containing known concentrations of X.

For quantitative evaluation, the differences $C_i - [X]$ are plotted as a function of the additions v_i of the standard solution. The horizontal section (or possibly the maximum value) of this curve is projected to the ordinate to obtain the concentration of bound X corresponding to the quantitative formation of A_rX_p: $(C - [X]_q)$. The initial concentration of A to be determined (C_A) can then be calculated from

$$C_A = (r/p)(C - [X]_q)(v_0 + v_i)/v_0 \tag{3}$$

Equation (1) is a general form representing protonation, or metal complex or precipitate formation, and X can denote protons, metal ions or ligands that can be determined by direct potentiometry.

The neutralization of weak acids in aqueous solution may be regarded as

hydroxide ion coordination (disregarding the dissociation step). If a strong base is used as the standard solution, X denotes the free hydroxide which can be measured potentiometrically with a glass electrode. Thus the procedure can also be applied for the determination of weak acids in aqueous solutions.

Sources of error

The total error of this procedure originates from two sources: (a) the state of the equilibrium at the saturation section of the $(C - [X])$ vs. v_i curve (theoretical error) and (b) the experimental error which arises mainly from the e.m.f. measurement but also depends on the accuracy of the concentration of the standard solution, of the volume measurement during titration, etc. Both types of error can be characterized by equilibrium calculations as shown for the following model reaction:

$$A + X \rightleftharpoons AX; \quad AX + X \rightleftharpoons AX_2 \tag{4}$$

The two steps may overlap, therefore the formation of AX_2 is accepted as the basis of the analytical procedure.

Theoretical error. According to the equilibrium model, $C_A = [A] + [AX] + [AX_2]$ and $C = [X] + [AX] + 2[AX_2]$. Along the saturation section of the curve representing $C - [X]$ vs. volume of titrant, $[AX_2] \gg [A] + [AX]$, and so $C - [X]_q = [AX] + 2[AX_2] \approx 2C_A$. The theoretical error (in relative %, $\Delta\%$) depending on the state of the equilibrium at this part of the curve is

$$\Delta\% = [2C_A - (C - [X]_q)]\ 100/2C_A \tag{5}$$

Substitution of the expressions given for C_A and $(C - [X]_q)$ into eqn. (5), description of $[AX]$ and $[AX_2]$ by the equilibrium constants K_1 and K_2 for eqns. (4), and appropriate reduction gives the expression

$$\Delta\% = (2 + K_1[X]_q)\ 100/2(1 + K_1[X]_q + K_1K_2[X]_q^2) \tag{6}$$

Thus the theoretical error can be calculated from the $[X]_q$ values measured on the maximum of the $(C - [X])$ vs. volume of titrant curve.

All these considerations reflect a principal advantage of the proposed method which lies in the fact that the standard reagent solution can be added in a suitable excess to ensure quantitative formation of the reaction product AX_2 (with a correspondingly low $\Delta\%$). Many chemical reactions which do not proceed quantitatively at the equivalence point of conventional titrations can therefore be utilized in this pseudotitration procedure.

Experimental error. The equation for the calculation of experimental errors resulting from error in the e.m.f. measurements can be derived simply by substituting $[X]$ from eqn. (2) into eqn. (5). The experimentally observed errors are presented in the discussion of the practical applications below. The data given indicate the high accuracy achieved even when measurements are made on a semimicro concentration scale.

The selectivity of the procedure

If two (or more) electron-pair donors A and B are simultaneously present in a solution, it will depend on their concentration ratio C_A:C_B and on the difference between the corresponding equilibrium constants, K_A and K_B, whether or not A (having the higher affinity for X) can be measured in the presence of B. With the aid of the following equilibrium calculations, it is easy to establish the correlation between the equilibrium constants K_A, K_B and the C_A:C_B ratio that permits the analysis to be done with a given error.

If the solution contains two donor molecules A and B, both of which contain only one donor group, then the usual mass-balance equations are

$$C_A = [A] + [AX] = [A]\ (1 + K_A\ [X]) \tag{7}$$

$$C_B = [B] + [BX] = [B]\ (1 + K_B\ [X]\ ) \tag{8}$$

and

$$C = [X] + [AX] + [BX] \tag{9}$$

where K_A and K_B are the formation constants of AX and BX, respectively. The expression used for the analytical evaluation of the experimental data is

$$C - [X] = [AX] + [BX] \tag{10}$$

If $K_A > K_B$ and A is to be determined with an error of Δ% (relative) in the presence of B, then at the saturation section of the curve $C - [X]$ vs. volume of standard solution,

$$[C_A - (C - [X]_q)]\ 100/C_A = \Delta \tag{11}$$

Substitution of $C - [X]$ from eqn. (10) into eqn. (11) and expression of [AX] and [BX] from eqns. (7) and (8) followed by appropriate reduction, with restriction to the saturation section of the curve, gives

$$C_A/C_B = \{K_B[X]_q(1 + K_A\ [X]_q)\}/\{(1 + K_B[X]_q)(1 - \delta - \delta\ K_A[X]_q)\} \tag{12}$$

where $\delta = \Delta/100$. This equation makes it possible to calculate the total concentration ratio of A and B which permits the determination of A in the presence of B with an error of Δ%, provided that K_A and K_B are known and $[X]_q$ is measured on the horizontal part (or maximum) of the analytical curve.

PRACTICAL APPLICATIONS

On the basis of the above discussion, the main groups of substances that can be analysed by this approach are: nitrogen bases, molecules containing carboxylate groups, weak acids containing a phenolic or imino proton, mono- and polyfunctional ligands binding heavy and transition metals, Lewis acids binding halide ions and many other complex systems.

A few examples chosen from these groups are used to illustrate the experimental analysis of the error incurred and its sources.

TABLE 1

Measurements of weak bases and acids

Compound	log K	Concn. (M)	Standard soln.	Observed total error (Δ %)	Calculated deviation (rel. %) fro mean value caused by error of	
					±0.2 mV in e.m.f.	±3% in v_i
Pyridine	5.15	0.1	0.2 M HCl	−0.01	±0.006	±0.4
		0.01	0.1 M HCl	−0.26	±0.04	±0.08
		0.001	0.1 M HCl	−2.9	±0.11	±0.01
Sodium acetate	4.76	0.1	0.2 M HCl	−0.39	±0.01	±0.5
		0.01	0.1 M HCl	−2.5	±0.09	±0.09
		0.001	0.1 M HCl	−4.1	±0.3	±0.01
Theophylline	5.20	0.1	0.2 M KOH	+0.65	±0.02	±0.5
		0.01	0.1 M KOH	−0.4	±0.06	±0.09
		0.001	0.1 M KOH	+1.3	±0.3	±0.01
Phenol	4.11	0.1	0.2 M KOH	−0.4	±0.03	±0.5
		0.01	0.1 M KOH	−3.8	±0.1	±0.01

Determinations based on protonation—deprotonation equilibria

The first model systems, weak monofunctional bases and acids, are shown in Table 1. The constants (log K) characterizing the corresponding equilibria $A + X \rightleftharpoons AX$ (where X is H^+ in the determination of bases and OH^- in that of acids) are listed. The experimentally observed total errors (% relative) refer to concentrations determined by independent methods. The calculated deviations from the mean value caused by an uncertainty of ±0.2 mV in the e.m.f. measurement or ±3% in the v_i value are also listed.

These analyses were done like conventional potentiometric titrations, with an Orion model 701A digital pH meter. An Orion 91-01-00 glass electrode was used for measurement of the free proton concentration, with a silver/silver chloride reference electrode in a Wilhelm bridge. The standard solution was measured from a Radiometer ABU12 automatic burette. The initial volume (v_0) of the sample solutions was 10.00 ml in the case of the 0.1 M solutions and 20.00 ml for the rest. The ionic strength of each solution was adjusted to 0.1 or 0.2 with potassium nitrate. The calculations needed for the construction of the curves of $C - [X]$ vs. ml of standard solution, based on the expressions for C_i and [X], were done with a programmable pocket calculator (TI 58).

The data in Table 1 clearly show that weak acids and bases which cannot be determined by the usual acid—base titrations in aqueous solutions can be measured using the proposed method even in 10^{-2}—10^{-3} M solutions with good accuracy.

Figure 1 presents, as examples, the primary curves for mV vs. ml of titrant and the corresponding curves for $C - [X]$ vs. ml derived from the primary

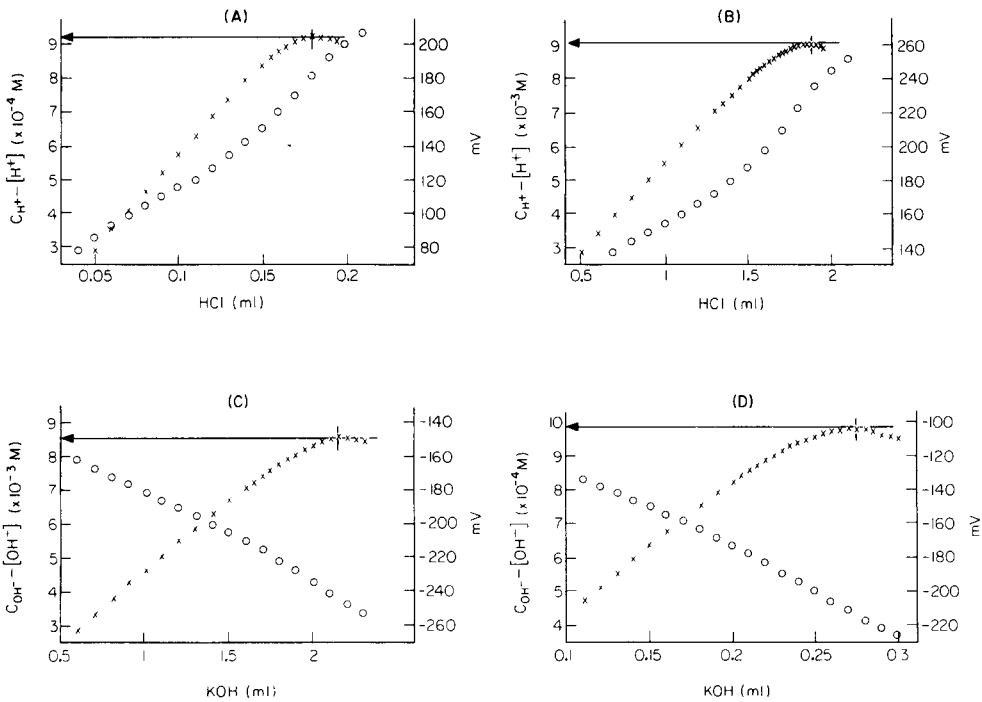

Fig. 1. The primary potentiometric titration curves for 20.00 ml of aqueous sample solution (○) and the derived curves $C_H - [H^+]$ (or $C_{OH} - [OH^-]$) vs. ml of titrant (×): (A) 0.001 M pyridine with standard 0.1 M HCl; (B) 0.01 M sodium acetate with standard 0.1 M HCl; (C) 0.01 M phenol with standard 0.1 M KOH; (D) 0.001 M theophylline with standard 0.1 M KOH. In all cases the ionic strength was adjusted to 0.1 with potassium nitrate.

curves, for titrations of 0.001 M pyridine and 0.01 M sodium acetate both with 0.1 M hydrochloric acid, and for titrations of 0.01 M phenol and 0.001 M theophylline both with 0.1 M potassium hydroxide. The weak acids must be determined either in CO_2-free solutions or the CO_2 content must be determined in a blank measurement. Comparison of the primary conventional titration curves with those constructed on the basis of the new approach gives immediate proof of the superiority of the latter. None of the primary titration curves showed an inflection which could be evaluated as the endpoint of the titration by conventional methods.

Determinations based on metal complex formation

The complex formation of methionine with silver(I) and the complex formation of angiotensin II polypeptide containing 8 amino acids (Asn—Arg—Val—Tyr—Ileu—His—Pro—Phe) with zinc(II) were selected as the first reactions to be examined. Both ligands coordinate only one metal ion per molecule. The complex formation proceeds quantitatively with good accuracy in the presence of an excess of the metal ion.

The free (uncomplexed) silver (I) concentration was measured by a Radiometer silver electrode (P 4011). For the determination of the uncomplexed zinc(II) concentration, a membrane electrode containing a benzalkonium-tetrathiocyanatozincate ion pair as electroactive substance incorporated into a polyvinyl chloride matrix was prepared. This zinc electrode was prepared as described previously [8] for a cobalt-selective electrode; the electrode showed a reversible Nernstian function in the zinc concentration interval of 10^{-1}—10^{-4} M with a slope of 29.2 mV.

For the methionine determination, a 5.00-ml aliquot of a 0.1 M solution was titrated with a standard 0.5 M silver nitrate solution. The ionic strength was maintained at 0.5 by potassium nitrate and the pH at 5 or 6 by 0.01 M sodium acetate—acetic acid buffer. A primary titration curve and the corresponding derived $C_{Ag} - [Ag]$ vs. ml of titrant curve are shown in Fig. 2.

For the determination of angiotensin II, a 7.00-ml portion of a 0.001 M solution was titrated with a standard 0.1 M zinc nitrate solution; the ionic strength was maintained at 3.0 with potassium thiocyanate and the pH at 5 or 6 by a 0.01 M sodium acetate—acetic acid buffer. Typical primary and derived curves are compared in Fig. 3.

The results of these determinations are presented in Table 2. The data indicate the good accuracy of the measurements.

Selective determinations

Bases having different protonation constants, or ligands having different complex stability constants, may be determined in mixtures. The feasibility of such analyses was demonstrated for the determination of theophylline in the presence of theobromine or caffeine, and for methionine in the presence of leucine. The results are presented in Table 3. Theophylline could be determined in a 20.00-ml portion of a 0.001 M solution by titration with 0.1 M potassium hydroxide titrant in the presence of 10^{-4} M theobromine or 10^{-2} M caffeine at ionic strength 0.1 (potassium nitrate). The selective deter-

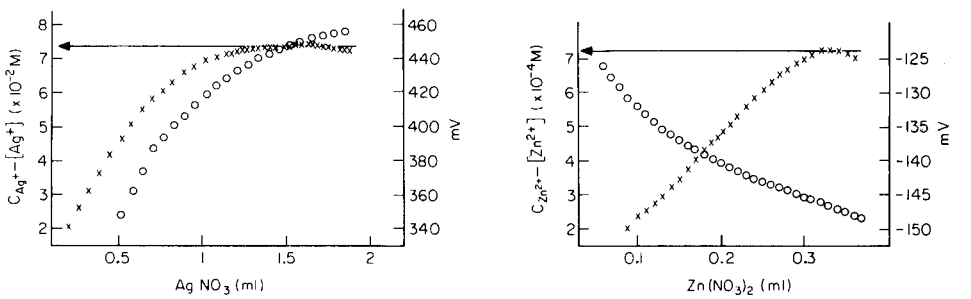

Fig. 2. The primary potentiometric titration curve for 5.00 ml of 0.1 M methionine in aqueous solution with standard 0.5 M $AgNO_3$ (○) and the derived curve $C_{Ag} - [Ag^+]$ vs. ml of titrant (×). Ionic strength adjusted to 0.5 with potassium nitrate.

Fig. 3. The primary potentiometric titration curve for 7.00 ml of 0.001 M angiotensin in aqueous solution with standard 0.1 M $Zn(NO_3)_2$ (○) and the derived curve $C_{Zn} - [Zn^{2+}]$ vs. ml of titrant (×). Ionic strength adjusted to 3.0 with potassium thiocyanate.

TABLE 2

The results of measurements based on complex formation

Compound	Concn. (M)	Standard soln.	Observed total error (Δ%)	Calculated deviation (rel. %) from mean value caused by an error of:	
				±0.2 mV in e.m.f.	±3% in v_i
Angiotensin pH ≈ 6	0.001	0.1 M $Zn(NO_3)_2$	+0.68	±3.7	±0.1
Angiotensin pH ≈ 5	0.001	0.1 M $Zn(NO_3)_2$	+2.62	±3.0	±0.1
Methionine pH ≈ 6	0.1	0.5 M $AgNO_3$	+1.5	±0.5	±0.5
Methionine pH ≈ 5	0.1	0.5 M $AgNO_3$	+0.3	±0.4	±0.4

TABLE 3

The results of selective determinations

Compound measured	Concentration (M)	Accompanying compound	Concentration ratio	Observed total error (Δ%)
Theophylline	0.001	—	—	−1.5
	0.001	Theobromine	20:1	+2.2
	0.001	Caffeine	1:10	−0.7
Methionine	0.1	—	—	+1.5
	0.1	Leucine	1:1	+0.5

mination of theophylline in the mixtures was made possible because its acidity is greater than that of the accompanying substances.

Methionine could be determined in the presence of an equal amount of leucine in a 5.00-ml portion of a 0.1 M solution by using 0.5 M silver nitrate as titrant, since methionine, which contains a thioether sulphur atom, has a higher affinity for silver ion than the other sulphur-free amino acids. The data in Table 3 reflect the good accuracy of these measurements.

REFERENCES

1 G. Gran, Acta Chem. Scand., 4 (1950) 559; Analyst, 77 (1952) 661.
2 F. Ingman and E. Still, Talanta, 13 (1966) 1431.
3 J. Buffle, Anal. Chim. Acta, 59 (1972) 439.
4 J. Buffle, N. Pathasarathy and D. Monnier, Anal. Chim. Acta, 59 (1972) 427.
5 P. Chakarova and O. Budevsky, Pharmazie, 30 (1975) 524; J. Electroanal. Chem., 73 (1976) 369.
6 H. Rossotti, Chemical Application of Potentiometry, Van Nostrand, London, 1969, p. 154; The Study of Ionic Equilibria, Longmans, London, 1978, p. 82.
7 J. Bjerrum, Metal Ammine Formation in Aqueous Solutions, Haase, Copenhagen, 1941.
8 K. Burger and G. Pethö, Anal. Chim. Acta, 107 (1979) 113.

Analytica Chimica Acta, 118 (1980) 101—108
© Elsevier Scientific Publishing Company, Amsterdam — Printed in The Netherlands

QUANTITATIVE PHOTOACOUSTIC SPECTROSCOPY OF CHEMICALLY-MODIFIED SILICA SURFACES

C. H. LOCHMÜLLER* and D. R. WILDER

Paul M. Gross Chemical Laboratory, Duke University, Durham, NC 27706 (U.S.A.)

(Received 31st January 1980)

SUMMARY

The degree of surface coverage on chemically-modified silica gel was determined by using photoacoustic spectroscopy. Vibrational overtones in the near-infrared were employed for the examination of modified materials containing bonded aliphatic, aromatic, and aminoalkyl functions. A linear relationship between photoacoustic signal amplitude and carbon or nitrogen content on the chemically-modified surface was obtained.

Photoacoustic spectroscopy (p.a.s.) has recently been shown to be a valuable method for the acquisition of molecular spectroscopic information from chemically-modified solid surfaces [1—5]. It is an especially useful technique when applied to the examination of modified microparticulate powders such as silica gel and alumina, and metal oxides, i.e., materials that find use as sorbents and catalysts. Photoacoustic spectroscopy can provide optical absorption data from the superstratum of immobilized molecules that make up the modified surface without experiencing interference from the powdered support matrix. The opacity and the light-scattering nature of the microparticulate substrates make examination of these surface-modified powders difficult by conventional transmission and reflectance techniques.

To date, photoacoustic studies of modified materials have focused on obtaining a qualitative spectroscopic characterization of the chemically-modified surface but the method has the potential for providing quantitative information about surface coverage on these materials as well. A recent report has demonstrated the value of p.a.s. for the accurate and sensitive determination of a solute sorbed on t.l.c. plates [6]. Surface-coverage determinations on derivatized microparticulate powders are typically made by using titrimetric methods if the immobilized function contains a chemically-active group [7], or by elemental carbon—hydrogen determinations for unreactive bonded species, e.g., surface-bound hydrocarbons. Photoacoustic spectroscopic analysis of these samples would offer significant advantages in terms of speed of analysis, ease of sample preparation, the non-destructive nature of a spectroscopic method, and the potential for the simultaneous acquisition of qualitative data. Although absolute quantitative determination in p.a.s. is more difficult than in conventional transmission spectrometry because of the

intimate dependence of signal amplitude in p.a.s. on such sample properties as thermal diffusion length, reflectivity, and luminescence yield, accurate results may nevertheless be obtained with the construction of calibration plots and the limitation of an analysis to similar sample types.

This work presents the results of a quantitative determination of surface coverage on chemically-modified silica gels. The materials examined typify those commonly used as chemically-bonded stationary phases in chromatographic applications and make use of alkyl-, phenyl-, and aminoalkyl-modified silicas, but the methods employed in this study should permit application to other modified solid substrates. The examination of these silicas was based on information obtained from the near-infrared spectral region. This region provides absorption data arising principally from vibrational overtones of the X—H stretch mode, where X is most commonly C, N, or O. While the molar absorptivity of these overtone bands is low, the degree of surface coverage that is normally obtained on high surface area silicas using current derivatization methods results in dense surface concentrations. These materials give rise to sufficiently intense absorption bands to allow for sensitive and reproducible measurement. In fact, the low molar absorptivities are an advantage in the case of these densely-covered materials because work becomes possible in a spectral region that is free from problems of photoacoustic saturation [8], a potential concern if the analysis were dependent upon strongly-absorbing ultraviolet or visible chromophores. The near-i.r. in p.a.s. is useful because it provides well-resolved absorption bands, relatively free from interferences, and, if the C—H stretch overtones are the absorptions monitored, the region is more universally useful than the u.v.—visible region. Transmission spectroscopy in the near-i.r. has been demonstrated previously to be of quantitative utility for hydrocarbonaceous samples [9, 10]. Since p.a.s. can provide optical absorption data that are essentially equivalent to those obtained by conventional methods, it seems reasonable to test its value, particularly in the near-i.r., for quantifying coverage on chemically-modified surfaces.

EXPERIMENTAL

Preparation of chemically-modified silicas

Derivatized microparticulate silica gels that afforded alkyl, phenyl, and aminoalkyl functions for quantitative study were prepared. Approximately 1 g of silica gel (LiChrosorb SI-100 (E.M. Laboratories), particle size 10 μm, surface area 420 $m^2\ g^{-1}$) was introduced into a reaction vessel containing 50 ml of dry toluene (distilled from calcium hydride and stored over sodium metal) in an atmosphere of dry nitrogen. An excess (6 mmol) of alkylmethyldichlorosilane or β-phenethylmethyldichlorosilane (Petrarch Systems, Levittown, PA) was added to the reaction flask, along with 2 ml of dry pyridine for use as a sequestering agent for evolved hydrogen chloride. The alkylsilanes used included those with hexyl, octyl, decyl, dodecyl, and octadecyl moieties. Reactions meant to produce alkyl-modified silicas were carried

out in refluxing toluene, but it was found that the phenethyl-derivatized silica was best prepared at reduced temperature (0°C) to afford sufficient differences in coverage to permit meaningful quantitative measurement. Aliquots of suspended silica were extracted from the reaction mixture at periodic intervals, washed with acetone, methanol, methanol—water, and acetone, and oven-dried at 110°C for 8 h. The resulting silylated silicas were stored in a vacuum desiccator until ready for photoacoustic analysis. After examination by p.a.s., portions of the material were submitted for elemental carbon and hydrogen analysis (MHW Laboratories, Phoenix, AZ). Aminopropyl-modified silica was prepared in a manner similar to that described above. The γ-aminopropylmethyldiethoxy silane (Petrarch Systems) was introduced into the reaction vessel by way of a buret to allow for controlled coverage of the silica gel. The reaction was run at room temperature and silica gel was extracted from the reaction vessel approximately 2 min after the introduction of each new increment of the silane reagent. The amine content on the modified silica was determined by non-aqueous acid—base titrimetry. A weighed amount of the aminated silica was transferred to a flask containing 10 ml of glacial acid and 20 ml of chloroform. Two drops of crystal violet indicator were added to the flask and the solution was titrated to a blue end-point with a standardized solution of perchloric acid in dioxane. Aminopropyl-modified silica gel meant to be examined by p.a.s. was stored in a vacuum desiccator.

Photoacoustic analysis

P.a.s. data were acquired by using a Princeton Applied Research model 6001 spectrometer. The spectral region between 1000 and 2000 nm was utilized in this study with a high-pressure xenon arc lamp providing the source of the near-i.r. radiation and one of the three gratings in the spectrometer affording wavelength isolation in this region. The silica gel samples were contained in cylindrical stainless-steel sample boats with a cavity volume of 0.10 ml. The silica was introduced into the sample cavity and the surface of the powder was carefully leveled (using a razor edge) parallel to the flat stainless-steel face of the sample boat to provide reproducible sample space filling. Such attention to reproducible filling is necessary because p.a.s. signal amplitude is magnified or diminished when the volume of air above the sample is increased or reduced. The filled boat was seated in the sample cell assembly and the upper portion of the cell was carefully screwed into place with a minimum of movement of the assembly so that collection of silica powder on the inside surface of the quartz window resulting from static charge could be avoided. Data were acquired in the form of a pen trace of the absorption band with the spectrometer scanning through a wavelength range sufficient to obtain the entire absorption envelope.

RESULTS AND DISCUSSION

Measurements of p.a.s. signal amplitude as a function of the percentage carbon content of octadecyl-modified silica gel are presented in Table 1. The signal amplitude values given in the Table represent the average of three scans performed on different aliquots of each modified silica sample, while carbon content (determined by elemental carbon analysis) was obtained from duplicate measurements. Photoacoustic signal amplitude was measured on the absorption trace as the distance to the peak maximum from a tangent drawn through the baseline. Amplitude data were obtained by using both the first and second overtones of the aliphatic C—H stretch vibrational mode, and it was found that both overtones provide a linear relationship between signal and carbon coverage. Linear correlation coefficients obtained from a regression analysis of the data are 0.995 and 0.999 for the first and second overtones, respectively. The reproducibility of measurements of signal amplitude was evaluated, both for replicate scans on one particular sample aliquot and for single scans on three portions of an apparently homogeneous sample aliquot. An average relative standard deviation of 0.01 was obtained for the replicate (three scans) determination on a single aliquot and a value of 0.02 was obtained from pooling the results of three single scans on three portions of each of the octadecyl-modified silica samples. The second aliphatic C—H stretch overtone (λ_{max}, 1184 nm) gave an especially well-resolved absorption band for these samples, permitting rapid and accurate measurement of peak height from the trace. The first overtone (λ_{max}, 1710 nm) produced a stronger photoacoustic signal, but determinations of signal

TABLE 1

Octadecyl-modified silica gel

Reaction time[a] (min)	P.a.s. signal amplitude		Carbon content of modified silica (%)
	1710 nm[b]	1188 nm[c]	
2	0.345	0.325	10.55 [0.94][d]
6	0.405	0.378	12.45 [1.11]
16	0.433	0.428	14.06 [1.25]
30	0.453	0.455	14.88 [1.32]
60	0.477	0.482	15.70 [1.40]
150	0.503	0.509	16.52 [1.47]
1260	0.517	0.517	16.78 [1.49]

[a]Times at which aliquots of silica were extracted from the reaction vessel. Reaction carried out in refluxing toluene.
[b]First overtone of the aliphatic C—H stretch vibrational mode. Acquired at an ordinate expansion factor of 4.
[c]Second overtone of the aliphatic C—H stretch vibrational mode. Acquired at an ordinate expansion factor of 10.
[d]Coverage values expressed as μmol m^{-2} appear in brackets.

amplitude were made more difficult because of an ascending baseline on the long wavelength side of the overtone band; this was due, in part, to the strong combination band arising from chemi- and physi-sorbed water on the silica substrate. Data from the second overtone amplitudes were used to construct a plot of p.a.s. signal (proportional to carbon coverage on the modified silica) vs. time of reaction for the octadecyl-modified silica gel; as may be seen in Fig. 1, essentially complete derivatization of the silica surface is accomplished after 2 h for the reaction conditions employed. Such rapid and easy acquisition of surface-coverage data made accessible by p.a.s. may be of value in studies related to optimization of surface derivatization reactions.

A small amount of heavily covered docosyl-modified silica gel was prepared for admixture with oven-dried native silica gel to assess the effect of sample dilution on quantitative response and to permit expansion of the range of apparent carbon content. Portions of the derivatized and native silica gel were carefully weighed and thoroughly mixed to obtain samples diluted by integral factors from 2 to 5 for a range of effective carbon content from 20.7% to 4.1%. As in the case of the octadecyl-modified silicas of variable coverage, a linear relationship between signal and effective carbon content was observed and regression analysis gave a correlation coefficient of 0.995. The native

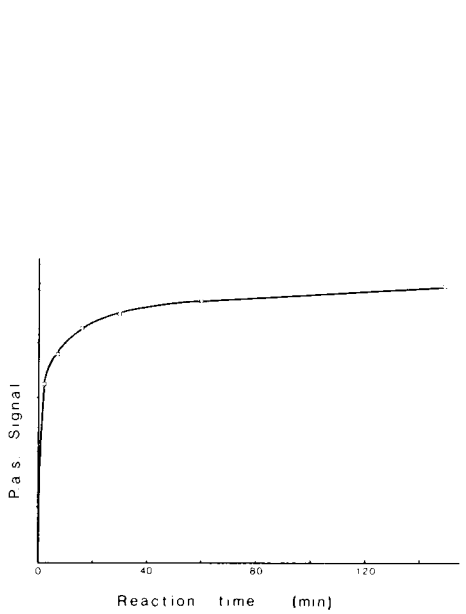

Fig. 1. The magnitude of p.a.s. signal amplitude as a function of time of reaction for octadecyl-modified silica gel.

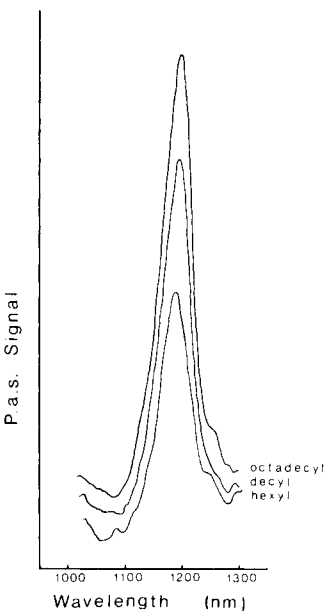

Fig. 2. Absorption bands arising from the second overtone of the aliphatic C—H stretch vibrational mode in octadecyl-, decyl-, and hexyl-modified silica gel.

silica diluent, then, appears to produce no measurable effect on quantitative response and the range of linear response for alkyl-modified silicas obtains over a relatively wide range of carbon coverage values.

An extension of the quantification scheme to include the analysis of modified silicas with bonded alkyl functions of differing chain length was attempted; the results of this analysis are contained in Table 2. As in the preceding determinations, a linear response was obtained with a linear correlation coefficient of 0.991 and a relative standard deviation of 0.03 as a measure of the reproducibility of each p.a.s. amplitude data point. Figure 2 provides an illustration of the second aliphatic C—H stretch overtones used for measurement, with the bands for several alkyl-modified silicas with different bonded carbon chain lengths overlaid. From these results it appears that samples that contain similar chemical groups, e.g., the methylene units in paraffinic species, may be analyzed interchangeably, and that the small qualitative differences that are produced upon shortening alkyl chain length do not measurably affect surface properties, i.e., thermal diffusion length or reflectivity, to the extent that p.a.s. signal amplitude is perceptibly altered.

The applicability of quantitative p.a.s. to the analysis of modified materials that contain unsaturated carbon was evaluated through the examination of silicas with surface-bound ethylbenzene groups. The point of attachment to the silica support matrix for this bonded moiety is through the ethyl function. This modified material presents a complication in that two spatially proximate signals are produced: one emanating from the C—H stretch from the aromatic portion of the molecule, and another from the saturated ethyl residue. The stronger, better-resolved aromatic C—H stretch overtone bands (λ_{max}, 1664 nm for the first overtone and λ_{max}, 1130 nm for the second overtone) were used for quantitative measurement. The results of the determination yielded, once again, a linear calibration plot of p.a.s. signal amplitude vs. carbon content, with correlation coefficients of 0.978 and 0.995 for

TABLE 2

Alkyl-modified silica gel

Chain length[a]	Signal amplitude 1182—1188 nm[b]	Carbon content of modified silica (%)
Hexyl	0.195	7.22 [1.72][c]
Octyl	0.260	9.06 [1.69]
Decyl	0.303	12.00 [1.86]
Dodecyl	0.331	12.56 [1.63]
Octadecyl	0.390	15.20 [1.35]

[a]Aliquots were extracted from each reaction flask approximately ten minutes after commencement of reaction. The reactions were carried out in refluxing toluene.
[b]Second overtone of the aliphatic C—H stretch vibrational mode. Acquired at ordinate expansion factor of 5.
[c]Coverage values in brackets are expressed as μmol m^{-2}.

the first and second overtones (see Table 3). A study of signal reproducibility for these aromatic C—H stretch overtones gave average relative standard deviation values of 0.04 and 0.09 for the first and second overtones when three separate portions from each silica aliquot were scanned once and the results were averaged. As a result of the lower carbon content of these samples and the effective dilution of signal because of the presence of two bands that are both indicative of carbon content, substantially noisier absorption traces resulted in a consequent impairment of the ability to measure peak height accurately. The aromatic C—H stretch overtones also manifested a relatively ill-defined shoulder on the long wavelength side of the bands which arose from the aliphatic C—H stretch overtone absorptions of ethyl and methyl groups. Both of these factors contributed to a less precise photoacoustic evaluation of carbon coverage in these samples.

The ability of p.a.s. to quantify coverage on silicas modified with reagents that introduce atoms in addition to carbon on the silica surface was evaluated through use of the first overtone of the N—H stretch vibrational mode in aminopropyl-modified silica gel. The extent of derivatization in these samples has previously been quantified in this laboratory by an acid—base titrimetric method, and results from these titrations usually closely parallel elemental nitrogen determinations. This method of amine determination, then, was employed in the comparison of p.a.s. signal and amine content of the modified silica. The results of the comparison are compiled in Table 4. As in the preceding case where the C—H stretch overtone was monitored, a straight-line relationship between signal amplitude and amine content was observed. Regression analysis gave a correlation coefficient of 0.997 and signal reproducibility measurements yielded an average relative standard deviation of 0.04 for individual measurements of portions of a single modified silica aliquot.

TABLE 3

β-Phenethyl-modified silica gel

Reaction time[a] (min)	Signal amplitude		Carbon content of modified silica (%)
	1664 nm[b]	1130 nm[c]	
1	0.278	0.155	6.68 [1.33][d]
4	0.300	0.163	8.06 [1.60]
10	0.355	0.183	9.50 [1.89]
20	0.395	0.193	9.79 [1.94]
120	0.410	0.208	10.69 [2.12]

[a]Times at which aliquots of silica were extracted from the reaction vessel. Reaction temperature, 0°C.

[b]First overtone of the aromatic C—H stretch vibrational mode. Acquired at an ordinate expansion factor of 4.

[c]Second overtone of the aromatic C—H stretch vibrational mode. Acquired at an ordinate expansion factor of 10.

[d]Coverage values in brackets are expressed in μmol m^{-2}.

TABLE 4

Aminopropyl-modified silica gel

Silane content[a] (mmol)	Signal amplitude 1520 nm[b]	Amine content[c] (mmol g^{-1})
0.25	0.055	0.087
1.25	0.230	0.302
2.50	0.320	0.467
4.50	0.397	0.576
7.50	0.463	0.638

[a]The γ-aminopropylmethyldiethoxy silane content of the reaction vessel. Aliquots of silica gel were withdrawn approximately 2 min after each new increment of silane was added.
[b]First overtone of the N—H stretch vibrational mode for primary aliphatic amines.
[c]Amine content was determined by non-aqueous acid—base titrimetry and results are expressed in terms of mmol of amine per gram of modified silica.

Quantification of coverage on samples of the type studied here necessarily involves a rigorous attempt to construct calibration plots using modified materials that very closely resemble the materials meant to be examined. Often, the molar absorptivity of a particular vibrational overtone will be altered enough through substituent effects that it may not be generally applicable to all compounds containing the particular atomic couple that give rise to the absorption. For example, the molar absorptivity of the N—H stretch overtone of a primary amine is substantially different from that of a secondary amine. Differences in surface properties pertinent to the strength of p.a.s. signal need also be considered in the construction of calibration plots that reliably mirror surface coverage. The production of signal from a chemical group anchored to a polymeric web on the support substrate surface may be considerably different than that which arises from a monolayer of molecules bonded directly to the support matrix.

This work was supported by a grant (to CHL) from the National Science Foundation, CHE-781807.

REFERENCES

1 M. J. D. Low and G. A. Parodi, Spectrosc. Lett., 11 (1978) 581.
2 D. E. Leyden, M. L. Steele, B. B. Jablonski and R. B. Somoano, Anal. Chim. Acta, 100 (1978) 545.
3 M. J. D. Low and G. A. Parodi, Appl. Spectrosc., 34 (1980) 76.
4 C. H. Lochmüller, S. F. Marshall and D. R. Wilder, Anal. Chem., 52 (1980) 19.
5 C. H. Lochmüller and D. R. Wilder, Anal. Chim. Acta, 116 (1980) 19.
6 S. L. Castleden, C. M. Elliott, G. F. Kirkbright and D. E. M. Spillane, Anal. Chem., 51 (1979) 2152.
7 C. H. Lochmüller and C. W. Amoss, J. Chromatogr., 108 (1975) 85.
8 E. M. Monahan, Jr. and A. W. Nolle, J. Appl. Phys., 48 (1977) 3519.
9 A. Evans and R. R. Hibbard, Anal. Chem., 23 (1951) 1604.
10 O. H. Wheeler, Chem. Rev., 59 (1959) 629.

Analytica Chimica Acta, 118 (1980) 109—114
© Elsevier Scientific Publishing Company, Amsterdam — Printed in The Netherlands

DETERMINATION OF ALUMINIUM IN BULK COAL SAMPLES BY NEUTRON ACTIVATION ANALYSIS

M. BORSARU and P. J. MATHEW*

CSIRO Division of Mineral Physics, P.O. Box 124, Port Melbourne, Victoria 3207 (Australia)

(Received 15th January 1980)

SUMMARY

The determination of Al_2O_3 in bulk coal samples to an accuracy of about 0.2% Al_2O_3 has been achieved by means of a thermal-neutron activation technique based on the reaction $^{27}Al(n, \gamma)^{28}Al$. In the analysed samples, which had widely different compositions, the Al_2O_3 concentrations ranged from 1 to 11% and the ash contents from 7 to 40%. Al_2O_3 concentrations measured by x-ray fluorescence showed a linear relationship with both the 1.78-MeV γ-ray count following the decay of ^{28}Al and the thermal-neutron count near the samples during irradiation. The linear relationship, which was obtained by regression analysis of the experimental data, determined the Al_2O_3 concentrations with a standard deviation of 0.24% Al_2O_3. The particle sizes in the samples ranged from −0.5 to −40 mm, the moisture contents ranged from 1 to 6%, and the sample weights ranged from 8 to 11 kg. However, inclusion of these parameters in the regression analysis did not significantly improve the results for Al_2O_3.

Several problems in the use of coal are attributable to its mineral content [1]. In order to eliminate such problems and thereby make more efficient use of a limited resource, accurate and continuous methods of monitoring ash and its components are needed.

Nuclear techniques are ideally suited to monitoring ash in bulk coal. In such techniques, the deeply penetrating neutrons and γ-rays produce a response representative of the bulk, whereas x-ray methods, because of their short range in matter, permit only a shallow region to be analysed. Nuclear activation analysis of bulk materials has several advantages over conventional methods: labour-intensive and time-consuming sampling and sample preparation are eliminated; substantial errors inherent in sampling are reduced; analytical results are available quickly enough for effective process control; and the method is easily automated. A programme for developing nuclear techniques and instrumentation was undertaken to exploit these advantages in determining, in the first instance, the aluminium content of bulk coal.

Established neutron methods that have been developed for small samples are not necessarily applicable to bulk samples because the bulk material distorts the neutron flux. The neutron flux is particularly sensitive to the amount of hydrogen in the bulk material because of the high thermalising

ability of hydrogen. The presence of elements with large neutron-absorption cross-sections can also alter the neutron flux significantly. Variations in the neutron flux affect the accuracy of content determinations unless corrections are made. Thus, the matrix effect is important in bulk analysis, and its contribution to the accuracy of individual measurements must be investigated.

The method used in the present work to determine aluminium in bulk coal samples consisted of neutron activation via the thermal-neutron reaction $^{27}Al(n, \gamma)^{28}Al$, which has a reaction cross-section of 230 mb. The β-decay of ^{28}Al ($t_{1/2}$ = 2.3 min) is followed by the emission of a 1.78-MeV γ-ray. This reaction was successfully used in earlier work to determine aluminium in bulk samples of iron ore [2] and bauxite [3], and the technique has been adapted to the determination of aluminium in bulk iron ore on a moving conveyer belt [4, 5].

Parker et al. [6] have used the fast-neutron reaction $^{27}Al(n, p)^{27}Mg$ induced by 14-MeV neutrons from a neutron generator to analyse bulk coal continuously for aluminium and other elements. Loska and Gorski [7] and Kurosawa [8] have used fast neutrons from neutron generators to determine aluminium and silicon simultaneously in small coal samples. However, using a neutron generator in an industrial environment has disadvantages such as the limited lifetimes of targets and components, the fluctuating neutron yield, and the need for skilled operators. Stewart and Hall [9] have employed a prompt irradiation method using a ^{252}Cf source to determine aluminium and other elements in coal moving at high tonnage rates. Instrumental neutron-activation analysis with a Ge(Li) γ-ray detector has been used to determine a large number of elements, including trace elements, in coal [10]. The small samples analysed were irradiated in a nuclear reactor. A strong correlation between Al_2O_3 and ash content may exist in some coals, and Wormald et al. [11] have developed a technique for monitoring the ash content of coal in moving wagons. A survey of the determination of aluminium in different ores and minerals by neutron activation has been given in Gijbels and Hertogen [12].

EXPERIMENTAL

A selection of 22 black-coal samples having a wide range of compositions was analysed. The samples were collected from nine different seams and locations in the eastern states of Australia. The ash contents of the samples varied from 7 to 40% (dry basis), the free moisture contents varied from 1 to 6%, and the Al_2O_3 contents in the ash varied from 15 to 35%, corresponding to 1—11% Al_2O_3 in the coal. The particle sizes of the samples ranged from −0.5 to −40 mm. The samples contained both fresh and washed coal.

The bulk samples, whose weights ranged from 8 to 11 kg, were put in a brass box (40 × 33 × 8 cm) for irradiation and counting. They were irradiated with a 36-μg ^{252}Cf neutron source located in a high-density polyethylene "howitzer" surrounded by paraffin, as shown in Fig. 1. This configuration

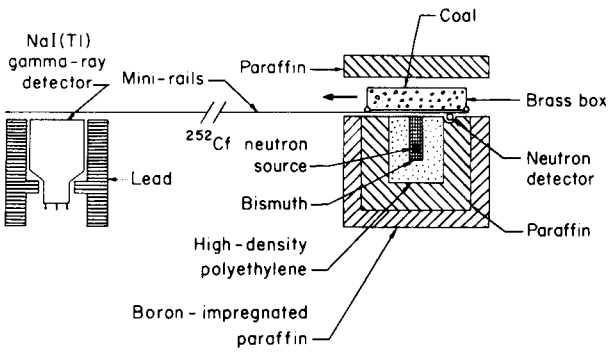

Fig. 1. Irradiation and counting facility.

produced the well thermalised neutron flux needed for the present work. In the irradiation position, the sample box sat above the howitzer. A ^{3}He neutron detector (15-cm active length), located below the sample box and shielded by a boron sheath against direct neutrons from the howitzer, was used to monitor the thermal-neutron flux in the vicinity of the bulk samples. An 18-cm-thick paraffin block was placed above the brass box to reflect neutrons back into the samples.

The counting station was situated 7 m away from the irradiation station and consisted of a 126 × 126-mm NaI(Tl) detector heavily shielded with lead to minimise the background γ-radiation produced by the neutrons and natural sources. Signals from the scintillation and neutron detectors were fed into amplifier/single-channel-analyser/scaler/printer chains controlled by timers. A Canberra Industries 1520 analogue gain stabiliser was used to stabilise the γ-ray spectrum. The stabiliser was locked on the 662-keV peak produced by a ^{137}Cs microsource placed near the scintillation detector.

The measurement consisted of irradiating the bulk sample for 6 min, followed by an interval of 15 s for transferring the sample to the counting station, and counting for 5 min. The sample box was transferred from the irradiation station to the counting station on a pair of rails. The weight of the sample, the thermal-neutron counts recorded by the ^{3}He neutron detector during irradiation, and the 1.78-MeV γ-ray counts were monitored for each sample.

RESULTS AND DISCUSSION

For each of the 22 samples analysed, stepwise regression analysis [13] was performed on the calculated values of the Al_2O_3 concentration (y) and on the measured values of the 1.78-MeV γ-ray count (γ), the neutron count (n), the moisture content, the particle size, and the sample weight. The best linear regression equation was computed to be

$$y = 22.1468 + 0.14403\gamma - 0.00270\,n$$
$$(\pm 3.5466) \quad (\pm 0.00098) \quad (\pm 0.00009)$$

where the numbers in parentheses are the standard errors of the regression coefficients.

The standard deviation of y for a single determination was 0.24% Al_2O_3. A comparison of the Al_2O_3 concentrations measured via neutron activation and those measured via x.r.f. is shown in Fig. 2. The standard deviation of y increases to 0.42% Al_2O_3 if n is omitted from the regression equation, which demonstrates the importance of the neutron count as a predictor of Al_2O_3.

The moisture content, the particle size, and the sample weight were found to be statistically insignificant in the regression equation. This shows that the Al_2O_3 content of coal can be determined from two easily measured parameters (γ and n).

The standard deviation of 0.24% Al_2O_3 includes an estimated x.r.f. error (from sampling and analysis) of 0.15% Al_2O_3 as well as the errors inherent in the neutron-activation method. If these two sources of error are independent, the standard deviation of the latter method is only about 0.18% Al_2O_3. Consequently, sources of error appreciably less than 0.18% Al_2O_3 can be regarded as negligible.

SOURCES OF INTERFERENCE

In Australian coals, the most commonly found elements that can interfere in the determination of Al_2O_3 are silicon, phosphorus, manganese, and iron.

Silicon is a major component of the mineral matter in coal, and the fast-neutron reaction $^{28}Si(n, p)^{28}Al$, which has an energy threshold of 3.8 MeV, could be a serious source of interference. The way to minimize this interference is to reduce the fast-neutron component in the irradiation flux. Irradiation and counting of pure silica in the apparatus used has shown that

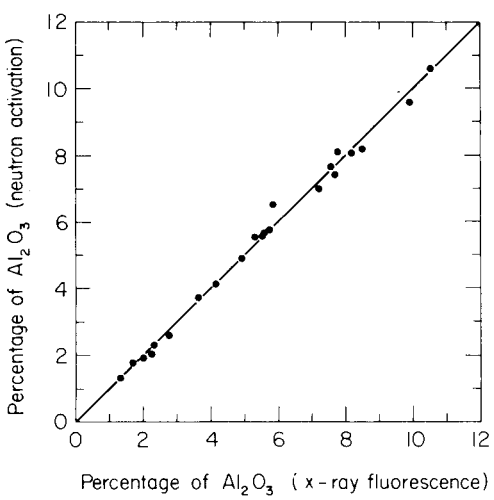

Fig. 2. Comparison of neutron-activation and x.r.f. assays of Al_2O_3 in coal samples.

the interference from silica corresponds to less than 0.1% Al_2O_3 for concentrations of up to 22% silica. The concentration of silica in the samples analysed was less than 22%.

The presence of phosphorus in coal can also produce ^{28}Al by the fast-neutron reaction $^{31}P(n, \alpha)^{28}Al$. The low concentration of phosphorus in Australian coals [14], the small reaction cross-section (1.5 mb at 5 MeV), and the small number of fast neutrons in the neutron flux preclude phosphorus as a source of interference.

^{56}Mn is produced by the thermal-neutron reaction $^{55}Mn(n, \gamma)^{56}Mn$, which has a high reaction cross-section (13.3 b). ^{56}Mn has a half-life of 2.58 h and emits γ-rays having energies of 0.847, 1.811, and 2.113 MeV. Since 1.811-MeV γ-rays cannot be resolved from 1.78-MeV γ-rays with a scintillation detector, the presence of manganese could cause interference. However, this interference is negligible because of the low concentration of manganese in Australian coals (mean content 150 ppm [14]) and because of the long half-life of ^{56}Mn in comparison with ^{28}Al.

^{56}Mn can also be formed by the fast-neutron reaction $^{56}Fe(n, p)^{56}Mn$, which has an energy threshold of 2.9 MeV. In order to estimate the amount of interference from ^{56}Mn, the residual radioactivity for the 1.78-MeV peak was measured after allowing the ^{28}Al activity to die away over a 25-min period. No statistically significant residual radioactivity could be detected. The samples checked for residual radioactivity were the ones containing the highest amount of MnO (0.08%) and Fe_2O_3 (2.9%).

It should be noted that if some coal samples contain high manganese concentrations, a correction to the intensity of the 1.78-MeV peak can easily be applied by monitoring the 2.113-MeV peak.

CONCLUSIONS

The present work shows that thermal-neutron activation analysis with a ^{252}Cf source can be used to determine Al_2O_3 in bulk coal with an accuracy corresponding to one standard deviation of 0.24% Al_2O_3. The Al_2O_3 content of the coal samples analysed ranged from 1 to 11%. The variations in particle size, moisture content, and sample weight encountered in the present work had virtually no effect on the accuracy of the method.

The presence of silicon, phosphorus, manganese, and iron in the concentrations commonly found in Australian coals does not cause any noticeable interference in the technique. An efficient thermal-neutron howitzer with a minimum number of fast neutrons in the thermal-neutron flux is needed to eliminate interference from fast-neutron reaction products.

The analysis time of 11 min per sample can be reduced by employing a stronger neutron source and a more efficient γ-ray counter.

In the light of previous work [4, 5], the present method could be adapted to analyse coal on a slow-moving side conveyor belt.

The authors thank H. L. Maltman and M. Pretor for their assistance in providing coal samples, and C. Ceravolo and Dr. G. W. Hill for valuable help. Support was provided under the National Energy Research, Development and Demonstration Program administered by the Commonwealth Department of National Development.

REFERENCES

1 R. A. Durie and D. J. Swaine, Coal Research in CSIRO, 45 (1971) 9.
2 M. Borsaru and R. J. Holmes, Anal. Chem., 48 (1976) 1699.
3 M. Borsaru and P. L. Eisler, Int. J. Radiat. Isot., in press.
4 R. J. Holmes, M. Borsaru and A. W. Wylie, Proceedings of the North Queensland Conference, Australasian Institute of Mining and Metallurgy, Melbourne, 1978, p. 235.
5 R. J. Holmes, A. J. Messenger and J. G. Miles, Proc. Australas. Inst. Min. Metall., in press.
6 C. V. Parker, Jr., T. C. Martin, K. R. Blake and I. L. Morgan, Mater. Eval., 25 (1967) 214.
7 L. Loska and L. Gorski, Radiochem. Radioanal. Lett., 10 (1972) 315.
8 R. Kurosawa, Nippon Kogyo Kaishi, 84 (1968) 101.
9 R. F. Stewart and A. W. Hall, Proceedings of the 13th Intersociety Energy Conversion Engineering Conference, Vol. 1, San Diego, 1978, p. 586.
10 C. Block and R. Dams, Anal. Chim. Acta, 71 (1974) 53.
11 M. R. Wormald, C. G. Clayton, I. S. Boyce and D. Mortimer, Int. J. Radiat. Isot., 30 (1979) 297.
12 R. H. Gijbels and J. Hertogen, Pure Appl. Chem., 49 (1977) 1555.
13 N. R. Draper and H. Smith, Applied Regression Analysis, J. Wiley, New York, 1968.
14 D. J. Swaine, Proc. 11th Symp. on Trace Substances in Environmental Health, University of Missouri, Columbia, 1977, p. 107.

Analytica Chimica Acta, 118 (1980) 115—122
© Elsevier Scientific Publishing Company, Amsterdam — Printed in The Netherlands

THE SEQUENTIAL DETERMINATION OF ARSENIC, SELENIUM, GERMANIUM AND TIN AS THEIR HYDRIDES BY GAS—SOLID CHROMATOGRAPHY WITH AN ATOMIC ABSORPTION DETECTOR

MARK H. HAHN, KEVIN J. MULLIGAN*, MICHAEL E. JACKSON and JOSEPH A. CARUSO

Department of Chemistry, University of Cincinnati, Cincinnati, Ohio 45221 (U.S.A.)

(Received 26th October 1979)

SUMMARY

Arsenic, germanium, selenium and tin were sequentially determined in single samples by using hydride generation followed by gas chromatography with an atomic absorption detector. Apparent detection limits varied from 3 ppb for As to 13 ppb for Ge with linear dynamic ranges of about 1.5 orders of magnitude. Relative standard deviations, evaluated in the middle of the working range, varied from 2% to 11%. Chromatographic parameters were chosen to allow for manual lamp selection and monochromator adjustment. Data handling was done by microcomputer. The analysis time was 5 min.

Hydride generation has been interfaced with a variety of detection techniques, particularly atomic spectrometry, for the determination of certain post-transition metals and metalloids. It offers several advantages over conventional solution nebulization. Among these are the capability for preconcentration of the analyte, the elimination of chemical and spectral interferences and the presentation of the analyte as a desolvated moiety to the atomization source. These advantages have led to as much as a thousand-fold improvement in detection limits [1].

Although plasma emission spectrometry and atomic fluorescence methods provide the lowest detection limits, most workers have used atomic absorption spectrometry, presumably because of its greater availability, lower cost, and ease of operation.

Multi-element determinations are generally faster and require less sample than a series of determinations of single elements. Since hydride generation usually presents the analytes as a plug to the detector, multi-element methods typically require some sort of multichannel detection system such as a plasma emission source coupled to a direct reading spectrometer [2, 3]. Depending on the demand in terms of throughput, sample availability and the analytical information desired, the cost of such systems can be prohibitive.

A compromise between the single-element and the multi-element approach has been achieved by separating the hydrides of As, Ge, Sb and Sn prior to a single-channel detector. Such separations have been employed as precursors to a mass spectrometer [4], a thermal conductivity detector [4, 5], a dual

flame detector [4] and a molecular emission source [6]. As a part of an extensive study, Kadeg and Christian [4] attempted to use atomic absorption spectrometry for this sequential determination but obtained unsatisfactory results.

Workers in this laboratory have used a chromatographic separation to remove spectral interferences and to stabilize the plasma during the determination of the hydrides of As, Ge, Sb, Se and Sn by microwave-induced plasma emission spectrometry [2, 3, 7, 8]. Conditions were suggested that could be applied to the sequential multi-element determination of these elements with a single-channel detector [2, 8].

This paper reports the development of a method in which the hydrides of As, Ge, Se and Sn are determined sequentially in a single run by atomic absorption spectrometry.

EXPERIMENTAL

System description

A diagram of the apparatus is provided in Fig. 1. Two modifications have been made to the system which is described in detail elsewhere [7, 8]. A 2-way valve (HFV) was introduced to bypass the needle valve (NVI). This permitted the flow rate of helium through the system to be dramatically increased

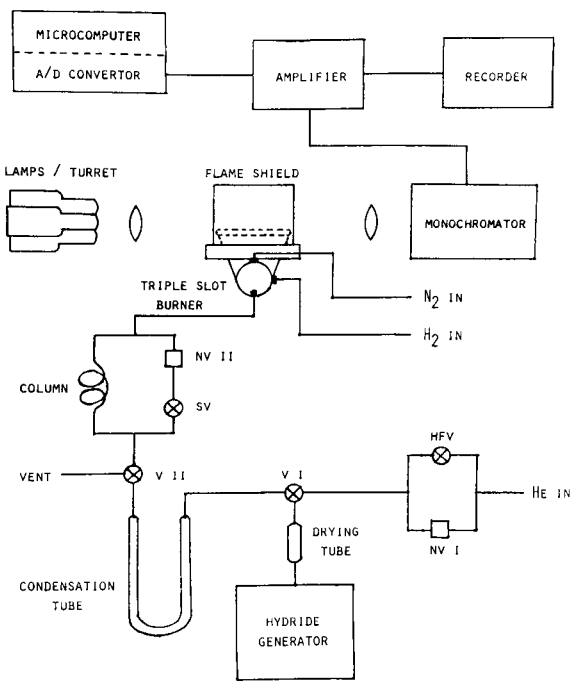

Fig. 1. Schematic diagram of the apparatus. NV = needle valve, V = 3-way valve and SV, HFV = 2-way valves.

(from 60 ml min^{-1} to 450 ml min^{-1}). Also a combination of a 2-way valve (SV) and a needle valve (NV II) served as a means of proportioning the plug of analytes leaving the condensation tube between the flame and the chromatographic column.

Hydride generation was accomplished by using a semi-automated hydride generator as described by Fiorino et al. [9].

The column consisted of a 3-ft length of Polypenco Nylaflow pressure tubing (4.7 mm i.d.) which was packed with Chromosorb 102 and was operated at ambient temperature (23°C).

A triple-slot burner equipped with a "homemade" flame shield similar to the one used by Fiorino et al. [9] served to maintain a nitrogen (15 ml min^{-1})—hydrogen (6 l min^{-1})—entrained air flame.

Finally, a Jarrell-Ash MV AA 82500 atomic absorption spectrometer was employed as a detector. Radiation was provided by hollow-cathode lamps (Westinghouse Inc.) for As, Ge, Se and Sn which were mounted in a lamp turret. The turret kept the lamps in a continuous state of operation (10 mA) and allowed them to be rapidly interchanged. This radiation was rendered parallel and after passing through the flame at a distance of 5 mm above the burner head was focused on the 100-μm entrance slit of a 0.5-m Ebert monochromator equipped with a 1180 groove mm^{-1} grating blazed at 300.0 nm. A Hamamatsu R106 PMT was positioned directly behind the 150-μm exit slit. Following a current-to-voltage conversion and suitable amplification the signal was recorded or input to a microcomputer system similar to the one described by Woodward and Reilley [10].

Hydride generation

A 20.0-ml aliquot of an aqueous acidic solution (5% v/v H_2SO_4 and 10% v/v HCl; Baker Analyzed Reagents) was introduced into the reaction tube of the hydride generator. Then the mixture was spiked with a known amount of a standard solution of the analytes which was prepared daily from a.a.s. standards (Alfa-Ventron Co. and Fisher Scientific Co.).

Upon initiation of the reaction cycle, 10 ml of the generating reagent was delivered to the reaction tube during a 10-s interval. This reagent consisted of a 4% (w/v) solution of sodium tetrahydroborate (MC/B 98%) in aqueous 5% w/v sodium hydroxide (MC/B Reagent Grade). After a 5-s delay, 10 ml of water was added to clear the delivery tube.

The volatile hydrides passed through a drying tube packed with $CaCl_2$ (Baker Reagent Grade; 8 mesh; anhydrous) and were directed by valve, VI, into a condensation tube which was immersed in liquid nitrogen. The condensation tube consisted of a thick-walled glass U-tube (1.5 cm i.d.) which had been filled to the extent of 40 cm with 1-mm glass helices. All glass surfaces were silanized.

While the hydrides were collected in this trap, the large amount of hydrogen which had been produced during the reaction was vented to the atmosphere through VII. One minute after the start of the reaction, VI was turned

to admit the helium carrier gas to the system. Then VII was adjusted so that the gas flow entered the remainder of the system.

Chromatographic separation and detection

The condensation tube was transferred to a hot water bath (75—80°C) and the collected hydrides were vaporized. The details of the subsequent procedure are contained in Table 1.

In summary, the plug of vaporized hydrides was split into two approximately equal portions. One of these was introduced directly into the flame and analyzed for selenium. The other passed through a chromatographic column which served to separate AsH_3, GeH_4 and SnH_4. Although this procedure resulted in a two-fold decrease in sensitivity for each analyte, it avoided separation problems associated with the marked chromatographic overlap of SeH_2 and SnH_4 which had been observed earlier [2, 8]. Also, the periodic step variation in flow rate during the chromatographic separation provided sufficient time for the necessary manipulations (lamp selection, etc.) and yet preserved peak shape and minimized the analysis time.

The peaks were quantified by integration with background subtraction after the data had been collected with the microcomputer system.

Data acquisition

Data were acquired by one of two methods. With the first method, the output from the amplifier was directed to a strip-chart recorder. The second method involved the use of a microcomputer. In this case, the analog output from the amplifier was converted to discrete digital data which were compatible with the microcomputer. By means of a programmable interval timer, real-time data acquisition was assured.

The microcomputer performed signal averaging during data collection. Signal averaging for the period of a 60-Hz wave improved the signal-to-noise ratio and virtually eliminated line frequency noise. Any random noise such as instrumental artifacts was conveniently and adequately handled by a soft-

TABLE 1

Time (s)	Operation
Set up	Select Se lamp. Monochromator to 196.0 nm. Open splitting valve, SV.
0	Transfer condensation tube to hot water bath.
48	Open bypass valve, HFV, to provide a high flow rate. Collect data on the Se channel.
65	Close HFV and then SV. Select the Ge lamp. Monochromator to 265.2 nm.
120	Open HFV. Collect data on the Ge channel.
140	Close HFV. Select As lamp. Monochromator to 193.7 nm.
165	Open HFV. Collect data on the As channel.
205	Close HFV. Select Sn lamp. Monochromator to 224.6 nm.
230	Open HFV. Collect data on the Sn channel.
300	Close HFV. Finished.

ware smoothing routine based on a modified ensemble-averaging algorithm.

Experimental control was provided by a BASIC interpreter language in the memory of the computer. Actual real-time acquisition, scaling, and smoothing were accomplished by software written in directly executable machine code. All other data manipulation was handled by the user and carried out under BASIC software control.

Following a graphical presentation of the data, the user selected the limits of integration for each peak. The interpolated value of the straight line defined by these points was subtracted from the corresponding data point to provide a background correction. Then, peak areas were calculated by a simple summation algorithm.

Ten successive treatments of the four analyte peaks at 1.25 μg yielded relative standard deviations of 1.2% to 1.8% in the value of each specific peak area.

RESULTS AND DISCUSSION

In preliminary experiments, the hydrides were generated individually and either introduced directly into the flame or passed through the column prior to the flame. A comparison of the peak areas obtained under these two conditions revealed that AsH_3, GeH_4 and SnH_4 were transferred quantitatively through the column. However, SeH_2 was not. With a freshly packed column, the selenium signal was significantly reduced. After about 10 runs at the microgram level, the signal for a chromatographed sample attained only about 40% of the value for a sample introduced directly into the flame, and remained constant thereafter.

The separation of the hydrides is illustrated in Fig. 2. Certain portions of the trace (which is continuous in time) have been deleted since lamp selection and monochromator adjustment were being done during these intervals. This separation at ambient temperature with digital flow programming is comparable to one which has been obtained by using temperature programming [4].

Antimony could have been included in this study. Under the above conditions, SbH_3 elutes after 8 min. The peak is rather broad, however. While BiH_3 and TeH_2 can be generated from the reaction mixture, it has so far proved impossible to chromatograph them. Apparently, the problem is due to decomposition within the cold trap and on the column.

Typical calibration curves are presented in Fig. 3. They reveal a linear range for each analyte of approximately 1.5 orders of magnitude. The lowest point of the linear portion of each curve has a relative standard deviation of about 25%. For this study, this point is defined as the detection limit, which probably corresponds to the smallest amount of analyte that can realistically be determined by this technique. With the data-handling routines employed (particularly ensemble averaging), the variation of the baseline with time was virtually eliminated. As a result, a definition of detection limits in terms of a signal-to-noise ratio would be misleading.

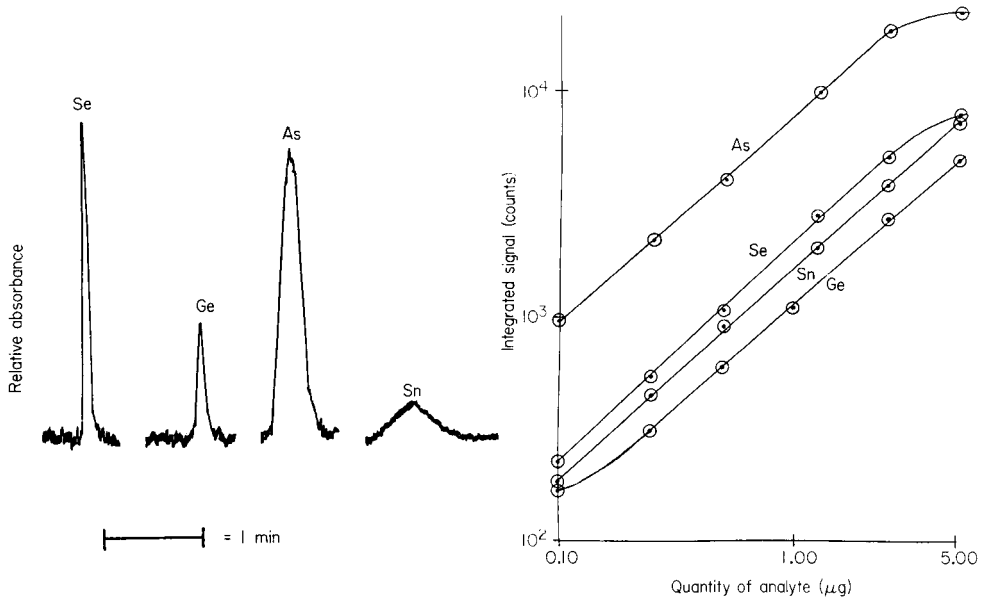

Fig. 2. Recorder tracing for a mixture containing 1.25 μg of each analyte. The trace is continuous in time. Certain portions have been deleted for reasons indicated above.

Fig. 3. Calibration curves obtained by plotting the integrated value for each peak against the quantity of analyte present in the mixture. These data were obtained with the microcomputer system.

Relative standard deviations were evaluated from ten determinations in the middle of the working range (1.25 μg). The results are: AsH_3, 2.2%; GeH_4, 7.5%; SeH_2, 8.7%; and SnH_4, 11.2%. While generally a bit high, the values seem reasonable in view of the amount of manipulation required during the course of the experiment.

A comparison of the atomic absorption technique with the sequential methods discussed earlier is contained in Table 2. Although the a.a.s. system lacks the sensitivity of the mass spectrometric detector, it offers a slightly wider linear range and probable advantages in terms of cost and convenience. Neither the molecular emission detector nor the thermal conductivity detector provide the speed of the above methods. Moreover, they lack specificity which may be useful in certain applications.

Table 3 contrasts the sequential a.a.s. technique with single-element a.a.s. determinations. Clearly, hydride generation represents a dramatic improvement over direct solution nebulization. Within the hydride generation category, the reduced sensitivity of the sequential method is principally due to two factors. The sequential approach requires that the plug of analytes be divided. This leads to a two-fold reduction in sensitivity. Also, band broadening within the chromatographic column leads to a greater portion of the analyte signal being lost to baseline noise. However, the sequential

TABLE 2

Comparison of sequential multi-element hydride techniques

Technique	Detection limit (ng)					Linear range	Analysis time (min)
	AsH_3	GeH_4	SbH_3	SeH_2	SnH_4		
Atomic absorption[a]	60	260	—	100	100	$10^{1.5}$	5
Molecular emission[b]	200	—	1000	—	—[c]	10^1	14
Thermal conductivity[d]	100	30	1000	—	—	10^3	20
Mass spectrometry[e]	10	5	100	—	50	10^1	8

[a]This work. See text for definition. [b]Ref. 5. S/N = 2. [c]The separation of SnH_4 from AsH_3, SbH_3 was illustrated but no detection limit was reported. [d]Ref. 6. S/N = 2. [e]Ref. 4.

TABLE 3

Comparison of sequential multi-element a.a.s. with other a.a.s. techniques[a]

Element	Solution nebulization[b]	Hydride generation[c]	Sequential determination[d]
As	630	0.8	3
Ge	20	4	13
Se	230	1.8	5
Sn	150	0.5	5

[a]The values in the table are detection limits expressed in ppb. [b]Ref. 11. [c]Refs. 12 and 13. [d]This work. The values are obtained by dividing the absolute amount (ng) of analyte by the solution volume (20 ml).

technique makes more efficient use of sample and reagents than a series of single-element determinations. As it stands, the sequential method is only slightly faster than multiple single-element runs. However, further automation of the system such as the use of a computer-controlled spectrometer and automated solenoid valves should enhance the time of analysis and, moreover, improve the precision of the technique.

The authors are grateful to the National Institute of Occupational Safety and Health for partial support of this work through research grant number OH-00739.

REFERENCES

1 W. B. Robbins and J. A. Caruso, Anal. Chem., 51 (1979) 889A.
2 W. B. Robbins and J. A. Caruso, J. Chromatogr. Sci., 17 (1979) 360.
3 K. J. Mulligan, M. H. Hahn, J. A. Caruso and F. L. Fricke, Anal. Chem., 51 (1979) 1935.
4 R. D. Kadeg and G. D. Christian, Anal. Chim. Acta, 88 (1977) 117.
5 R. K. Skogerboe and A. P. Bejmuk, Anal. Chim. Acta, 94 (1977) 297.
6 R. Belcher, S. L. Bogdanski, E. Henden and A. Townshend, Anal. Chim. Acta, 92 (1977) 33.

7 F. L. Fricke, W. B. Robbins and J. A. Caruso, J. Assoc. Off. Anal. Chem., 61 (1978) 1118.
8 W. B. Robbins, J. A. Caruso and F. L. Fricke, Analyst, 104 (1979) 35.
9 J. A. Fiorino, J. W. Jones and S. G. Capar, Anal. Chem., 48 (1976) 120.
10 W. S. Woodward and C. N. Reilley, Pure Appl. Chem., 50 (1978) 785.
11 Perkin-Elmer Corp., Reprint AA-322G, Technique and Applications of Atomic Absorption, 1978.
12 K. C. Thompson and D. R. Thomerson, Analyst, 99 (1974) 575.
13 A. E. Smith, Analyst, 100 (1975) 300.

Analytica Chimica Acta, 118 (1980) 123—128
© Elsevier Scientific Publishing Company, Amsterdam — Printed in The Netherlands

DETERMINATION OF EUROPIUM(III) IN RARE EARTH OXIDE SULFIDE PHOSPHORS BY LIFETIME MEASUREMENTS

YVES CHARREIRE**, MARKKU LESKELÄ* and LAURI NIINISTÖ

Department of Chemistry, Helsinki University of Technology, Otaniemi, SF-02150 Espoo 15 (Finland)

JEAN LORIERS

C.N.R.S., 1 Place A. Briand, F-92190 Meudon-Bellevue (France)

(Received 26th November 1979)

SUMMARY

The lifetimes for three transitions, $^5D_2 \rightarrow {}^7F_0$, $^5D_1 \rightarrow {}^7F_1$ and $^5D_0 \rightarrow {}^7F_2$, in the luminescence spectra of $Eu_x^{3+}:Y_{2-x}O_2S$ (x=0.001—0.12) are reported. The relation between the lifetime of the transition $^5D_0 \rightarrow {}^7F_2$ and the europium concentration is sufficiently linear in the concentration range 2—10% for the lifetime method to be used for the determination of europium in rare earth oxide sulfides. The accuracy of the method is compared with that of the linear intensity ratio method.

Europium-activated yttrium oxide sulfide is widely used as a red phosphor in color television screens; the color and brightness depend on the europium concentration to a greater extent than in other common phosphors activated by europium(III), such as $Eu:Y_2O_3$ or $Eu:YVO_4$ [1]. When the europium(III) concentration in yttrium oxide sulfide is small, the emission is yellow, but it shifts towards red with increasing activator concentration [2]. Satisfactory methods for the determination of europium(III) in rare earth oxide sulfides are therefore important industrially.

There are several requirements for a suitable procedure: it must be rapid, accurate, economical of sample, and independent of the method of preparation of the phosphor. But, most critically, it must measure only the activator concentration within the crystal lattice of the rare earth oxide sulfide and not the total europium(III) concentration. The normal analytical methods do not meet all these conditions, especially the last.

It is possible, however, to determine the europium by indirect methods, based on concentration quenching of europium-activated phosphors. With increasing activator concentration the intensity of the luminescence begins to decrease. The quenching of different transitions occurs differently, and for europium the quenching order is $^5D_2 > {}^5D_1 > {}^5D_0$ [3]. The changes in europium concentration also affect the luminescence lifetime.

Forest and Ozawa [4, 5] have developed a method for the determination

**Permanent address: C.N.R.S., 1 Place A. Briand, F-92190 Meudon-Bellevue, France.

of europium(III) in rare earth oxide sulfides, making use of the quenching of intensity. Their method, the linear intensity ratio method, is based on the intensity ratio of the peaks in the emission spectra, i.e. $I(^5D_1)/I(^5D_0)$, which changes with europium(III) concentration. The best results are obtained from the intensity ratio for the transitions $^5D_0 \rightarrow {}^7F_0$ (583.0 nm) and $^5D_1 \rightarrow {}^7F_3$ (589 nm).

According to van Uitert [6], the luminescence intensity depends on the activator concentration:

$$I/I_0 = [1 + \beta(C/C^*)^{\theta/3}]^{-1} \quad (1)$$

where I is the intensity, I_0 is the intensity under dilute conditions, C is the quenching ion concentration, and C^* the critical transfer concentration; θ equals 6, 8 and 10 for dipole–dipole, dipole–quadrupole, and quadrupole–quadrupole interactions, respectively; β is a constant characteristic of each transition [7]. The values of θ are normally 6 for the $^5D_1$ and 8 for the $^5D_2$ emitting levels of europium(III). Concentration quenching from the $^5D_0$ level occurs by magnetic dipole interaction [8]. However, the dependence of the intensity on the lifetime of the emission follows the equation [9]:

$$I(t) = \exp[-(t/\tau) - \Gamma(1 - 3/\theta)(C/C^*)(t/\tau_0)]^{3/\theta}$$

where $I(t)$ is the intensity at time t after excitation has stopped and τ_0 is the lifetime under dilute conditions. Γ is a function of argument unity [9].

The lifetime of the emission depends on the concentration in an analogous way to the luminescence intensity in eqn. (1). If there is no interaction between the lanthanide ions, I/I_0 can be replaced by τ_e/τ_0, where τ_e is the time required for the intensity $I(t)$ to fall to $1/e$ (0.368) of its value at t=0. Because of multipolar interactions, this cannot be done, but van Uitert [6] employed this relation to define an arbitrary lifetime τ_a:

$$\tau_a/\tau_0 = [1 + \beta'(C/C^*)^{\theta/3}]^{-1}$$

τ_a is calculated from the tangent of the I–t plot [6]. A good approximation of τ_a is obtained experimentally when linear regression is used to establish the slope of the log I–t plot. This is used to determine τ, resulting in an exponential curve which fits the real decrease.

Since this I–t plot is not in general an exponential function, there is no unique way of defining the decay time. In their determination of lifetime, Inokuti and Hirayama [9] used τ_m, the mean duration of I:

$$\tau_m = {}_0\int^{\infty} tI(t)\mathrm{d}t_0 / \int^{\infty} I(t)\mathrm{d}t \quad (2)$$

The integrals can easily be calculated from the experimental I–t curve with use of Simpson's equation. τ_a was found to be a good approximation of τ_m. The integral limits from zero time to the time where I=0.1I_0 give satisfactory values and 20 intervals in Simpson's equation are sufficient to achieve a precision greater than 0.1%. The two calculation methods [6, 7] give equally good approximations for the decrease curves. The final precision depends on the apparatus used.

In the study reported here, the dependence of the decay time of some transitions in the emission spectrum of $Eu^{3+}:Y_2O_2S$ on the europium concentration was examined. The transitions investigated were: $^5D_0 \rightarrow {}^7F_2$ (626 nm), $^5D_1 \rightarrow {}^7F_1$ (539 nm) and $^5D_2 \rightarrow {}^7F_0$ (476 nm). The calculations were performed by means of eqn. (2).

EXPERIMENTAL

Preparation of the compounds

The starting materials used were lanthanide oxides of purity 99.99% (Rhone-Poulenc, France). The europium concentrations in yttrium oxide sulfides varied from 0.1 to 12 mol-%. Two series of $Eu^{3+}:Y_2O_2S$ phosphors were prepared, the first by reducing the corresponding sulfites with carbon monoxide [10] and the second by the reaction of coprecipitated lanthanide oxides with a sulfurizing flux containing sulfur, sodium carbonate and tripotassium phosphate [11].

Lifetime measurements

The lifetime measurements were carried out by inducing cathodoluminescence. A schematic representation of the apparatus used for measurements is shown in Fig. 1. The phosphor sample was placed on a copper support at room temperature and excited by a periodic electron beam (Fig. 2) (15—20 keV, a few μA cm^{-2}). The period T of one cycle was variable; $T > 3\tau_e$ was used. The fluorescence was detected by reflection through a monochromator of 0.45-m focal length equipped with a grating of 1200 lines mm^{-1}. The detector was a photomultiplier sensitive between 180 and 950 nm. The observation of the lifetime was made either by taking a photograph of the decay of the luminescence from an oscilloscope or by using an x—y recorder

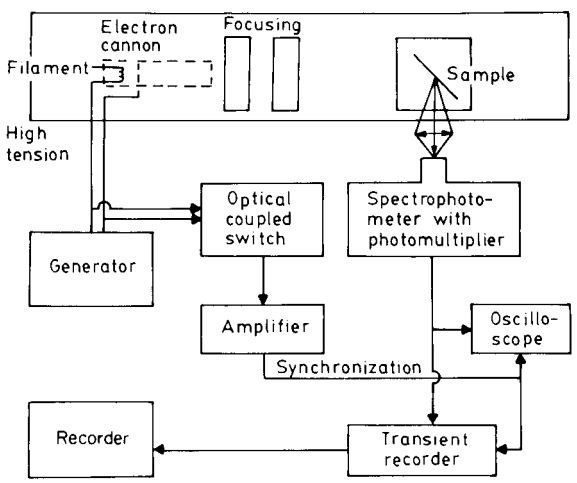

Fig. 1. Schematic representation of the apparatus used in lifetime measurements.

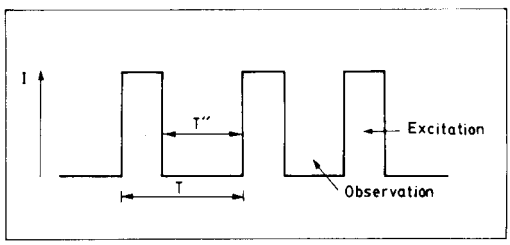

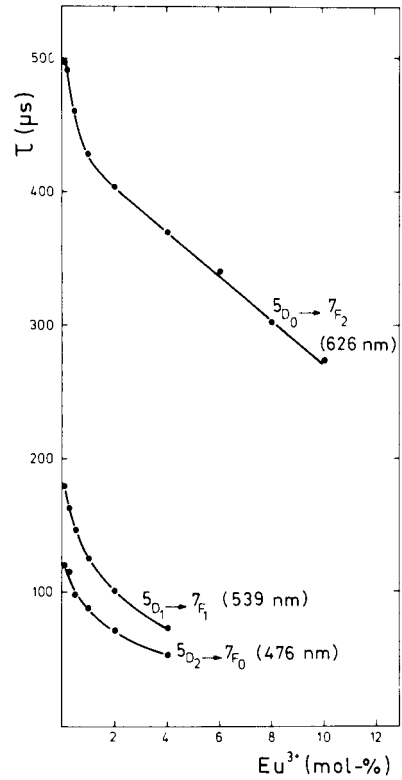

Fig. 2. Representation of the excitation signal. The intensity under observation, I (T'') $\leqslant I_0/10$, when $T'' > 3\tau_e$.

Fig. 3. Lifetime vs. europium concentration for three transitions in the luminescence spectrum of Eu^{3+}:Y_2O_2S.

with a large band-pass electrical integrator (10 MHz) type ATN or a boxcar integrator. The time constant of the complete apparatus and detector was less than 1 μs.

RESULTS AND DISCUSSION

The lifetime vs. concentration curves for the transitions $^5D_0 \rightarrow {}^7F_2$, $^5D_1 \rightarrow {}^7F_1$ and $^5D_2 \rightarrow {}^7F_0$ in the luminescence spectra of Eu^{3+}:Y_2O_2S are shown in Fig. 3. The emission from $^5D_2$ is quenched first, then that from $^5D_1$, and the emission from $^5D_0$ has the longest lifetime, as expected. The differences between the lifetimes of the transitions from the three levels are significant. For the transition $^5D_0 \rightarrow {}^7F_2$ the decay times were 300—500 μs; for $^5D_2 \rightarrow {}^7F_0$, 50—100 μs. When the europium concentration exceeded 4%, the lifetimes were difficult to measure for the $^5D_2$ and $^5D_1$ transitions owing to their low intensity. In commercial Eu^{3+}:Y_2O_2S phosphors, the activator concentrations are seldom more than 4%, however.

The results from the lifetime measurements are interesting but not in agreement with the above equation for τ_a/τ_0, as the curves were not logarithmic. The curves of transitions $^5D_2 \rightarrow {}^7F_0$ and $^5D_1 \rightarrow {}^7F_1$ appeared logarithmic (Fig. 3) but a plot of log τ against concentration shows two linear portions, indicating the possibility of two different quenching mechanisms (Fig. 4). The intersection of the lines occurred at 1% europium. This was also found by Ozawa and Jaffe [3] for oxides and oxide sulfides, where the experimental results corresponded well with theory for the oxides but deviated slightly for the oxide sulfides. The lifetime vs. concentration curve of the $^5D_0 \rightarrow {}^7F_2$ transition differs from the other curves because its quenching mechanism is different.

In the concentration range 2—10 mol-% europium(III), the dependence of the lifetime on concentration was linear. The linearity was so good that the lifetime measurement of the red emission could be used to determine the activator concentration. A change of 1 mol-% in the europium concentration caused the lifetime to change by about 20 μs. As the detection limit of the apparatus was about 2 μs, the europium concentration could thus be determined to within 0.2 mol-%, which is very satisfactory for practical purposes.

The linear intensity ratio curve ($f(C) = I_{589.0\ nm}/I_{583.0\ nm}$) obtained from the samples is shown in Fig. 5. In the normal concentration region the intensity ratio varied between 0.5 and 2. When the europium concentration changed by 1 mol-% the ratio changed by 0.2—0.3. The precision of this

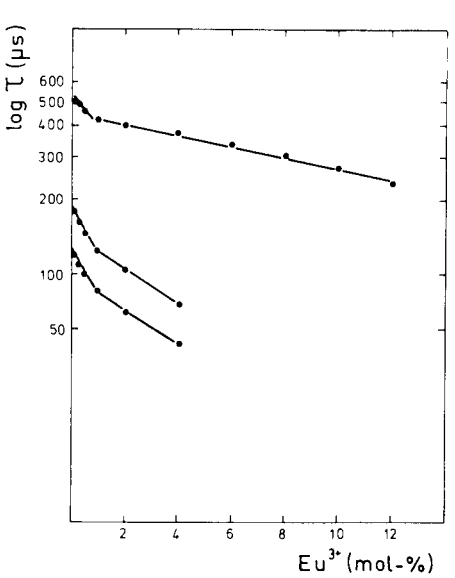

Fig. 4. Log (lifetime) vs. europium concentration for the data in Fig. 3.

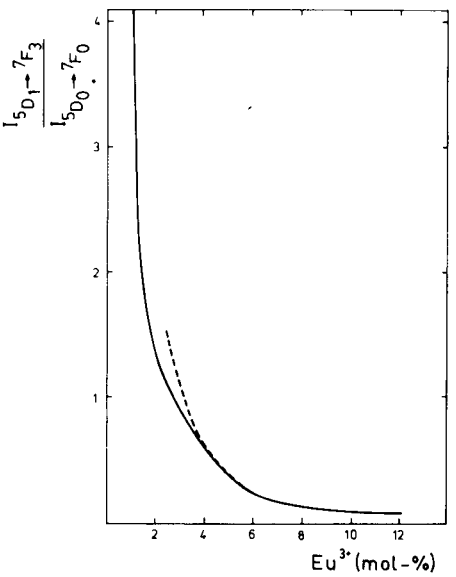

Fig. 5. Linear intensity ratio (LIR) vs. europium concentration for transitions $^5D_1 \rightarrow {}^7F_3$ and $^5D_0 \rightarrow {}^7F_0$ at 589 and 583 nm, respectively. The broken line represents values given in ref. 5 for 587 and 583 nm, respectively.

method is reported to be within 0.05% in the range 2—6 mol-% of europium [5], but such high reproducibility could not be attained here.

The shape of the linear intensity ratio curve (Fig. 5) is in agreement with that obtained by Ozawa and Forest [5] for europium concentrations exceeding 3.5%. Below 3.5%, the intensity ratio was found to be significantly smaller and at 2.5% the two curves differed by an amount corresponding to 0.5% europium. This is probably due to our use of the peak at 589 nm (instead of 587 nm) because it is sharper and can thus give better accuracy.

The results from the lifetime measurements were independent of anodic voltage and intensity of the electric current. The absolute lifetime values are not comparable to those measured by optical excitation (flash lamp, pulse laser), however. Struck and Fonger [12] have shown that the lifetime of a single transition depends on the excitation wavelength. Also, the self-quenching concentration is evidently different for different types of excitation [13]. When Y_2O_2S containing 0.1% Eu is excited at 77 K in three different ways (i.e. excitation to the $4f$ states at 397 nm, excitation to a charge-transfer state at 350 nm, and direct $^5D_2$ excitation at 300 nm), the corresponding lifetimes for $^5D_2$ are 240, 205, and 180 μs, respectively [12]. The differences are so large that optical excitation cannot be used in analytical applications in the way that cathode-ray excitation can.

Conclusion

Measuring the lifetime of the Eu^{3+} transition $^5D_0 \rightarrow {}^7F_2$ provides a practical and rapid analytical method for the determination of europium concentration in rare earth oxide sulfides. Its precision to within 0.2% is high enough for industrial use. An advantage of this method over the linear intensity ratio method is that fresh calibration is not needed for every determination, because the lifetime is an absolute value. In the analytical use of lifetime measurements the excitation must be by cathode rays.

Y.C. thanks the Finnish Ministry of Education for a fellowship. Financial aid from the Finnish Cultural Foundation to M.L. is gratefully acknowledged.

REFERENCES

1 J. E. Mathers, in O. B. Michelsen (Ed.), Analysis and Applications of Rare Earth Materials, Universitetsforlaget, Oslo, 1973, p. 241.
2 M. R. Royce, U.S. Pat. 3 418 246 (1968).
3 L. Ozawa and P. M. Jaffe, J. Electrochem. Soc., 118 (1971) 1678.
4 H. Forest, J. Electrochem. Soc., 120 (1973) 695; U.S. Pat 3 793 527 (1974).
5 L. Ozawa and H. Forest, Anal. Chem., 45 (1973) 978.
6 L. G. van Uitert, J. Electrochem. Soc., 114 (1967) 1048.
7 D. L. Dexter and J. H. Schulman, J. Chem. Phys., 22 (1954) 1063.
8 L. Ozawa, J. Electrochem. Soc., 126 (1979) 106.
9 M. Inokuti and F. Hirayama, J. Chem. Phys., 43 (1965) 1978.
10 M. Koskenlinna, M. Leskelä and L. Niinistö, J. Electrochem. Soc., 123 (1976) 75.
11 M. R. Royce, S. M. Thomsen and P. N. Yocom, U.S. Pat. 3 502 590 (1970).
12 C. W. Struck and W. H. Fonger, J. Lumin., 1/2 (1970) 456.
13 L. Ozawa and H. N. Hersh, Appl. Phys. Lett., 28 (1976) 727; J. Electrochem. Soc., 124 (1977) 482.

Analytica Chimica Acta, 118 (1980) 129—135
© Elsevier Scientific Publishing Company, Amsterdam — Printed in The Netherlands

EXTRACTION OF TIN(IV) WITH SALICYLIDENEAMINO-2-THIOPHENOL IN THE PRESENCE OF AUXILIARY COMPLEXING AGENTS

HISANORI IMURA and NOBUO SUZUKI*

Department of Chemistry, Faculty of Science, Tohoku University, Sendai, 980 (Japan)

(Received 2nd January 1980)

SUMMARY

The effect of auxiliary complexing agents on the extraction of tin(IV) with salicylideneamino-2-thiophenol in benzene is described. When masking agents such as lactic acid and tartaric acid are used, the extraction of tin(IV) is very slow. 8-Quinolinol-5-sulphonic acid is the most suitable masking agent. Amino-2-thiophenol has a catalytic effect on the extraction of tin(IV); the rate of extraction is increased 27 times on adding amino-2-thiophenol. The quantitative extraction of tin(IV) at pH 0.5—2.0 is described.

Tin(II) readily reacts with chelating reagents containing sulphur and nitrogen donors, such as dithiol [1], diethyldithiocarbamate [2], and dithizone [3], and the resulting chelate can be extracted into organic solvents. However, since tin(II) is readily oxidized to tin(IV) in air, a study of the extraction behaviour of tin(IV) is desirable. Tin(IV) in aqueous solutions readily forms an insoluble hydrated oxide above pH 1 [4], so that addition of masking agents to prevent this hydrolysis is necessary in its extraction in this pH region. The coordination number of tin(IV) is six (except in simple tin(IV) complexes such as halides) so that extraction of tin(IV) with bidentate chelating reagents such as 8-quinolinol (oxine) [5], thenoyltrifluoroacetone [6], or *N*-benzoyl-*N*-phenylhydroxylamine [7] is possible only as a mixed ligand complex such as $SnCl_2$ $(oxine)_2$.

Salicylideneamino-2-thiophenol (SATP) is a tridentate ligand with nitrogen, oxygen, and sulphur donors, forms a stable and extractable chelate with tin(II) and tin(IV), and has been applied to the photometric determination of tin [8, 9]. The expected tin(IV) species, $Sn(SATP)_2$, has been confirmed by applying the mole-ratio method to complex formation in benzene [10], and by elemental analysis of the precipitate obtained by addition of SATP to aqueous solutions of tin(IV) [8]. However, little is known on the acid dissociation and the two-phase distribution of SATP, and the extraction behaviour of the tin(IV)—SATP chelate has not been studied.

In the present paper, the stability and distribution of SATP, and the effects of various complexing agents on the extraction of tin(IV) with SATP are reported.

EXPERIMENTAL

Reagents and apparatus

The purity of SATP (Dojin Chemical Laboratory) was checked by elemental analyses for C, H, N, and S. The reagent was dissolved in benzene before use. 8-Quinolinol-5-sulphonic acid (QS) was purified by recrystallization from acidic aqueous solutions after shaking with benzene at pH 6—8. Amino-2-thiophenol (Tokyo Kasei Kogyo Co.) was diluted with benzene. The solution was stored in a dark bottle.

A tin(IV) standard solution (1.09×10^{-2} M) was prepared by dissolving tin (99.999% pure) in a small quantity of concentrated sulphuric acid and diluting with 2 M hydrochloric acid.

The radioisotope tin-113 used as a tracer (New England Nuclear, U.S.A.) was added to the tin(IV) standard solution. Isotopic equilibrium was achieved by standing for a few days.

Other reagents were of analytical-reagent grade.

A Nippon Atomic Industry Group Co. single-channel analyzer with a 50 × 50 mm NaI(Tl) well-type scintillation detector was used for the γ-counting. An Iwaki KM-Shaker was used for agitation of aqueous and organic phases at 330 strokes per min.

Procedures

Extraction and back-extraction procedure. In a 50-ml centrifuge tube with a ground-glass stopper, 10 ml of benzene containing 10^{-3}—10^{-2} M SATP and 10^{-5}—10^{-3} M amino-2-thiophenol was placed, and 10 ml of buffer solution (pH 0—12) containing 10^{-5}—10^{-4} M tin(IV) labelled with ^{113}Sn and 10^{-4}—10^{-2} M QS was added. Then the contents were shaken for 30—120 min at room temperature. After centrifugation, 3-ml portions were taken from each phase and allowed to stand for 18 h in order to establish the radioactive equilibrium for ^{113}Sn ($t_{1/2}$ = 115 d) with ^{113m}In ($t_{1/2}$ = 1.66 h). Then the radioactivity was counted and the distribution ratio (D) of tin(IV) was calculated. The pH value was measured before and after extraction in all cases.

In the back-extraction procedure, 5 ml of the organic phase obtained as described above, was shaken with 5 ml of a buffer solution containing 10^{-5}—10^{-3} M QS for 5—30 min. The distribution ratio and the percentage back-extraction ($\%E_b$) were determined in the same manner as in the extraction procedure.

Determination of rate constant. The rate of extraction of a metal ion (M), $-\mathrm{d[M]}/\mathrm{d}t$, can be related to the observed rate constant, k_{obs}, by the equation $-\mathrm{d[M]}/\mathrm{d}t = k_{obs}[\mathrm{M}]$, hence $\ln[\mathrm{M}]_t/[\mathrm{M}]_{t=0} = -k_{obs}t$; here t is the extraction time measured from the start of the shaking (t=0). The experiment was carried out as follows: 10 ml of benzene containing SATP and amino-2-thiophenol was shaken with 10 ml of an aqueous phase containing radioactive tin(IV) and QS for various periods (0.5—15 min) at 20 ± 0.5°C. After centrifugation, a 3-ml portion was taken from each phase and allowed to stand for

18 h. Then the γ-activity of each phase was counted, and $\ln[M]_t/[M]_{t=0}$ was plotted against t.

Determination of SATP in benzene. To a 30-ml centrifuge tube with a ground-glass stopper were added 3—5 ml of 10^{-6}—10^{-4} M SATP in benzene, 1 ml of 0.1 M Cu(II) solution (excess), 0.05 ml of pyridine (py) and 5 ml of 0.1 M acetate buffer solution pH 5.0. The contents were shaken for 1—3 min. Then the concentration of SATP was determined spectrophotometrically by measuring the absorbance of the Cu(II)—SATP—py complex [11] at 415 nm against benzene.

RESULTS AND DISCUSSION

Stability and distribution of SATP

The stability and distribution behaviour of SATP as a function of pH were investigated. Figure 1 shows the equilibrium concentration of SATP in benzene after shaking with an equal volume of an aqueous phase. Low values were obtained below pH 1 and above pH 9 because of the decomposition and dissociation of SATP. The relative concentration of SATP in benzene is plotted against shaking time at different pH values in Fig. 2. The rate of lowering of SATP concentration in benzene was pH-dependent; the higher the acidity or the basicity of the aqueous phase, the faster the depression of SATP concentration. These phenomena are probably due to the decomposition of SATP in the presence of acid and of base, which is characteristic of most Schiff bases. However, between pH 2 and 8, SATP was found to be quite stable even after shaking for over 2 h. The distribution coefficient of SATP between the aqueous and the benzene phases, $[SATP]_{org}/[SATP]_{aq}$, was determined as follows: (1) 10 ml of 1.0×10^{-2} M SATP in benzene was

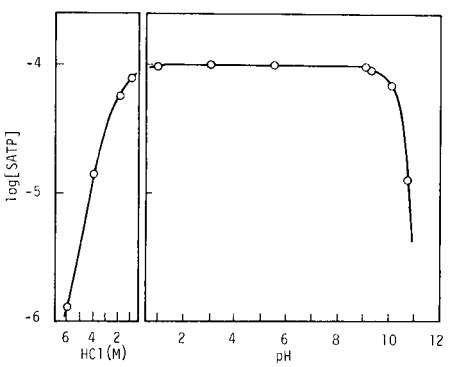

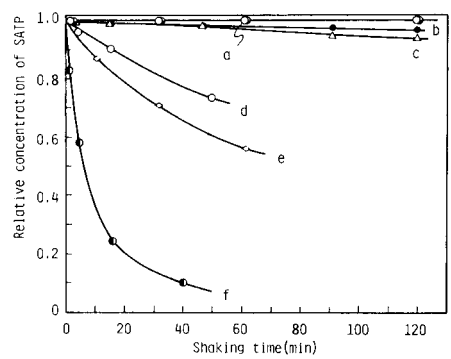

Fig. 1. Effect of pH and acidity on the concentration of SATP in benzene. Initial concentration of SATP, 0.97×10^{-4} M; shaking time, 30 min.

Fig. 2. Change in concentration of SATP (initially 1.0×10^{-4} M) in benzene on shaking with an aqueous phase of various pH values for different times. (a) pH 5.9 and pH 6.5; (b) pH 8.9; (c) pH 1.1; (d) pH 0.2; (e) pH 10.2; (f) pH 10.7.

shaken with 10 ml of aqueous solution (pH 5.5, ionic strength 0.1) for 1 min, and the concentration of SATP in the aqueous phase was measured; (2) the aqueous phase thus obtained was shaken again with pure benzene for 1 min, and then the concentration of SATP in the benzene phase was determined. These two procedures gave a value of 980 ± 8.

Effect of masking agents

In order to achieve quantitative and rapid extraction of tin(IV) with SATP, it was necessary to prevent hydrolysis of tin(IV). Several complexing agents were tested, with the results shown in Table 1. The distribution ratio at a constant shaking time can be taken as a measure of the rate of extraction; thus, the rate of extraction in acidic media decreased in the order: QS > lactic > oxalic > tartaric > citric > glycine > EDTA. For the series from lactic acid to EDTA, the extraction rate decreased as the formation constant of the tin(IV) complex increased. This is compatible with the observation that the rate of reaction of tin(IV) with SATP in an ethanolic aqueous solution was increased by the addition of lactic acid, but not by tartaric or oxalic acid [8]. In contrast, at pH 9.5, the extraction of tin(IV) was greatly enhanced in the presence of all the carboxylic acids. It is known that the tin(IV)—EDTA complex dissociates above pH 8 [4], so the behaviour of other tin(IV)—carboxylate complexes may be similar. The increase in the distribution ratio of tin(IV) may thus be due to the rapid reaction of free tin(IV) with the anionic form of SATP. However, as SATP is susceptible to decomposition at pH 9.5 (see above), this pH is not suitable for the extraction of metal ions.

Table 2 shows that the extraction rate of tin(IV) with SATP increased with increasing QS concentration at low pH values, while the opposite trend was observed at high pH. In the masking reaction of tin(IV) with QS (pK_1 = 3.8 and pK_2 = 8.4), complexes of 1:1 to 1:3 composition may be formed successively with increasing pH. The rate-determining step in the present extraction system is the formation of the 1:1 tin(IV)—SATP complex (see below); this 1:1 complex formation may proceed rapidly via the substitution

TABLE 1

Effect of masking agents on the distribution ratio of 10^{-4} M tin(IV) in the 1.0×10^{-2} M SATP—benzene system for a shaking time of 60 min

Masking agent	pH 2.2	pH 4.0	pH 9.5
10^{-3} M QS	990	0.72	0.33
10^{-2} M lactic acid	9.0	0.53	76
10^{-3} M tartaric acid	3.3	0.65	66
10^{-3} M oxalic acid	5.0	0.43	110
10^{-3} M citric acid	0.58	0.12	55
10^{-3} M glycine	0.34	0.22	99
6×10^{-4} M EDTA	0.011	0.012	49

TABLE 2

Effect of the concentration of QS on the distribution ratio of 10^{-4} M tin(IV) in the 1.0×10^{-2} M SATP—QS system on shaking for 30 min

[QS] (M)	5.0×10^{-4}	1.0×10^{-3}	5.0×10^{-3}
D at pH 1.3	3.0	14	99
D at pH 9.5	0.33	0.14	0.05

reaction of the lower tin(IV)—QS complex with SATP. The increase in the distribution ratio at low pH with increasing QS concentration reflects the formation of the lower tin(IV)—QS complex; at pH 9.5, the extraction decreases because of formation of the higher tin(IV)—QS complex.

Effect of auxiliary agents

The effects on the extraction rate of other complexing agents soluble in the organic solvent were investigated. 4-Picoline, amino-2-phenol, and amino-2-thiophenol, a decomposition product of SATP, were added to the SATP—QS—benzene system. Neither 4-picoline nor amino-2-phenol had an appreciable effect on the rate of extraction of tin(IV), whereas the addition of 9.4×10^{-4} M amino-2-thiophenol increased the distribution ratio to 158 at pH 1.2 and 89 at pH 2.2. The variation in the extent of extraction under these conditions at different pH values is shown in Fig. 3.

The effect of amino-2-thiophenol was studied as follows; if the rate-determining step in extraction in the SATP—QS—amino-2-thiophenol system is the formation of the 1:1 chelate of tin(IV) with SATP, the rate of extraction can be described by the general equation: $-d[Sn]/dt = k_{obs}[Sn] = k[Sn][SATP]$, where k is a rate constant combining various factors such as the acid dissociation and the distribution coefficient of SATP as well as the stability constant and the concentration of the auxiliary masking agents. The log k_{obs} vs. log [SATP] ($>3.0 \times 10^{-3}$ M SATP) plots in the presence of 2.8×10^{-4} M amino-2-thiophenol and in its absence gave straight lines with slopes of 1.1 and 0.98, respectively. This indicated that the formation of the 1:1 tin(IV)—SATP complex is indeed the rate-determining step. Log k_{obs} was also plotted against log [amino-2-thiophenol], the equilibrium concentration in the aqueous phase obtained by colorimetry. The result is shown in Fig. 4: the value of k_{obs} increased with the concentration of amino-2-thiophenol in the aqueous phase, and the extraction rate of tin(IV) with SATP was increased 27 times by 10^{-3} M amino-2-thiophenol. This increase in k_{obs} can be explained on the assumption [12] that the tin(IV)—amino-2-thiophenol complex is formed in the aqueous phase, and that it then reacts faster with SATP than hydrated tin(IV). A plateau region above 10^{-4} M amino-2-thiophenol is seen in Fig. 4; this suggests that the formation of the 1:1 tin(IV)—SATP chelate then proceeds mainly via the reaction of the tin(IV)—amino-2-thiophenol complex with SATP. Similar phenomena have been observed in the extraction of nickel(II) and zinc(II) with dithizone in the presence of acetate and thiocyanate as auxiliary complexing reagents [13].

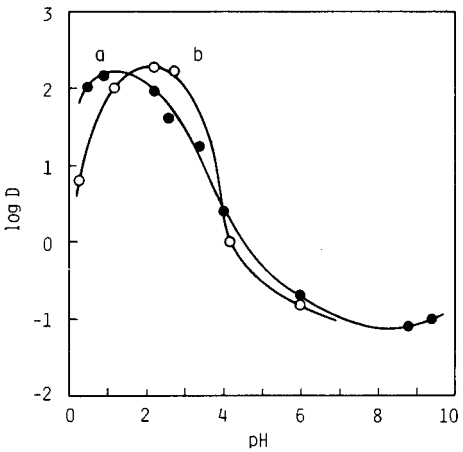

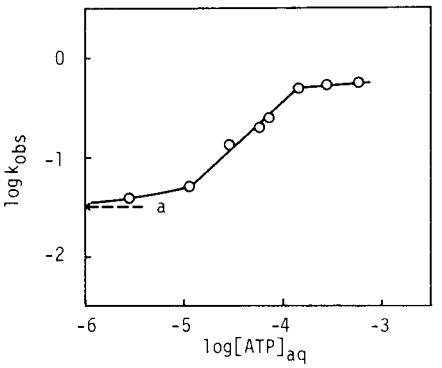

Fig. 3. Extraction of tin(IV) with SATP in benzene from an aqueous phase of various pH values containing 1×10^{-3} M QS in the presence of amino-2-thiophenol (ATP) (a) [SATP] = 6.0×10^{-3} M, [ATP] = 9.4×10^{-4} M, [Sn] = 1.0×10^{-4} M, shaking time = 30 min; (b) [SATP] = 1.0×10^{-2} M, [ATP] = 9.4×10^{-5} M, [Sn] = 1.0×10^{-4} M, shaking time = 60 min.

Fig. 4. Dependence of k_{obs} on the concentration of amino-2-thiophenol in the aqueous phase in the 6.0×10^{-3} M SATP—1.0×10^{-3} M QS—ATP system at pH 1.60. The dashed line indicates k_{obs} in absence of amino-2-thiophenol.

The effect of the pH value of the aqueous phase on k_{obs} is shown in Fig. 5. The plots in the presence or the absence of amino-2-thiophenol are similar in trend, thus the complex formation of tin(IV) with QS in the aqueous phase plays some part in the extraction. As described above, the higher complexes formed in the aqueous phase react less readily with SATP. Thus, k_{obs} increases with the formation of the 1:1 tin(IV)—QS complex, and then decreases with the formation of higher complexes.

Back-extraction of the tin(IV)—SATP complex in the presence of auxiliary agents

The back-extraction behaviour of tin(IV) in the presence and absence of amino-2-thiophenol was investigated. As shown in Fig. 6, the back-extraction of tin(IV) was not affected by amino-2-thiophenol. This indicates that amino-2-thiophenol participated in the chelate formation process of tin(IV) with SATP, but was not involved in the extracted Sn(IV)—SATP chelate. The increase in the back-extraction with shaking time below pH 1 and above pH 10 may be attributed to the decomposition of SATP during back-extraction. The distribution coefficient of the tin(IV)–SATP complex between benzene and the aqueous phase was estimated from the minimum values in the percentage back-extraction (Fig. 6) as more than 3000.

In conclusion, 8-quinolinol-5-sulphonic acid was the most suitable complexing agent in the extraction of tin(IV) with SATP. The catalytic action of

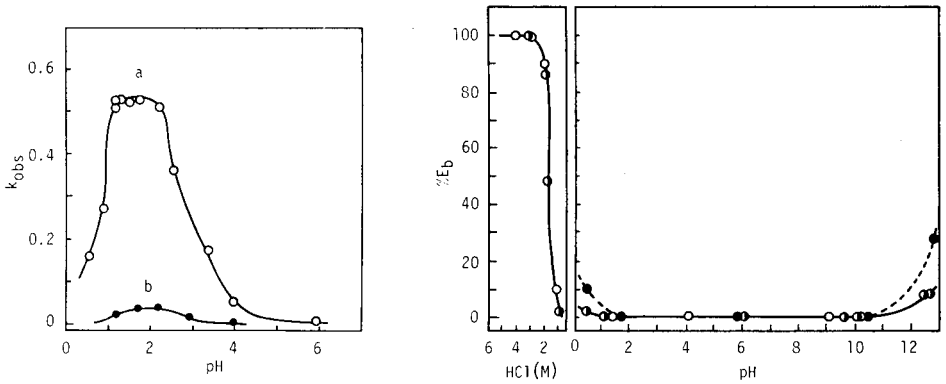

Fig. 5. Dependence of k_{obs} on the pH value of the aqueous phase. (a) 6.0×10^{-3} M SATP—9.4×10^{-4} M amino-2-thiophenol—1.0×10^{-3} M QS system; (b) 6.0×10^{-3} M SATP—1.0×10^{-3} M QS system.

Fig. 6. Back-extraction behaviour of the tin(IV)—SATP chelate into the aqueous phase containing 1.0×10^{-3} M QS. (○) Organic phase prepared from the 6.0×10^{-3} M SATP—1.0×10^{-3} M QS system, shaking time 5 min; (◑) organic phase prepared from the 6.0×10^{-3} M SATP—9.4×10^{-4} M amino-2-thiophenol—1.0×10^{-3} M QS system, shaking time 5 min; (●) as for (○) except that the shaking time was 30 min.

amino-2-thiophenol increases the rate of extraction of tin(IV) with SATP 27 times.

REFERENCES

1 M. Farnsworth and J. Pekola, Anal. Chem., 26 (1954) 735.
2 H. Bode and F. Neumann, Fresenius Z. Anal. Chem., 172 (1960) 1.
3 G. Morrison and H. Freiser, Solvent Extraction in Analytical Chemistry, J. Wiley, New York, 1957, p. 178.
4 J. Kragten, Talanta, 22 (1975) 505.
5 A. R. Eberle and M. W. Lerner, Anal. Chem., 34 (1962) 627.
6 J. R. Stokeley and F. L. Moore, Anal. Chem., 36 (1964) 1203.
7 M. Koeva, N. Jordanov and S. Mareva, Anal. Chim. Acta, 104 (1979) 161.
8 G. R. E. C. Gregory and P. G. Jeffery, Analyst, 92 (1967) 293.
9 S. Maekawa and K. Kato, Bunseki Kagaku, 20 (1971) 474.
10 H. Imura and N. Suzuki, The 28th Annual Meeting of the Japan Society for Analytical Chemistry, Koriyama, October 1979, Abstr. No. 1F04.
11 H. Ishii and H. Einaga, Nippon Kagaku Zasshi, 91 (1970) 734.
12 S. Funahashi, Sakukeisei Hanno, Japan Society for Analytical Chemistry, Maruzen, Tokyo, 1974, p. 288.
13 P. R. Subbaraman, S. M. Cordes and H. Freiser, Anal. Chem., 41 (1969) 1878.

Analytica Chimica Acta, 118 (1980) 137—143
© Elsevier Scientific Publishing Company, Amsterdam — Printed in The Netherlands

Short Communication

SAMPLE CONTAMINATION FROM A COMMERCIAL GRINDING UNIT

R. VAN GRIEKEN*, R. VAN DE VELDE and H. ROBBERECHT

Department of Chemistry, University of Antwerp (U.I.A.), Universiteitsplein 1, B-2610 Wilrijk (Belgium)

(Received 14th February 1980)

Summary. The contamination of ground samples by a commercially available Lovibond McCrone Micronizing Mill is discussed. Tracer and weighing experiments showed that abrasion of corundum grinding elements was important, introducing 6—20 mg of abrasion products per minute of wet grinding. Agate grinding elements were abraded at $\leqslant 6$ mg min^{-1}. The abrasion products and grinding elements were analyzed by x-ray fluorescence, spark-source mass spectrometry and neutron activation analysis. Contamination in trace element analysis of geological materials is likely to be negligible for agate grinding elements and, except for a few transition metals, also for corundum grinding elements. Contamination of typical biological samples is significant for a few elements even when agate elements are used, and is absolutely prohibitive for trace analysis when corundum elements are used.

A grinding and homogenization step is often necessary prior to the analysis of particulate samples, such as geological material and ashed biological specimens. This is particularly so for emission spectrometry and spark-source mass spectrometry, where only a small sample weight is analyzed, and in x-ray fluorescence (x.r.f.), where particle size effects can be troublesome. The material to be analyzed is usually reduced to a fine powder using conventional mortars and pestles or special grinding devices. All these procedures use abrasion and impact to break down the sample particles, and with respect to the trace elements, important contamination might be introduced.

After several authors had reported on contamination from hardened steel and ceramic rotating disks, Thompson and Bankston [1] examined contamination caused by grinding in the boron carbide, alumina and agate mortars and pestles, and in tungsten carbide, alumina—ceramic and lucite vials, that were commercially available around 1970. They noted significant contamination in several cases. The purpose of the present work is to evaluate the effect on the sample composition of grinding in a micronizing mill that is presently commercially available and allows fast and practical particle size reductions at reasonable cost. Special attention is paid to geological and biological samples.

Experimental

Grinding unit. The grinding device studied is a Lovibond McCrone Micronizing Mill. It is a vibroenergy laboratory mill powered by a 1/30 h.p. motor. The grinding vessel is a 125-ml polypropylene jar fitted with a polythene

closure. This jar is packed with an ordered array of identical cylindrical grinding elements, in 6 regular layers of 8 elements each. During the grinding process, the jar with the 48 elements is vigorously shaken, and, as each element moves with respect to its neighbours, grinding occurs between the plane ends and along the cylindrical sides of the elements, while the powder moves continuously between these surfaces. Normally grinding in a liquid slurry is preferred because it appears to be faster and more efficient. The mill can accept about 5 cm^3 of material with particle sizes up to 0.5 mm diameter and is normally operated for a few minutes. The grinding elements normally supplied with the mill are of fine-grained non-porous sintered corundum (alumina). At additional cost, agate elements are also available. Contamination from both types was studied in this work. Hot-pressed boron carbide elements were not considered because of their high price.

Measuring equipment. The x-ray fluorescence (x.r.f.) analysis unit included a Siemens Kristalloflex-2 high-voltage generator (usually operating at 40 kV—40 mA) and a Kevex-0810 subsystem with a tungsten-anode x-ray tube and a secondary target and filter assembly, of for example, molybdenum. The collimated characteristic x-ray beam was measured by a 30-mm^2 Si(Li) detector connected to an amplifier, ADC converter and multichannel analyzer. The x.r.f. spectra were stored on magnetic tape for off-line computer evaluation.

Gamma-spectrometry for tracer experiments and neutron activation analysis (n.a.a.) was performed on a 63-cm^3 coaxial Ge(Li) detector, Philips APY 45 A/N, also connected to a multichannel analyzer. The neutron irradiations, at 10^{12} n s^{-1} cm^{-2}, were carried out in the Thetis reactor of Ghent State University.

The unit for spark-source mass spectrometry (s.s.m.s.) was a radiofrequency spark-source double-focusing instrument with Mattauch-Herzog geometry (JEOL JMS-O1-BM-2) with spherical electric field. Ilford Q2 38 cm × 5 cm ion-sensitive plates were used as detectors. The transmittance of the exposed plates was measured with a single-beam microdensitometer (JEOL JMD-2C) controlled by a JEOL JEC-6 minicomputer, and the data were recorded on a magnetic type unit for processing by a PDP 11/45 computer.

Procedures. In order to evaluate the abrasion of the grinding elements and the resulting sample contamination, 1-g aliquots of biological and geological material were ground with 7 ml of doubly-distilled water for a certain time. After grinding, the resulting slurry was poured out of the mill and the jar and elements were rinsed with 7 ml of water. Both slurries were combined for analysis. To sample the abrasion product from the elements and jar, the grinding unit was operated with only 7 ml of doubly-distilled water present, and afterwards rinsed with 7 ml of water. The suspension was filtered off on a 0.4-μm pore-size, 47-mm diameter Nuclepore membrane. The chemical composition of the filter load is representative of the contaminating material, if none of the grinding unit material is soluble in water.

For x.r.f. analysis the loaded Nuclepore filters were dried and suspended

on teflon rings fitting in the x.r.f. unit. Of the 14-ml biological or geological material slurries, 1 ml was pipetted onto a mylar foil suspended on a teflon ring and dried. The targets were irradiated for 1000—5000 s via a molybdenum secondary fluorescence source. The characteristic spectra were analyzed by means of a non-linear least-squares fitting routine [2], using commercially available thin films for calibration. The material weight was evaluated by a method based on the scatter peaks in the spectrum [3].

For s.s.m.s. analyses of the abrasion material, 1 g of Specpure graphite powder, spiked with indium as an internal standard, was placed into the grinding unit. The resulting slurry was evaporated in a Rotavapor, and electrodes were compressed from the residue. The s.s.m.s. measurements made use of a 2.5-kV anode voltage, 29.8-kV acceleration voltage, 20-μs pulse time and 3-kHz pulse frequency, settings of 20 μm for the main slit and of 0.5 mm for the α- and β-slits. Fifteen exposures were made on each photographic plate, ranging from 0.2 to 200 nC. The developed plates were evaluated by microdensitometry and analyzed by a computer routine [4] based on relative sensitivity coefficients determined for pure graphite [5].

For n.a.a. and tracer measurements, 4 corundum and 4 agate grinding elements were irradiated for 32 h at 10^{12} n s^{-1} cm^{-2}. After one week of cooling, the induced activities were analyzed by Ge(Li)-spectrometry, with a simple background subtraction peak evaluation procedure, and comparison with spotted solution calibration standards. As a tracer for the rate of abrasion into different materials, the released ^{51}Cr and ^{46}Sc activities were measured in the ground product.

TABLE 1

Elemental concentrations in corundum and agate grinding elements or their abrasion products

Element	Concentration (μg g^{-1})		Element	Concentration (μg g^{-1})		Element	Concentration (μg g^{-1})	
	Corundum elements	Agate elements		Corundum elements	Agate elements		Corundum elements	Agate elements
Na	<1350[c]	<280[c]	Co	0.6[c]		Sb	0.05[c]	0.3[c]
Mg	1900[b]	1200[b]	Ni	20[a]	<32[a]	Cs	0.7[c]	0.01[c]
Si	7600[b]		Cu	50[a]	30[a]	Ba	25[b]	
P	72[b]	65[b]	Zn	160[a]	70[a]	La	2.5[c]	0.01[c]
S	110[b]	200[b]	Ga	50[a]	<8[a]	Ce	5.3[c]	0.02[c]
Cl	60[b]	300[b]	Ge	<7[a]	<20[a]	Nd	2.0[c]	
K	1300[a]	<550[a]	As	<10[a]	0.1[c]	Sm, Eu, Tb	0.1 to 0.3[c]	0.01 to 0.1[c]
Ca	1200[a]	1000[a]	Se	<6[a]	<10[a]			
Sc	1.3[b]	0.001[c]	Br		0.3[c]	Yb, Lu, Hf, Ta, W	0.03 to 0.2[c]	
Ti	500[a]	<160[a]	Rb	15[a]	20[a]			
V	40[a]	<77[a]	Sr	25[a]	35[a]	Pb	35[a]	60[a]
Cr	290[a]	70[a]	Y	60[a]	110[a]	Th	0.6[c]	
Mn	80[a]	40[a]	Zr	12[b]		U	0.3[c]	
Fe	2500[a]	1000[a]	Ag	5[b]				

[a]Determined by x.r.f. on the abrasion material when the mill is operated on doubly-distilled wate alone; the uncertainties are generally <15%.
[b]Determined by s.s.m.s. on the abrasion material; the uncertainties are up to a factor of 3 (see text
[c]Determined by n.a.a. on the grinding elements alone.

TABLE 2

Estimated maximum contamination for wet grinding of 1-g geological and biological sample (Abrasion rate: 20 mg min^{-1} for corundum elements; 6 mg min^{-1} for agate elements; grinding el

Element	Corundum grinding elements						
	Absolute contamination ($\mu g\ min^{-1}$)	Typical relative contamination (% min^{-1})					
		Rocks and soils	Sediments	Land plants	Land animals	Marine plants	Marine animals
Na	<27	<0.2	<0.58	<2.2	<0.67	<0.08	<0.06–0.
Mg	38	0.27		1.2	3.8	0.7	0.8
Si	150	N		3–75	2.5–125	0.8–10	15–200
P	1.4	0.16		0.07	N	N	N
S	2.2	0.46		0.07	N	N	N
Cl	1.2	1.0		0.06	N	N	N
K	26	0.15	0.15	0.19	0.35	N	0.09–0.
Ca	24	0.1	0.08	0.13	N–12	0.24	0.1–1.6
Sc	0.026	1.7	0.24	325	9–L		
Ti	10	0.19	0.26	L	L	12–80	50–500
V	0.8	0.68	0.97	50	L	40	40–L
Cr	5.8	5.8	5.9	L	L	L	L
Mn	1.6	0.18	0.11	0.30	L	3.0	3–150
Fe	50	0.11	0.13	36	31	7.1	12
Co	0.012	0.07	0.09	2.4	40	1.7	0.24–2
Ni	0.4	0.7	1.1	13	50	13	2–100
Cu	1	2.7	4.1	7	40	9	2–25
Zn	3.2	5.3	1.5	3.2	2	2.1	0.2–50
Ga	1	6		L	L	200	200
As	<10	<250	<45			<30	
Br							
Rb	0.3	0.32	0.28	1.5	1.8	4	1.5
Sr	0.5	0.15	0.36	2	3.6	N–0.2	0.1–2.1
Y	1.2	3 ?		>200			L
Zr	0.24	0.1		38	>80	>1.2	24–240
Ag	0.1	85	14	160	10–L	40	1.5
Sb	0.001	0.1 ?	0.09	1.7	17		0.5
Cs	0.014	0.4	0.15	7	22	20	
Ba	0.5	0.1	0.14	3.6	67	1.7	17–250
La	0.05	0.17	0.14	60	19–L	0.5	50
Ce	0.11	0.2	0.16	>0.03	L		
Nd	0.04	0.14	0.10	>0.01		0.8	8
Sm	0.006	0.1	0.08	110	60		10
Eu	0.002	0.17	0.14	10	1–L		3–20
Tb	0.004	0.45	0.53	N–L	L		50
Yb	0.002	N	0.08	>130	0.2–L		10
Lu	0.0006	0.12		>0.01	7.5–500		20
Hf	0.004	0.13	0.05	<40 ?	<10	<1	
Ta	0.002	0.1	0.21				
W	0.004	0.32		5.7	80	11	8–L
Pb	0.7	6	1.2	26	35	8	120
Th	0.012	0.16	0.13		12–400		40–400
U	0.006	0.32–6	0.25	16	50		0.2–15

[a]N = negligible contamination, below 0.05%, L = very important contamination, above 500%.

ents composition as given in Table 1)[a]

gate grinding elements						
bsolute ntami- ation g min^{-1})	Typical relative contamination (% min^{-1})					
	Rocks and soils	Sediments	Land plants	Land animals	Marine plants	Marine animals
.7	<0.01	N	<0.14	N	N	N
.2	0.05		0.22	0.72	0.13	0.15
.39	N		N	N	N	N
.2	0.09		N	N	N	N
.8	1.6		0.09	0.06	N	N
.3	N	N	N	N	N	N—0.06
	N	N	N	N—3	0.06	N—0.04
00001	N	N				
.0	N	N	<100		1.2—8	5—50
.5	0.42	0.61	30	330	25	25—350
.42	0.42	0.42	180	L	42	42—210
.24	N	N	N	120	0.5	0.5—20
	N	N	4.3	3.7	0.9	1.4
.2	<0.3	<0.5	<6	<25	<6	<1—50
.18	0.5	0.74	1.3	7.2	1.6	0.4—4
.42	0.7	0.20	0.42	0.26	0.28	N—6.6
05	<0.3		<85		<10	<10
.001	N	N	N	≤0.5	N	0.3—20
.002	N	N	N	N	N	N
.12	0.13	0.11	0.60	0.72	1.6	6
.21	0.06	0.15	0.84	1.5	N—0.08	N—1.0
.66	1.6 ?		>110			450
.002	0.2 ?	0.17	3.4	34		1
.00006	N	N	N	0.09	0.09	
.00006	N	N	0.07	N—60	N	0.06
.0001	N	N	N	3.0		
.00006	N	N	1.1	0.6		0.1
.00006	N	N	0.3	N—50		0.1—0.6
.00001	N	N	N—>0.7	2.5		0.13
.36	3	0.60	13	17	4	60

Results and discussion

Abrasion rate. After the mill had been operating for 10—15 min on 7 ml of doubly-distilled water alone, the weight of the grinding elements was found to be decreased by an average of 17 ± 2 mg per min of grinding time for the corundum elements and 5.8 ± 0.2 mg min^{-1} for the agate elements. At the same time, the weight of the polypropylene jar decreased by 0.72 ± 0.05 mg min^{-1} during the grinding with corundum elements. The chemical composition of the abrasion products did not change significantly with time, since the amounts of transition metals in the suspended abrasion products, as determined by x.r.f., appeared to increase linearly with grinding time. The weight of the corundum elements was found to decrease by only 11 mg min^{-1} during wet grinding of plankton powder (MA-A-1, IAEA) and 6.4 ± 2.4 mg min^{-1} for seaweed powder (SP-M-1, IAEA). The radioactivity found in the slurries, after grinding with radioactivated corundum grinding elements, also provided a measure for the abrasion rate. (In the case of agate elements, the induced radioactivity was too low to be measured.) When the mill had been operating on doubly-distilled water alone, the ^{51}Cr and ^{46}Sc activities corresponded to a mean abrasion rate of 23 ± 2 mg min^{-1}. When slurries with 1 g of material had been ground, the results were: 17 ± 1 mg min^{-1} for a lake sediment (SL-1, IAEA), 14 ± 1 mg min^{-1} for a soil sample (Soil-5, IAEA), 6 ± 1 mg min^{-1} for seaweed powder (SP-M-1, IAEA) and 7 mg min^{-1} for leaves (orchard leaves, NBS-SRM 1571). Clearly, the highest abrasion rates are found when only water is present in the jar, and the elements abrade each other, with no softer material available between the elements. In view of the above results, it seems reasonable to conclude that the maximum abrasion rate is 20 mg min^{-1} for corundum and 6 mg min^{-1} for agate elements.

Of course, the reliability of such data is rather limited, since they may vary somewhat with the amount of wear on the elements and jar.

Composition of grinding elements. Table 1 lists the analytical results for eight x.r.f. measurements on the suspension filtered off after the mill had been operating on a 7-ml water sample, for single s.s.m.s. measurements on the same material, or for two n.a.a. measurements on the grinding elements themselves. The x.r.f. results are the most reliable. In view of the uncertainties in the relative sensitivity coefficients, s.s.m.s. analyses are quoted only where no x.r.f. data are available; their uncertainty can be up to a factor of three. In cases of overlap, the average difference between x.r.f. and s.s.m.s. determinations amounted to 24%. The n.a.a. results cannot be compared to the x.r.f. and s.s.m.s. results, since they deal with the grinding elements themselves, not the abrasion products. N.a.a. data are quoted only when no other result was available.

Contamination of biological and geological samples. Contamination rates were estimated from the product of the abrasion rates and the composition of the abrasion material. Measurements of the apparent composition of reference materials as a function of the grinding time allowed only the most important elemental contaminations to be observed above the random scatter.

As mentioned above the abrasion rates for corundum elements were 6—20 mg min^{-1}, depending on the charge and 6 mg min^{-1} or less for agate elements. The highest of these numbers and the data in Table 1 were used to calculate the maximum absolute contamination rates that are included in Table 2. These data are in agreement with the results of, for instance, Thompson and Bankston [1], who reported significant contamination by Li, B, Al, Ti, Cr, Mn, Fe, Co, Cu, Zn, Ga, Zr and Ba from alumina and alumina—ceramic mortars and vials, and only mild B and Cu contamination from agate mortars. Relative contamination rates for the grinding of 1-g samples were calculated using average elemental compositions of igneous rocks and soils, land plants, land animals, marine plants and marine animals [6], and averages for rather polluted Ems river sediments [7]. In view of the possibly important uncertainties, the results should not be used to carry out contamination corrections. They do give useful information, however, as to the expected contamination levels and the applicability of the Lovibond Micronizing Mill.

It appears from Table 2 that geological material contamination is negligible for agate grinding elements and only serious for a few elements, e.g. Ag, Cr, Cu, Zu and Pb, when grinding is done with corundum. When typical biological materials are ground, however, the contamination from corundum grinding elements is absolutely intolerable for most trace elements and permissible only for abundant constituents like Na, Mg, P, S, Cl, K, Ca, Rb and Sr. Agate grinding elements may induce into biological material important contamination by Ti, V, Cr, Mn, Fe and Pb, while many other elements can probably be determined safely.

We are grateful for the help of L. Van't dack, W. Blommaert and E. Michiels. H. Robberecht acknowledges financial support during part of this work from the Belgian Ministry of Health (Project Selenium Impact, promoter: D. Vanden Berghe).

REFERENCES

1 G. Thompson and D. C. Bankston, Appl. Spectrosc., 24 (1970) 210.
2 P. Van Espen, H. Nullens and F. Adams, Nucl. Instrum. Methods, 142 (1977) 243.
3 P. Van Espen, L. Van't dack, F. Adams and R. Van Grieken, Anal. Chem, 51 (1979) 961.
4 B. Vanderborght and R. Van Grieken, Anal. Chim. Acta, 103 (1978) 223.
5 B. Vanderborght and R. Van Grieken, Talanta, 26 (1979) 461.
6 H. J. M. Bowen, Trace Elements in Biochemistry, Academic Press, London, 1966.
7 Bundesanstalt für Gewässerkunde: Report on 2nd Intercomparison Run "Spurenmetalle in Sedimenten", Koblenz, FRG, 1977.

Analytica Chimica Acta, 118 (1980) 145—148
© Elsevier Scientific Publishing Company, Amsterdam — Printed in The Netherlands

Short Communication

A VERY SIMPLE AIR-GAP CYANIDE SENSOR

JAROSŁAW FLIGIER*, PIOTR CZICHON and ZBIGNIEW GREGOROWICZ

Department of Analytical and General Chemistry, Silesian Polytechnic University, 44-101 Gliwice (Poland)

(Received 30th January 1980)

Summary. A simple and cheap cyanide electrode is described. Based on the air-gap concept, the sensor consists of an ordinary calomel electrode and a silver wire mounted in a ground-glass joint. A minute volume of the dicyanoargentate(I) solution serves as electrolyte. The sensor responds linearly to cyanide concentration in the range 10^{-3}—10^{-6} M in the usual double-Nernstian way. The selectivity is very good.

Cyanide-selective electrodes have been commercially available for several years; they are solid-state electrodes with silver iodide, silver sulphide or a mixture of these two compounds in the membrane. Practical measurements with such electrodes nearly always require preceding elimination of interfering ions, and often preliminary separation of cyanide by distillation [1]. The lifetime of these solid-state electrodes is limited because of the solubility of the products of the electrode reaction. This is why the structure of the electrodes has been changed to facilitate regeneration [2]. Another type of cyanide-selective electrode is the gas-sensing electrode described by Frant et al. [3], who based their method on their earlier potentiometric determination of cyanide by the standard addition technique [4].

This communication deals with a very simple sensor, the operation of which is based on the reaction $Ag(CN)_2^- \rightleftharpoons Ag^+ + 2CN^-$. Construction of the sensor with an air-gap [5] allows considerable simplification compared to Frant's solution, as well as significant improvement in response time and selectivity.

Experimental

Reagents. Analytical-grade reagents and deionized oxygen-free water were used. A 10^{-3} M potassium cyanide stock solution was standardized by Liebig's method. The electrolyte, 10^{-2} M potassium dicyanoargentate(I), was adjusted to pH 9.5 with 0.1 M borax and 0.5% (w/w) methylcellulose was added. The standard solutions and samples were acidified with 1 M tartaric acid.

Apparatus. The sensor (Fig. 1) consisted of a calomel electrode (1; K-401 Radiometer) and a silver electrode (2) made from silver wire (1 mm diameter) slightly flattened at its curved lower part as shown. Both these electrodes were mounted in a 19/26 ground-glass joint (3) by means of a silicone resin (Polasistil, Erg, Poland). For the measurements, the sensor was attached to a

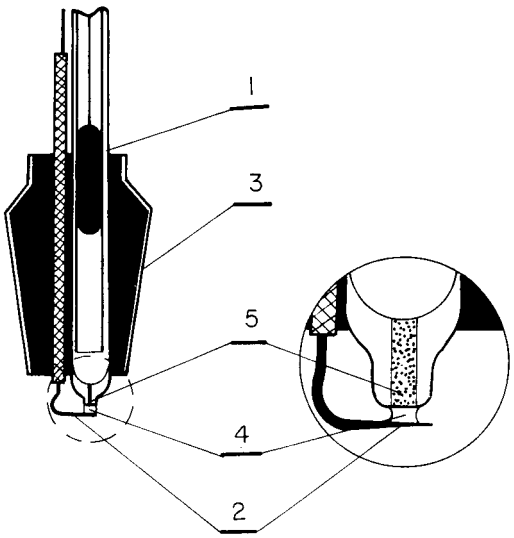

Fig. 1. Construction of the cyanide sensor. For details, see text.

conical glass flask of about 20-cm^3 capacity with a 19/26 ground-glass joint. Stirring was done magnetically with a small teflon-coated bar. A Meratronik N-517 digital pH/mV meter was used.

Measuring technique. The electrolyte (4) was applied between the porous pin of the calomel electrode (5) and the end of the silver electrode as shown in Fig. 1. The gap between the electrodes was 1.0 mm. Next 15.0 ml of the standard solution or sample, previously adjusted to pH $\leqslant$11 if necessary, was pipetted into the glass vessel and 1.0 ml of 1 M tartaric acid was added. Immediately, the vessel was closed with the sensor and the magnetic stirrer was started simultaneously. Readings were made after a steady state had been reached (1—3 min), with an accuracy of 1 mV. After each measurement, the electrolyte layer was removed with distilled water, the electrodes were dried with paper tissue, and a fresh layer of electrolyte was applied.

Results and discussion

Choice of the electrodes and electrolyte. The use of the Radiometer K-401 calomel electrode proved to be very convenient. The good reproducibility of its potential, the slight leakage of the potassium chloride solution (5 μl in 24 h) and the axial position of the porous pin at the bottom of the electrode, guaranteed adequate stability of the reference half-cell and simplified the construction of the sensor. The seepage of chloride did not cause precipitation of silver chloride in the electrolyte because of the very low dissociation constant of the dicyanoargentate complex. In contrast to the silver iodide/sulphide membranes, the silver indicator electrode does not react directly with the cyanide, so that its regeneration consisted merely of occasional cleaning of the surface. The closeness of the two electrodes facilitated quick application of the electrolyte in an amount of 2—3 μl.

Methylcellulose (0.5%) was added both to stabilize the electrolyte mechanically and to retard seepage of the potassium chloride solution from the calomel electrode. The appropriate concentration of methylcellulose was chosen by measuring the stability of the baseline as well as response time of the sensor. The 10^{-2} M dicyanoargentate(I) solution used as electrolyte was selected after tests of the slope of the calibration graph and its linear range for electrolyte concentrations around 10^{-2} M.

Response time, stability and selectivity. As the time required for the sensor signal to return to the baseline was 10—30 min, depending on the concentration of cyanide, it was preferable to renew the electrolyte layer between measurements; this normally took 1 min. The small distance between the electrodes and the sample surface (2—3 mm), as well as the insignificant volume of the electrolyte, improved the response time of the sensor compared to those of the Radiometer electrode or the electrode of Frant et al. [3]. In the range 10^{-3}—10^{-5} M cyanide in the sample, the time needed to reach a 99% steady state varied from 0.5 to 2 min. The stability of the sensor above 3×10^{-5} M cyanide solution was good; after 30 min, the potential decreased only 1% from the initial steady state.

The lack of direct contact between the electrode and the sample solution improves the selectivity of the sensor compared with solid-state electrodes; the only possible interferences arise from compounds which are volatile after the acidification. The proposed sensor is of course insensitive to compounds which change the diffusion conditions in the polymeric membrane [6].

The selectivity coefficients were determined at a fixed cyanide concentration (3.3×10^{-5} M) with varying concentrations of the interfering ions. The presence of sulphide in the sample caused silver sulphide precipitation in the electrolyte and the silver electrode became covered with a layer of sulphide. Sulphide could, however, be separated initially by the addition of a slight excess of a lead or cadmium salt. In the case of carbonate and sulphite, the mean selectivity coefficients were 5×10^{-5} and 8×10^{-5}, respectively.

Reproducibility of measurements. Over a period of 4 weeks of operation (4—6 hours daily) the calibration graph was checked every 2—3 days. The changes of the potentials at different concentrations of cyanide are summarized in Table 1. The potentials were checked by using the same as well as freshly prepared electrolyte. After 4 weeks, the silver electrode was cleaned by dipping into concentrated nitric acid and washing with 0.1 M potassium cyanide and water. After this operation, the potential values were 10—15 mV lower than the lower limits presented in Table 1 for the respective concentrations of cyanide. These low values (±2 mV) were, however, maintained

TABLE 1

Reproducibility of the cyanide sensor over 4 weeks of operation

$[CN^-]$ (M)	10^{-6}	10^{-5}	10^{-4}	10^{-3}
E.m.f. (mV)	86—96	202—206	316—319	426—432

TABLE 2

Recovery of known amounts of cyanide added to the effluent from a coking plant[a]

Present (μg)	Added (μg)	Found (μg)	Recovery (%)
6.6[b]	2.6	9.3	101.2
	6.5	12.8	97.8
	13.0	20.0	102.0
	26.0	32.2	98.8

[a]10.0 ml of effluent, 1.0 ml of 0.1 M Pb^{2+} solution, standard solution and water to a total volume of 15.0 ml. The results shown are the averages of triplicate determinations.
[b]Average for 10 determinations.

after the sensor had been conditioned for 12 h in electrolyte. This cleaning procedure was repeated 4 times with much the same results. The slope of the calibration graphs was not affected by the cleaning.

Calibration and testing of the sensor. For 6.66×10^{-5} M cyanide, the standard deviation amounted to 1.33 mV for 10 determinations, which corresponds to an error of 2.9%. The accuracy of measurement was evaluated by determining the concentration of cyanide in effluents containing sulphide, collected from a coking plant, and making known additions of cyanide (Table 2).

Conclusion

The simple structure of the cyanide sensor, operating on the air-gap principle, makes it easy to construct in the laboratory within a few hours. Unlike the solid-state electrodes, which deteriorate quickly at high cyanide concentrations, the lifetime of the proposed sensor is practically unlimited, provided that the surface of the silver electrode is periodically cleaned. The double-Nernstian response of the sensor to the cyanide concentration enhances the accuracy of the measurements, despite the slightly poorer reproducibility compared with manufacturer's data for the commercial electrodes. The positioning of the sensor above the sample surface makes it possible to measure also the partial pressure of hydrogen cyanide in any system, analogously to the case of sulphur dioxide [7].

REFERENCES

1 J. Koryta, Anal. Chim. Acta, 91 (1977) 1.
2 C. Harzdorf, Anal. Chim. Acta, 86 (1976) 103.
3 M. S. Frant, J. M. Riseman and J. A. Krueger, U.S. Patent 3, 950, 231, April 13, 1976.
4 M. S. Frant, J. W. Ross and J. H. Riseman, Anal. Chem., 44 (1972) 2227.
5 J. Růžička and E. H. Hansen, Anal. Chim. Acta, 69 (1974) 129.
6 J. W. Ross, J. H. Riseman and J. A. Krueger, Pure Appl. Chem., 36 (1973) 473.
7 J. Fligier, P. Czichon and Z. Gregorowicz, Chem. Anal. (Warsaw), in press.

Analytica Chimica Acta, 118 (1980) 149—151
© Elsevier Scientific Publishing Company, Amsterdam — Printed in The Netherlands

Short Communication

COLOR TEST FOR TERMINAL PROLYL RESIDUES IN THE SOLID-PHASE SYNTHESIS OF PEPTIDES

E. KAISER*, C. D. BOSSINGER, R. L. COLESCOTT and D. B. OLSEN

Armour Pharmaceutical Company, P.O. Box 511, Kankakee, Illinois 60901 (U.S.A.)

(Received 19th November 1979)

Summary. Reaction with isatin in the presence of BOC-phenylalanine provides a rapid, sensitive and selective test. A blue complex is formed on the resin beads. The accuracy of the test is similar to that of the first cycle of an Edman degradation.

The presence of a free prolyl group at the N-terminal end of a solid-phase peptide sequence is indicated by a reddish-brown color in the ninhydrin test [1]. When the amount of the prolyl residue is small, the color is weak and may remain undetected. Yet, even weak proline ninhydrin colors could indicate that sizable amounts of terminal free prolyl residues still remained unreacted during the coupling. Also, in some cases, rapidly developing blue colors, caused perhaps by a breakdown of the peptide sequences by diketopiperazine formation at the prolyl end, may obscure the brown color on the beads. There is a need to complement the ninhydrin test for proline with a proline-specific color test.

Proline is known to form a blue color with isatin. A color test with isatin has been used to identify proline in paper and column chromatography [2—5] and proline has been determined with isatin in protein hydrolysates [6, 7]. The detection with an isatin reagent of free prolyl groups at the N-terminal of solid-phase peptides is described in this communication.

In the work discussed here, the proline—isatin complex formation was investigated first in organic solvents. Isatin was dissolved in ethanol [6], acetone [7], methanol, or benzyl alcohol, in various concentrations, and samples of these solutions were heated with small amounts of proline. Blue colors were observed, which were weak and fast-fading in ethanol and acetone, somewhat stronger and more stable in methanol, and were strongest and most stable in benzyl alcohol.

Yet, disappointingly, even saturated solutions of isatin in benzyl alcohol failed to yield a blue color on heating to 100°C with a Pro-Leu-Glu-(Bz)-Phe-resin solid-phase peptide sequence. That the presence of the solid-phase peptide did not inhibit the color formation could be shown by the addition of a few crystals of proline, which almost immediately produced a blue color in the solution. The addition of carboxylic acids, which by themselves did not cause formation of a blue color with isatin in benzyl alcohol, was then

tested. Carboxylic acids tried were: acetic acid, malonic acid, benzoic acid, BOC-glycine, and BOC-phenylalanine, all of which yielded blue colors when added to isatin solutions in benzyl alcohol, in which a solid-phase peptide with an N-terminal prolyl group was suspended. The blue complex was tightly bound to the solid-phase beads, while the color of the supernatant liquid remained unchanged. Aromatic carboxylic acids produced more intense colors on the beads than the aliphatic ones. The most satisfactory color was obtained with BOC-phenylalanine. It was found to be advantageous to use saturated solutions of isatin in benzyl alcohol and to add BOC-phenylalanine in a 5% concentration.

Experimental

Reagent preparation. A large excess of isatin (4 g) is added to 120 ml of benzyl alcohol and the mixture stirred for 2 h at room temperature. The part of the isatin which remains insoluble, is removed by filtration, and 5 g of BOC-phenylalanine is added to 100 ml of the filtrate.

Procedure. As in the ninhydrin test, 12 × 75 mm test tubes are used, into which small amounts of beads to be tested are placed and then 2 or 3 drops of the isatin—BOC-phenylalanine solution are added. The tubes are heated in a heating block to 100°C for 5 min, with occasional swirling. If a blue color appears on the beads, then the isatin test is positive; the absence of a blue color is regarded as a negative isatin reaction. The blue color on the beads can even be better observed when the supernatant liquid is removed from the test tube by decantation and the beads repeatedly washed by decantation with acetone.

The isatin reagent is very stable. A 4-year old reagent solution produced colors of intensity equal to those obtained with a freshly prepared reagent solution.

Results and discussion

This isatin test made it possible to detect incomplete couplings to proline in cases when the ninhydrin test was so weak that it could be regarded as negative. The positive isatin test became negative when the coupling reaction was repeated or the reaction time prolonged. The quantitative significance of such an isatin-negative coupling reaction was explored with the help of the Edman degradation.

To a resin peptide, such as Pro-Leu-Glu-(Bz)-Phe-resin, various α-BOC-amino acids were coupled [α-BOC-Phe, α-BOC-Trp, α-BOC-Lys (ε-Z)]. Coupling reactions of the α-BOC-amino acids were regarded to be complete when tests with the isatin reagent were negative. After acidic removal of the α-BOC groups, the resin pentapeptides remained isatin-negative (no blue beads in the test). They then were subjected to Edman degradation. In the first cycle only the phenylthiohydantoins of the terminal amino acid residues appeared; proline phenylthiohydantoin was not previewed. As expected, proline—PTH was the product of the second cycle. These findings indicate

that a negative isatin test has the same level of accuracy as the first cycle of an Edman degradation.

The selectivity of the isatin test was also investigated. The residues of the following amino acids were tested on the solid phase with the isatin reagent: Ala, Arg, Asp, Asn, Cys, Glu, Gln, His, Leu, Met, Thr, Phe and Val. All tests were negative; blue color on the beads could not be detected. Only with terminal prolyl residues did the color of the beads become blue. An α-BOC protection of the prolyl group prevented the formation of blue beads, even on prolonged heating.

To rationalize the need for an acid group to promote the reaction between isatin and the solid-phase prolyl group, it is suggested that the condensation reaction takes place between isatin and the solid-phase prolyl terminal group to yield the blue beads with elimination of water. The suggested structure for the product possesses an extended conjugated system

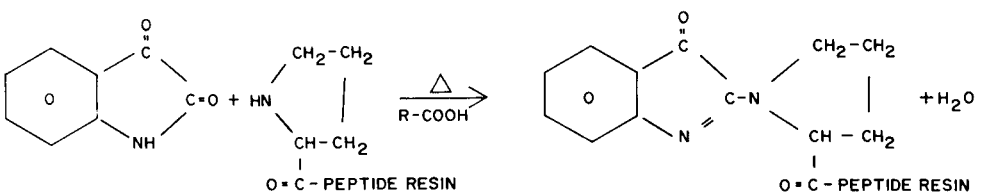

We thank Mr. B. Laken for carrying out the Edman degradations.

REFERENCES

1 E. Kaiser, R. L. Colescott, C. D. Bossinger and P. I. Cook, Anal. Biochem., 34 (1970) 595.
2 R. Archer, C. Fromageot and M. Jutisz, Biochim. Biophys. Acta, 5 (1950) 81.
3 I. N. Smith, Nature, 171 (1953) 43.
4 A. E. Pasieka and J. F. Morgan, Proc. Soc. Exptl. Biol. Med., 93 (1956) 54.
5 E. Hrabetova and J. Tupy, J. Chromatogr., 3 (1960) 199.
6 F. N. Boctor, Anal. Biochem., 43 (1971) 66.
7 R. J. Elliott and D. L. Gardner, Anal. Biochem., 70 (1976) 268.

Analytica Chimica Acta, 118 (1980) 153—157
© Elsevier Scientific Publishing Company, Amsterdam — Printed in The Netherlands

Short Communication

RAPID SEMI-AUTOMATIC ATOMIC ABSORPTION SPECTROMETRIC DETERMINATION OF COPPER IN BOVINE SERUM

C. B. LAWRENCE* and M. PHILLIPPO

Department of Nutritional Biochemistry, Rowett Research Institute, Bucksburn, Aberdeen AB2 9SB (Gt. Britain)

(Received 21st January 1980)

Summary. A system is described for the determination of copper in bovine serum. After semi-automatic dilution of the serum, up to 170 fully automatic atomic absorption analyses per hour are possible. An alarm circuit provides warning of any nebulizer blockage. The coefficient of variation of the method is <2.5%, recovery is 97%, and sensitivity is 0.055 μg Cu ml^{-1}.

A demand for analyses of large numbers of serum samples for copper necessitated the development of an automatic method. An account is given of a procedure found to be fully suitable for routine use.

Experimental

Sample and standard preparation. For each analysis about 0.4 ml of diluted bovine serum (0.2 ml of serum diluted with 0.4 ml of 1.5 × 10^{-3} M hydrochloric acid) was required. This dilution was achieved semi-automatically in a 2-ml plastic cup by using a Compu-Pet 100 (Warner and Co., Eastleigh, Hants). Normally 140 dilutions were completed in 35 min. Standards containing 0.2, 0.5 and 1.0 μg Cu ml^{-1} in 10^{-3} M hydrochloric acid were made from $CuCl_2 \cdot 2H_2O$. Twice-distilled water from glass apparatus was used in the preparation of all solutions. All chemicals were of analytical-reagent grade.

Apparatus. The automatic system (Fig. 1) required a proportioning pump (C.P.P. 15, Chemlab Instruments Ltd., Hornchurch, Essex) which was connected to a sampler—turntable (Chemlab C.S. 40). The sampler, which had an alarm for nebulizer blockage and air failure attached to it, was linked to a Varian AA 1000 spectrometer; the output signal was displayed on a Varian Aerograph A25 recorder.

The automatic system. The proportioning pump was used to introduce a 10^{-3} M hydrochloric acid wash solution to the reservoir in the sampler (Fig. 2) at 3.9 ml min^{-1} and to remove any excess wash solution, up to 2.5 ml min^{-1}, not taken up by the spectrometer when the sampling probe was in the upper position in the reservoir during the probe wash period. If the nebulizer became blocked, the pump was used to remove any waste sample and wash through an emergency line on the pump manifold. The automatic sampler had a normal rate of sampling from 2-ml plastic cups on the attached

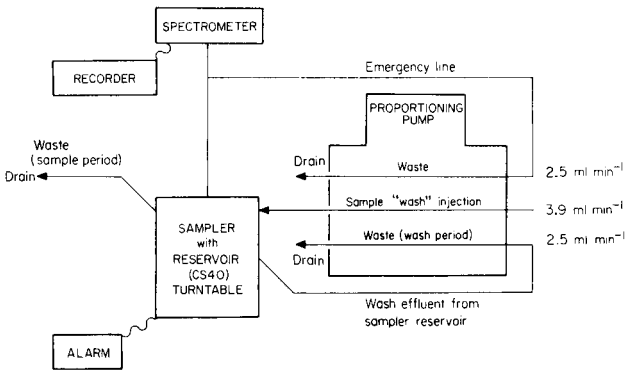

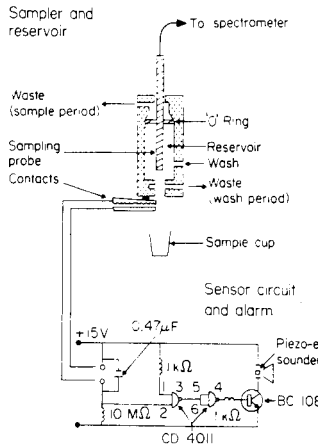

Fig. 1. Automatic system for atomic absorption spectrometry.

Fig. 2. Sampler and reservoir with alarm circuit.

turntable of 170 h^{-1}, this required settings on the variable timer of 6 s for sample aspiration and 15 s for wash of the sampler probe and line. However, for one person to supervise analyses and dilution concurrently a 120 h^{-1} sampling rate with settings of 8 s for "sample" and 22 s for "wash" was more convenient.

The novel detector and alarm giving audible warning of nebulizer blockage was fitted to the base of the sampler reservoir (Fig. 2). The sampling probe of the sampler moved down from its upper wash position in the reservoir to sample from the plastic cup on the turntable. The sample flowed by nebulizer suction to the spectrometer for aspiration into the flame. If partial or complete blockage of the nebulizer or sample line occurred (or the air supply failed), wash fluid was not fully aspirated when the probe moved back to the reservoir. Thus if a partial blockage reduced fluid uptake by the spectrometer to less than 1.4 ml min^{-1}, wash fluid dropped from the bottom outlet of the reservoir and completed the conductivity sensing circuit between the contacts, activating a piezo-electric audible alarm. The system did not need to be shut down if blockage occurred in the nebulizer capillary (the most likely location) as further flooding at the sampler was prevented by connecting the sample line to the emergency line on the pump.

The spectrometer had a single-slot, 10-cm long burner. Optimal operating conditions were as follows: air, 40 psi (5.9 on flow meter); acetylene, 9 psi (1.75 units on flow meter); lamp current 3 mA; wavelength, 324.7 nm; slit width, 0.2 mm; scale expansion, × 2; damping, mode B. The recorder was set on the 2-mV range at chart speed 2.5 cm min^{-1}.

Method assessment. In order to obtain data on precision and accuracy, analyses of a bulk control serum alone, and with 0.2 μg of copper added were carried out, within several measurement sequences, and a number of sera were

analysed alone and plus 0.2 μg or 0.4 μg of copper in the same sequence. The standard used for addition contained 1.0 μg Cu ml^{-1}. The concentrations of copper were measured in various control sera at the start and finish of the proposed operational procedure. Finally, the copper concentrations of 5-ml aliquots of bulk serum were determined in (1 + 19) sulphuric acid (with appropriate standards and blanks) after wet digestion in HNO_3, $HClO_4$, H_2SO_4 and were compared with the values obtained by direct serum dilution.

Results

Comparison with manual measurements. Results for copper obtained after (1 + 2) dilution of sera with 10^{-3} M hydrochloric acid by Compu-pet or calibrated glass pipette were identical, and proved that dilution was accurate. With a (1 + 2) dilution the viscosity problem was negligible (the aspiration rate of diluted serum was only 2% lower than that of a standard copper solution). This dilution was therefore selected for further use, as it generally provided adequate peak height. Attempts to enhance peak height (by about 10%) with 6% butanol [1] were abandoned as a gradual precipitation occurred in the cups awaiting analysis and this had an adverse effect on the accuracy. The criteria for internal consistency in the proposed method were satisfied, in that sera diluted 3, 5 and 6 times gave the same original copper concentration. These results indicated that the serum constituents did not cause matrix effects.

In Fig. 3, a recorder trace showing the automatic analysis of replicate dilutions of a serum sample by the normal proposed procedure is contrasted with that of a similar analysis, having alternate 10^{-3} M hydrochloric acid blank cups interposed between samples, and with manual operation. The peak heights obtained with the automatic method were only slightly lower than those obtained when manual aspiration was continued to attain a plateau value. The mean serum values, without correction for recovery, by the three

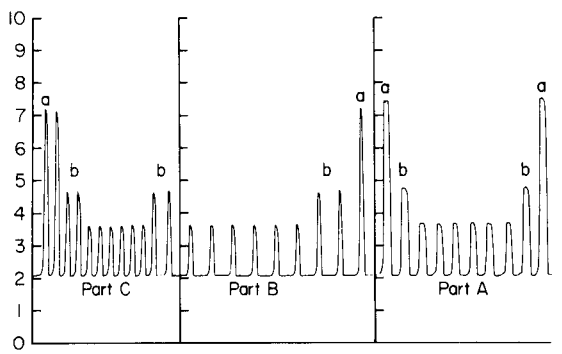

Fig. 3. Automatic analyses of bulked sera after dilution by the proposed method (part C), with blank cups interposed (part B) and by manual analysis (part A). The standards shown are 1.0 μg Cu ml^{-1} (a) and 0.5 μg Cu ml^{-1} (b). The smallest peaks are for a diluted serum.

procedures in Parts A, B and C (Fig. 3) obtained from each of these, were 0.89, 0.92 and 0.91 μg Cu ml^{-1}, respectively. For six serum samples, the mean copper concentrations as measured by the automatic and manual techniques were statistically the same (paired *t*-test) for concentrations in the range 0.50—1.22 μg Cu ml^{-1}.

Automatic analysis. The operational sequence finally decided upon involved analysis of 0.2, 0.5 and 1.0 μg Cu ml^{-1} standards, followed by analyses of the 1.0 μg ml^{-1} standard diluted (1 + 2) by the Compu-Pet (as were the samples) to double check the accuracy of dilution. The peak height was verified to correspond to the correct concentration on the standard graph. On completion of the analyses of standards, 130—160 serum samples were analysed with 0.5 μg Cu ml^{-1} standards after every fifth sample. A control serum was analysed at the beginning and end of the run, which was completed with analyses of fresh aliquots of the initial standards. The burner head was then removed for cleaning because of slight build-up of a deposit in the slot.

With automatic measurement, the chart baseline showed a slow increase with a maximum of 0.5—1.0 chart divisions per hour. Standard peak heights, used for the calculation of results, decreased during an analytical run; however, the difference between the first and last standards for runs with about 140 samples was always less than 15%. The results of analyses on bulk control sera at the beginning and end of such runs, showed that any variation in serum copper concentrations with run position was not statistically significant at the ($P > 0.05$) by a paired *t*-test (Table 1). Sample results were therefore affected neither by baseline drift nor peak-height depression.

The sensitivity was usually 0.055 μg Cu ml^{-1} for 0.0044 absorbance. The peak-height repeatability was better than 2% for a 0.91 μg Cu ml^{-1} solution (see Fig. 3). In other trials where sera levels varied from 0.46 to 1.22 μg ml^{-1}, a coefficient of variation of 2.5% was not exceeded.

The precision of the overall method was calculated from the results of analyses of a bulk control serum carried out within a number of analytical runs on different days over a 10-day period. The coefficient of variation was always less than 2.5%, with serum copper levels of 0.91 μg ml^{-1} or 0.59 μg ml^{-1}, the latter level being found in animals of presumed low copper status. As an example, results for the latter serum fell in the range 0.58—0.60 μg Cu ml^{-1} over a 7-day period.

TABLE 1

Analyses of control sera before and after 140 serum analyses

Sample	A	B	C	D	E	F
Cu found (μg ml^{-1})						
Before	0.45	0.52	0.54	0.55	0.79	0.83
After	0.48	0.52	0.53	0.57	0.80	0.85

TABLE 2

Accuracy of the automatic determination of copper in bovine sera

Serum sample	Cu found (μg ml^{-1})		Serum aliquot	Cu found (μg ml^{-1})	
	Std. addn.	Direct +3%		Direct +3%	Wet digestion
1	0.29	0.29	A	0.89	0.90
2	0.44	0.44	B	0.89	0.90
3	0.51	0.52	C	0.89	0.89
4	0.60	0.60	D	0.88	0.89
5	0.72	0.72	E	0.88	0.89
6	0.72	0.72	F	0.88	0.89

The within-run recovery of 0.2 μg copper added to 0.2-ml aliquots of different sera finally diluted to 0.6 ml (with 1.5×10^{-3} M hydrochloric acid) was found to be 97%. Inter-run recovery from a bulk control serum was 97 ± 2.1% (mean ± s.d.). Because the recoveries from different sera were consistent but slightly low, it is probable that the low recoveries were due to the higher uptake rate of standard compared with diluted serum. The factor responsible for this slight difference in uptake rate (possibly protein) was still exerting an effect at 6-fold dilution, and any further dilution was impracticable for routine analysis.

For the most accurate determinations of serum copper concentrations, results were calculated from the standard additions procedure. These results are contrasted with those obtained by the normal direct procedure, corrected by a factor of +3% for "recovery", as described in Table 2. Both sets of results are in good agreement. The accuracy of the corrected routine procedure is further substantiated by the close similarity of results obtained by analyses of a control serum prepared by direct dilution and by wet digestion (Table 2).

Conclusion

The reported automatic method is of sufficient accuracy, sensitivity, precision, speed and reliability to make it of special use in the large-scale screening of samples. Although it has been developed for the determination of copper in bovine sera, the system can be used with minor changes in instrumental settings in analyses for other elements. With appropriate manifold modifications, the system should be applicable to any atomic absorption spectrometer. Coupling and operation takes only about 1 min, uncoupling is equally easy, and the system may therefore be used for other automatic processes.

The authors thank Mr. A. Allan for construction of the alarm circuit.

REFERENCE

1 S. Meret and R. I. Henkin, Clin. Chem., 17 (1971) 369.

Analytica Chimica Acta, 118 (1980) 159—162
© Elsevier Scientific Publishing Company, Amsterdam — Printed in The Netherlands

Short Communication

THE DETERMINATION OF TRACE AMOUNTS OF SELENIUM IN PHOSPHORIC ACID BY NON-DISPERSIVE FLAME ATOMIC FLUORESCENCE SPECTROMETRY WITH HYDRIDE GENERATION

TAKETOSHI NAKAHARA*, TATSUSHI WAKISAKA and SÔICHIRÔ MUSHA

Department of Applied Chemistry, College of Engineering, University of Osaka Prefecture, Sakai, Osaka 591 (Japan)

(Received 16th January 1980)

Summary. A sensitive, fast and simple method of determining selenium in phosphoric acids has been developed, based on hydride generation followed by non-dispersive atomic fluorescence spectrometry with a premixed argon(entrained air)—hydrogen flame. A standard addition method showed that selenium was present in the range 6—13 ng Se ml^{-1} in the reagent-grade phosphoric acids used.

During an investigation of the general applicability of non-dispersive atomic fluorescence spectrometry for the determination of selenium in biological materials and waste waters [1], a marked enhancing effect of analytical-reagent grade phosphoric acid was observed on selenium atomic fluorescence signals, the extent of which was directly proportional to the concentration of phosphoric acid. This was due to the presence of ppb concentrations of selenium in the phosphoric acid used. Present Japanese Industrial Standards [2] and American Chemical Society [3] specifications for phosphoric acid do not include selenium. From the previous work [1], it was apparent that the extremely sensitive non-dispersive flame atomic fluorescence method coupled with hydride generation could be used to determine selenium in reagent-grade phosphoric acid. This was carried out with the use of a premixed argon (entrained air)—hydrogen flame produced by a specially-designed burner [4]. The 3σ-detection limit obtained previously [1] was 20 pg ml^{-1}.

Experimental

Apparatus. The experimental system used was as described previously [1]. When a dispersive measuring system was required, a grating monochromator (0.3-m Ebert mounting, JE-30, Nippon Jarrell-Ash Co.) equipped with a R-106 UH photomultiplier (Hamamatsu TV Co.) was used.

Reagents. Most reagents were as previously described [1]. Sodium tetrahydroborate was used to form hydrogen selenide, since it was more efficient in the presence of phosphoric acid than zinc [1].

Procedure. The experimental conditions and general procedure for generating hydrogen selenide and measuring atomic fluorescence intensity were similar to those described previously [1]. All atomic fluorescence signals

were measured by peak height and peak area. The results of at least triplicate measurements of each test solution were averaged, unless otherwise stated. Blanks were run throughout and their values were subtracted to give the net values reported.

Five 20-ml aliquots of reagent-grade phosphoric acid (as sample) were added to 100-ml volumetric flasks, and 12.5 ml of 4.0 M hydrochloric acid was added to each, followed by 0, 5, 10, 15 and 20 ml of a 50 ng ml^{-1} selenium standard in sequence, before diluting to volume with distilled water. For measurement of atomic fluorescence intensity, a 20-ml portion of each solution was transferred to the hydride generation unit, and the determination was completed as before.

Results and discussion

Analytical data. Linear logarithmic working curves for $1—10^4$ ng of selenium were obtained by peak-height and peak-area measurements. The 3σ detection limit [5] was 0.4 ng of selenium, equivalent to 20 pg ml^{-1} for a 20-ml sample. The reagent blank had a value of ca. 3 ng of selenium in 20 ml of sample. Table 1 shows the precision obtained when the method was applied to aqueous selenium(IV) standard solutions.

Dispersive study. Winefordner and co-workers [6, 7] have demonstrated PO fluorescence bands at 220—275 nm in a flame fluorescence background and that the PO was formed in the flame from phosphine present in the acetylene. If gaseous phosphorus compounds such as phosphine are produced during the reduction, the PO fluorescence bands may obscure the atomic fluorescence of selenium when measured with a non-dispersive system. To investigate this possibility, therefore, the atomic fluorescence intensities at four major selenium atomic fluorescence lines were measured with a dispersive system by using an aqueous selenium(IV) standard solution and also dilute phosphoric acid. The results obtained by peak-height measurements (Table 2) confirm the absence of flame background fluorescence arising from PO molecules or from contaminants of the phosphoric acid. Thus the non-dispersive method described here is applicable to the determination of traces of selenium in phosphoric acid.

Recovery of selenium added to phosphoric acid. From the interference study of diverse elements and mineral acids in the selenium determination described previously [1], the maximum arsenic levels found in phosphoric

TABLE 1

Precision of the method for selenium with peak-height and peak-area measurements

Selenium (ng)		5	50	500	5000
R.s.d. (%)[a]	Height	4.9	3.5	2.7	3.7
	Area	4.6	3.0	2.5	2.9

[a] 10 determinations.

TABLE 2

Dispersive study of selenium atomic fluorescence

Wavelength (nm)	196.03	203.99	206.28	207.48
Relative intensity 100 ng Se ml^{-1}	100	69.4	24.2	9.7
7.5 M H_3PO_4	100	70.0	25.0	9.0

acid would be expected to cause low results in the determination of selenium. A recovery study was carried out by adding known amounts of selenium to phosphoric acid and applying the recommended procedure. The added selenium was not recovered quantitatively, as is shown in Table 3; the effect of phosphoric acid itself and/or other interferences such as arsenic was small but not negligible. For accurate determinations, therefore, a standard addition method was essential.

Determination of selenium in phosphoric acids. All samples were obtained from several Japanese manufacturers. The results of the determinations obtained by standard addition plots are shown in Table 4. For a comparative study, attempts were made to apply atomic emission spectrometry with an inductively coupled plasma (Nippon Jarrell-Ash Model ICAP-50SM) with a pneumatic nebulizer and without any pre-concentration and separation steps, but results were poor because of the poor sensitivity of the method for selenium and the difficulty in obtaining steady nebulization of concentrated phosphoric acid.

The data indicate that the sensitivity and precision of the method described are adequate for the determination of traces of selenium in analytical-reagent grade phosphoric acids. No reference materials, however, were available to establish the absolute accuracy of this method and, although the results quoted above are those expected from other considerations, a formal check by an independent method would be desirable.

TABLE 3

Recovery study for selenium in phosphoric acid

Phosphoric acid (M)	Se added (ng)	Peak height		Peak area	
		Se found (ng)	Recovery (%)	Se found (ng)	Recovery (%)
1.5	50	48	96	47	94
	100	94	94	95	95
	200	190	95	192	96
3.0	50	46	92	47	94
	100	90	90	93	93
	200	186	93	182	91

TABLE 4

Determination of selenium in phosphoric acids by the standard addition method

Sample No.	Peak height		Peak area	
	ng Se ml^{-1} [a]	R.s.d. (%)	ng Se ml^{-1} [a]	R.s.d. (%)
1	10.3	4.1	11.5	4.0
2	6.0	5.2	5.6	5.1
3	7.0	4.8	7.7	4.8
4	8.6	4.5	9.4	4.3
5	8.5	4.7	8.9	4.5
6	13.0	4.2	13.4	4.2

[a]Mean of 9 determinations.

The authors gratefully acknowledge the technical assistance of Mr. Kôji Hatanaka and financial support for this project by the Ministry of Education of Japan.

REFERENCES

1 T. Nakahara, S. Kobayashi, T. Wakisaka and S. Musha, Appl. Spectrosc., 34 (1980) 194.
2 Phosphoric Acid, JIS K-9005, Japanese Industrial Standards Committee, Japanese Standards Association, Tokyo, Japan, 1972.
3 Reagent Chemicals, American Chemical Society Committee on Analytical Reagents, 5th edn., American Chemical Society, Washington, DC, 1974.
4 T. Nakahara, T. Tanaka and S. Musha, Bull. Chem. Soc. Jpn., 51 (1978) 2046.
5 IUPAC, Nomenclature, Symbols, Units and Their Usage in Spectrochemical Analysis, Part II, Section 4.1, Revision 1975, Pure Appl. Chem., 45 (1976) 99.
6 H. Haraguchi, W. K. Fowler, D. J. Johnson and J. D. Winefordner, Spectrochim. Acta, Part A, 32 (1976) 1539.
7 W. K. Fowler and J. D. Winefordner, Anal. Chem., 49 (1977) 944.

Analytica Chimica Acta, 118 (1980) 163—168
© Elsevier Scientific Publishing Company, Amsterdam — Printed in The Netherlands

Short Communication

ELECTROTHERMAL ATOMIC ABSORPTION SPECTROMETRIC DETERMINATION OF LITHIUM, SODIUM, POTASSIUM AND COPPER IN URANIUM WITHOUT PRELIMINARY CHEMICAL SEPARATION

B. M. PATEL, NEELAM GUPTA, PARU PUROHIT and B. D. JOSHI*

Radiochemistry Division, Bhabha Atomic Research Centre, Trombay, Bombay 400085 (India)

(Received 21st January 1980)

Summary. Graphite furnace atomization is used for the direct determination of Li (0.25—4 ppm), Na (8—70 ppm), K (20—300 ppm) and Cu (0.5—25 ppm) in uranium dissolved in nitric acid, with relative standard deviations of 4—9%. Only iron seriously depresses the signals from the alkali metals.

The direct determination of trace metals in uranium solutions by atomic absorption spectrometry (a.a.s.) with electrothermal atomization offers advantages compared with methods involving chemical separation, viz. shorter analysis time and reduced chances of contamination from reagents. Cadmium, chromium and cobalt at ppm levels can be directly determined in this way, using a 0.1-mg uranium sample dissolved as uranyl nitrate [1]. This technique can be extended to lithium, sodium, potassium and copper in uranium as described below.

Experimental

Apparatus. A Varian-Techtron carbon rod atomizer (CRA-63) and atomic absorption spectrometer (AA-6) were used. All other facilities were as reported previously [1]. Varian-Techtron single-element hollow-cathode lamps were used for copper and lithium and a multi-element lamp for potassium and sodium. All were operated at 10 mA, except for the lithium lamp (5 mA). The spectral bandwidths were 0.2 nm for copper and 0.5 nm for the other elements. An Excalibur 5-μl syringe with disposable teflon tips was used for dispensing solutions.

Reagents. All reagents were of analytical grade. The nitric acid and water were doubly-distilled in quartz apparatus. Specpure chemicals (Johnson Matthey, London) were used in the preparation of solutions. Stock solutions (2000 μg ml^{-1}) of each element were prepared by dissolving appropriate weights of metal or compound in 3 M nitric acid. Working standards were made by suitable dilution with water, the acid concentration in all diluted solutions being adjusted to 0.1 M with nitric acid. All these solutions were stored in PVC containers. To prepare the stock solution of uranium (200 mg ml^{-1}), high-purity uranium was dissolved in concentrated nitric acid, the

solution was evaporated to dryness and this uranyl nitrate was dissolved in 0.1 M nitric acid.

For the study of the direct determination of copper and lithium, standard solutions were prepared each containing 20 mg U ml^{-1} and various concentrations of analytes in the range of 5—500 ng ml^{-1}, singly as well as in presence of the 15 elements Al, B, Ca, Cd, Co, Cu, Fe, Mg, Mo, Ni, Si, Sn, Ti, V and Zn, each in the concentration range 1—500 ng ml^{-1}. For the study of potassium and sodium, the series of standard solutions contained 100 mg U ml^{-1} and analytes in the range 0.5—50 μg ml^{-1}, singly as well as in presence of the 15 elements mentioned above, each in the range 1—500 ng ml^{-1}.

Determination of Cu, Li, Na and K in uranium metal or oxide. For Cu and Li, uranium metal (200 mg) or U_3O_8 (235.9 mg) and for Na and K, uranium metal (500 mg) or U_3O_8 (589.7 mg) was dissolved in concentrated nitric acid, evaporated to dryness and made up to 10 ml and 5 ml, respectively, with 0.1 M nitric acid. The standard solutions, prepared as described above, contained exactly the same amount of uranium. A 5-μl aliquot of standard or sample solution was injected into the carbon tube atomizer and the optimal program settings given in Table 1 were used. The inert atmosphere around the atomizer was provided with an argon flow of 4.5 l min^{-1}. At least five peak height absorption measurements were made on each solution. A 10-μl injection of xylene was used each time for pretreating the carbon furnace before injection of the sample solution, as this gave increased reproducibility and tube life, as reported earlier [1, 2].

Results and discussion

The influence of the uranium matrix on the atomization behaviour of the analytes was examined. The results are shown in Fig. 1. All the analytes

TABLE 1

Optimum conditions for atomization

Element and wavelength (nm)	Sample type[a]	Settings[b] and time		
		Dry	Ash	Atomize
Li 670.7	(A)	5.5, 135°C, 30s	—	7.5, 2250°C, 4 s
	(U)	6,150°C, 50 s	8, 900°C, 45 s	8.5, 2550°C, 3 s
Na 330.3	(A)	7, 200°C, 35 s	—	8.5, 2550°C, 3 s
	(U)	7.5, 230°C, 45 s	8, 900°C, 40 s	8, 2400°C, 3 s
K 404.4	(A)	6.5, 160°C, 40 s	—	8, 2400°C, 4 s
	(U)	8, 250°C, 50 s	8, 900°C, 40 s	8, 2400°C, 3 s
Cu 324.7	(A)	7, 200°C, 30 s	—	8, 2400°C, 3 s
	(U)	7.5, 230°C, 40 s	8, 900°C, 40 s	8, 2400°C, 3 s

[a] (A) 0.1 M HNO_3 solution, (U) uranyl nitrate solution.
[b] Temperatures as provided by the manufacturers.

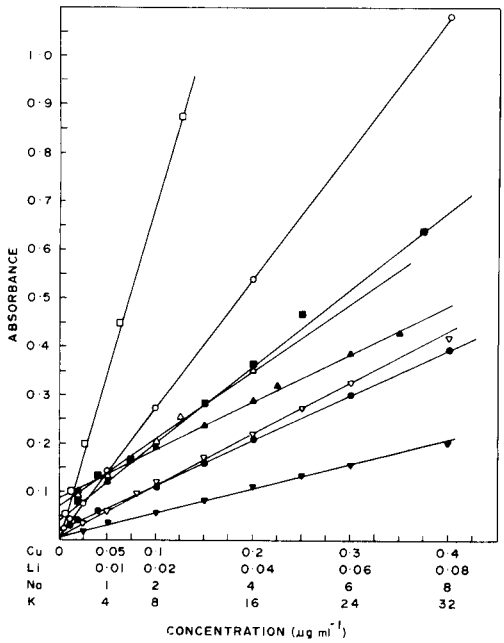

Fig. 1. Comparison of absorption signals in the presence and absence of uranium matrix. (□) Potassium; (○) copper; (△) sodium; (▽) lithium. Open symbols, without uranium; closed symbols, with uranium.

showed decreased signals in the presence of uranium, probably because of a decrease in the efficiency with which ground-state atoms are produced. It is essential, therefore, to have standards containing the same amount of uranium for the direct analysis of uranium samples. Possible non-specific absorbance from the uranium, examined using a hydrogen continuum lamp, was found to be insignificant.

Repeated atomization of an analyte from the uranyl nitrate solution when a new carbon tube was used showed a large scatter in the signal for the initial 20—30 atomization cycles. Subsequent atomizations produced more reproducible signals and even after 80—90 cycles, the reproducibility was unaffected in spite of the uranium accumulated in the tube.

The copper signals from two sets of standard solutions, one having copper alone in uranium and the other containing copper along with Al, B, Ca, Cd, Co, Cr, Fe, Mg, Mo, Ni, Si, Sn, Ti, V and Zn at trace concentrations in uranium, were not significantly different. Similar studies with the other analytes also did not show significant difference in the slopes of the calibration graphs or the range of linearity when these 15 elements were present. The levels used, except for Ca, Fe, Si and Zn, were those which typically would be found in uranium. Since the maximum permissible concentrations of calcium, iron, silicon and zinc in the reactor-grade uranium are generally much higher than those used above, their effects (1000 ppm of each) on the signals from

5 ppm copper, 2 ppm lithium, 40 ppm potassium and 40 ppm sodium in a uranium sample were examined. The results of 8—10 replicate measurements are shown in Fig. 2. It can be seen that the absorbance of copper is not affected by the presence of iron, zinc and calcium but is slightly suppressed (18%) by silicon. The signals of lithium in the presence of zinc, calcium and silicon, and of sodium in the presence of calcium and zinc, are unaffected. The potassium signal is not affected by zinc, silicon and calcium. The presence of iron seriously suppresses the signals from lithium, sodium and potassium. With the exception of iron, therefore, interferences by these other elements are not serious.

The influence of different concentrations of iron on the absorbance of 2 ppm lithium, 40 ppm sodium and 40 ppm potassium was investigated in the presence of uranium. The results (Fig. 3) show that increasing amounts of iron cause the signals to decrease nearly exponentially.

The analytical ranges, precisions and the smallest amounts of the elements that can be determined in solution with and without uranium are listed in Table 2. The smallest amounts of copper and lithium determined in uranium in this work are lower by factors of 20 and 80, respectively, than those reported for the King furnace [3]. Comparison with results obtained by direct atomization of uranium solutions into a flame [4] shows that the present procedure is about 4 times more sensitive for copper whereas there is little difference for sodium. In the present work, the less sensitive sodium

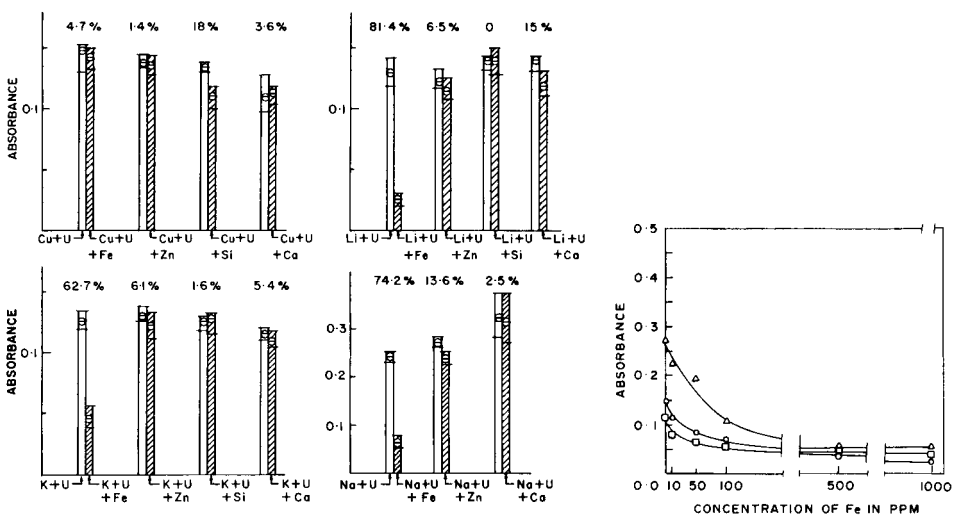

Fig. 2. Influence of 1000 ppm of Ca, Fe, Si and Zn on the absorbances of 5 ppm Cu, 2 ppm Li, 40 ppm Na and 40 ppm K, in the presence of uranium. Percentages are mean % change in presence of interferent. The spreads in the absorbances are shown by the horizontal bars; the circles represent mean absorbances.

Fig. 3. Effect of various concentrations of iron on the signals of (○) 2 ppm Li, (△) 40 ppm Na and (□) 40 ppm K.

TABLE 2

Analytical data for measurements for lithium, sodium, potassium and copper in uranium solutio

Analyte	Concentration (μg ml^{-1})	Peak absorbance	S.d.	R.s.d.[a] (%)	Linear analytical range (μg ml^{-1})	Linear analytical range (ppm)	Smallest amount determined (g)
Li	0.01	0.035	0.002	6.0	0.002—0.06[b]	—	4×10^{-12}[b]
	0.04	0.141	0.009	6.4	0.005—0.08[c]	0.25—4[d]	25×10^{-12}
Na	1.0	0.164	0.015	9.1	0.4—4[b]	—	2×10^{-9}[b]
	2.0	0.177	0.016	9.0	0.8—7[c]	8—70[e]	4×10^{-9}
	6.0	0.315	0.022	7.0			
K	2.0	0.074	0.006	8.3	0.5—10[b]	—	2.5×10^{-9}[b]
	8.0	0.201	0.017	8.2	2—30[c]	20—300[e]	10×10^{-9}
	12.0	0.284	0.013	4.0			
Cu	0.02	0.044	0.003	6.8	0.005—0.4[b]	—	25×10^{-12}[b]
	0.08	0.111	0.005	4.5	0.01—0.5[c]	0.5—25[d]	50×10^{-12}
	0.2	0.217	0.007	3.2			

[a]Calculated from 10 or more replicate measurements. [b]In uranium-free solution. [c]In urani
[d]Based on 0.1 mg of uranium in 5 μl of solution. [e]Based on 0.5 mg of uranium in 5 μl of soluti

line at 330.3 nm and potassium line at 404.4 nm were used, with reduced analytical ranges. The smallest amounts that can be determined for sodium and potassium at these lines are 2 ng and 2.5 ng, respectively, in aqueous solution and 4 ng and 10 ng, respectively, in uranium. The relative standard deviations of the method for all four analytes (Table 2) lie in the range 4—9%.

Spiked sample solutions were prepared for the four analyte elements following dissolution of uranium metal. Results of the analyses of these

TABLE 3

Results of determination of lithium, sodium, potassium and copper in spiked uranium samples

Element	Concentration of spike[a]				Element	Concentration of spike[a]			
	Added		Measured			Added		Measured	
	(μg ml^{-1})	(ppm)[b]	(μg ml^{-1})	(ppm)[b]		(μg ml^{-1})	(ppm)[b]	(μg ml^{-1})	(ppr
Li	0.04	2.0	0.039	1.9	K	2.0	20.0	2.1	21.
	0.05	2.5	0.048	2.4		12.0	120.0	12.0	120.
	0.08	4.0	0.08	4.0					
					Cu	0.025	1.25	0.024	1.
Na	1.4	14.0	1.44	14.4		0.040	2.0	0.044	2.
	3.0	30.0	3.08	30.8		0.104	5.2	0.102	5.
	4.0	40.0	3.75	37.5		0.30	15.0	0.306	15.

[a]20 mg U ml^{-1} for Cu and Li; 100 mg U ml^{-1} for Na and K.
[b]In uranium sample.

samples are shown in Table 3, based on 6—8 replicate measurements for each solution. The concentrations determined are in very good agreement with the spike concentrations added to the uranium.

The recommended technique is suitable for the determination of ppm levels of lithium, sodium, potassium and copper. The analysis is rapid and the risk of contamination is considerably reduced since no chemical separation of the uranium matrix is required. However, because of the suppressive effects of uranium, standards and sample solutions must contain approximately the same concentration of uranium. Further, the presence of iron in the sample will cause interference in the determination of the alkali metals.

The authors are grateful to Dr. M. V. Ramaniah, Director, Radiological Group, for his keen interest and constant encouragement.

REFERENCES

1 B. M. Patel, Paru M. Bhatt, Neelam Gupta, M. M. Pawar and B. D. Joshi, Anal. Chim. Acta, 104 (1979) 113.
2 B. M. Patel, Ph.D. Thesis, University of Bombay, 1978, Ch. 3 (on a.a.s.).
3 M. Buffereau and J. Robichet, Methodes Phys. Anal. (GAMS), 7 (1971) 138.
4 M. Buffereau and J. Robichet, Rept. CEA-R-3870 (1969).

Analytica Chimica Acta, 118 (1980) 169—174
© Elsevier Scientific Publishing Company, Amsterdam — Printed in The Netherlands

Short Communication

DETECTION LIMITS FOR ORGANIC SALTS IN SECONDARY ION MASS SPECTROMETRY

S. E. UNGER, T. M. RYAN and R. G. COOKS*

Department of Chemistry, Purdue University, West Lafayette, IN 47907 (U.S.A.)

(Received 26th December 1979)

Summary. Trimethylisopropylammonium iodide is detected at the picogram level by secondary ion mass spectrometry (s.i.m.s.). The intact organic cation can be monitored; the effects of experimental conditions on its abundance are discussed. Mixtures of organic salts can be analyzed without matrix effects at 1:100 weight ratios. The effects of other matrices and the mechanism of sputtering are considered. S.i.m.s. provides greater sensitivity for direct ionization of polyatomic salts than for cationization of molecules.

Recent reports have shown the value of secondary ion mass spectrometry (s.i.m.s.) as a method for the determination of organic compounds. Rabalais and co-workers [1] have obtained s.i.m.s. spectra of species such as frozen benzene, while Jonkman et al. [2] have employed matrix isolation methods for sample preparation of various hydrocarbons and recorded their s.i.m.s. spectra. Benninghoven and Sichtermann [3, 4] have recorded the s.i.m.s. spectra of biological compounds, including amino acids, peptides, alkaloids, and vitamins. There has been some consideration of the mechanism of ionization and the sensitivity of the method in these and other papers [5].

Earlier reports [6, 7] from this laboratory have shown the formation of metal adducts with intact organic molecules, $(C+M)^+$. The cationization process is quite general for various types of metals (alkali, transition, and main group), as well as for various types of organic compounds [8, 9]. A second and distinct ionization process is the direct emission of the intact cation of organic salts [10, 11]. Both cationization and the emission of ions from the solid to the gas phase have analogies with processes occurring in field desorption [12, 13] and plasma desorption [14, 15].

Large intensities of the organic cation are observed in the s.i.m.s. spectra of organic salts [10], suggesting that the method is very sensitive for these species. In fact, Benninghoven et al. [16] have predicted picogram detection limits for certain organic compounds. This conclusion is based on extrapolation rather than actual demonstration. Data showing the identification of organic ammonium salts at the picogram level are presented here.

Experimental

Instrumentation. S.i.m.s. spectra shown here were taken with a commercial Riber system. The Riber SQ 156 L quadrupole mass filter has a mass range

of 1000 and an associated electrostatic analyzer which serves as an energy prefilter. Both positive and negative ion s.i.m.s. spectra are obtainable with this system. Ion counting employing a Princeton Applied Research 1121 amplifier and discriminator is used for signal processing. Typical operating pressure inside the main chamber is $2—3 \times 10^{-9}$ torr. A differentially pumped primary ion gun produces beams (generally Ar^+) of kinetic energies from 100 eV to 5 keV and primary ion currents from 1×10^{-11} to 1×10^{-6} A. The primary ion beam profile, measured using a 150-μm Faraday cup, is 1 mm (FWHM).

Sample preparation. Aqueous solutions of the organic salts were prepared by serial dilution from a prepared standard. The organic salts were either obtained commercially or prepared from the corresponding amine by reaction with an alkyl iodide. An appropriate solution (20 μl) was then deposited from a syringe onto a 1-cm^2 silver foil, which had been roughened with 320-grit silicon carbide paper, then rinsed twice with distilled water and 100% ethanol. Once dried, the sample was transferred to an independently pumped preparation chamber. Subsequent transfer to the main chamber and positioning of the sample relative to the primary ion beam and detector system finalized preparation procedures.

Results

The relative efficiency of cationization versus direct emission of organic salts, the two main ionization processes in s.i.m.s., was tested in the particular case of a 1:1 mole mixture of copper(II) sulfate and dicyanobenzene versus $\dot{N}(C_2H_5)_4I^-$. Pellets of each were made and their spectra recorded under identical conditions (3×10^{-10} A; 3×10^{-8} A cm^{-2}; Ar^+, 5 keV). The signal due to the cation $\dot{N}(C_2H_5)_4$ at *m/z* 130 was more than two orders of magnitude larger than the $(Cu+M)^+$ signal at *m/z* 191, 193 from dicyanobenzene. These results provide an example of the efficiency and sensitivity of the direct emission process for organic salts over other operative ionization processes in s.i.m.s.

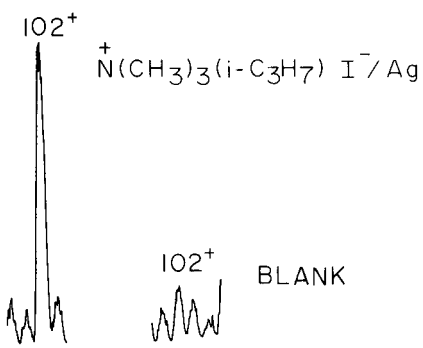

Fig. 1. S.i.m.s. spectrum (selective region scan) of the intact cation and of the blank. For experimental detail, see text.

Figure 1 shows the s.i.m.s. spectrum of the intact cation (*m/z* 102) for 10 pg of $\overset{+}{N}(CH_3)_3(i\text{-}C_3H_7)I^-$ deposited on 1 cm^2 of silver. The sample was prepared by depositing 20 μl of a 0.5 $\mu g\ l^{-1}$ aqueous solution of the organic salt onto a roughened silver foil. Under the experimental conditions used (5×10^{-9} A; 5×10^{-7} A cm^{-2}; Ar^+, 5 keV), the cation signal remains above background for approximately one minute. This quantity of material and sampling time are adequate for detection of the compound, provided that a selected region or a particular mass is monitored. Static s.i.m.s. conditions (10^{-9}—10^{-10} A cm^{-2}) show little deterioration in signal for organic salts at absolute limits of 10 ng cm^{-2} or higher, thereby allowing complete spectra to be recorded.

Relative detection limits for mixtures of organic salts were also studied. The presence of another organic salt at higher concentration has no effect on the spectrum of the salt of interest. The absence of matrix effects is seen in Fig. 2 where 100 μg of $\overset{+}{N}(CH_3)_3(C_2H_5)I^-$ and 1 μg of $\overset{+}{N}(CH_3)_3(C_6H_5)I^-$ are co-deposited onto a 1-cm^2 silver foil. The gram ratio of the two salts is 100:1, mole ratio is 155:1, and the cation signal intensity is approximately 130:1. Considering the discrimination of the quadrupole analyzer against higher mass ions, this result suggests that the phenyl salt is slightly more stable than the ethyl salt. A 10:1 gram ratio of these salts showed similar results, as well as characteristic fragment ions of both ammonium salts.

At high primary ion currents (10^{-7}—10^{-8} A; 10^{-5}—10^{-6} A cm^{-2}; Ar^+, 5 keV) profound matrix effects can occur in the s.i.m.s. spectra of organic salts [10]. For example, an equimolar mixture of KF, KCl, KBr, KI, and $\overset{+}{N}(CH_3)_3(C_6H_5)I^-$ burnished onto a platinum foil shows an entirely different s.i.m.s. spectrum than it does under static conditions or than does pure $\overset{+}{N}(CH_3)_3(C_6H_5)I^-$ on platinum foil. The cation at *m/z* 136 and associated fragment ions at *m/z* 120 and 121 disappear in the mixture spectrum as the current density is raised. In its place, ions at *m/z* 77 ($C_6H_5^+$), 96 ($C_6H_5F^+$), 112 and 114 ($C_6H_5Cl^+$), 156 and 158 ($C_6H_5Br^+$), and 204 ($C_6H_5I^+$) are observed in the s.i.m.s. spectrum. Similar results are obtained for $\overset{+}{As}(C_6H_5)_4I^-$ mixed with

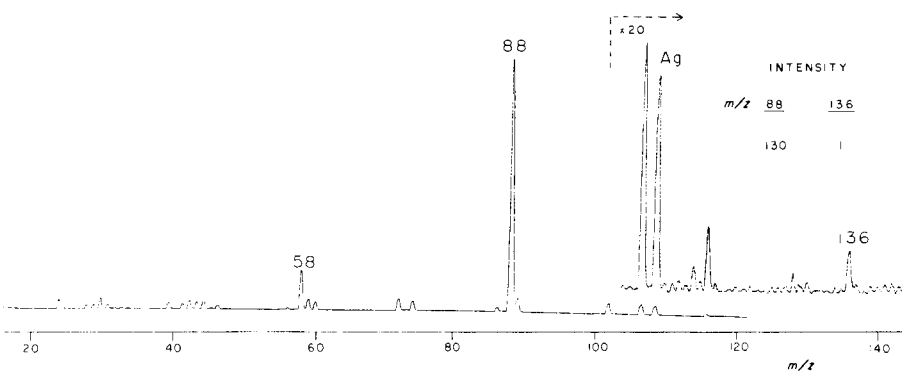

Fig. 2. S.i.m.s. spectrum of 100 μg of $\overset{+}{N}(CH_3)_3(C_2H_5)I^-$ and 1 μg of $\overset{+}{N}(CH_3)_3(C_6H_5)I^-$ co-deposited on a 1-cm^2 silver foil. Conditions: 5 keV, 5×10^{-7} A cm^{-2}.

potassium halide salts, demonstrating the occurrence of thermally mediated effects in these spectra. A related case which is not controlled by primary ion current density occurs in the s.i.m.s. spectrum of methylviologen (*N,N'*-dimethyl-4,4'-bipyridinium chloride) on silver foil which shows a large signal at *m/z* 186 due to the reduced cation and at *m/z* 171 due to $CH_3\cdot$ loss from $186^{\dagger}$. However, a 1:1 mole mixture of methylviologen and 2,9-dimethylphenanthroline on silver foil shows no ions characteristic of methylviologen, only those related to 2,9-dimethylphenanthroline on silver. Systematic investigations into such matrix effects are in hand.

S.i.m.s. spectra of organic salts may also be affected by changes in primary ion current. Table 1 shows an increase in four main fragment ions from the intact cation of $\overset{+}{N}(CH_3)_3(C_2H_5)I^-$ on platinum foil with an increase in primary ion current. These results are general for other ammonium salts such as choline esters, as well as for organic sulfonium salts, demonstrating the control of fragmentation in s.i.m.s. by selection of primary ion current.

Discussion

At lower mass ($m/z < 100$) the detection limit for organic salts is often determined by the background signal from residual gas adsorption, alkali salt contaminants such as NaCl and KCl, and fragment ions from background species. For most organic salts the observation of the intact cation above the background is not a problem since the molecular weight of the cation is generally above *m/z* 100. Often, however, at low concentrations various lower mass fragments will be obscured in the background noise. For trace determinations, selected region or selected ion monitoring of the intact cation is often desirable, therefore, this problem may be avoided. If selected ion monitoring is used, static s.i.m.s. conditions [17] employing low primary ion currents are necessary to minimize fragmentation, thus maximizing the relative intensity of the cation.

TABLE 1

Relative intensity versus primary ion current[a]

Primary ion current[b]		Intensity of *m/z*			
A	A cm^{-2}	58	60	72	74
5×10^{-10}	5×10^{-8}	33	4.8	6.1	7.2
5×10^{-9}	5×10^{-7}	45	29	16	29
5×10^{-8}	5×10^{-6}	85	81	27	67
2×10^{-7}	2×10^{-5}	102	102	32	77

[a] 8.0 mg cm^{-2} $\overset{+}{N}(CH_3)_3(C_2H_5)I^-$ on Pt foil, ion intensities are referenced to the cation $\overset{+}{N}(CH_3)_3(C_2H_5)$ at *m/z* 88 which is assigned an intensity of 100.

[b] Ar^+ primary ion beam with a kinetic energy of 5 keV (similar results observed at lower kinetic energies); initial currents measured for a circular beam FWHM of 1 mm and adjusted to A cm^{-2}.

Fragment ions of organic salts in s.i.m.s. arise by gas-phase reactions characteristic of closed-shell structures [18]. For example, the fragment ions of $\overset{+}{N}(CH_3)_3(C_2H_5)I^-$ shown in Table 1 correspond to *m/z* 58 $(M-I-C_2H_6)^+$, *m/z* 60 $(M-I-C_2H_4)^+$, and *m/z* 72 $(M-I-CH_4)^+$. The ion at *m/z* 74 may correspond to carbene loss from the cation or may arise by rearrangement involving dealkylation ($C_2H_5\cdot$) with subsequent realkylation ($CH_3\cdot$) to form $\overset{+}{N}(CH_3)_4$. Such ions have been observed in electron impact mass spectra of these salts [19].

Also present in the s.i.m.s. spectra of this and other salts are ions corresponding to $(M-I+14)^+$ and $(M-I+28)^+$, here at *m/z* 102 and 116 respectively (Fig. 2). The $(M-I+14)^+$ ions seen in field desorption spectra of organic salts have been explained as a consequence of intermolecular alkylation [20]. Evidence that these ions arise in s.i.m.s. from a mechanism other than dealkylation followed by realkylation is seen in the spectra of $\overset{+}{N}(C_2H_5)_4OH^-$ and $N(CH_3)_4Cl^-$. Both these salts show an $(M-I+14)^+$ peak, but the symmetric nature of the cations argues against direct scrambling of the alkyl groups as the mechanism. Carbene insertion directly into the intact cations, or indirectly into an alkyl fragment (followed by realkylation), are more likely processes.

The results for quaternary ammonium salts parallel those reported by Benninghoven and Sichtermann [3, 4] for various biological compounds, for which maximum secondary ion yields for $(M+H)^+$ ions were obtained when the sample was deposited on the surface from low pH solutions. Under these conditions one assumes that the organic compound is present as a salt. Both sets of results suggest that instead of using cationization [7] many organic compounds may be determined by s.i.m.s. if they are first converted to the respective salt. This may be accomplished by protonation with aqueous acid to form the salt or quaternization with an alkyl iodide to form the ammonium salt. Similar procedures are successful with sulfur, phosphorus, and arsenic-containing organic compounds [10].

This work was supported by the National Science Foundation CHE 78-08728 and the MRL Program DMR 77-23798.

REFERENCES

1 G. M. Lancaster, F. Honda, Y. Fukuda and J. W. Rabalais, J. Am. Chem. Soc., 101 (1979) 1951.
2 H. T. Jonkman, J. Michl, R. N. King and J. D. Andrade, Anal. Chem., 50 (1978) 2078.
3 A. Benninghoven and W. K. Sichtermann, Anal. Chem., 50 (1978) 1180.
4 A. Benninghoven and W. K. Sichtermann, Org. Mass. Spectrom., 12 (1977) 595.
5 R. J. Colton, J. S. Murday, J. R. Wyatt and J. J. DeCorpo, Surf. Sci., 84 (1979) 235.
6 H. Grade, N. Winograd and R. G. Cooks, J. Am. Chem. Soc., 99 (1977) 7725.
7 H. Grade and R. G. Cooks, J. Am. Chem. Soc., 100 (1978) 5615.
8 R. J. Day, S. E. Unger and R. G. Cooks, J. Am. Chem. Soc., 101 (1979) 499.
9 R. J. Day, S. E. Unger and R. G. Cooks, Anal. Chem., 50 (1980) 353.
10 R. J. Day, S. E. Unger and R. G. Cooks, J. Am. Chem. Soc., 101 (1979) 501.
11 R. Ullmann, Mikrochim. Acta, (1979) 221.

12 D. F. Hunt, J. Shabanowitz and F. K. Botz, Anal. Chem., 49 (1977) 1160.
13 D. A. Brent, D. J. Rouse, M. C. Sammons and M. M. Bursey, Tetrahedron Lett., 42 (1973) 4127.
14 R. D. MacFarlane and D. F. Torgerson, Science, 191 (1976) 920.
15 G. W. Wood and P. Y. Lau, Org. Mass Spectrom., 10 (1975) 1147.
16 A. Benninghoven, B. Jaspers and W. Michtermann, Appl. Phys., 11 (1976) 35.
17 A. Benninghoven, Surf. Sci., 28 (1971) 541.
18 H. H. Gierlich, F. W. Rollgen, F. Borchers and K. Levsen, Org. Mass Spectrom., 12 (1977) 387.
19 D. Zakett and R. G. Cooks, unpublished results.
20 G. W. Wood and P.-Y. Lau, Org. Mass Spectrom., 10 (1975) 1147.

Analytica Chimica Acta, 118 (1980) 175—178
© Elsevier Scientific Publishing Company, Amsterdam — Printed in The Netherlands

Short Communication

DETERMINATION OF TOTAL ZINC IN SOILS BY EXTERNAL-BEAM PROTON-INDUCED X-RAY EMISSION SPECTROMETRY

M. ABDULLAH, M. B. ZAMAN, M. KHALIQUZZAMAN and A. H. KHAN*

Atomic Energy Centre, P.O. Box 164, Dacca (Bangladesh)

(Received 28th January 1980)

Summary. A rapid non-destructive determination of total zinc in soils is reported. The 1 mm thick targets were prepared without a binder. Multiple standard additions were used for calibration. For a 10-μC irradiation with 2-MeV protons, the detection limit was about 2 ppm of zinc. The precision was within 5% and good agreement was found with spectrophotometric measurements of zinc.

The determination of zinc in soils is important because of the important role of this element in agricultural science. Soil scientists generally use extraction procedures for the separation of available zinc from soils and then apply atomic absorption spectrometry (a.a.s.) in order to study the quantity of zinc available to plants under different soil conditions [1]. However, for an in-depth understanding of the relationship between the total zinc and the extractable zinc, it is also necessary to have accurate data on total zinc. Many laboratories routinely apply wavelength-dispersive x-ray fluorescence for trace analysis of silicate materials. In recent years, the use of energy-dispersive x-ray fluorescence methods has also become important [2—4]. Applications of proton-induced x-ray emission (p.i.x.e.) for trace analysis of soils are rather limited, although applications in biological and environmental sciences have been widely reported [5]. Baum et al. [6] and Navarrete et al. [7] recently studied the p.i.x.e. method for soil analysis, using both destructive and non-destructive methods of target preparation and the conventional irradiation of targets in vacuo. In view of the large disagreement between the p.i.x.e. and a.a.s. data on zinc and lead and the overall complexity of soil analysis, it was considered worthwhile to investigate this problem further.

In this communication a non-destructive analytical procedure for the determination of total zinc in soils is reported; the external-beam p.i.x.e. method where the samples are irradiated as pellets is utilized.

Experimental

Target preparation. Soil samples in powdered form were obtained from the Forest Research Institute, Chittagong, Bangladesh. For the preparation of the calibration curve, a 10-g portion of sample was ground to a fine powder in an agate mortar and its moisture content was determined at 110°C.

Four 1-g fractions were taken from the dried sample into clean platinum crucibles. Measured volumes of a standard zinc solution in ultrapure nitric acid (Merck) were added to the samples to give concentrations of added zinc in the range 25—150 ppm. The samples were dried to constant weight at 110°C. Preliminary mixing of the soil mass with the added zinc was then done with a glass rod, and the sample was quantitatively transferred to an agate mortar and ground finely in order to obtain a homogeneous mixture.

From this mixture, duplicate standard pellets (70 mg each, 1 mm thick, 8 mm diameter) were prepared with a stainless steel pellet maker under a pressure of 3 tons. The pellets thus prepared were strong enough to withstand mechanical handling. They were mounted in 35-mm slide frames with adhesive tape and stored in a desiccator until irradiation. Pellets for sample analysis were prepared under similar conditions except for the addition of zinc. Prior to the preparation of soil pellets, a sample of chromatographic-grade cellulose powder (Whatman) was ground in the mortar for blank correction, if any.

Irradiation. The external-beam p.i.x.e. facility recently developed in this laboratory was used; details of the experimental set-up have been reported [8]. Kapton foils (1.12 mg cm^{-2} thick) were used as the proton exit window. Proton beams (2.5 MeV) were obtained from the 3-MeV Van de Graaff accelerator at the Atomic Energy Centre, Dacca. After energy loss in the exit window and the air path, the beam energy on the target was about 2 MeV. The beam spot at the exit window was 4 mm in diameter and the irradiation spot on the target was well within this diameter.

The targets were irradiated with a beam intensity of 10—15 nA at 45° with respect to the beam direction. The characteristic x-rays were detected with a 30-mm^2 Ortec Si(Li) detector having a resolution of 180 eV at 5.9 keV. A plastic absorber (44 mg cm^{-2}) was used to reduce the argon background in air. A typical x-ray spectrum obtained with these experimental arrangements from a soil sample without added zinc is shown in Fig. 1. The Zn K_α peak area was integrated manually, a straight-line background being assumed. It was corrected for the Cu K_β contribution by using the K_α/K_β ratio of copper measured separately with a cellulose target.

Results and discussion

The p.i.x.e. spectrum shown in Fig. 1 was obtained from a 4-μC irradiation; the x-ray lines of several elements are obviously well resolved. This is largely because in the absence of charging of the target in air during irradiation, better peak-to-background ratios are obtained than is the case for irradiation in vacuo. This aspect of the method has been clearly demonstrated by Katsanos and Hadjiantoniou [9]. Although the present investigation is concerned only with the determination of zinc, the spectral quality achieved from the external-beam p.i.x.e. method illustrates the possibility of multi-element trace analysis of soils.

Calibration of the method was done by multiple standard additions. The

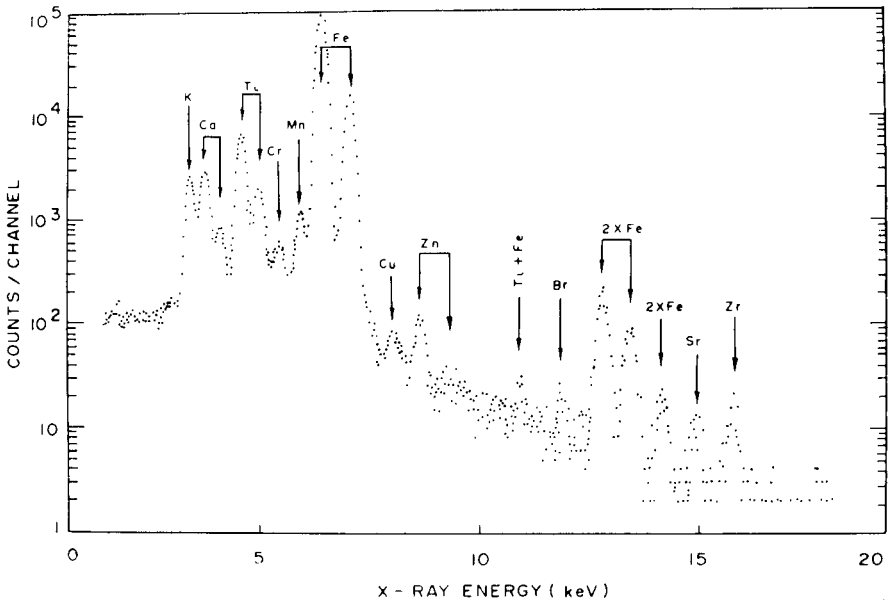

Fig. 1. A typical p.i.x.e. spectrum from a soil sample irradiated in air as a 1-mm thick pellet.

peak areas averaged from duplicate measurements were used to construct the calibration plot by least-squares fitting. From the slope of the curve, the calibration factor (number of Zn K_α x-rays per microcoulomb per ppm for a given geometry) was calculated; this factor, 4.08 in the present case, was used to obtain the concentration of zinc (ppm) in a given sample from the equation ppm = $Y_x TW/4.08\ Q$, where Y_x is the x-ray yield of zinc, Q is the total charge in microcoulombs, W is the dry sample weight and T is the dead-time correction factor.

The uncertainty in the results is determined primarily by the uncertainty in the calibration curve. The error in the individual data points in the curve varied between 1.0 and 3.6%, the maximum being at the 25 ppm level. Another source of error is sample inhomogeneity. The homogeneity of samples after the addition of zinc was tested by irradiating several pellets from the same material; the variations were within 4%. The blank correction was negligible. Thus, the overall error in the determination of zinc by the present procedure is estimated to be about 5%.

From consideration of the statistical errors in counting, the limit of detection was calculated; this limit is defined here as the amount of zinc in ppm which would yield an x-ray intensity equal to 3 times the standard deviation of the background in a one FWHM energy interval. For a 10-μC irradiation, this was found to be 2 ppm. This value is better than that indicated for zinc in soils by Van Grieken et al. [3] in their thin-film energy-dispersive x.r.f. measurements.

In order to test the accuracy of the procedure, a few soil samples were analyzed for zinc by p.i.x.e. and by a spectrophotometric method. For

TABLE 1

Comparison between p.i.x.e. and spectrophotometric (Sp) determinations of total zinc in soils

Sample	Zn found (ppm)		Deviation (%)[a] $C_p \times 100$	Error (%)[b]
	p.i.x.e. (C_p)	Sp(C_s)		
FRI-5	64 ± 3	68 ± 4	6.2	7.8
FRI-7	60 ± 4	61 ± 5	1.6	10.6
FRI-10	58 ± 3	55 ± 5	5.2	10.0
FRI-15	69 ± 4	71 ± 1	2.8	6.0

[a] $100\,(C_p - C_s)/C_p$. [b] $100(\Delta C_p^2 + \Delta C_s^2)^{1/2}/C_p$.

spectrophotometry, the samples were dissolved in mixed perchloric and hydrofluoric acids; after extraction into tetrachloromethane in the presence of selective masking agents, zinc was determined as its dithizonate in a conventional manner. The results (Table 1) are in good agreement.

The above results prove that the external-beam p.i.x.e. method with thick targets and multiple standard additions is satisfactory and convenient for the determination of zinc in soils. The method is very rapid, a typical irradiation taking 3—4 min; the sensitivity is quite reasonable and there is little possibility of contamination in sample preparation. The method can therefore be very economical for a large-scale study of zinc levels in soil.

Although this study is concerned only with analysis for zinc, it can be easily extended to multielement trace analysis of soils by using the zinc data as the internal standard. In that case, 8—10 elements can be easily determined from a single irradiation.

This work was supported in part by the International Atomic Energy Agency, Vienna. The authors are grateful to A. A. Katsanos for valuable suggestions, to M. Husain, I. Ahmed and S. Akhter for their enthusiastic cooperation and to A. H. M. Habibul Islam, Director, AECD, for his interest and encouragement.

REFERENCES

1 F. Ahmed, Geoderma, 16 (1976) 71.
2 C. G. Clayton and T. W. Packer, Proc. Int. Symp. on Nuclear Techniques in Exploration, Extraction and Processing of Minerals, IAEA, Vienna, IAEA-SM-216/44, 1977.
3 R. Van Grieken, L. Van 't Dack, C. C. Dantas and H. D. S. Dantas, Anal. Chim. Acta, 108 (1979) 93.
4 R. D. Giauque, R. G. Garrett and L. Y. Goda, Anal. Chem., 49 (1977) 62.
5 S. A. E. Johansson and T. B. Johansson, Nucl. Instr. Methods, 137 (1976) 473.
6 R. Baum, W. F. Gutknecht, R. D. Willis and R. L. Walter, Anal. Chim. Acta, 85 (1976) 323.
7 V. R. Navarrete, G. Izawa, T. Shiokawa, K. Ishii and S. Morita, Radiochem. Radioanal. Lett., 27 (1976) 27.
8 A. H. Khan, M. Khaliquzzaman, M. Husain, M. Abdullah and A. A. Katsanos, Nucl. Instr. Methods, 165 (1979) 253.
9 A. A. Katsanos and A. Hadjiantoniou, Nucl. Instr. Methods, 149 (1978) 469.

Analytica Chimica Acta, 118 (1980) 179—183
© Elsevier Scientific Publishing Company, Amsterdam — Printed in The Netherlands

Short Communication

CHEMILUMINESCENCE METHOD FOR THE DETERMINATION OF NANOGRAM AMOUNTS OF HIGHLY TOXIC ALKYLPHOSPHATES

U. FRITSCHE

Fraunhofer-Institut für Toxikologie und Aerosolforschung, D-5948 Schmallenberg-Grafschaft (Federal Republic of Germany)

(Received 17th December 1979)

Summary. The method is based on the Schoenemann reaction with sodium perborate and then with luminol. The reaction medium contains EDTA and is 5 M in sodium chloride, thus improving the detection limit 1000 times to ca. 1 ng for the highly toxic alkylphosphates. "Non-toxic" alkylphosphates are indifferent.

Alkylphosphates are widely used as insecticides, and several others are considered to be potential chemical warfare agents, because of their extremely high toxicity to mammals. On account of their high toxicity, analytical methods for the detection of such compounds should be as sensitive as possible [1]. The methods recommended for this purpose are based on cholinesterase inhibition [2], flame emission [3], reaction with oximes and potentiometric measurement of the liberated cyanide [4], the piezoelectric effect [5] or plasma chromatography [6]. All these methods have advantages, but are not satisfactory in all respects. For example, the cholinesterase method is very sensitive, but the detection limit depends on the reaction time available and the calibration curve is not linear. The flame photometric detector is also very sensitive, but it responds to all phosphorus compounds.

The Schoenemann reaction [7] is the reaction of an alkylphosphate (or alkylphosphonate) with hydrogen peroxide to produce a peroxophosphate (or peroxophosphonate), followed by the rapid oxidation of an amine by the product, in an alkaline medium. Sodium perborate or sodium peroxodiphosphate is preferred to hydrogen peroxide because their stability is greater. The most commonly used amines and the corresponding measurement procedures [8] are 3,3'-dimethoxybenzidine (spectrophotometry), indole (fluorimetry) and luminol (chemiluminescence measurement). Up to now the most sensitive variant of the Schoenemann reaction was the indole procedure, with a detection limit for, e.g., sarin (*O*-isopropylmethylfluorophosphonate) of 30 ng, whereas the luminol procedure had a detection limit of 0.5 μg [9]. With respect to the high toxicity of this and some similar alkylphosphates, the sensitivities of these methods are inadequate to determine dangerous levels of these compounds.

This communication describes an improvement of the chemiluminescence method which increases its sensitivity by about three orders of magnitude.

This is achieved by using chloride, which promotes the luminescence strongly, and EDTA, which suppresses background emission caused by catalysis by metal ion impurities. The detection limit is best for the most highly toxic alkylphosphates, the so-called nerve gases, which are fluorophosphonates and cyanophosphates.

Insecticides can also be detected, an aspect which is now under investigation. Weber and Matković [10] found for the insecticide *O,O*-dimethyl-(1-hydroxy-2,2,2-trichlorethyl)phosphonate (dipterex) that halide ions had a promoter effect in the luminol reaction.

Experimental

Apparatus. Any commercially available luminometer used for the estimation of ATP can be applied. The detector does not have to be extremely sensitive. In this investigation a luminometer constructed in the laboratory was used (Fig. 1). The light-tight box contains a 1-cm diameter reaction cell. The photomultiplier receives the light from the cell as shown, and the amplified signal is recorded automatically versus time. To protect the photomultiplier from external light, the window is rotated through 90° before the apparatus is opened.

Reagents and solutions. All chemicals used were of analytical grade. Deionized water was used throughout. For the luminol solution, a solution 0.1 M in luminol and 0.5 M in trisodium phosphate was mixed with 5 M NaCl and 0.02 M EDTA solutions in the ratio 5:100:1 by volume. This can be used for at least 1 year. The sodium perborate solution (0.1 M) was stored in a refrigerator.

Procedure. Mix 100 µl of sodium perborate solution and 2 ml of the luminol solution in the cell of the luminometer. Record the background emission signal for 4 min. Add, with mixing, a methanolic solution of the alkylphosphate (20 µl) and record the signal. Measure the maximum intensity above the background signal.

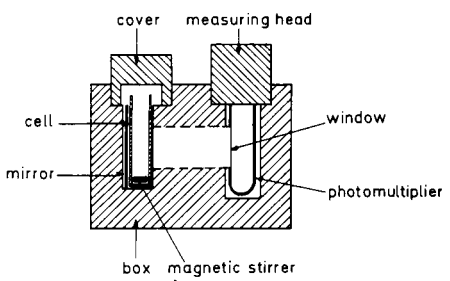

Fig. 1. Luminometer used.

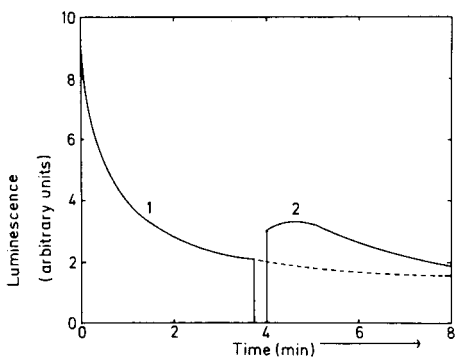

Fig. 2. Luminescence—time response for an experiment with 5 ng of DFP: (1) background; (2) DFP response.

Results

Figure 2 gives an example of the responses obtained. The initial emission is the background. This signal decreases, and after 4 min is nearly constant. The short interruption of the signal indicates the removal of the photomultiplier before addition of the alkylphosphate. The subsequent increase in signal results from the increased oxidative ability of the peroxophosphate formed. There is a linear relationship between the area under the curve (after correction for the background) and the amount of alkylphosphate added. The same applies to the maximum intensity. Calibration graphs based on either measurement are linear over more than three decades of concentration. For practical purposes it is more convenient to measure the maximum intensity. The time interval between injecting the sample and the maximum is characteristic for the individual alkylphosphate, as is the rate of increase and decrease of the luminescence signal. This is summarized in Table 1. These values are quoted at 20°C and are independent of the concentration of the alkylphosphate. They can be used to help identify the compound. If more than one kind of alkylphosphate is present, the curves are superimposed.

TABLE 1

Time to maximum luminescence (t_{max}) and half-life of the luminescence decay ($t_{1/2}$) for some alkylphosphates

Compound	Soman	Sarin	DFP	Tabun
$t_{max}(s)$	4	1	16	6
$t_{1/2}(s)$	34	27	35	17

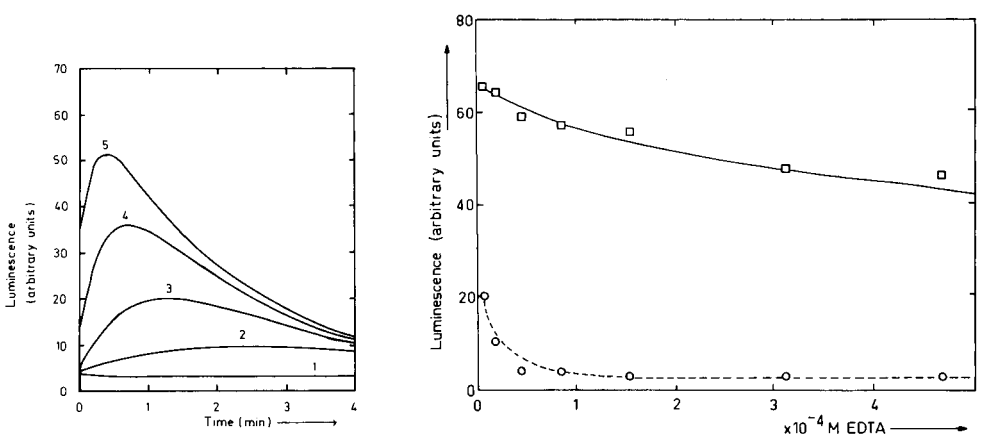

Fig. 3. Luminescence–time responses for 200 ng of DFP using luminol solutions prepared with NaCl solutions of concentrations: (1) 0.00, (2) 2.50, (3) 3.75, (4) 5.00 M. The time scale begins after the 4-min background decay period.

Fig. 4. Effect of EDTA on (○) background luminescence and (□) peak height of 200 ng of DFP.

The luminescence—time responses for diisopropylfluorophosphate (DFP) as a function of chloride concentration, are shown in Fig. 3. It is evident that increasing chloride concentrations lead to greater emissions. The influence of the EDTA is plotted in Fig. 4. The luminescence caused by the alkylphosphate is slightly suppressed, but the background luminescence is decreased to a much higher degree. The concentration in EDTA is not critical, but very high concentrations suppress the alkylphosphate signal. The responses for various alkylphosphates, obtained under identical experimental conditions, are compared in Fig. 5.

The detection limits [11] (statistical probability $\geqslant 95\%$) obtained were: DFP, sarin and soman (1,2,2-trimethylpropylmethylfluorophosphonate), 0.5 ng; tabun (dimethylaminoethylcyanophosphate), 1 ng; VX (*O*-ethyl-*S*-(*N*,*N*-diisopropylaminoethyl)methylthiolphosphonate), 10 ng. Although the method is less sensitive for VX than for the other substances, it is better than other available methods. The standard deviations of the procedure [12] for the range 10—100 ng alkylphosphate, calculated from 24 measurements per agent, were 2.8 ng, 2.0 ng and 2.7 ng for soman, DFP and tabun, respectively.

Temperature affects the shape and height of the response (Fig. 6), but the area under the curves, which represents the total emission, is constant for temperatures between 15 and 35°C. Consequently, this allows a quantitative evaluation of the curves independent of the temperature.

The solvents methanol, ethanol, ether, isobutyl methyl ketone, chloroform, *N*,*N*-dimethylformamide, n-hexane, cyclohexane and toluene (20 µl) had no effect on the luminescence reaction. Acetone gave an increased signal, whereas pyridine and dimethylsulfoxide decreased the emission.

Interferences. Representative "non-toxic" alkylphosphates investigated were trimethylphosphate, tri-n-butylphosphate and tri-*p*-cresylphosphate. They do not give emission and do not interfere in amounts up to at least 20 µg.

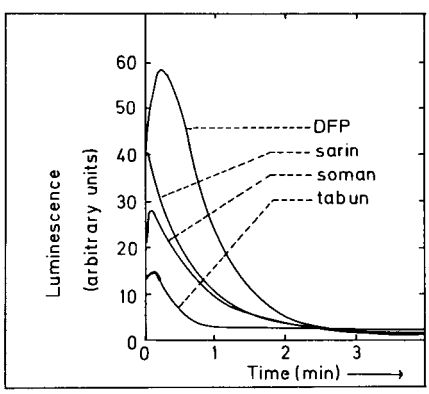

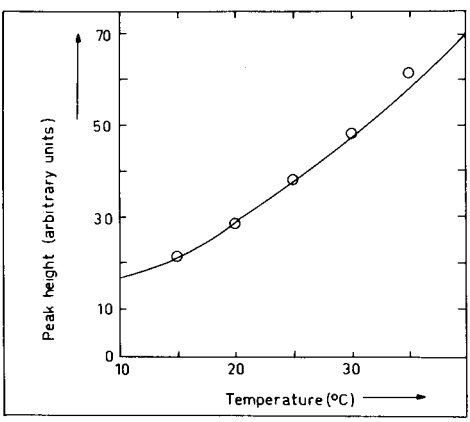

Fig. 5. Luminescence—time responses for 2 nmol of various alkylphosphates.

Fig. 6. Effect of temperature on peak height for 200 ng of DFP.

In experiments to investigate the effect of inorganic substances, 20 μg of a cation or anion was applied. In the following results, increasing effect on the luminescence is classified by the symbols (+), (++), (+++), and a decrease by (−), (− −), (− − −); indifferent substances are symbolized by (±):

Na^+(±), K^+(±), Mg^{2+}(+), Ca^{2+}(±), Al^{3+}(±), Pb^{2+}(±), Mn^{2+}(+++), Cu^{2+}(+++), Zn^{2+}(++), Cd^{2+}(+), Hg^{2+}(+), Fe^{3+}(+++), Co^{2+}(+++), Ni^{2+}(+++), UO_2^{2+}(±), NH_4^+(±). Anions: F^-(±), Cl^-(±), ClO_3^-(±), Br^-(±), I^-(−−), SO_4^{2-}(±), S^{2-}(+++), NO_3^-(±), NO_2^-(±), PO_4^{3-}(+), AsO_4^{3-}(±), CO_3^{2-}(±), CH_3COO^-(±), CN^-(− −), CrO_4^{2-}(±), MnO_4^{2-}(+).

Most heavy metal ions interfere, because they promote the decomposition of the oxidant and catalyse the oxidation of luminol by the oxidant, in addition to the effect of the alkylphosphate. The interference by small concentrations of these cations is suppressed by EDTA.

Discussion

The improved chemiluminescence method has several advantages. The detection limit has been improved by three orders of magnitude. The method is now the most sensitive variant of the Schoenemann reaction procedure, and has a linear calibration range over more than three decades. "Non-toxic" alkylphosphates do not interfere. Since the emission—time curve is characteristic of an individual alkylphosphate, it is possible to discriminate between different alkylphosphates. Finally, the equipment used is relatively simple.

It seems promising to try an adaptation of this procedure for the analysis of gaseous samples, which is now under investigation, in parallel with continuing investigations on insecticides. In addition, kinetic studies aimed at explaining the influence of chloride will be carried out.

REFERENCES

1 K. H. Lohs and P. Franz, Acta Chim. Hung., 26 (1961) 29.
2 H. U. Bergmeyer, Methoden der enzymatischen Analyse, Verlag Chemie, Weinheim/Bergstr., 3. edn., 1974, Vol. 1, p. 862.
3 J. H. Glover, Analyst, 100 (1975) 449.
4 E. J. Poziomek, E. V. Crabtree and D. N. Kramer, Microchem. J., 14 (1969) 150.
5 W. M. Shackelford and G. G. Guilbault, Anal. Chim. Acta, 73 (1974) 383.
6 J. M. Preston, Anal. Chem., 49 (1977) 1746.
7 R. B. R. Schoenemann, PB 119887, lecture Spandau 1944, cited in [8].
8 E. J. Poziomek and E. V. Crabtree, J. Assoc. Off. Anal. Chem., 56 (1973) 56.
9 J. Goldenson, Anal. Chem., 29 (1957) 877.
10 K. Weber and J. Matković, Arh. Hig. Rada, 15 (1964) 151.
11 O. G. Koch and G. A. Koch-Dedic, Handbuch der Spurenanalyse, Springer-Verlag, Berlin, 2. edn., 1974, Vol. 1, p. 23.
12 G. Gottschalk, Fresenius Z. Anal. Chem., 276 (1975) 81.

Analytica Chimica Acta, 118 (1980) 185—189
© Elsevier Scientific Publishing Company, Amsterdam — Printed in The Netherlands

Short Communication

THE SPECTROPHOTOMETRIC AND SPECTROFLUORIMETRIC DETERMINATION OF PERCHLORATE BY EXTRACTION WITH AMILORIDE HYDROCHLORIDE

D. THORBURN BURNS* and P. HANPRASOPWATTANA

Department of Analytical Chemistry, The Queen's University of Belfast, Northern Ireland (U.K.)

(Received 28th January 1980)

Summary. Perchlorate can be determined by spectrophotometric or fluorimetric measurement after extraction into 4-methyl-2-pentanone as an ion pair with amiloride at pH 4. The effects of pH and diverse ions are reported. The system is applied to the determination of down to 0.003% (w/w) perchlorate in samples of potassium chlorate after prior destruction of chlorate.

Relatively few spectrophotometric and no spectrofluorimetric methods have been reported for the determination of perchlorate ions. The spectrophotometric methods can be classified into three main categories: (i) indirect by removal of a reagent by precipitation, (ii) extraction of ion pairs, and (iii) redox reactions. Examples of the first category are the use of methylene blue [1, 2], nitron [3], and the tetrapyridinecuprate(II) ion [4]. Suitable counter-ions for ion-pair extraction include brilliant green [5, 6], methylene blue [7], chelate cations of copper(I) with cuproin [8], neocuproin [8], or with 6-methylpicolinealdehydeazine [9], tetrabutylphosphonium [10], and n-tetrahexylammonium used as the picrate [11] or as the erdmannate [12]. In the last two cases, an amount of the coloured ion equivalent to the perchlorate ion present is displaced into the aqueous phase. Perchlorate may also be determined by measurement of vanadyl ion formed by oxidation of vanadium(III) sulphate [13], or through its interference in the reaction of perrhenate, reduced by tin(II), with α-furildioxime [14].

Persson [15] has described the extraction of the fluorescent protonated secondary amine protriptyline with a variety of ions including perchlorate, but these studies were not extended to the determination of perchlorate. Protriptyline is suitable for the determination of cobalt as tetrathiocyanatocobaltate(II) [16]. In the work reported here, the properties of amiloride [3,5-diamino-*N*-(aminoiminomethyl)-6-chloropyrazinecarboxamide], which forms a highly fluorescent cation at suitable pH, were examined. The protonated amiloride—perchlorate ion pair could be extracted into 4-methyl-2-pentanone, which formed the basis of spectrophotometric and spectrofluorimetric determinations of perchlorate.

Experimental

Apparatus. A Unicam SP8000 recording spectrophotometer and a Baird Atomic SFR100 spectrofluorimeter were used. The wavelengths employed were 365 nm for absorption, and 368 and 410 nm for fluorescence excitation and emission, respectively. Quartz 1-cm cells were used, except in estimating the precision of the spectrophotometric method and in analyses of potassium chlorate, when 4-cm cells were preferred.

Amiloride hydrochloride. The reagent (3,5-diamino-*N*-(aminoiminomethyl)-6-chloropyrazinecarboxamide hydrochloride dihydrate; Merck, Sharp and Dohme International) was used as supplied. Elemental analysis for carbon, hydrogen and nitrogen was satisfactory for the dihydrate. A 0.01 M stock solution was made by dissolving 0.3021 g of the reagent in 100 ml of distilled water.

Stock solution of perchlorate ion. A 1000 ppm perchlorate solution was prepared by dissolving 0.1393 g of potassium perchlorate (analytical-reagent grade dried to constant weight at 105°C) in 100 ml of distilled water. More dilute solutions were prepared as required.

Universal buffer [17]. Citric acid (6.008 g), potassium dihydrogenphosphate (3.893 g), boric acid (1.769 g), and diethylbarbituric acid (5.266 g) were dissolved in 1 l of distilled water. Aliquots (100 ml) were titrated with 0.2 M sodium hydroxide to produce buffer solutions of the desired pH values within the range 2.6—12.0. All reagents were of analytical grade.

Choice of solvent. A variety of solvents including alcohols, ketones, esters, ethers and chlorinated and aromatic hydrocarbons was examined for extraction efficiency by mixing 5-ml aliquots of a 10 ppm perchlorate solution with 5 ml of 0.01 M amiloride hydrochloride solution and extracting with 20 ml of solvent. The organic phase was separated and filtered to remove water, and the absorbance of the extract was measured at 365 nm against the solvent as blank. 4-Methyl-2-pentanone was the most efficient extractant with a low blank in the absence of perchlorate; this is considered to be due to the weak proton-accepting properties of the perchlorate ion and the donor-acceptor properties of the ion pair and solvent, respectively [18].

pH effects. The pH of aqueous solutions was adjusted by addition of 10 ml of buffer solution of defined pH prior to extraction. The reagent blank was constant in the range pH 3--7, whilst the apparent extraction of perchlorate decreased linearly (by 20%) between pH 3 and 7. Solutions buffered at pH 4 were used in all later work.

Optimum amount of reagent. The effect of amiloride hydrochloride concentration on the extraction was studied by using 5-ml aliquots of solutions in the concentration range $0.1—2.0 \times 10^{-2}$ M. Above a concentration of 0.6×10^{-2} M, the absorbances of extracts increased slowly with reagent concentration, 30% from 0.6×10^{-2} M to 1.2×10^{-2} M. A 1.0×10^{-2} M solution was therefore chosen as a reasonable quantity for further studies of the system.

Composition of the complex. This was established spectrophotometrically by Job's method of continuous variations [19] to be a 1:1 ion pair $C_6H_9ClN_7O^+ ClO_4^-$. The curvature of the plot indicated that the complex is appreciably dissociated.

Analysis of potassium chlorate samples. As chlorate interferes in the determination it is necessary to remove or destroy it prior to extraction of perchlorate by evaporation with concentrated hydrochloric acid which also removes other interfering ions [6, 10, 20] such as bromides, iodide and nitrate.

For the analysis, place 5.00 g of sample in an evaporating dish and add 100 ml of concentrated hydrochloric acid. Evaporate to dryness using an infrared lamp in the final stages. Evaporate to dryness a further three times after successive additions of 20 ml of water, in order to remove all the acid. Dissolve the residue in distilled water and dilute to 100 ml in a volumetric flask. To 10-ml aliquots add 5 ml of 1.5×10^{-2} M amiloride hydrochloride solution and 10 ml of pH 4 buffer. Extract with 25-ml and 20-ml portions of 4-methyl-2-pentanone, collecting the organic phases in a 50-ml volumetric flask. Make up to volume, mix well, and determine the absorbance at 365 nm or the fluorescence at 410 nm with excitation at 368 nm.

Results and discussion

Linear calibration graphs were obtained over the range 0—50 μg of perchlorate ion (in 20 ml of aqueous solution) for both fluorescence and absorbance measurements. For 40 μg of perchlorate, the coefficients of variation

TABLE 1

Effect of diverse ions[a] on the determination of perchlorate
(Ions causing a change in absorbance or fluorescence of less than 3% are regarded as non-interfering)

Ion	Ratio to ClO_4^- (w/w)	Change in fluorescence (%)	Change in absorbance (%)	Ion	Ratio to ClO_4^- (w/w)	Change in fluorescence (%)	Change in absorbance (%)
ClO_3^-	200	34	64	SCN^-	100	485	804
	50	—	—		1	2	18.6
	200[b]	—	—		100[c]	—	—
NO_3^-	200	2	40	Cu^{2+}	200	42	111
	20	—	—		200[d]	—	—
	200[b]	—	—				
				Hg^{2+}	200	860	285
I^-	200	43	894		200[d]	—	—
	5	—	—				
	200[c]	—	—	MnO_4^-	20	—	—

[a]Cations added as chloride and anions added as sodium salts. [b]After treatment with concentrated hydrochloric acid. [c]Ag_2SO_4 added: 1:1 molar ratio to the interfering ion. [d]EDTA added: 5 ml of 0.1 M solution.

TABLE 2

Determination of perchlorate in potassium chlorate based on the standard calibration graph (method A) and on standard addition (method B)

Method	$KClO_4$ added (μg)	Total $KClO_4$ found (μg)		$KClO_4$ in $KClO_3$ (%)	
		Fluorimetry	Spectrophot.	Fluorimetry	Spectrophot.
A	0	11.4 ± 0.3	11.8 ± 0.6	0.00228± 0.00006	0.00236± 0.00012
A	10	22.4 ± 0.3	22.7 ± 0.3	0.00248± 0.00006	0.00254± 0.00006
A	30	42.4 ± 0.3	42.0 ± 0.3	0.00248± 0.00006	0.00240± 0.00006
B	—	—	—	0.00224± 0.00004	0.00248± 0.00006

estimated from 7 replicates were 1.6 and 1.8%, respectively. The detection limits were 0.75 and 0.73 μg of perchlorate for fluorescence and absorbance measurements. The molar absorptivity at pH 4 was calculated as 12850 l mol^{-1} cm^{-1}.

The possible interferences of diverse ions on the solvent extraction of 50 μg of perchlorate were examined. There was no interference on either absorbance or fluorescence measurements from 300 mg of chloride or from 10-mg amounts of sulphate, bromide, acetate, chromate, citrate, Mn^{2+}, Ni^{2+}, Zn^{2+}, Fe^{3+} or Co^{2+}. Other results are listed in Table 1. The interferences of chlorate, iodide, nitrate and thiocyanate were significant. These may be removed by evaporation with hydrochloric acid; alternatively, iodide and thiocyanate can be masked by addition of silver sulphate. Mercury(II) and copper(II) interfere seriously but can be masked with EDTA.

The results for the direct and standard addition analysis of samples of analytical-grade potassium chlorate (4 replicates, 95% confidence limits) are shown in Table 2. The results are more precise than those obtainable by earlier methods [6, 10] and the procedures are more convenient. Protriptyline hydrochloride and cyproheptadine hydrochloride were examined as an alternative to amiloride hydrochloride; they behaved similarly but the molar absorptivities were poorer at 8842 l mol^{-1} cm^{-1} and 5720 l mol^{-1} cm^{-1}, respectively.

One of us (P. H.) thanks the Queen's University of Belfast for financial support and Kasetsart University for leave of absence.

REFERENCES

1 F. W. Atack, J. Soc. Dyers Colour., 31 (1915) 183.
2 G. M. Nabar and C. R. Ramachandran, Anal. Chem., 31 (1959) 263.
3 S. Shahine and S. Khamis, Microchem. J., 20 (1975) 409.
4 W. Bodenheimer and H. Weiler, Anal. Chem., 27 (1955) 1293.
5 G. Reusmann, Fresenius Z. Anal. Chem., 226 (1967) 346.
6 A. G. Fogg, C. Burgess and D. Thorburn Burns, Analyst, 96 (1971) 854.

7 I. Iwasaki, S. Utsami and C. Kang, Bull. Chem. Soc. Jpn., 36 (1963) 325.
8 Y. Yamamoto, N. Okamoto and E. Tao, Anal. Chim. Acta, 47 (1969) 127.
9 M. Valcarcel and F. Pino, Ann. Quim., 68 (1972) 385.
10 A. G. Fogg, D. Thorburn Burns and E. H. Yeowart, Mikrochim. Acta, (1970) 974.
11 A. B. Hassle, British Patent 1332043.
12 H. M. N. H. Irving and A. D. Damodaran, Analyst, 90 (1965) 443.
13 D. A. Zatko and B. Kratochvil, Anal. Chem., 37 (1965) 1560.
14 N. L. Trautwein and J. C. Guyon, Anal. Chem., 40 (1968) 639.
15 B.-A. Persson, Acta Pharm. Suec., 7 (1970) 337.
16 D. Thorburn Burns and P. Hanprasopwattana, Anal. Chim. Acta, 115 (1980) 389.
17 W. C. Johnson and A. J. Lindsey, Analyst, 64 (1939) 490.
18 R. Modin and G. Schill, Talanta, 22 (1975) 1017.
19 P. Job, Ann. Chim. (Paris), 9 (1928) 113.
20 A. G. Briggs, W. P. Hayes, P. A. Howling and D. Thorburn Burns, Mikrochim. Acta, (1970) 888.

ACA announcements

ANNOUNCEMENTS OF MEETINGS

Vth INTERNATIONAL SYMPOSIUM ON COLUMN LIQUID CHROMATOGRAPHY

The Vth International Symposium on Column Liquid Chromatography will be held 11–15th May, 1981 in Avignon, France. The programme will comprise discussion papers as well as poster papers dealing with all areas of column liquid chromatography and related techniques. A poster session will be organised.

Notification of discussion papers and poster communications submitted for consideration should arrive not later than 14 November, 1980 together with a 1 page, 300 word, abstract. The papers will be submitted for publication in a special issue of Journal of Chromatography and authors will be requested to hand their manuscripts to the Editor at the meeting.

Further details from: Prof. G. Guiochon, Ecole Polytechnic, Laboratoire de Chimie Analytique Physique, Route de Saclay, 91128 Palaiseau Cedex, France.

4th INTERNATIONAL SYMPOSIUM ON AFFINITY CHROMATOGRAPHY AND RELATED TECHNIQUES

The 4th International Symposium on Affinity Chromatography and Related Techniques – Theoretical Aspects, Industrial and Biomedical Applications will be held from June 22–26, 1981 in the University of Nijmegen, The Netherlands. The scope of the meeting will cover the following topics:

Theoretical Aspects – Ligand/ligate interaction in homogeneous and heterogeneous systems. General theory of electrostatic, hydrophobic and charge-transfer interaction. Theoretical analyses of affinity separations. Matrix structure. Column/batch procedures.

Polymeric Matrices and Ligand Immobilization – Natural and synthetic polymers. Immobilization of ligand molecules.

Applications – Isolation and purification.

The proceedings of the symposium will be published by Elsevier Scientific Publishing Company in the Analytical Chemistry Symposia Series.

Plenary lectures will be presented by invited speakers. Participants wishing to present a paper and/or poster should address themselves for detailed information to the organizing committee at the following address: Secretariat, Department of Organic Chemistry/Faculty of Sciences, Katholieke Universiteit, Toernooiveld, 6525 ED Nijmegen, The Netherlands.

9th INTERNATIONAL CONFERENCE ON ATOMIC SPECTROSCOPY AND COLLOQUIUM SPECTROSCOPICUM INTERNATIONALE

The conference will be held on 4–8 September, 1981 in Tokyo, Japan and will consider all aspects of analytical spectroscopy. Emphasis will be given to spectrochemical methods in the u.v. visible region utilizing emission, absorption and fluorescence spectroscopy in the "gas phase".

Further details: The Japan Society for Analytical Chemistry, 9th ICAS/XXII CSI, Gotanda Sanhaitsu, 26-2 Nishigotanda 1-chome, Shinagawa-ku, Tokyo 141, Japan.

CALENDAR OF FORTHCOMING MEETINGS

Aug. 4–8, 1980 Denver, Colo., U.S.A.	**Conference on Applications of X-Ray Analysis** Contact: Mrs. Mildred Cain, Denver Research Institute, University of Denver, Denver, Colo., 80208, U.S.A. Tel. 303/753-2141
Aug. 4–9, 1980 Ottawa, Canada	**7th International Conference on Raman Spectroscopy** Contact: Mr. Ken Charbonneau, Conference Services, National Research Council of Canada, Ottawa, Ontario, Canada K1A OR6.

Aug. 17–23, 1980 Wolfeboro, N.H., U.S.A.	**Gordon Research Conference on Vibrational Spectroscopy** Contact: Dr. Erich Ipsen, Bell Laboratories, Holmdel, N.J. 07733, U.S.A.
Aug. 18–22, 1980 Brighton, Great Britain	**Micro 80** Contact: The Royal Microscopial Society, 37/38 St. Clements, Oxford OX4 1AJ, Great Britain.
Aug. 24–29, 1980 San Francisco, Calif., U.S.A.	**ACS 180th National Conference – 2nd Chemical Congress of the North Amer. Continent** Contact: A.T. Winstead, 1155 16th Street, N.W. Washington, D.C. 20036, U.S.A.
Aug. 24–31, 1980 Rzeszów, Poland	**2nd International Summer School on Data Processing in Chemistry DPC '80** Contact: Prof. Dr. Z. Hippe, Dept. of Physical Chemistry, Technical University, 35-959 Rzeszów, Poland. (Further details published in Vol. 122, No. 1)
Aug. 25–29, 1980 Prague, Czechoslovakia	**J. Heyrovský Memorial Congress on Polarography** Contact: Czechoslovak Academy of Sciences, J. Heyrovský Institute of Physical Chemistry and Electrochemistry, Vlasská 9, CS-118 40 Praha 1, Czechoslovakia. (Further details published in Vol. 113, No. 2)
Aug. 25–30, 1980 Graz, Austria	**8th International Microchemical Symposium** Contact: Prof. Dr. A. Holasek, Institut für Medizinische Biochemie, Universität Graz, Harrachgasse 21, A-8010 Graz, Austria. Tel. 0 316) 32 5 32 or 76 5 91. (Further details published in Vol. 109, No. 1 and Vol. 110, No. 2).
Aug. 25–30, 1980 Delft, The Netherlands	**Joint ISMAR–Ampère International Conference on Magnetic Resonance** Contact: ISMAR-Ampère 1980, Postbus 30424, NL.2500 GK Den Haag, The Netherlands.
Aug. 31–Sept. 5, 1980 Kuparovice Castle, Czechoslovakia	**IIIrd Brno Symposium on MolecularBiophysics: Electroanalysis of Biopolymers** Contact: Dr. E. Palecak, Institute of Biophysics, Czechoslovak Academy of Sciences, Královopolská 135, 612 65 Brno, Czechoslovakia.
Sep. 2–5, 1980 Prague, Czechoslovakia	**VII European Symposium on Connective Tissue Research** Contact: Dr. Z. Deyl, Physiological Institute Czechoslovak Academy of Sciences, 142 20 Budejovická 1083, Prague 4, Czechoslovakia.
Sep. 6–12, 1980 Liège, Belgium	**International Solvent Extraction Conference (ISEC '80)** Contact: Conference Secretariat ISEC '80, Department of Chemistry, University of Liège, Sart Tilman, B–4000 Liège, Belgium. (Further details published in Vol. 107)
Sep. 6–12, 1980 Bath, Great Britain	**IMLS Triennial Conference** Contact: K. Case, Area Central Laboratory, Royal United Hospital, Bath BA1 3NG, Great Britain.
Sep. 7–12, 1980 Florence, Italy	**IUPAC International Symposium on Macromolecules (Structural Order in Polymers)** Contact: Macro IUPAC 80, Fondazione Giovanni Lorenzini, Via Monte Napoleone 23, 20121 Milan, Italy.
Sep. 8–10, 1980 Oxford, Great Britain	**Photoelectrochemistry Discussion** Contact: Dr. M.D. Archer, Dept. of Physical Chemistry, Univ. of Cambridge, Lensfield Road, Cambridge, Great Britain.

Sep. 9–11, 1980 Eindhoven, The Netherlands	**2nd International Symposium on Isotachophoresis** Contact: ITP 80, Afd. Instrumentele Analyse, Technische Hogeschool Eindhoven, Postbus 513, 5600 MB Eindhoven, The Netherlands.
Sep. 16–19, 1980 Bratislava, Czechoslovakia	**6th International Symposium on Advances and Application of Chromatography in Industry** Contact: Dr. Ján Remeň, Analytical Section ČS VTS, pri n.p. Slovnaft, 82300 Bratislava, Czechoslovakia.
Sep. 17–18, 1980 Amsterdam, The Netherlands	**New Techniques in Analytical Chemistry** Contact: Robert S. First, Inc., 707 Westchester Avenue, White Plains, N.Y. 10604, U.S.A.
Sep. 22–26, 1980 Cannes, France	**8th International Vacuum Congress – 4th International Conference on Solid Surfaces – 3rd European Conference on Surface Science** Contact: Société Francaise du Vide, 19 Rue Renard, F–75004 Paris, France.
Sep. 22–26, 1980 Paris, France	**European Conference on Chemical Pathways in the Environment** Contact: Dr. C. Troyanowsky, Société de Chimie physique, 10, rue Vauquelin, F-75005 Paris, France. Tel. 707-54-48.
Sep. 23–25, 1980 Cardiff, Great Britain	**Chemical Society/Analytical Division – CS Autumn meeting: Trace and Ultratrace Analysis** Contact: The Secretary, Analytical Division, The Chemical Society, Burlington House, London W1V 0BN, Great Britain.
Sep. 24–28, 1980 Hamburg, F.R.G.	**EMBO-EMBL** **Workshop on X-ray and Neutron Scattering of Biological Structure** Contact: Prof. H. Stuhrmann, EMBL c/o DESY, Notkestrasse 85, D-2000 Hamburg 52, F.R.G.
Sep. 28–Oct. 3, 1980 Smolenice Castle, Czechoslovakia	**International Symposium on n.m.r. Spectroscopy** Contact: Ing. Igor Goljer, n.m.r. Laboratory, Faculty of Chemical Technology, Jánska 1, 880 37 Bratislava, Czechoslovakia.
Sep. 28–Oct. 3, 1980 Philadelphia, Pa., U.S.A.	**7th Annual Meeting of Federation of Analytical Chemistry and Spectroscopy Societies (FACSS)** Contact: Mrs. J.G. Graselli, c/o Standard Oil Co., 4440 Warrensville Road, Cleveland, Ohio 44128, U.S.A.
Sep. 29–Oct. 3, 1980 York, Great Britain	**Modern Radiochemical Practice** Contact: The Secretary, Analytical Division, Chemical Society, Burlington House, London W1V 0BN, Great Britain.
Oct. 6–9, 1980 Houston, Texas, U.S.A.	**EXPOCHEM '80** Contact: Professor A. Zlatkis, Chemistry Department, University of Houston, Houston, Texas, 77004, U.S.A. Tel. (713) 749-2623. (Further details published in Vol. 116, No. 1)
Oct. 6–9, 1980 Houston, Texas, U.S.A.	**Chromatography '80 – 15th International Symposium on Advances in Chromatography** Contact: Professor A. Zlatkis, Chemistry Department, University of Houston, Houston, Texas 77004, U.S.A. Tel. (713) 749 2623. (Further details published in Vol. 115)

Oct. 7–9, 1980 Gatlinburg, Tenn., U.S.A.	**Analytical Chemistry in Environmental Regulation and Control** Contact: W.S. Lyon, Technical Program Chairman, Oak Ridge National Laboratory, P.O. Box 8, Oak Ridge, Tenn. 37830, U.S.A. Tel: (615) 574-4882.
Oct. 9–15, 1980 Dusseldorf, West Germany	**INTERKAMA '80 – International Congress and Trade Fair for Instrumentation and Automation** Contact: German/American Chamber of Commerce, 666 Fifth Avenue, New York, NY 10019, U.S.A.
Oct. 15–17, 1980 Toyohashi, Japan	**Fifth International Conference on Computer in Chemical Research and Education (VICCCRE)** Contact: Prof. S. Sasaki, Toyohashi University of Technology, Tempaku, Toyohashi, Japan 440.
Oct. 16–17, 1980 Teddington, Middx., Great Britain	**Quantitative Surface Analysis** Contact: The Meetings Officer, The Institute of Physics, 47 Belgrave Square, London SW1X 8QZ, Great Britain.
Oct. 19–23, 1980 Washington, D.C., U.S.A.	**Annual Meeting of Assoc. of Official Analytical Chemists** Contact: K.M. Fominaya, Box 540, Benjamin Franklin Station, Washington, D.C. 20044, U.S.A.
Oct. 22–24, 1980 Rome, Italy	**Workshop on TCDD and Related Compounds** Contact: Prof. Dr. O. Hutzinger, University of Amsterdam, Nieuwe Achtergracht 166, Amsterdam, The Netherlands. (Further details published in Vol. 122, No. 1)
Oct. 27–31, 1980 Endorf bei Rosenheim/ Bayern, F.R.G.	**EUCHEM – CONFERENCE: Die Darstellung logischer Strukturen in der Chemie durch Modelle und die Lösung chemischer Probleme mittels Computern** Contact: GDCh–Geschäftsstelle, P.O. Box 90 04 40, D–6000 Frankfurt/M 90, F.R.G.
Nov. 11–15, 1980 Milan, Italy	**1st African and Mediterranean Congress of Clinical Chemistry and 6th Congress of the Italian Society of Clinical Biochemistry** Contact: 1st African and Mediterranean Congress of Clinical Chemistry, Via Keplero, 10-20124 Milan, Italy.
Nov. 19–21, 1980 New York, N.Y., U.S.A.	**19th Eastern Analytical Symposium** Contact: Norman Gardner, Exposition Manager, 73 Ethel Street, Metuchen, N.J. 08840, U.S.A. Tel. (201) 548 7377.
Dec. 8–12, 1980 Porte de Versailles, Paris, France	**2ème Congrès de Chimie Analytique – 34ème Congrès du G.A.M.S.** Contact: Secrétriat du G.A.M.S. (Congrès), 88, Boulevard Malesherbes, 75008 Paris, France.
Dec. 16–17, 1980 Brighton, Great Britain	**Chromatography, Equilibria and Kinetics** Contact: Mrs. Y.A. Fish, The Chemical Society, Burlington House, London W1V 0BN, Great Britain. Tel. 01-7349971.
Apr. 13–16, 1980 Cardiff, Wales United Kingdom	**International Symposium on Electroanalysis in Clinical Environmental and Pharmaceutical Chemistry** Contact: Short Courses Section (Electroanalysis Symposium), UWIST, Cardiff CF1 3NU, Wales, United Kingdom. (Further details published in Vol. 116, No. 1)

(continued from outside of cover)

Short Communications

VOL. 118 No. 1 ANALYTICA CHIMICA ACTA JULY 1, 1980

CONTENTS

(continued on inside page of cover)

© Elsevier Scientific Publishing Company, 1980.
All rights reserved. No part of this publication may be reproduced, stored in a retrieval system or transmitted in any form or by any means, electronic, mechanical, photocopying, recording or otherwise, without the prior written permission of the publisher, Elsevier Scientific Publishing Company, P.O. Box 330, 1000 AH Amsterdam, The Netherlands.

Submission of an article for publication implies the transfer of the copyright from the author to the publisher and is also understood to imply that the article is not being considered for publication elsewhere.

Submission to this journal of a paper entails the author's irrevocable and exclusive authorization of the publisher to collect any sums or considerations for copying or reproduction payable by third parties (as mentioned in article 17 paragraph 2 of the Dutch Copyright Act of 1912 and in the Royal Decree of June 20, 1974 (S. 351) pursuant to article 16 b of the Dutch Copyright Act of 1912) and/or to act in or out of court in connection therewith.

Printed in The Netherlands.